

**UNIVERSIDADE DE SÃO PAULO**  
Faculdade de Ciências Farmacêuticas  
Departamento de Farmácia

Programa de Pós-Graduação em Fármaco e Medicamentos  
Área de Insumos Farmacêuticos

**Targeting the *h*TRPV6 with capsaicinoid inhibitors**

**Micael Rodrigues Cunha**

Tese para obtenção do Título de  
DOUTOR

**Orientador:**  
Prof. Dr. Roberto Parise-Filho  
Universidade de São Paulo

**São Paulo**  
**2019**



**UNIVERSIDADE DE SÃO PAULO**  
Faculdade de Ciências Farmacêuticas  
Departamento de Farmácia

Programa de Pós-Graduação em Fármaco e Medicamentos  
Área de Insumos Farmacêuticos

**Targeting the *h*TRPV6 with capsaicinoid inhibitors**

**Micael Rodrigues Cunha**

VERSÃO ORIGINAL

Tese para obtenção do Título de  
DOUTOR

**Orientador:**  
Prof. Dr. Roberto Parise-Filho  
Universidade de São Paulo

**São Paulo**  
**2019**

Autorizo a reprodução e divulgação total ou parcial deste trabalho, por qualquer meio convencional ou eletrônico, para fins de estudo e pesquisa, desde que citada a fonte.

Ficha Catalográfica elaborada eletronicamente pelo autor, utilizando o programa desenvolvido pela Seção Técnica de Informática do ICMC/USP e adaptado para a Divisão de Biblioteca e Documentação do Conjunto das Químicas da USP

Bibliotecária responsável pela orientação de catalogação da publicação:  
Marlene Aparecida Vieira - CRB - 8/5562

C972t Cunha, Micael Rodrigues  
Targeting the hTRPV6 with capsaicinoid  
inhibitors / Micael Rodrigues Cunha. - São Paulo,  
2019.  
197 p.

Tese (doutorado) - Faculdade de Ciências  
Farmacêuticas da Universidade de São Paulo.  
Departamento de Farmácia.  
Orientador: Parise-Filho, Roberto

1. TRPV channels. 2. capsaicin. 3.  
bioisosterism. 4. Ligand-Based Drug Design. I. T.  
II. Parise-Filho, Roberto, orientador.

Micael Rodrigues Cunha

**Targeting the *h*TRPV6 with capsaicinoid inhibitors**

Comissão julgadora

---

Prof. Roberto Parise-Filho, PhD  
Orientador e Presidente

---

Prof. \_\_\_\_\_  
Primeiro examinador

---

Prof. \_\_\_\_\_  
Segundo examinador

---

Prof. \_\_\_\_\_  
Terceiro examinador

São Paulo, 3 de dezembro de 2019

*“Grandes são as obras do SENHOR; nelas meditam todos os que as apreciam.”*  
*Sl. 111.2*

*“Great are the Works of the LORD; they are pondered by all who delight in them.”*  
*Ps. 111.2*

---

## Table of Contents

Acknowledgments .....	i
Resumo .....	iii
Abstract .....	iv
Abbreviations .....	v
List of Figures .....	viii
List of Tables.....	xi
List of Schemes .....	xii
1. Introduction .....	1
1.1 Aim of the Thesis .....	1
1.2 TRP channels.....	1
1.2.1 TRP Vanilloid (TRPV) subfamily.....	2
1.3 TRPV6 Channel .....	4
1.3.1 The role of TRPV6 in diseases.....	5
1.3.2 TRPV6 modulation by small molecules.....	6
1.4 Capsaicin (CPS) .....	6
1.4.1 Capsaicin and TRPV channels .....	7
1.5 Rationality behind Drug Design.....	9
1.5.1 Design of bioisosteric and hybrid capsaicinoids .....	12
2. Results and Discussion.....	14
2.1 Synthesis of bioisosteric capsaicinoids.....	14
2.2 Synthesis of hybrid capsaicinoids .....	17
2.3 TRPV6 Cd <sup>2+</sup> assay for screening of compounds .....	20
2.4 Hit optimization.....	21
2.4.1 Confocal imaging .....	26
2.4.2 <i>In vitro</i> metabolism.....	26
2.4.3 Antiproliferative activity .....	28
3. Conclusion and Outlook.....	30
4. Contributions .....	31
5. Experimental Part .....	32
5.1 Chemistry .....	33
5.1.1 Synthesis of the bioisosteric capsaicinoids.....	33
5.1.2 Synthesis of the hybrid capsaicinoids.....	40
5.2 Biology .....	56
5.2.1 TRPV FLIPR assay. ....	56
5.2.2 Confocal imaging. ....	57
5.2.3 <i>In vitro</i> Polypharmacology and metabolism.....	58

5.2.4 Antiproliferative activity.....	58
5.3 Purity.....	60
6. References.....	61
7. Supplementary Data.....	67
7.1 Time-course confocal microscopy.....	67
7.2 Inhibition curves of <i>cis</i> -22a against SKOV-3 and HEK-wt.....	68
7.3 In vitro Polypharmacology and metabolism.....	68
7.4 Copy of NMR spectra, ESI-HRMS and HPLC traces.....	69
7.5 Curriculum Vitae.....	175
7.6 Student's Record.....	177

## Acknowledgments

Thanks to the Department of Pharmacy of the University of São Paulo, and to the Graduation Program in Drugs and Medicines for this great opportunity, for financial and technical support.

Thanks to the Coordenação de Aperfeiçoamento de Pessoal de Nível Superior (CAPES, Finance Code 001), and to the Fundação de Amparo à Pesquisa do Estado de São Paulo (FAPESP, Grant nr: 2017/00689-0) for the financial support during this work.

I would like to thank my wife, Mariana Etchebehere Berthault Cunha. As I said before, I would never conclude this part of my life without your constant support. Thank you for giving up many of your dreams to be with me, I cannot express how deeply it impacted my life. Thank you for taking me out of home, for making me breathe. Thank you for always being there. Essentially, all this work was only possible because I had someone like you reminding me of what is important in life.

To my beloved parents, Jonas Moraes Cunha and Yara Rodrigues Cunha. Thank you for all the effort, all the sacrifice and dedication without which I would not have come this far. To my brother, Mateus Rodrigues Cunha, thank you for all your prayers and advice. Thank you all for always believing in my dreams.

To my in-laws, Claudio Berthault and Roberta Etchebehere Berthault, and my brother-in-law João Pedro Etchebehere Berthault. Thank you for all our shared moments, for your support abroad, and for welcoming me so well into your family.

To my supervisor, Prof. Dr. Roberto Parise-Filho. Among all the people, I thank you with all my heart for accepting to guide me. Few today would do what you did for me at the beginning of my academic career. Thank you for your guidance, trust, friendship, and opportunities.

Thank you all the actual and former members of Roberto's group: Rosania, Alfredo, Mauricio, Gustavo, Thais, Nuno, Karinne and Victor. Despite the difficulties in doing science these days, you have helped to make my burden lighter. Stay firm!

Thanks also to the Pharmacy Department, especially to David for your gigantic administrative support, to Dr. Inês for the NMR services, and to Dr. Monica that in spite of the short time we have met, you have helped me a lot to get this work done.

I would like to thank the Swiss Confederation, for the financial support which allowed me to complete a big part of this work. Also, I would like to thank many people during my 20 months working within the NCCR TransCure at the University of Bern - Switzerland.

Special thank goes to Prof. Dr. Jean-Louis Reymond for accepting me at your lab, for your trust in my work and for inserting me in many exciting projects, also, thank you very much for the scientific and financial support.

I am particularly grateful to Dr. Rajesh Bhardwaj in the group of Prof. Dr. Matthias Hediger for teaching me how to think and how to do proper biochemistry; for mentoring me during my - several - stress crisis of living abroad; for testing my compounds and never giving up from so many projects we did together. Thank you also for all the other members of Hedger's group.

Thank you too, Dra. Tamis Darbe, for the chemistry comments and discussions, but especially for having some time of Portuguese conversation. Thank you all the former members of the Reymond's group: Thissa, Mahendra, Ivan, Vala, Jérémy, Marion, Clémence, Marc and Bee Ha, I hope all of you are doing well. Thank you also to the current members: Geo, Manuel, Stephen, Lazo, Giorgio, Sven, Alice, Susana, Kris, Daniel, Elena, Dina, Joseph, and Amol for the wonderful atmosphere in the lab, for the áperos, the hiking, the barbecues and for letting me (and my wife) being part of your lives in Bern.

A big thank you to Dr. Sacha Javor, for introducing me to Molecular Dynamics world, and the big support on chemistry.

I would also like to thank all the administrative team within the Department of Chemistry and Biochemistry and the International Office of the UniBe, namely, Sandra Zbinden, Beatrice Thönen and Jasmin Fallahi, for all the support with letters, translations, and documentation. Thanks to the team of the Werkstatt, the Ausgabe, the NMR and MS services for all the requested equipment, chemicals, and analysis.

To all of you, Obrigado!

## Resumo

CUNHA, M. R. **Targeting the *h*TRPV6 with capsaicinoid inhibitors**. 2019. 197p. Tese de Doutorado – Faculdade de Ciências Farmacêuticas. Universidade de São Paulo, São Paulo, 2019.

Capsaicina é uma substância produzida por pimentas do gênero *Capsicum* com extensa atividade biológica relatada na literatura. Entre esses estudos, sugeriu-se que a atividade antitumoral esteja relacionada à modulação dos canais TRPV (do inglês, *Transient Potential Receptor Vanilloid*). Sabe-se que a capsaicina se liga com altíssima afinidade ao TRPV1 ( $IC_{50} \approx 7$  nM), desencadeando a sensação de queimação seguida de analgesia. No entanto, estudos recentes sugeriram que os efeitos pró-apoptóticos da capsaicina são mediados pelo TRPV6. Visando o exposto, este trabalho relata o desenvolvimento de um novo inibidor do TRPV6 usando duas estratégias diferentes para o planejamento dos compostos. Geramos séries de capsaicinoides diretos e quiméricos com base nos compostos da literatura, capsaicina e *cis*-22a. Esses análogos foram analisados contra HEK-*h*TRPV6 e os análogos mais promissores foram otimizados. Com base na REA e em otimizações químicas anteriores, encontramos **56h**, chamado MRC-130, um derivado que inibiu notavelmente o TRPV6 na faixa nanomolar ( $IC_{50} = 83 \pm 4$  nM), possui alta seletividade e estabilidade *in vitro* e menor inibição de *h*ERG em comparação com o composto de referência, *cis*-22a. Espera-se que essas novas moléculas contribuam significativamente para o estudo da função do TRPV6 e seu papel na fisiopatologia tumoral.

**Palavras-chave:** Capsaicina, Bioisosterismo, Receptor TRPV, Citotoxicidade.

## Abstract

CUNHA, M. R. **Targeting the *h*TRPV6 with capsaicinoid inhibitors.** 2019. 197p. Doctoral Theses – Faculty of Pharmaceutical Sciences. University of São Paulo, São Paulo, 2019.

Capsaicin is a substance produced by *Capsicum* peppers with extensive biological activity reported in the literature. Among these studies, it was suggested that the anti-tumor activity is related to modulation of the Transient Potential Receptor Vanilloid (TRPV) channels. Capsaicin is known to bind with very high affinity to TRPV1 ( $IC_{50} \approx 7$  nM), triggering the burning sensation followed by analgesia. However, recent studies have suggested that the pro-apoptotic effects of capsaicin are TRPV6-mediated. Herein we report the development of a novel inhibitor of the TRPV6 using two different strategies for compounds design. We generated a series of direct and chimeric capsaicinoids based on the literature compounds, capsaicin, and *cis-22a*. These analogs were probed against HEK-*h*TRPV6 and the hits were further optimized. Based on the previous SAR and chemical optimization, we found **56h**, named MRC-130, a derivative that remarkably inhibited TRPV6 in the nanomolar range ( $IC_{50} = 83 \pm 4$  nM), possess high selectivity and stability *in vitro*, and lesser *h*ERG inhibition compared to the reference compound, *cis-22a*. It is expected that these new molecules would contribute significantly to the study on the TRPV6 function and its role in tumor pathophysiology.

**Key-words:** Capsaicin, Bioisosterism, TRPV Channel, Cytotoxicity.

---

## Abbreviations

<b>2-APB</b>	2-Aminoethoxydiphenyl borate
<b>ADMET</b>	Absorption, Distribution, Metabolism, Excretion, Toxicity
<b>AEA</b>	N-arachidonoyl ethanolamide
<b>Akt</b>	Protein kinase B
<b>CADD</b>	Computer-Aided Drug Design
<b>CaM</b>	Calmodulin
<b>CB</b>	Cannabinoid Receptor
<b>cDNA</b>	Complementary Deoxyribonucleic acid
<b>COSY</b>	Correlated Spectroscopy
<b>CPS</b>	Capsaicin
<b>cryo-EM</b>	Cryo-Electron Microscopy
<b>DCM</b>	Dichloromethane
<b>DMAP</b>	4-Dimethylaminopyridine
<b>DMSO</b>	Dimethylsulfoxide
<b>EC<sub>50</sub></b>	Median Effective Concentration
<b>ECN</b>	Econazole
<b>EDCI</b>	1-ethyl-3-(3-dimethyl aminopropyl)carbodiimide hydrochloride
<b>ESI</b>	Electron Spray Ionization
<b>Et<sub>2</sub>O</b>	Diethyl Ether
<b>EtOAc</b>	Ethyl Acetate
<b>FBS</b>	Fetal Bovine Serum
<b>FLIPR</b>	Fluorescent Imaging Plate Reader
<b>HA</b>	Heavy Atom
<b>HEK</b>	Human Embryonic Kidney
<b>hERG</b>	Human Ether-a-go-go-related Gene
<b>HPLC</b>	High-Performance Liquid Chromatography
<b>HRMS</b>	High-Resolution Mass Spectrometry
<b>HTS</b>	Highthroughput Screening
<b>IC<sub>50</sub></b>	Half Maximal Inhibitory Concentration
<b>IGF1R</b>	Insulin-Like Growth Factor 1 Receptor
<b>LBDD</b>	Ligand-Based Drug Design
<b>LBS</b>	Ligand-Binding Site

<b>LE</b>	Ligand Efficiency
<b>LLE</b>	Lipophilic Ligand Efficiency
<b>MCN</b>	Miconazole
<b>MD</b>	Molecular Dynamics
<b>mRNA</b>	Messenger Ribonucleic Acid
<b>NCF</b>	Nominal Calcium Free buffer
<b>NFAT</b>	Nuclear Factor of Activated T-Cells
<b>NMR</b>	Nuclear Magnetic Resonance
<b>PI3K</b>	Phosphoinositide 3-Kinase
<b>PIP2</b>	Phosphatidylinositol 4,5-bisphosphate
<b>PKC</b>	Protein Kinase C
<b>PMS</b>	Phenazine Methosulfate
<b>PPTS</b>	Pyridinium <i>para</i> -Toluenosulfonate
<b>ROS</b>	Reactive Oxygen Species
<b>RP-HPLC</b>	Reversed-Phase Ultra-High-Performance Liquid Chromatography
<b>RTx</b>	resiniferatoxin
<b>SAR</b>	Structure-Activity Relationship
<b>SBDD</b>	Structure-Based Drug Discovery
<b>SBVS</b>	Structure-Based Virtual Screening
<b>SCLC</b>	Small Cell Lung Cancer
<b>SD</b>	Standard Deviation
<b>SEM</b>	Standard Error of Mean
<b>siRNA</b>	small interfering Ribonucleic Acid
<b>TBAF</b>	Tetrabutylammonium Fluoride
<b>TBDMS</b>	<i>tert</i> -Butyldimethylsilyl
<b>TFA</b>	Trifluoroacetic Acid
<b>THF</b>	Tetrahydrofuran
<b>TLC</b>	Thin Layer Chromatography
<b>TNH</b>	Transient Neonatal Hyperparathyroidism
<b>TRP</b>	Transient Receptor Potential
<b>TRPA</b>	Transient Receptor Potential Ankyrin
<b>TRPC</b>	Transient Receptor Potential Canonical
<b>TRPM</b>	Transient Receptor Potential Melastatin
<b>TRPML</b>	Transient Receptor Potential Mucolipin

<b>TRPN</b>	Transient Receptor Potential No mechanoreceptor potential C
<b>TRPP</b>	Transient Receptor Potential Polycystic
<b>TRPV</b>	Transient Receptor Potential Vanilloid
<b>TsOH</b>	<i>para</i> -Toluenosulfonic Acid
<b>VR1</b>	Vanilloid Receptor 1

## List of Figures

<b>Figure 1.</b> Phylogenetic tree of human TRP channels and similarities with the mouse (TRPC2) and zebrafish (TRPN1). <sup>a</sup> .....	2
<b>Figure 2.</b> Single-channel recordings of TRPV1 currents after activation by CPS/PIP2 (A) and by heat at different temperatures (B). <sup>18,19</sup> .....	3
<b>Figure 3.</b> Top view of the tetrameric assembly of TRPV channels achieved by Cryo-EM. Proteins are depicted as cartoon and were colored as cyan, green, yellow, and magenta. Below each structure is the PDB code used to generate the figure. ....	3
<b>Figure 4.</b> (A) Structure of hTRPV6 in the closed state bound to Ca <sup>2+</sup> -CaM. (B) Bottom view of the TRPV6 shown as a light-gray surface. Proteins are depicted as cartoon and were colored as cyan, green, yellow, and magenta. CaM is depicted in dark-blue and Ca <sup>2+</sup> atoms as green spheres. ....	4
<b>Figure 5.</b> (A) Structure of apo-hTRPV6 in the open state. TRPV6 is depicted as a cartoon and was colored as cyan, green, yellow, and magenta. (B) Side view of the highlighted region in (A) displaying the protein as light gray surface and the electron density maps of the putative lipids are shown as dark-blue mesh. ....	5
<b>Figure 6.</b> Chemical structure of TRPV6 modulators.....	6
<b>Figure 7.</b> Antiproliferative activities of CPS and analogs developed in our group against tumor cell lines.....	7
<b>Figure 8.</b> A computational model of CPS (light magenta sticks) bound to TRPV1. <sup>108</sup> .....	8
<b>Figure 9.</b> The workflow of SBDD and LBDD in drug discovery. Adapted from Lu and colleagues, 2018. <sup>126</sup> .....	9
<b>Figure 10.</b> An example highlighting how the bioisosteric replacements of CPS led to the discovery of potent TRPV1 modulators. ....	11
<b>Figure 11.</b> Chemical structures of CPS and AEA highlighting the pharmacophore used on the design of arvanil.....	12
<b>Figure 12.</b> (A) Structure of the CPS and <i>cis</i> -22a used to design bioisosteric (B and C) and hybrid capsaicinoids (D). ....	13
<b>Figure 13.</b> General routes for the synthesis of substituted hydrazones. Note that for sulfonyl hydrazones and sulfonylglycine hydrazones instead of an amide the compounds present a sulfonamide moiety.....	15
<b>Figure 14.</b> Crystal structure of a sulfonylhydrazone revealing its E-antiperiplanar stereochemistry. <sup>165</sup> .....	16
<b>Figure 15.</b> Possible conformers of E- <b>12b</b> . ....	16
<b>Figure 16.</b> <sup>1</sup> H-NMR spectra of compound <b>12b</b> at 20 °C (A), 75 °C (B) and cooled to 30 °C (C).17	
<b>Figure 17.</b> <sup>1</sup> H-NMR (A) and <sup>13</sup> C-NMR (B) spectra of compound <i>cis</i> - <b>24f</b> (black line) and <i>trans</i> - <b>24f</b> (blue line).....	19
<b>Figure 18.</b> Crystal structure of compound <i>cis</i> - <b>24f</b> .....	20
<b>Figure 19.</b> Cd <sup>2+</sup> (50.0 μM) influx into HEK293- <i>h</i> TRPV6 cells. Data were normalized to the maximum entry in the vehicle group (buffer/DMSO). BC = bioisosteric capsaicinoids; HC = hybrid	

---

capsaicinoids. One-way ANOVA, Boferroni's post-test. \*P < 0.05; \*\*\*P < 0.001. Data shown are mean + SEM ( $n = 3$  or  $6$ ). ..... 20

**Figure 20.** Design of the 3-pyridones from compound **24f** and literature compounds *cis-12b*<sup>76</sup> and azo-**9d**.<sup>179</sup> ..... 22

**Figure 21.** HEK-*h*TRPV6 cells co-stained with Leadmium Green and Alexa Fluor 298. Images were collected at time 0 min and 30 min after treatment with vehicle (A) or MRC-130 (10  $\mu$ M, B) followed by the addition of Cd<sup>2+</sup> (50  $\mu$ M) using confocal microscopy (Nikon Eclipse TE2000-E, 100X). White bars denote 25  $\mu$ m. .... 26

**Figure 22.** Intrinsic clearance in human liver microsomes of *cis-22a* (blue bars) and MRC-130 (red bars). Data shown are mean  $\pm$  SEM ( $n = 2$ ). The experiments were conducted by Eurofins Cerep SA, France. .... 27

**Figure 23.** In vitro polypharmacology for selected human targets of *cis-22a* (blue bars) and MRC-130 (red bars). Data shown are mean  $\pm$  SEM ( $n = 2$ ). The data for *cis-22a* was extracted from the ref.<sup>76</sup> The experiments were conducted by Eurofins Cerep SA, France. .... 27

**Figure 24.** Photomicrographs show the morphological aspects of the control cultures of T47D cells (A), and treated with MRC-130 (100  $\mu$ M, B); *cis-22a* (100  $\mu$ M, C); doxorubicin (10  $\mu$ M, D). Cells were imaged at 20X with an inverted microscope (Nikon Eclipse TiU). .... 29



## List of Tables

<b>Table 1.</b> TRPV Activity of active capsaicinoids. <sup>a</sup> .....	21
<b>Table 2.</b> TRPV Activity Evaluation of Optimized Capsaicinoids. <sup>a</sup> .....	25
<b>Table 3.</b> Percentage of viable cells treated with MRC-130, <i>cis</i> -22a, and doxorubicin. <sup>a</sup> .....	28

## List of Schemes

<b>Scheme 1.</b> Synthetic route of sulfonylhydrazones <b>5a-b</b> and <b>8a-b</b> . <sup>a</sup> .....	14
<b>Scheme 2.</b> Synthetic route of N-acyl hydrazones <b>11a-b</b> and <b>12a-b</b> . <sup>a</sup> .....	14
<b>Scheme 3.</b> Synthetic route of sulfonylglycine hydrazones <b>17a-b</b> and <b>18a-b</b> . <sup>a</sup> .....	15
<b>Scheme 4.</b> Synthetic route of compounds <b>24c-f</b> . <sup>a</sup> .....	18
<b>Scheme 5.</b> Synthetic route of compounds <b>28c-f</b> . <sup>a</sup> .....	18
<b>Scheme 6.</b> Synthetic route of 3-pyridones <b>32e-f</b> and <b>36e-f</b> . <sup>a</sup> .....	22
<b>Scheme 7.</b> Synthetic route of pyridine substituted analogues of <b>32f</b> . <sup>a</sup> .....	23
<b>Scheme 8.</b> Synthetic route of optimized 3-pyridones <b>53g-i</b> and <b>56h-i</b> . <sup>a</sup> .....	24

# 1. Introduction

## *1.1 Aim of the Thesis*

The Laboratory for Design and Synthesis of Bioactive Substances (LAPESSB) aims to rationally develop drug-candidates and tools-compounds to assist in understanding the physiological role of biological targets and their participation in diseases. Among the strategies for the generation of chemical compounds, LAPESSB is based on the selection of privileged frameworks and proposition of analogs for chemical synthesis, through molecular modifications.

The aim of this thesis was to develop innovative compounds with modulatory activity on the TRPV6 membrane receptor. Based on literary data, capsaicin was selected as a prototype for the design of bioisosteric and hybrid analogs.

The introduction has been subdivided into three parts to facilitate the reader's contextualization. First, the TRPV receptor family will be addressed; followed by the literature review on the prototype; and methods for generating analogs.

## *1.2 TRP channels*

The study of the phototransduction in flies is considered the starting point of TRP discovery. The bright-light blindness in mutated *Drosophila melanogaster* (common fruit flies) rendered a *transient receptor potential (trp)* in electroretinogram (ERG), losing 50 % of signal amplitude after several light flashes. Under the same conditions, the recorded potential for wild-type flies was sustained during the whole experiment.<sup>1</sup> 20-years later, the gene mutation that caused defective photoreception was linked to the production of a putative light-sensitive ion channel responsive to phosphatidylinositol 4,5-bisphosphate (PIP<sub>2</sub>).<sup>2</sup> A few years later, the similarity observed in calcium (Ca<sup>2+</sup>) transduction in mammalian and *Drosophila* tissues was investigated in depth. The results revealed gene homologs widely expressed in human tissues.<sup>3,4</sup>

The Transient Receptor Potential (TRP) superfamily plays a massive role in Ca<sup>2+</sup> homeostasis.<sup>5</sup> Currently, it is subdivided into seven subfamilies: TRPC (canonical), TRPV (vanilloid), TRPM (melastatin), TRPP (polycystin), TRPML (mucolipin), TRPA (Ankyrin) and TRPN (NO-mechano-potential) (**Figure 1**), with 27 representatives in humans.<sup>6</sup> Their function triggers different cellular responses ranging from epithelial Ca<sup>2+</sup> reabsorption to neuronal sensory transduction.<sup>7,8</sup> The ability of TRPs to unleash a plethora of cell signaling,

and the possibility of modulation by small molecules place this family as one of the most important targets for drug discovery.<sup>9,10</sup>

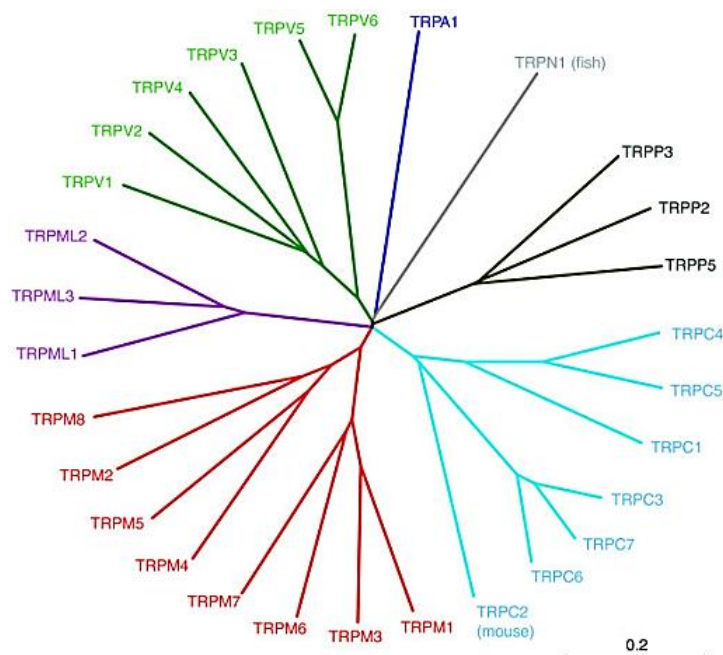


**Figure 1.** Phylogenetic tree of human TRP channels and similarities with the mouse (TRPC2) and zebrafish (TRPN1).<sup>a</sup>

### 1.2.1 TRP Vanilloid (TRPV) subfamily

The TRP Vanilloid subfamily comprises a total of six isoforms (TRPV1-6) found in almost every cell type in both excitable and non-excitable tissues and responds to a wide range of physical and chemical stimuli including binding of intracellular and extracellular messengers, changes in temperature, and osmotic pressure and mechanical stimulation.<sup>11</sup>

The TRPV term was coined owing to the discovery of its first representative, TRPV1, by the time referred to as VR1 (Vanilloid Receptor 1). The pungent sensation caused by vanilloid compounds, such as capsaicin (CPS)<sup>12-14</sup> and resiniferatoxin (RTx)<sup>15,16</sup> had been linked to the depolarization of sensory neurons by increasing the permeability of the plasma membrane to cations. In 1997, Caterina and coworkers were able to generate HEK-transfected cells from a library of cDNA from dorsal root ganglion-derived mRNA, which underwent the same features observed in CPS and RTx-treated neurons.<sup>17</sup> Currently, it is established that TRPV1 also responds to noxious heat in a similar manner found by CPS-activation (**Figure 2**),<sup>18,19</sup> and the thermal hyperalgesia resulting from cutaneous inflammation.<sup>20</sup> Subsequently, TRPV2 to 6 were identified mainly by expression-cloning in an attempt to identify mechanisms of thermo-sensitivity in TRPV1-knockout mice responsive to mild-heat, hypoosmolarity and mechanical nociception, and Ca<sup>2+</sup> transport in kidney and intestines.<sup>21-31</sup>

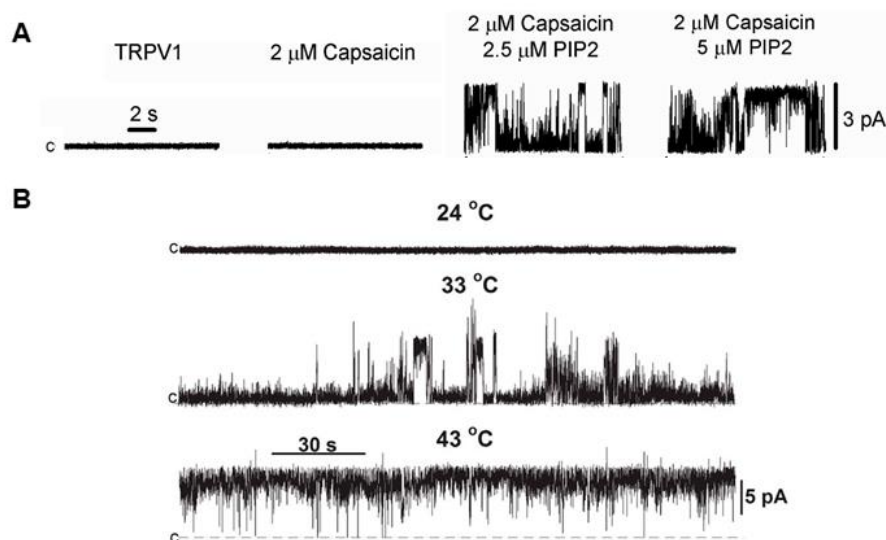


**Figure 2.** Single-channel recordings of TRPV1 currents after activation by CPS/PIP2 (A) and by heat at different temperatures (B).<sup>18,19</sup>

TRPV channels are membrane proteins that contain six transmembrane domains (S1-S6) and a pore helix. TRPV subunits may form hetero- and homotetramers, each subunit swapped with the S5-S6 pore domain of the following subunit.<sup>32–36</sup> The pore region confers to TRPV5 and TRPV6 their constitutive activity and high  $\text{Ca}^{2+}$ -selectivity, unique among the whole TRP family.<sup>23,28</sup> The N- and C-terminal regions are both intracellular and are involved in channel traffic to the plasma membrane, correct tetramerization and regulation of phosphorylation sites.<sup>37–39</sup> Very recently, the structure of all the TRPV members was elucidated by X-ray crystallography and cryoelectron-microscopy (cryo-EM) methods (**Figure 3**).<sup>32,40–46</sup>

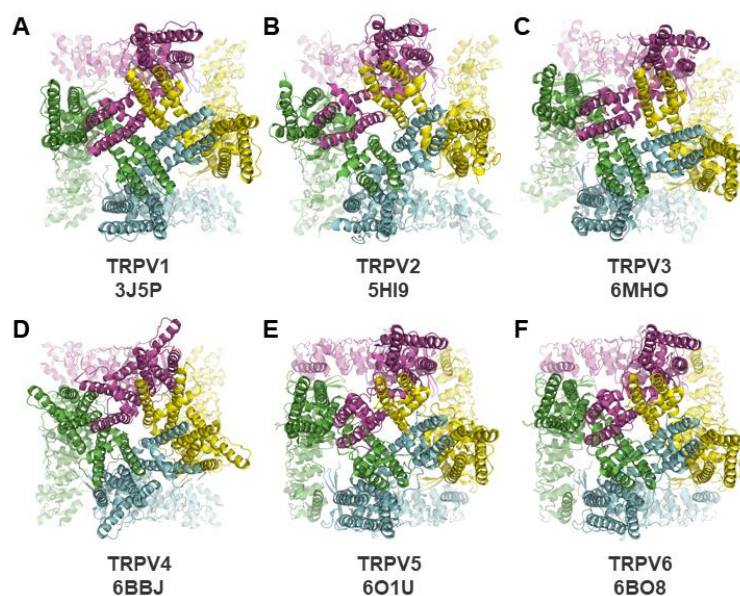


**Figure 3.** Top view of the tetrameric assembly of TRPV channels achieved by Cryo-EM. Proteins are depicted as cartoon and were colored as cyan, green, yellow, and magenta. Below each structure is the PDB code used to generate the figure.

### 1.3 TRPV6 Channel

TRPV6 is a  $\text{Ca}^{2+}$ -selective ( $P_{\text{Ca}}/P_{\text{Na}} \sim 130$ ) member of the TRPV family, referred to as the gatekeeper of transepithelial  $\text{Ca}^{2+}$  transport.<sup>31,46,47</sup> The channel does not require voltage-dependent activation and is activated by PIP2. TRPV6 is primarily found in human and murine intestines, kidney, pancreas, prostate, testis, placenta and exocrine tissues.<sup>36,48</sup> It has been found that its expression is upregulated by  $1\alpha,25(\text{OH})_2\text{D}_3$ , the biologically active form of vitamin D.<sup>49,50</sup>

The biochemical mechanisms for controlling intracellular levels of  $\text{Ca}^{2+}$  due to TRPV6 constitutive activity is dependent on many factors. A fast-inactivation occurs by  $\text{Ca}^{2+}$  itself exerting a negative feedback mechanism on TRPV6 activity, mediated by the loop connecting S2 and S3 helices.<sup>51,52</sup> Secondly, in high intracellular concentration of  $\text{Ca}^{2+}$  (7 - 60  $\mu\text{M}$ ), a messenger protein named calmodulin (calcium-modulated protein, CaM) binds to it forming a complex ( $\text{Ca}^{2+}$ -CaM) that directly blocks the pore region of TRPV6 (**Figure 4**), inducing a closed conformation of the channel.<sup>53,54</sup> The high-affinity binding site for CaM ( $K_d \sim 65$  nM) is located in the C-terminal region, between residues 735-756. This region comprises the phosphorylation site of protein kinase C (PKC) at Thr742 that can prevent CaM-mediated inactivation.<sup>55</sup>

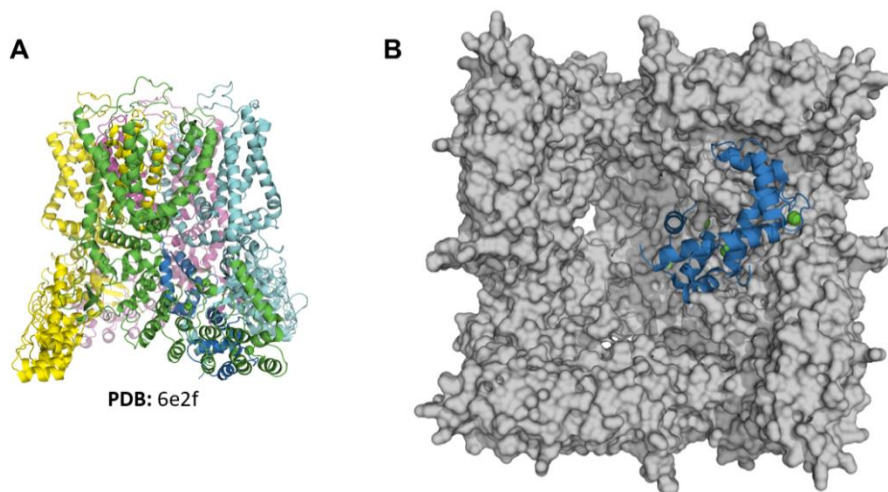


**Figure 4.** (A) Structure of *h*TRPV6 in the closed state bound to  $\text{Ca}^{2+}$ -CaM. (B) Bottom view of the TRPV6 shown as a light-gray surface. Proteins are depicted as cartoon and were colored as cyan, green, yellow, and magenta. CaM is depicted in dark-blue and  $\text{Ca}^{2+}$  atoms as green spheres.

A different mechanism of TRPV6 regulation involves the binding of PIP2 to their Lipid Binding Sites (**Figure 5**) conserved across the TRPV family. PIP2 activates TRPV6 channel which, in turn, induces negative feedback for channel closure by activating  $\text{Ca}^{2+}$ -sensitive phospholipase C isoform (PLC) which is able to hydrolyze PIP2.<sup>56,57</sup> Other TRP channels, such as TRPV1,<sup>58</sup> presents high affinity for PIP2 at the S4-S5 loop (LBS-2),

which interacts with a positively charged arginine residue. By mutating TRPV6 in order to present the same residue (R488G), the channel became insensitive to PIP2 hydrolysis and to  $\text{Ca}^{2+}$  fast inactivation.<sup>59</sup>

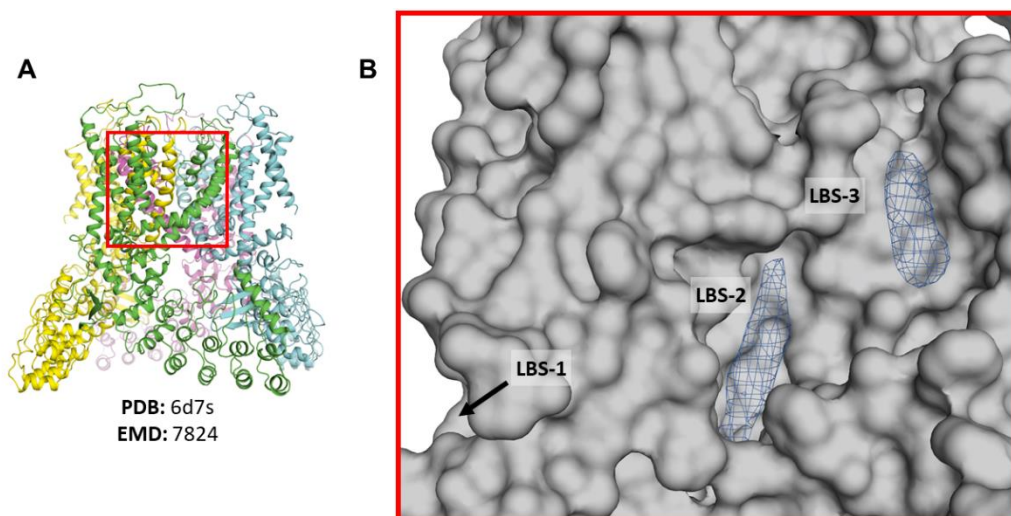


**Figure 5.** (A) Structure of apo-*h*TRPV6 in the open state. TRPV6 is depicted as a cartoon and was colored as cyan, green, yellow, and magenta. (B) Side view of to the highlighted region in (A) displaying the protein as light gray surface and the electron density maps of the putative lipids are shown as dark-blue mesh.

### 1.3.1 The role of TRPV6 in diseases

The current physiopathology establishes that TRPV6 might have an important contribution to multifactorial syndromes and tumors.<sup>55,60,61</sup> Several authors have described that TRPV6-deficient mice have diminished fertility, osteopenia and reduced body weight,<sup>48,62</sup> whilst human TRPV6 mutations, in which the channel was less functional, caused Transient Neonatal Hyperparathyroidism (TNH) and skeletal abnormalities.<sup>63,64</sup> In  $\text{Ca}^{2+}$  stone formers with idiopathic hypercalciuria, the polymorphism of TRPV6 results in increased  $\text{Ca}^{2+}$  transport and slower  $\text{Ca}^{2+}$ -inactivation.<sup>65</sup> These pathological findings are related to tissues in which TRPV6-expression at normal levels is essential for  $\text{Ca}^{2+}$  homeostasis.

On the other hand, TRPV6 expression was found abnormally upregulated in numerous human tumor tissues, especially in the prostate (mRNA and protein level).<sup>66</sup> Curiously, in normal prostate tissue the expression of TRPV6 is undetectable.<sup>67,68</sup> Also, when HEK cells were transfected with TRPV6, their proliferation rate was exacerbated compared to the wild-type.<sup>69</sup> In breast and prostate models overexpressing TRPV6 (respectively, T47D and LNCaP cells) the TRPV6 siRNA knockout decreased cell proliferation by 20 and 15%, respectively.<sup>70,71</sup> The involvement of TRPV6 on cell division appears to be organism-dependent, for instance, in a zebrafish model, inhibition of TRPV6 activates the IGF1R-PI3K-Akt signaling, increasing cell proliferation.<sup>72</sup> On the other hand, the pharmacological

block of *h*TRPV6 reduced prostate tumor growth by diminished NFAT activity.<sup>70,73</sup> These data suggest that the development of a tool compound able to strongly and selectively inhibit TRPV6 might facilitate the investigation of its cellular role.

### 1.3.2 TRPV6 modulation by small molecules

Since its discovery, several small molecules were found to be TRPV6 inhibitors (**Figure 6**). Econazole (ECN) and miconazole (MCN) were studied due to their unspecific inhibition of ion channels in non-excitabile cells, specially TRPV5.<sup>74,75</sup> Due to high homology with TRPV6 (75% of protein identity), both compounds also showed activity on TRPV6.<sup>76</sup> Compound TH-1177 was found in a screening of Ca<sup>2+</sup> current blockers<sup>77</sup> and further optimization yielded a more potent compound, named #3.<sup>78</sup> 2-aminoethoxydiphenyl borate (2-APB) is a small molecule able to modulate without specificity many TRP channels. For instance, 2-APB inhibits TRPV6,<sup>79</sup> TRPM2/7, and TRPC3/6/7,<sup>10,80,81</sup> and activates TRPA1, TRPM6, and TRPV1/2/3.<sup>82-84</sup>

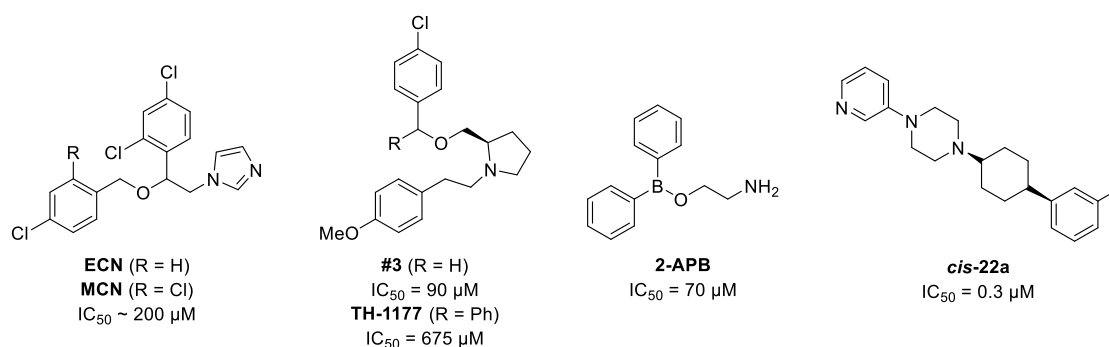


**Figure 6.** Chemical structure of TRPV6 modulators.

The first potent TRPV6 inhibitors were reported in 2015<sup>76</sup> using a ligand-based virtual screening workflow followed by chemical synthesis. The Structure-Activity Relationship (SAR) resulted in the discovery of the (*cis*-4-phenyl-cyclohexyl)piperazine as the pharmacophore for TRPV6 inhibition. This scaffold was subsequently optimized to improve potency resulting in compound *cis*-22a (**Figure 6**). *Cis*-22a demonstrated high potency in HEK-TRPV6 based assays (IC<sub>50</sub> = 0.3 μM) and selectivity over the TRP family. However, *cis*-22a only decreased the cell viability of an overexpressing-TRPV6 tumor cell line at high concentrations. Also, the compound inhibited other ion channels, such as *h*ERG, dopamine and muscarinic receptors, suggesting a major polypharmacology issue.<sup>85</sup>

## 1.4 Capsaicin (CPS)

Capsaicin is a natural secondary metabolite produced by plants of genus *Capsicum* widely known to induce a burning sensation after dietary consumption. The spiciest

peppers, such as jalapeño (*Capsicum annuum*), habanero (*C. chinense*), and tabasco (*C. frutescens*), possess high contents of CPS in its fruits.<sup>86–89</sup> The isolated compound possesses a large number of biological activities, such as analgesic,<sup>90,91</sup> anti-inflammatory,<sup>92</sup> insulin-secretion modulatory,<sup>93</sup> cardioprotective,<sup>94</sup> and anti-obesity.<sup>95,96</sup>

CPS has also shown high pro-apoptotic activity in more than 40 types of tumors, attracting the attention of many researchers as a promising drug candidate for cancer treatment.<sup>5,92,97–99</sup> Upon treatment with CPS, tumor cells reveal disrupted the mitochondrial membrane, increase in ROS generation, and caspase-3 and -9 activities.<sup>100</sup> *In vivo* mice models revealed that CPS was able to significantly reduce (>50%) tumor growth in breast and leukemic cancers without toxic effects.<sup>101,102</sup>

In our group, the replacement of the amide moiety for different chemical functions as well as the ring closure to the fused benzo[d][1,3]dioxole system, yielded weakly to moderate cytotoxic compounds (**Figure 7**).<sup>103–106</sup> Amongst them, compound RPF101 and RPF151 were able to induce cell cycle arrest, mitochondrial and microtubule disruption, and reduced tumor volume *in vivo*.<sup>105,106</sup>

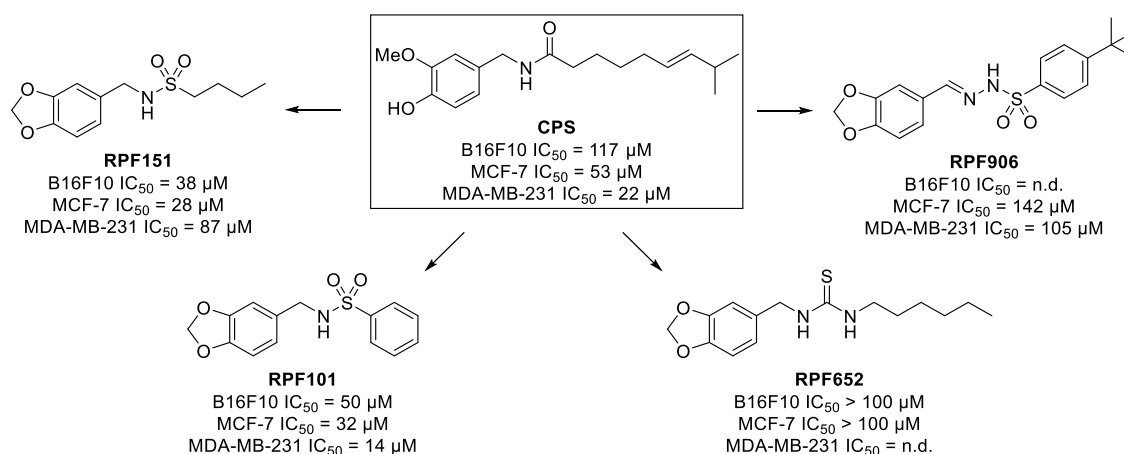


**Figure 7.** Antiproliferative activities of CPS and analogs developed in our group against tumor cell lines.

### 1.4.1 Capsaicin and TRPV channels

Despite the low structural resolution of CPS bound to TRPV1,<sup>107</sup> subsequent studies of mutagenesis, molecular docking, and dynamics allowed to elucidate the mode of interaction at the atomic level.<sup>108,109</sup> Due to its high lipophilicity, CPS is able to diffuse into the plasma membrane, reaching the vanilloid pocket of TRPV1 (analogous to the LBS-2) located at the interface of the protein-plasmatic membrane. The phosphatidylinositide cofactor is displaced by CPS which binds to TRPV1 through polar interactions of the vanillin ring and amidic linker with hydrophilic residues (Tyr511, Ser512, Thr550) located in S3 and S4 helices, at the bottom of the pocket. The hydrophobic chain of CPS is oriented towards the

top of the channel, interacting with a series of hydrophobic residues (**Figure 8**). Once bound to CPS, TRPV1 rearranges the S4-S5 linker, pulling the S6 helix away from the central axis of the channel ( $\sim 2$  Å), widening the selectivity filter, therefore increasing  $\text{Ca}^{+2}$  influx.<sup>107</sup> In sensory neurons the increase in  $\text{Ca}^{+2}$  transport results in propagation of the neuronal stimulus establishing the central perception of pain and burning.<sup>110</sup>

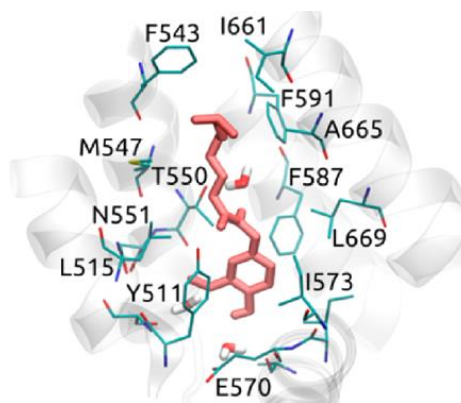


**Figure 8.** A computational model of CPS (light magenta sticks) bound to TRPV1.<sup>108</sup>

In addition to the high affinity for TRPV1, several studies have pinpointed that CPS might modulate TRPV6 activity in the prostate (LNCaP),<sup>111,112</sup> gastric (AGS),<sup>113</sup> and human small cell lung cancer (SCLC)<sup>114</sup> cells. Importantly, the pro-apoptotic stimulus was selective to the tumor cells compared to the non-tumoral in both studies. According to the authors, TRPV6 knockdown drastically reduced CPS pro-apoptotic activity in AGS and SCLC cells (>70%), while TRPV1 knockdown did not alter its activity. In human SCLC cells, the activation of TRPV6 by CPS triggered high intracellular  $\text{Ca}^{+2}$  levels followed by activation of calpain-1 and -2. This activation was significantly lower ( $\sim 50\%$ ) by TRPV6 knockdown. Calpains are  $\text{Ca}^{2+}$ -dependent cysteine proteases implicated in the cell cycle. Once activated, calpains are responsible for membrane degradation, leading to the collapse of cellular architecture and apoptosis.<sup>115</sup>

Despite the apparent activity of CPS on the TRPV6 receptor, it is noteworthy that none of the cited literature had conducted studies that prove the potency on the target. Furthermore, the development of capsaicinoid analogs with selectivity over TRPV6 has not been reported. Thus, the optimization of small molecules driven by the CPS scaffold with modulatory activity on TRPV6 is of high interest for the study of its pathophysiological function.

### 1.5 Rationality behind Drug Design

Drug discovery is a complex multidisciplinary area that pursues the development of effective and safe compounds, as drug candidates. The different modalities for compound generation can be categorized into main groups, such as serendipity;<sup>116</sup> natural products;<sup>117</sup> chemical synthesis and High Throughput Screening (HTS);<sup>118</sup> and more recently, computer-assisted drug discovery.<sup>119</sup> Once biologically tested, medicinal chemists often seek for those active compounds that can be optimized.<sup>120,121</sup>

There are two drug design strategies for compound optimization which have been widely used in academia and industry. Their rationality resides either in the structural data of the target protein (SBDD) or in bioactive compounds (LBDD).<sup>122</sup> If this data is available for both strategies, it might be combined to increase the chance of obtaining compounds with optimized biological activity (**Figure 9**).<sup>123</sup> It is worth noting that the use of computational techniques through the Computer-Assisted Drug Design (CADD) permeate the current drug discovery process and, has been exponentially used.<sup>124,125</sup>

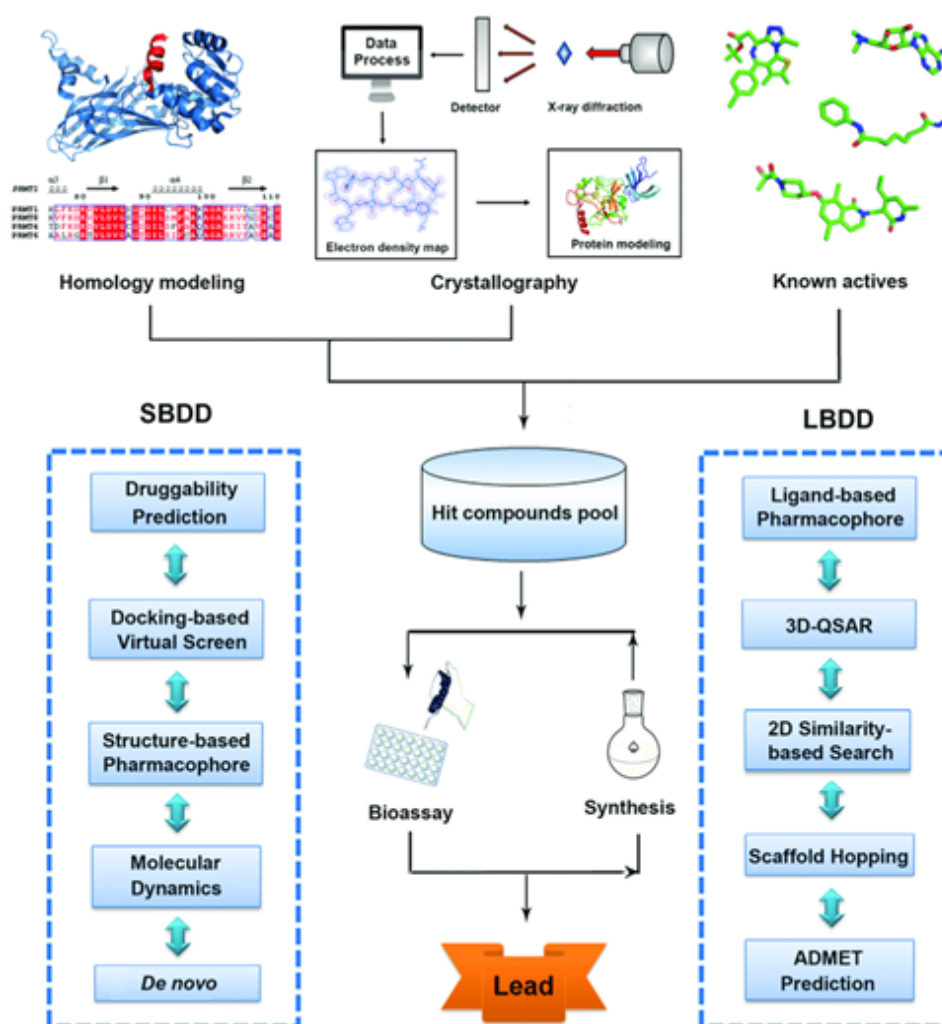


**Figure 9.** The workflow of SBDD and LBDD in drug discovery. Adapted from Lu and colleagues, 2018.<sup>126</sup>

The Structure-Based Drug Design (SBDD) uses the three-dimensional data of target proteins.<sup>127</sup> The field has been dramatically changed due to technological advances in computer science and structural biology, especially with the advent of cryo-EM.<sup>128</sup> If the target structure is not known, its conformation and spatial arrangement can be determined by methods existing in CADD.<sup>129–131</sup> With the structural data of the target, it is possible to determine the mode of interaction of the bioactive compounds, as well as to characterize the interactions between them. The most frequently used SBDD methods for such study are Molecular Docking, Molecular Dynamics (MD) and Structure-Based Virtual Screening (SBVS).<sup>132</sup> These methods allow the design and optimization of compounds with precise shape-complementarity with the target protein, leading to modulation of its activity and the desired pharmacological effects.<sup>133</sup>

The Ligand-Based Drug Design (LBDD) strategy is used when there is no structural data of the target protein, but the biological activity of a set of compounds is known. Thus, the physicochemical, electronic, steric and topological properties of this set are computed and correlated for the proposition of pharmacodynamically optimized molecules.<sup>123,134</sup> Based on the pharmacophore of the prototype, molecular modifications are proposed in order to confer similar interactions with the target as those expected for the original compound.<sup>135</sup>

Molecular modifications guide the development of new compounds and can be employed either in LBDD or SBDD, as the aim is to provide better compound complementarity with the target, therefore enhanced activity.<sup>136</sup> Among the various molecular modifications that exist in medicinal chemistry, this work was based particularly on two of them, namely bioisosterism and molecular hybridization.

Bioisosterism is one of the most important tools in medicinal chemistry to rationally modify an atom or functional groups by others that exhibit “*near-equal molecular shapes and volumes, approximately the same distribution of electrons, and which exhibit similar physical properties...*”<sup>137</sup> to give the new compound beneficial changes in pharmacokinetic and dynamic parameters.<sup>136,138</sup> Bioisosteres can be classified into two main categories: classical, and non-classical. The first category comprises atoms or functional groups that have the same valence, or equivalent rings; the second comprises isosteres that do not completely fulfill the steric and electronic definitions of the previous category.<sup>139</sup> Currently, computer-based approaches are also employed in order to prioritize the best bioisosteric replacements for correct modulation of potency and lipophilicity.<sup>140–142</sup>

A massive synthetic effort has been made to produce capsaicin-related compounds as TRPV1-mediated analgesic drugs. The strategy for compound generation essentially involved hundreds of bioisosteric replacements of the vanilil ring (Region A),<sup>143</sup> amide linker (region B),<sup>143</sup> and the alkyl tail (Region C).<sup>144</sup> With the SAR of each region of the molecule, the authors reached a conclusion that in terms of TRPV1 activation the vanilil moiety is crucial; the bioisosteric replacement of the linker by the urea or thiourea is largely beneficial; and the hydrophobicity in the side chain is clearly important.<sup>145</sup> Noteworthy, the authors reached a very approximate conclusion of the mode of interaction of CPS with TRPV1 without previous crystallographic data or computer models of TRPV1. From their work, other widely important compounds for the TRPV1 study were developed and further optimized for *in vivo* profiling, such as the antagonist capsazepine (CPZ)<sup>146</sup> and the non-pungent agonist, SDZ 249-665<sup>147</sup> (**Figure 10**).

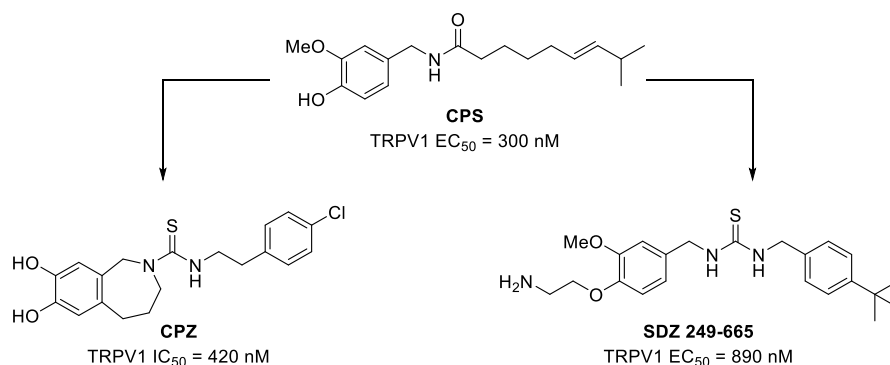


**Figure 10.** An example highlighting how the bioisosteric replacements of CPS led to the discovery of potent TRPV1 modulators.

Molecular hybridization consists of the rationale strategy of merging two or more pharmacophores, aiming to obtain a new chemical entity, referred to as a hybrid compound, which would avoid molecular redundancy in drug discovery campaigns.<sup>148</sup> Ideally, the hybrid would present either an optimized affinity towards the target of interest or the capability to modulate the original targets associated with the prototypes.<sup>149</sup>

The study of *Cannabis sativa* neuroactive metabolites led to the discovery of the endocannabinoid system (cannabinoid receptors, CB<sub>1</sub> and CB<sub>2</sub>).<sup>150</sup> Surprisingly, several endocannabinoid ligands, such as anandamide (N-arachidonoyl ethanolamide, AEA), were found to also activate TRPV1.<sup>151,152</sup> The structures of CPS and AEA can be overlapped (**Figure 11**) to construct, through the molecular hybridization process, hybrids that target TRPV1/CB<sub>1</sub>, such as arvanil, with pronounced analgesic activity *in vivo*.<sup>153,154</sup> Although CPS is inactive against CB receptors<sup>155</sup> and AEA has comparable activities against TRPV1 and CB<sub>1</sub>,<sup>156</sup> the molecular hybridization process was able to enhance in 52-fold and 1260-

fold the activity towards TRPV1 (comparing to CPS and AEA, respectively) and decreased CB<sub>1</sub> potency.<sup>157</sup>

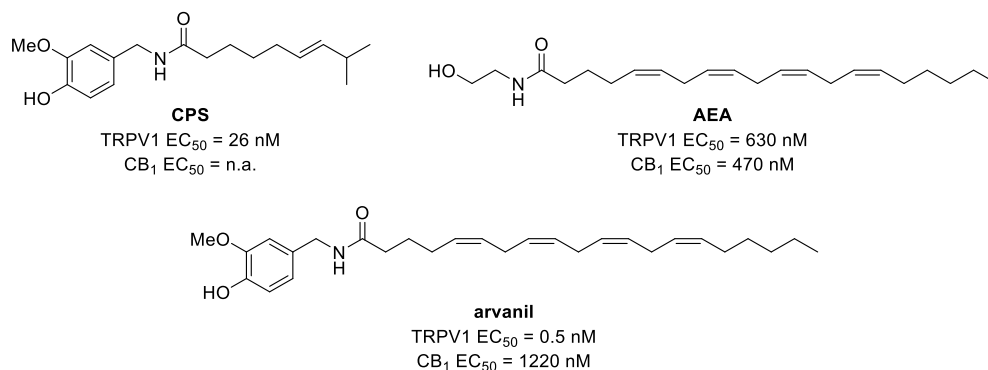


**Figure 11.** Chemical structures of CPS and AEA highlighting the pharmacophore used on the design of arvanil.

Although CPS has a large spectrum of targets *in vivo*,<sup>158,159</sup> the examples from the literature of bioisosterism and molecular hybridization illustrate that through different medicinal chemistry approaches its framework can be modified to achieve selective and optimized compounds.

### 1.5.1 Design of bioisosteric and hybrid capsaicinoids

Based on literature reports of CPS activity on TRPV6,<sup>113,114</sup> we decided to have a proof of concept if CPS itself, as well as new capsaicinoids, could modulate TRPV6 ion transport (**Figure 12A**). Several bioisosteric groups, such as sulfonylhydrazone, N-acyl hydrazone, and sulfonylglycine hydrazones were used to replace the amide found in CPS.<sup>160,161</sup> These substitutions should be able to balance the physicochemical properties of the compounds, especially by offering hydrogen bonding interactions with the target. The literature also reports that reducing the methylene units in the CPS hydrophobic tail decreased its affinity towards TRPV1.<sup>162</sup> Therefore, we expected that smaller n-alkyl groups would mimic the lipophilic chain but reduce TRPV1 affinity (**Figure 12B**). We also generated benzo[d][1,3]dioxole versions of the bioisosteric capsaicinoids based on the ring cyclization of the vanilloid moiety, as described for related analogs in our group (**Figure 12C**).<sup>103,105,106,163,164</sup>

In our second approach, the overlapping pharmacophores of CPS and *cis*-22a were combined into a hybrid compound. The use of *cis*-22a was based on its similarity with CPS, an aromatic region (in blue) linked to a hydrophobic moiety (in green) by an amide bioisoster (in red). The essential *cis*-cyclohexyl-piperazine moiety was maintained due to its high activity on TRPV6. In order to confer a more CPS-like compound, a carbonyl was appended at the piperazine. Finally, we intended to analyze the influence of the size and

lipophilicity of this region by attaching different commercially available cyclohexanones (Figure 12D).

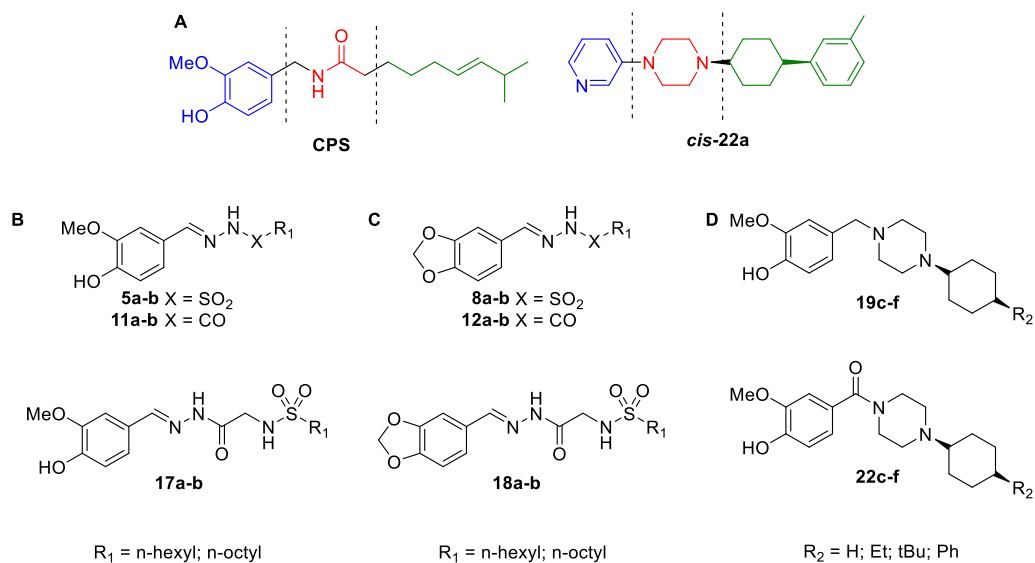


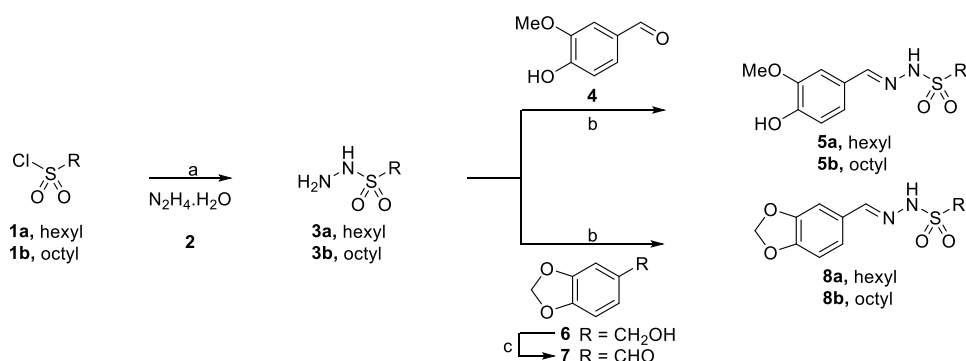
**Figure 12.** (A) Structure of the CPS and *cis-22a* used to design bisosteric (B and C) and hybrid capsaicinoids (D).

## 2. Results and Discussion

### 2.1 Synthesis of bioisosteric capsaicinoids

The synthesis of bioisosteric capsaicinoids was divided into three synthetic routes depicted in **Scheme 1-3**, according to the bioisosteric replacement of CPS amide. The reaction of sulfonyl chlorides (**1a-b**) with hydrazine hydrate (**2**) led to the sulfonyl hydrazide intermediates **3a-b**, which were subsequently condensed with vanillin (**4**) to form the desired sulfonyl hydrazones **5a-b**.<sup>165</sup> For the benzo[d][1,3]dioxole derivatives, the piperonyl alcohol (**6**) was subjected to mild oxidation to the correspondent aldehyde (**7**),<sup>166,167</sup> then was condensed with **3a-b** to yield the derivatives **8a-b**.

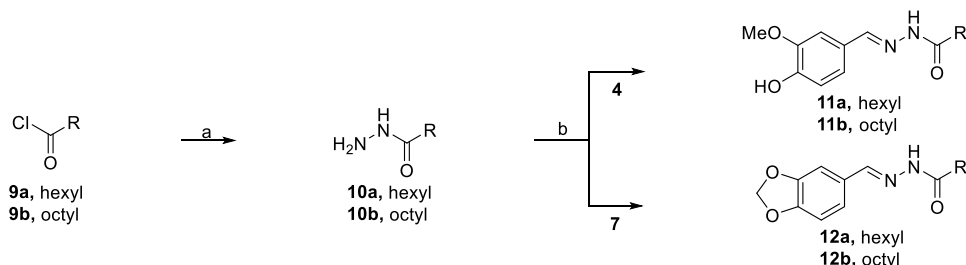
**Scheme 1.** Synthetic route of sulfonylhydrazones **5a-b** and **8a-b**.<sup>a</sup>



<sup>a</sup>Reagents and conditions. (a) **2**, THF, 0 °C to r.t., 2 h (60-82 %); (b) **4**, MeOH, rf., 2 h (89-93 %); (c) MnO<sub>2</sub>, CH<sub>2</sub>Cl<sub>2</sub>, r.t., 4 h (73 %).

The N-acyl hydrazones (**Scheme 2**) were similarly prepared by reacting the appropriate acyl chlorides **9a-b** with **2**. The intermediates **10a-b** were directly used in the next step of condensation with **4** or **7** to yield **11a-b** and **12a-b**.<sup>168</sup>

**Scheme 2.** Synthetic route of N-acyl hydrazones **11a-b** and **12a-b**.<sup>a</sup>

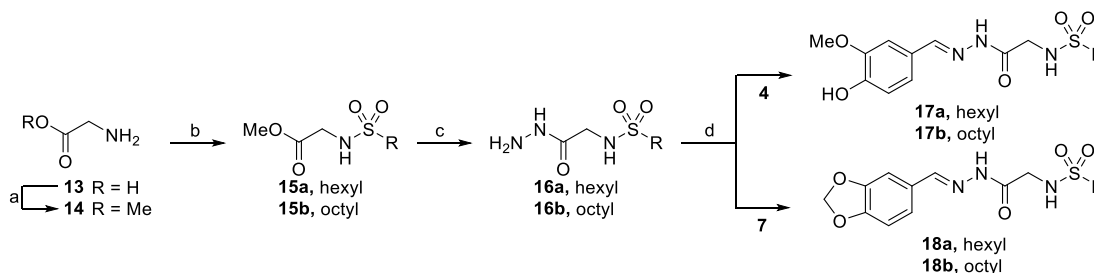


<sup>a</sup>Reagents and conditions. (a) **2**, CH<sub>2</sub>Cl<sub>2</sub>, 0 °C to r.t., 2 h; (b) **4** or **7**, EtOH, AcOH (cat.), r.t., 2 h (25-31 %, over 2-steps).

The third series of bioisosteric capsaicinoids is referred to as sulfonylglycine hydrazones (**Scheme 3**). We envisaged using this group as a peptide-mimetic structure seeking to increase the water solubility of the analogs and to improve the binding to the protein via

hydrogen bonds. The synthesis started with the methyl esterification of glycine (**13**) to generate the intermediate **14**, which reacted with **1a-b** to generate the sulfonamide intermediates **15a-b**. Then, hydrazinolysis of the methyl ester by **2** afforded **16a-b**, which were further condensed with **4** or **7** to give the desired compounds **17a-b** and **18a-b**.<sup>169,170</sup>

**Scheme 3.** Synthetic route of sulfonylglycine hydrazones **17a-b** and **18a-b**.<sup>a</sup>



<sup>a</sup>Reagents and conditions. (a)  $\text{SOCl}_2$ , MeOH, rf., 12 h (63 %); (b) **1a-b**,  $\text{Et}_3\text{N}$ ,  $\text{CH}_2\text{Cl}_2$ , 0 °C to r.t., 6 h (45-52 %); (c) **2**, MeOH, r.t., 3 h (75-99 %); (d) **4** or **7**, EtOH, AcOH (cat.), r.t., 24 h (87-89 %).

Once the main functional group in this thesis derived from an imine bond formation ( $\text{N}=\text{CH}$ ), the mechanism can be generalized to all the bioisosteric capsaicinoids (**Figure 13**). In Step I, a nucleophilic attack occurs between the primary amine present of **2** or **14** to either sulfonyl (**1a-b**) or acyl chlorides (**9a-b**), eliminating HCl. Then, in Step II, the activated aldehyde (**4** or **7**) is subjected to an addition to the carbonyl by the primary amine of hydrazide (**3a-b**; **10a-b**; **16a-b**), which after proton transferring, eliminates  $\text{H}_3\text{O}^+$  and forms the hydrazone.<sup>165</sup>

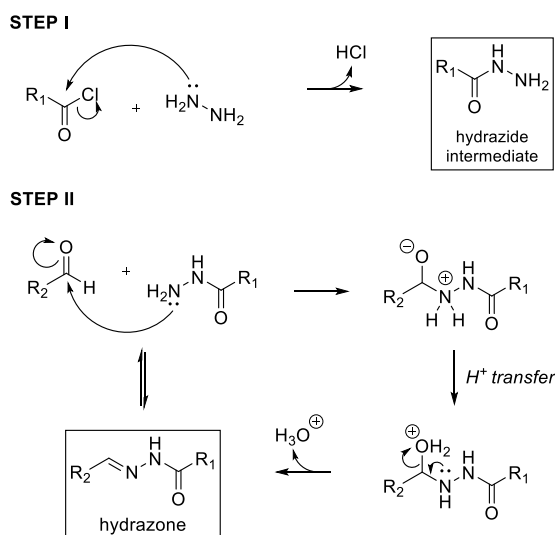


**Figure 13.** General routes for the synthesis of substituted hydrazones. Note that for sulfonyl hydrazones and sulfonylglycine hydrazones instead of an amide the compounds present a sulfonamide moiety.

The literature establishes N-acyl or sulfonyl hydrazones may exist as  $\text{C}=\text{N}$  double bond stereoisomers (*E/Z*), and as syn/anti-periplanar conformers of the amide  $\text{CO-NH}$  or

sulfonamide SO<sub>2</sub>-NH bonds.<sup>171,172</sup> We observed that the *E*-isomer was preferably formed during synthesis, once this isomer is less hindered and thermodynamically more stable.<sup>173</sup> This was particularly clear for sulfonyl hydrazones which <sup>1</sup>H-NMR revealed a single isomer, as reported in the literature.<sup>174,175</sup> During the synthesis of other sulfonyl hydrazones, our group was able to demonstrate by X-ray crystallography, that these compounds adopt a stable *E* and antiperiplanar configuration (**Figure 14**).<sup>165</sup> It is worth noting that the selective synthesis of *Z*-sulfonyl hydrazones was already described depending on the reaction conditions and proper aldehyde-substitutions.<sup>176–178</sup>

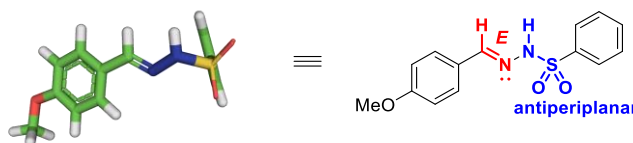


**Figure 14.** Crystal structure of a sulfonylhydrazone revealing its *E*-antiperiplanar stereochemistry.<sup>165</sup>

N-acyl hydrazones and sulfonyl-glycine hydrazones presented conformers that could be identified by 1D-<sup>1</sup>H-NMR and 2D-COSY in DMSO-*d*<sub>6</sub> at various temperatures. As illustrated for compound **12b** (**Figure 15**), the duplicated signals presented a total coalescence, with an exception for the N=CH proton at 8.38 ppm (partial coalescence). This effect was reverted by cooling the sample down to the room temperature (30 °C) (**Figure 16**). Upon heating, the gain in energy would overcome the rotational barrier favoring the fast conversion between amide conformers.<sup>171</sup>

The current photochemical literature of N-acyl hydrazones establishes that the thermodynamically stable *E*-conformer can be switched to the *Z*-conformer under UV-light irradiation, a behavior very characteristic of azobenzenes (N=N).<sup>179</sup> *Z*-conformers should return to the stable *E*-conformation under heating or progressive back-isomerization at room temperature.<sup>180,181</sup> Therefore, we assume that only the *E*-conformer was formed and the duplicated signal is due to the presence of a syn- and antiperiplanar mixture. Moreover, the HPLC spectra of N-acyl hydrazones and sulfonyl-glycine hydrazones attest the presence of a single conformer.<sup>173</sup>

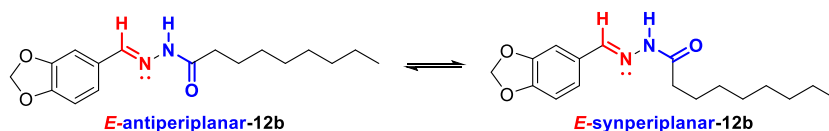


**Figure 15.** Possible conformers of E-**12b**.

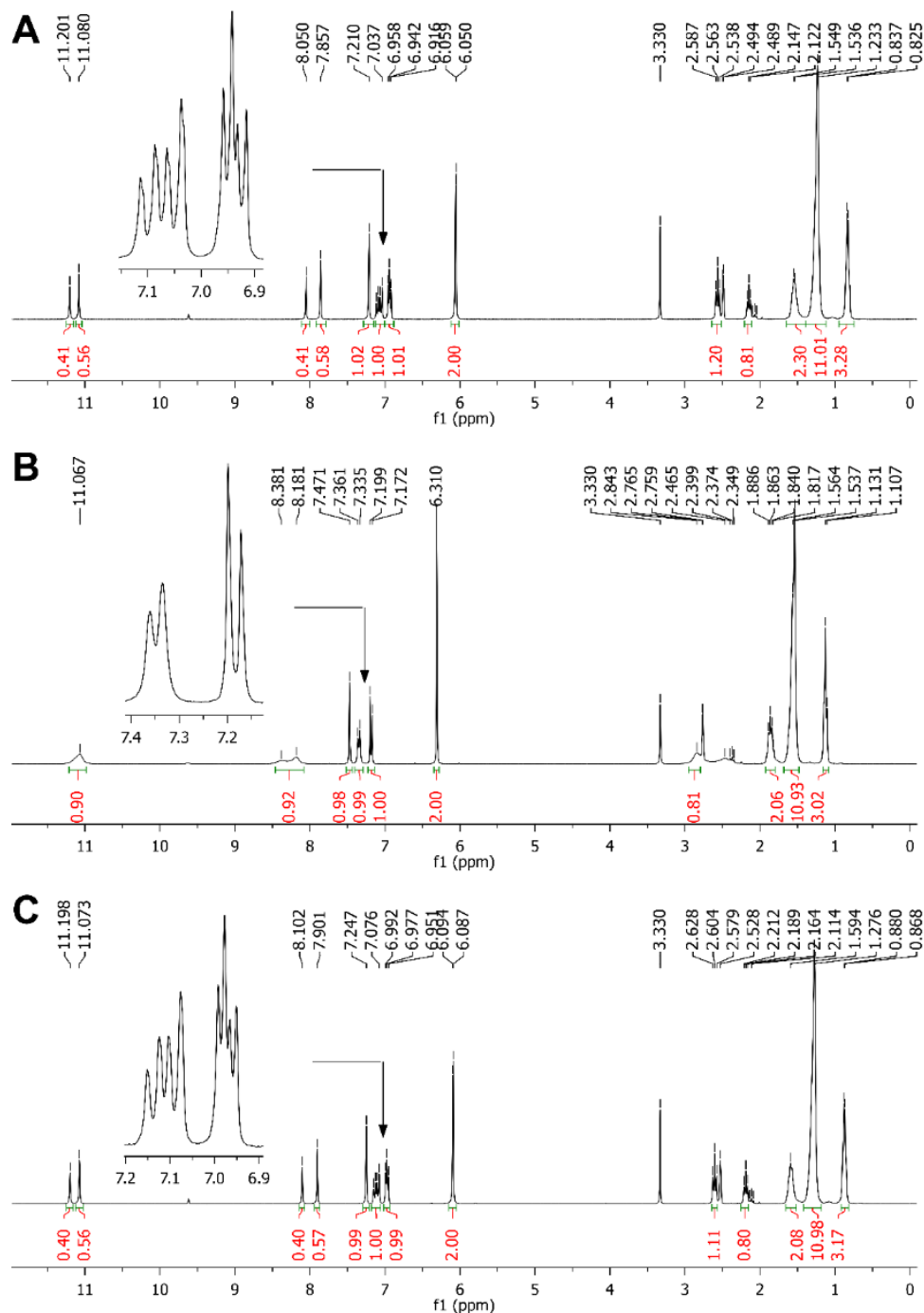


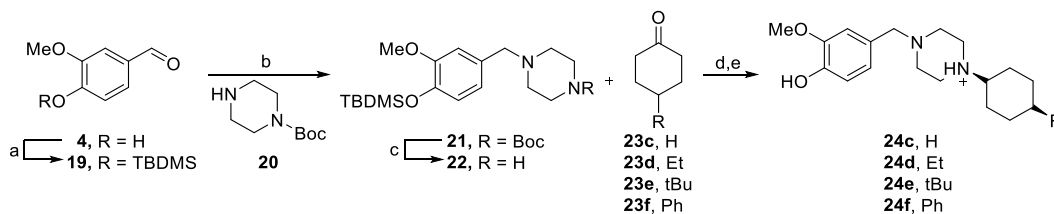
**Figure 16.**  $^1\text{H-NMR}$  spectra of compound **12b** at 20 °C (A), 75 °C (B) and cooled to 30 °C (C).

## 2.2 Synthesis of hybrid capsaicinoids

The synthetic routes for the hybrid capsaicinoids are illustrated in **Schemes 4** and **5**. Analogs **24c–f** were prepared by first converting **4** into the corresponding TBDMS-vanillin intermediate **19**, followed by reductive amination with Boc-piperazine (**20**) to generate **21**, and Boc removal to the free piperazine **22**, as described before.<sup>76,179</sup> Then, a second reductive amination of the free nitrogen of the piperazine was performed with different

cyclohexanones (**23c-f**) followed by phenol-deprotection with tetrabutylammonium fluoride (TBAF) to give the desired compounds **24c-f**.

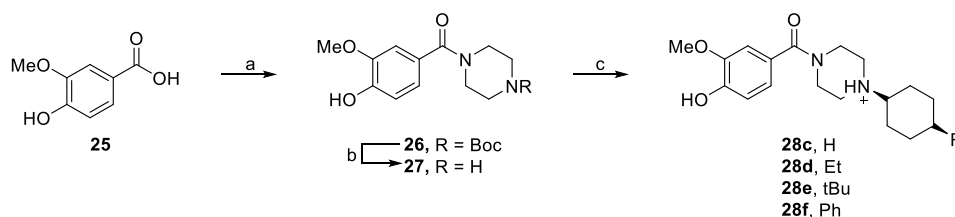
**Scheme 4.** Synthetic route of compounds **24c-f**.<sup>a</sup>



<sup>a</sup>Reagents and conditions. (a) TBDMSCl, DMAP, Imidazole, DCM, r.t., 2 h (quant.); (b) **20**, AcOH, NaBH(OAc)<sub>3</sub>, DCE, r.t., 48 h; (c) TFA, DCM, r.t., 1 h (45 %, over 2-steps); (d) **23c-f**, NaBH(OAc)<sub>3</sub>, Et<sub>3</sub>N, DCE, r.t., 48 h; (e) TBAF, THF, r.t., 3 h (30-59 %, over 2-steps).

Analogs **28c-f** were obtained from the vanillic acid (**25**) by coupling it with **20** under standard Steglich esterification conditions<sup>182</sup> to generate the acyl-piperazine-intermediate **26**, followed by the described procedures of Boc removal to afford **27** and reductive amination with **23c-f**.

**Scheme 5.** Synthetic route of compounds **28c-f**.<sup>a</sup>



<sup>a</sup>Reagents and conditions. (a) **20**, EDCI, DMAP, CH<sub>2</sub>Cl<sub>2</sub>, r.t., on; (b) TFA, DCM, r.t., 1 h, (60 %, over 2-steps); (c) **23c-f**, NaBH(OAc)<sub>3</sub>, Et<sub>3</sub>N, DCE, r.t., 48 h (21-31 %, over 2-steps).

The pharmacophore of the TRPV6 inhibitors must have *cis*-orientation, therefore we did not isolate the *trans*-counterparts. In all cases, the *cis*-1,4-cyclohexyl diastereoisomer was isolated either by column chromatography or RP-HPLC, and the *cis*-isomer consistently eluting before the *trans*-counterpart. All compounds obtained as free-bases were precipitated as dihydrochloride salts.

The synthesis of di-substituted cyclohexanones by reductive amination is known to afford two diastereoisomers.<sup>76,179</sup> In general, by analysis of the crude (TLC and HPLC), the *cis*-isomer was majority formed. According to several authors, the bulky reagent NaBH(OAc)<sub>3</sub> preferably attack the less hindered side of the intermediate iminium ion, favoring the *cis*-isomer.<sup>183</sup> To unambiguously determine the stereoconfiguration of the isolated compounds we carried out <sup>1</sup>H- and <sup>13</sup>C-NMR analysis associated with X-ray crystallography.

**Figure 17** below, illustrates that in  $C_6D_6$ , the ArCH and NCH of the *cis*-isomer (black line) commonly split into a triplet of triples of 1H around 2.52 ppm ( $J = 3.7, 11.1$  Hz) and a broad multiplet of 1H that resembles a pentet around 2.11 ppm. On the other hand, the *trans*-counterpart presented two triplets of triples superimposed as a multiplet of 2H around 2.22 ppm. The differences in  $^{13}C$ -NMR are pronounced due to the chemical shift that occurred of the CH carbon at 58.8 ppm (*cis*) to 63.3 ppm (*trans*).

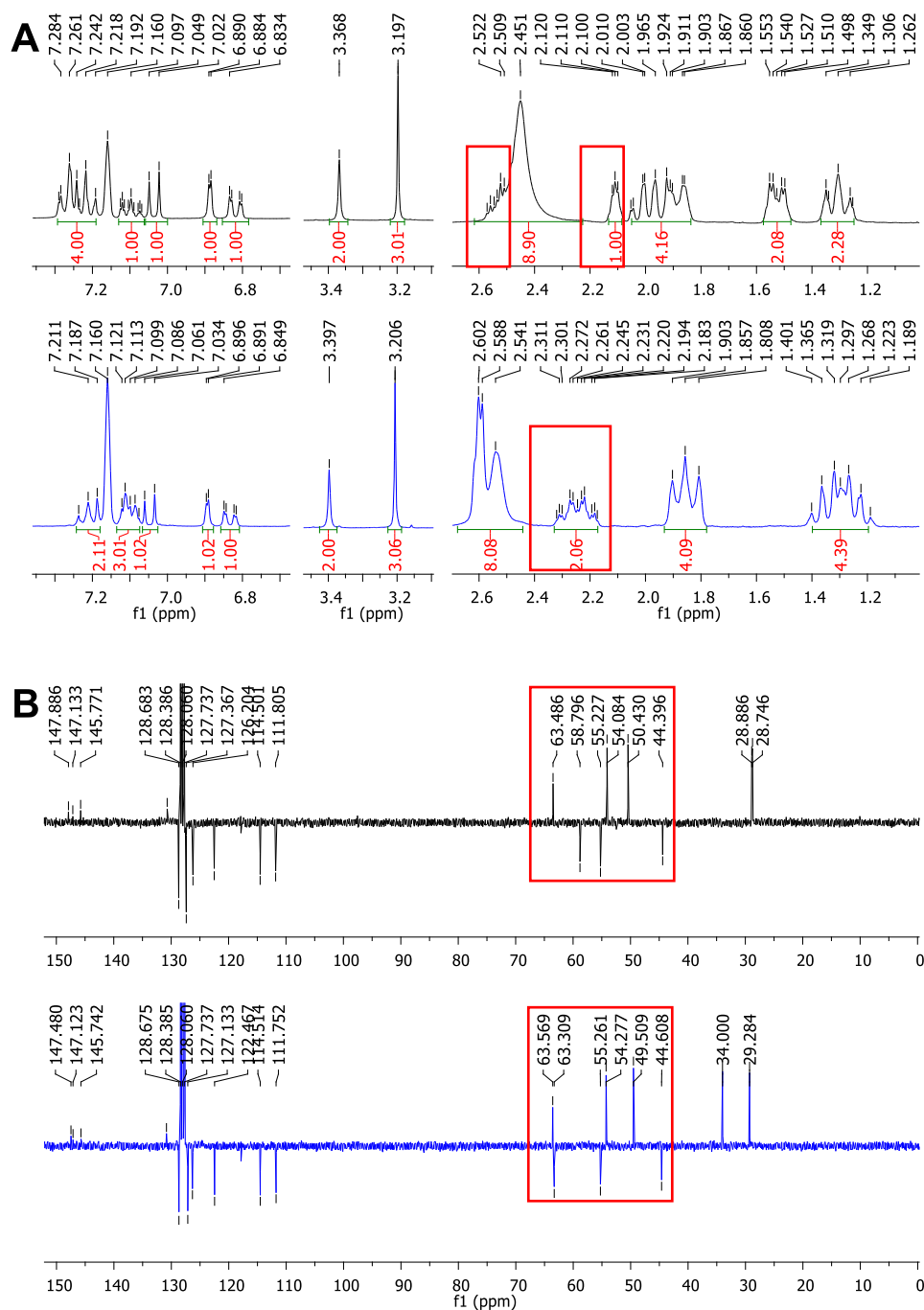


**Figure 17.**  $^1H$ -NMR (A) and  $^{13}C$ -NMR (B) spectra of compound *cis*-24f (black line) and *trans*-24f (blue line).

The structure of *cis*-**24f** was confirmed by X-ray crystallography which showed that the piperazine was equatorial and the phenyl substituents were axial relative to the cyclohexane ring (**Figure 18**).



**Figure 18.** Crystal structure of compound *cis*-**24f**.

### 2.3 TRPV6 $\text{Cd}^{2+}$ assay for screening of compounds

The obtained capsaicinoids from both approaches were subjected to a fluorescent assay<sup>76</sup> by means of cadmium ( $\text{Cd}^{2+}$ ) uptake into HEK293 cells stably overexpressing human TRPV6 (HEK-*h*TRPV6) (**Figure 19**).

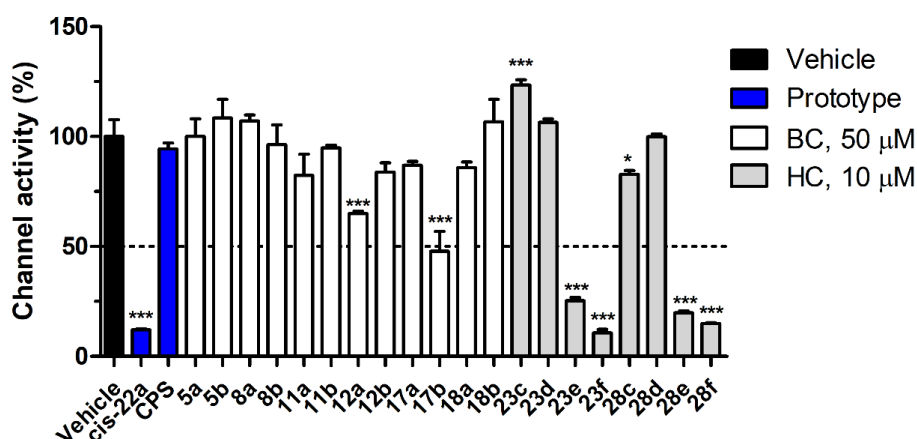


**Figure 19.**  $\text{Cd}^{2+}$  (50.0  $\mu\text{M}$ ) influx into HEK293-*h*TRPV6 cells. Data were normalized to the maximum entry in the vehicle group (buffer/DMSO). BC = bioisosteric capsaicinoids; HC = hybrid capsaicinoids. One-way ANOVA, Bonferroni's post-test. \* $P < 0.05$ ; \*\*\* $P < 0.001$ . Data shown are mean + SEM ( $n = 3$  or 6).

As illustrated in **Table 1**, compounds derived from the hybrid-capsaicinoids bearing a *tert*-butyl (**23e** and **28e**) or phenyl (**23f** and **28f**) at the *cis*-cyclohexyl ring revealed promising activity, whilst the remaining compounds were inactive. Intriguingly CPS was found to be ineffective to induce changes in TRPV6 activity, in accordance with a recent publication.<sup>164</sup> Once the active compounds were found by merging the scaffolds of CPS and *cis*-22a, these compounds were also tested against HEK cell transiently transfected with TRPV1.<sup>164</sup> By stimulating the channel with 100 nM of CPS, it was observed that at 10  $\mu\text{M}$ , compound **23e**, **23f**, and **28f** inhibited TRPV1  $\text{Cd}^{2+}$  influx between 27 to 81 %.

Ligand metrics, such as Ligand Efficiency (LE) and Lipophilic Ligand Efficiency (LLE), are defined as a normalized way of comparing and selecting compounds with a

range of activities, molecular weight, and lipophilicity for lead-optimization.<sup>184</sup> The optimal values for a drug candidate should be  $>0.4$  and  $>4.0$  for LE and LLE, respectively.<sup>185</sup> In terms of ligand metrics, the active compounds found in this screening were still far from the optimal values, especially when compared to *cis*-22a. Taken all these results together, a series of hit-optimizations was conducted aiming to increase the potency towards TRPV6 and enhance the ligand metrics.

**Table 1.** TRPV Activity of active capsaicinoids.<sup>a</sup>

Cpd	Structure	TRPV6 IC <sub>50</sub> (nM) <sup>b</sup>	TRPV1 % Inh <sup>d</sup>	LE <sup>e</sup>	LLE <sup>f</sup>
<i>cis</i> -22a		50 ± 3 <sup>c</sup>	16	0.40	2.7
23e		2383	81	0.30	-0.1
23f		1566	60	0.28	0.5
28e		2090	-5	0.29	0.6
28f		428	27	0.30	1.7

<sup>a</sup>Active compounds were defined as able to inhibit at least 50% of TRPV6 activity. Data shown are mean ± SEM ( $n = 6$ /concentration) of a single<sup>b</sup> or at least two<sup>c</sup> independent experiments. <sup>d</sup>Compounds were tested at 10 μM against a stimulus of 100 nM of CPS. Data shown is mean ( $n = 2$ ) of a single experiment. <sup>e</sup>LE: Ligand Efficiency =  $1.37 \times \text{pIC}_{50} / \text{number of heavy atoms}$ ; <sup>f</sup>LLE: Lipophilic Ligand Efficiency =  $\text{pIC}_{50} - \text{cLogP}_{\text{ow}}$ . Based on mean oral drug values that provide the acceptable values for drug candidates, LE and LLE should ideally be above 0.4 and 4.0, respectively.<sup>185</sup>

## 2.4 Hit optimization

Previously it was identified that the benzylic substitution of the second nitrogen of the piperazine for a *meta*-substituted pyridine is important for potent TRPV6 inhibition.<sup>76</sup> A recent publication also demonstrated that substitution at *para*-position of the pyridine with an azobenzene afforded compounds with potency in the low μM range.<sup>179</sup> The *para*-position appears to be a hot-spot for polar substituents, hence, we envisaged to attach a *para*-phenol, present in the vanillyl ring of the active compounds **24c-f** and **28c-f**, to the *meta*-substituted pyridine aiming to improve the binding affinities of the compounds to the protein. It is important to note that this group is stably found as the 3-pyridone (**Figure 20**).

Analogues containing the 3-pyridone **32e-f** and **36e-f** were obtained using the same reactions described before, respectively using 6-hydroxynicotinaldehyde (**29**) and 6-hydroxynicotinic acid (**33**, **Scheme 6**).

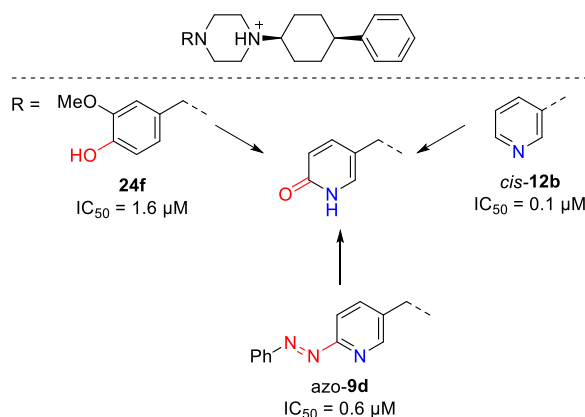
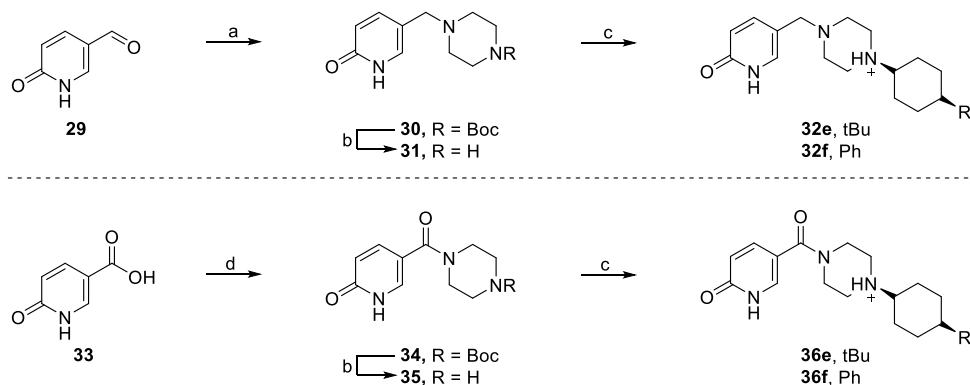


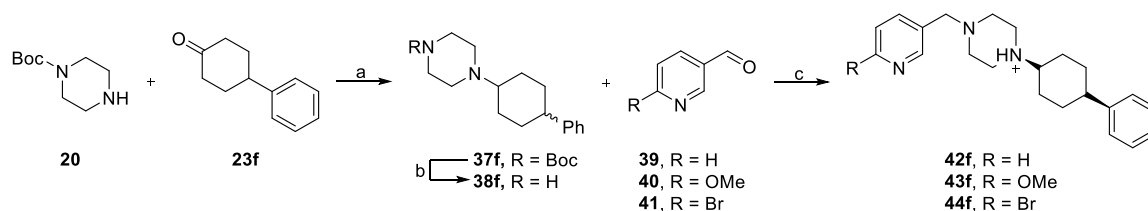
**Figure 20.** Design of the 3-pyridones from compound **24f** and literature compounds *cis*-**12b**<sup>76</sup> and azo-**9d**.<sup>179</sup>

**Scheme 6.** Synthetic route of 3-pyridones **32e-f** and **36e-f**.<sup>a</sup>



<sup>a</sup>Reagents and conditions. (a) **20**, AcOH, NaBH(OAc)<sub>3</sub>, DCE, r.t., 48 h; (b) TFA, DCM, r.t., 1 h (70-78 %, over 2-steps); (c) **23e-f**, NaBH(OAc)<sub>3</sub>, Et<sub>3</sub>N, DCE, r.t., 48 h (6-45 %); (d) **20**, EDCl, DMAP, CH<sub>2</sub>Cl<sub>2</sub>, r.t., on.

The replacement of the vanillin ring with 3-pyridone led to a 4-fold improvement in TRPV6 inhibitory potency of compound **32f** ( $IC_{50} = 373$  nM, **Table 2**). Compounds **32e** and **36f** showed the same activity of their vanilloid pairs, while compound **36e** was inactive. Notably, the replacement significantly improved the LLE of **32f** compared to its pair **24f** (3.0 and 0.5, respectively). To determine the influence of the pyridone moiety on TRPV6 inhibition, we prepared analogs of the hit **32f** by first coupling **20** to **23f** under reductive amination conditions, followed by Boc-removal of **37f** to the free piperazine **38f** (**Scheme 7**). Then, the piperazine reacted with the commercially available pyridine-carboxaldehyde (**39-41**) to generate the desired compounds **42f-44f**.

**Scheme 7.** Synthetic route of pyridine substituted analogues of **32f**.<sup>a</sup>

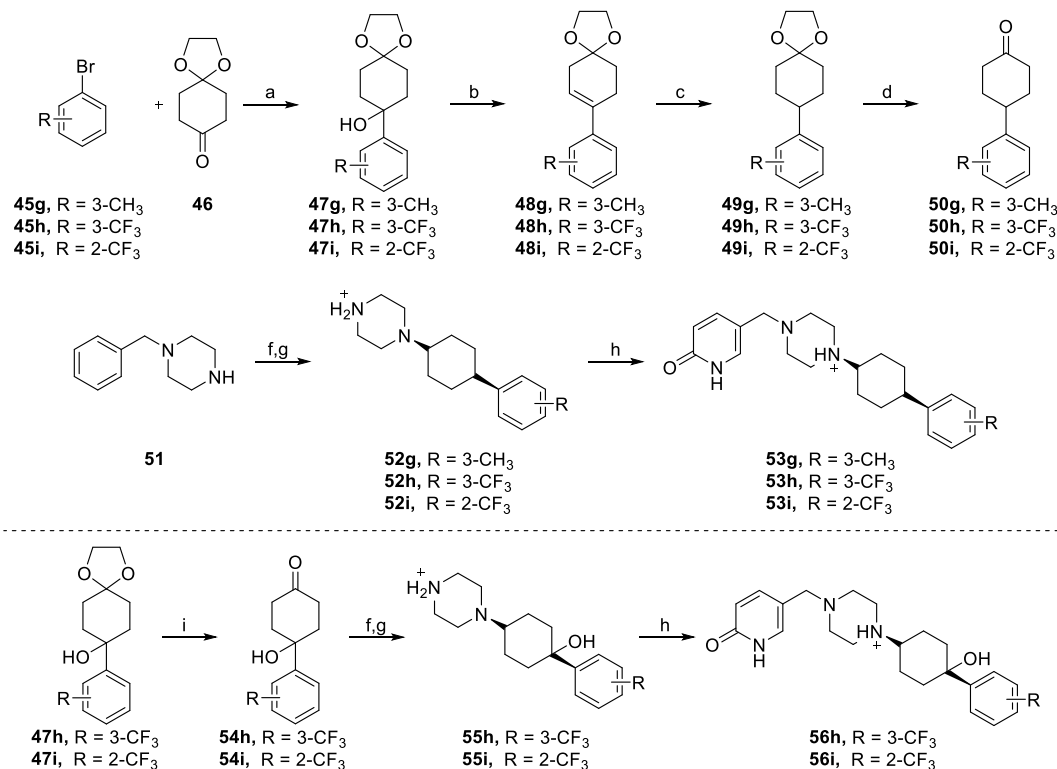
<sup>a</sup>Reagents and conditions. (a) AcOH, NaBH(OAc)<sub>3</sub>, DCE, r.t., 48 h; (b) HCl, H<sub>2</sub>O, rf., 90 min (88 %, over 2-steps); (c) AcOH, NaBH(OAc)<sub>3</sub>, DCE, r.t., 48 h (43-68 %).

The removal of the pyridone carbonyl in **32f** resulted in a slight decrease in potency for compounds **42f** and **43f** ( $IC_{50} \approx 550$  nM, **Table 2**). On the other hand, the substitution of the carbonyl by 4-Bromo (**44f**) resulted in a 2-fold increase in potency against TRPV6 ( $IC_{50} = 172$  nM), suggesting that a halogen bound<sup>186</sup> might stabilize the complex ligand-protein. The LE of compounds **42f-44f** ranged from 0.32 to 0.36 as observed for the hit compound **32f**. In spite of that, LLE was remarkably reduced (<2.0), meaning that removal of the pyridone-carbonyl has more influence on lipophilicity rather than TRPV6 inhibition. With this additional information in hands, another optimization was conducted on the *cis*-phenyl-cyclohexyl moiety of compound **32f**.

SAR studies had shown that only small hydrophobic substituents are allowed on the *cis*-4-phenyl-cyclohexyl group, specifically the methyl group at *meta*-position.<sup>76</sup> Hence, we envisaged to generate an analog of **32f** with the methyl group, as observed in the structure of *cis*-22a. We also decided to explore the influence of the trifluoromethyl group as a methyl bioisostere<sup>187,188</sup> at *ortho*- or *meta*-positions (**53h-i**). The trifluoromethyl group might increase lipophilicity compared to a methyl group. Once the synthetic intermediate is a tertiary alcohol that increases water solubility, we decided to generate two additional analogs (**56h-i**). These compounds were prepared according to **Scheme 8**, by first forming the Grignard reagents (**45g-i**) then reacting it with 1,4-cyclohexanedione monoethylene acetal (**46**) to generate the tertiary alcohols **47g-i**.<sup>76,189</sup> These alcohols were subjected to dehydration with *para*-toluenesulfonic acid hydrate (**48g-i**) followed by hydrogenation with Pd/C under H<sub>2</sub> atmosphere (**49g-i**), and acetal deprotection with pyridinium *para*-toluene sulfonate (PPTS) under mild conditions to the free cyclohexanones **50g-i**.<sup>190</sup> Subsequently, the ketones were coupled to **51** under reductive amination. The *cis*-diastereomers were isolated and the benzyl-piperazine was deprotected with Pd/C under H<sub>2</sub> atmosphere to the free piperazines **52g-i**. These compounds were condensed with **29**, to yield the desired final compounds **53g-i**. The tertiary alcohols **47h-i** were subjected to PPTS deprotection (**54h-i**), then, the synthetic route followed the same procedures of reductive

amination with **51** followed by benzyl deprotection to **55h-i** and a second reductive amination with **29**, to yield the desired final compounds **56h-i**.

**Scheme 8.** Synthetic route of optimized 3-pyridones **53g-i** and **56h-i**.<sup>a</sup>



<sup>a</sup>Reagents and conditions. (a) (i) Mg, **45g-i**, THF, Ar., r.f., 30 min, (ii) **46**, THF, Ar., r.f., 30 min; (b) TsOH.H<sub>2</sub>O, toluene, Ar., r.f., 4 h; (c) Pd/C, H<sub>2</sub>, AcOEt, r.t., on.; (d) PPTS, Acetone, H<sub>2</sub>O, 60 °C, 6 h (19-68 %, 4-steps); (f) **51**, NaBH(OAc)<sub>3</sub>, DCE, r.t., 48 h; (g) Pd/C, H<sub>2</sub>, AcOH, MeOH, r.t., on. (9-38 %, over 2-steps); (h) **29**, AcOH, NaBH(OAc)<sub>3</sub>, DCE, r.t., 48 h (17-81 %); (i) PPTS, Acetone, H<sub>2</sub>O, 60 °C, 6 h (72-90 %).

Compared to **32f**, the addition of a *meta*-methyl substitution in the phenyl-cyclohexyl ring (**53g**) improved the potency in 3.3-fold (IC<sub>50</sub> = 113 nM, **Table 2**) while retained the ligand metrics. Replacement to *meta*-trifluoromethyl (**53h**) gave a 6-fold increase in potency (IC<sub>50</sub> = 62 ± 8 nM), however, by moving it to the *ortho*-position (**53i**) the activity dropped 11-fold. The insertion of the hydroxyl group at the cyclohexyl ring slightly reduced the potency of compound **56h** (IC<sub>50</sub> = 83 ± 4 nM) and restored the activity of the analog **56i**. Due to an increase in the number of HA, the LE of **56h** was maintained in 0.31, and the LLE was significantly enhanced to an optimal value of 4.5. Based on the values of ligand metrics and modest potency against TRPV6, we chose compound **56h**, named MRC-130, for further investigation.

To fully evaluate the advantage of compound MRC-130, we probed its activity against the homolog channel TRPV5 along with **53h**, and *cis*-22a. Remarkably either MRC-130 or *cis*-22a possesses a TRPV5/TRPV6 selective index of 6.8. The hydroxylation solely

conferred a 3.2-fold improvement in selectivity when compared to **53h**. The optimized TRPV6 inhibitors were also tested against the TRPV1. At a concentration of 10  $\mu\text{M}$ , MRC-130 were able to block 51% of  $\text{Ca}^{2+}$  influx towards TRPV1, while the other compounds remained inactive.

**Table 2.** TRPV Activity Evaluation of Optimized Capsaicinoids.<sup>a</sup>

Cpd	Structure	TRPV6 IC <sub>50</sub> (nM) <sup>b</sup>	TRPV5 IC <sub>50</sub> (nM) <sup>b</sup>	TRPV1 % Inh <sup>d</sup>	LE <sup>e</sup>	LLE <sup>f</sup>
<b>32e</b>		2477	b	33	0.32	1.8
<b>32f</b>		373	b	14	0.34	3.1
<b>36f</b>		598	b	36	0.32	2.0
<b>42f</b>		551	b	13	0.34	1.7
<b>43f</b>		553	b	10	0.32	0.8
<b>44f</b>		172	b	1	0.36	1.2
<b>48g</b>		113	b	9	0.35	3.1
<b>53h</b>		62 ± 8 <sup>c</sup>	133	10	0.33	2.9
<b>53i</b>		688	b	6	0.28	1.9
<b>56h</b>		83 ± 4 <sup>c</sup>	561	51	0.31	4.5
<b>56i</b>		128	b	-10	0.30	4.3

<sup>a</sup>Active compounds were defined as able to inhibit at least 50% of TRPV6 activity. Data shown are mean  $\pm$  SEM ( $n = 6/\text{concentration}$ ) of a single<sup>b</sup> or at least two<sup>c</sup> independent experiments. <sup>d</sup>Compounds were tested at 10  $\mu\text{M}$  against a stimulus of 100 nM of CPS. Data shown is mean ( $n = 2$ ) of a single experiment. <sup>e</sup>LE: Ligand Efficiency =  $1.37 \times \text{pIC}_{50} / \text{number of heavy atoms}$ ; <sup>f</sup>LLE: Lipophilic Ligand Efficiency =  $\text{pIC}_{50} - \text{cLogP}_{\text{o/w}}$ . Based on mean oral drug values that provide the acceptable values for drug candidates, LE and LLE should ideally be above 0.4 and 4.0, respectively.<sup>185</sup>

### 2.4.1 Confocal imaging

To further detail the TRPV6 inhibitory activities of MRC-130, we co-stained HEK-*h*TRPV6 cells with specific dyes. Leadmium Green is a  $\text{Ca}^{2+}$ -insensitive intracellular dye which complexes specifically with Lead and  $\text{Cd}^{2+}$ , generating a green fluorescence within the cytosol. Alexa Fluor 594 was used as control of the plasmatic membrane.<sup>191,192</sup> In control cells (treated with vehicle), the application of  $\text{Cd}^{2+}$  (50  $\mu\text{M}$ ) revealed an increase in green fluorescence after 30 min, indicating  $\text{Cd}^{2+}$  transport through TRPV6 (**Figure 21A**). When cells were treated with 10  $\mu\text{M}$  of MRC-130 prior to the addition of  $\text{Cd}^{2+}$ , the fluorescence was significantly less pronounced (**Figure 21B**). We also performed time-course imaging of  $\text{Cd}^{2+}$  uptake within 30 min and we plotted total fluorescence over time (**Figure S1**). Compared to the MRC-130 treated cells, the influx at non-treated cells was more pronounced in the first 12 minutes of the experiment, and after that, a plateau was reached.

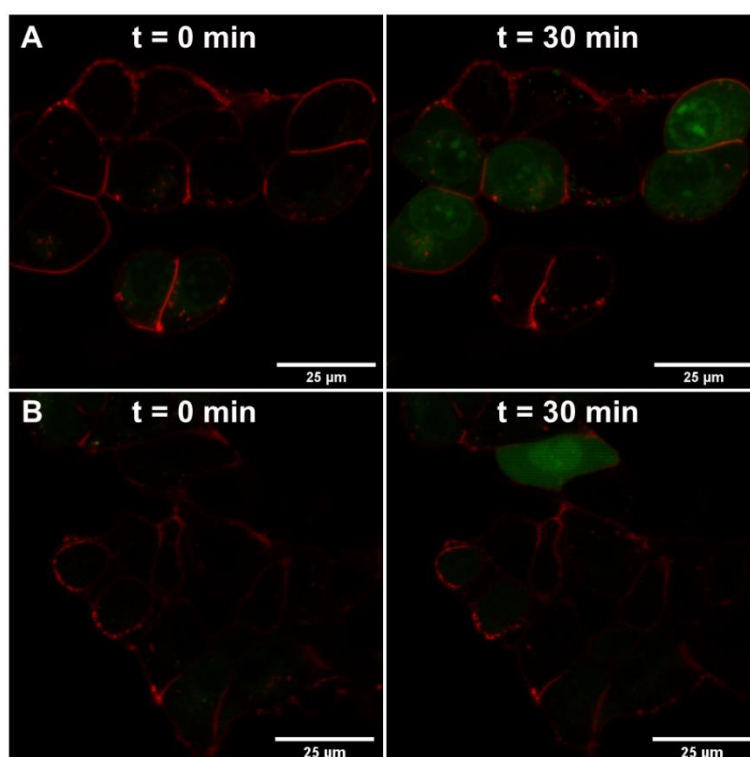


**Figure 21.** HEK-*h*TRPV6 cells co-stained with Leadmium Green and Alexa Fluor 298. Images were collected at time 0 min and 30 min after treatment with vehicle (A) or MRC-130 (10  $\mu\text{M}$ , B) followed by the addition of  $\text{Cd}^{2+}$  (50  $\mu\text{M}$ ) using confocal microscopy (Nikon Eclipse TE2000-E, 100X). White bars denote 25  $\mu\text{m}$ .

### 2.4.2 *In vitro* metabolism

One important step of drug discovery is to improve ADMET parameters of lead compounds. It is well known that compounds bearing a reactive methyl group can be readily metabolized by enzymes present in the cytochrome P450.<sup>193,194</sup> One possibility to

improve stability consists of the bioisosteric replacement of methyl group with trifluoromethyl.<sup>187,188</sup> In this view, we compared the liver microsomal stability of *cis*-22a and MRC-130 (**Figure 22**). As expected, *cis*-22a displayed a low human liver microsomal stability (half-life of 6 min) while MRC-130 remained stable over the course of the experiment (half-life > 60 min).

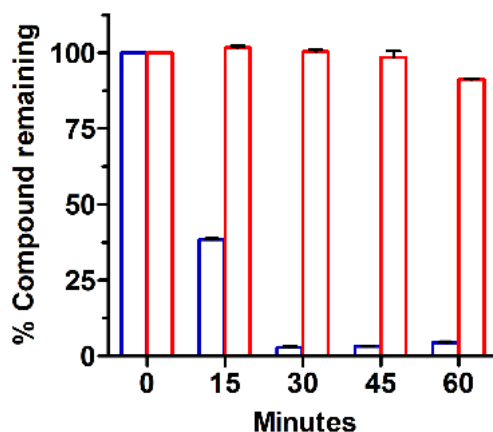


**Figure 22.** Intrinsic clearance in human liver microsomes of *cis*-22a (blue bars) and MRC-130 (red bars). Data shown are mean  $\pm$  SEM ( $n = 2$ ). The experiments were conducted by Eurofins Cerep SA, France.

In the discovery of *cis*-22a, a set of human ion channels were selected to evaluate its polypharmacology.<sup>76</sup> Although *cis*-22a displayed a selective activity towards the TRPV6 channel, at the concentration of 10  $\mu$ M *cis*-22a displayed > 50% of inhibition against several channels found in Cardiovascular and Central Nervous Systems (**Figure 23**). Outstanding, MRC-130 displayed no significant inhibition against the same channels at 10  $\mu$ M. Noteworthy, the activity over *h*ERG was completely abolished. The high stability in liver microsomes and weak inhibitory activity against off-targets constitutes an improvement relative to the original compound *cis*-22a.

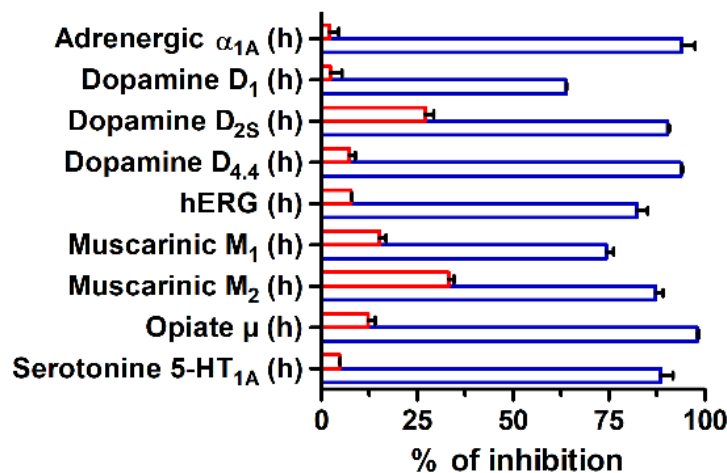


**Figure 23.** *In vitro* polypharmacology for selected human targets of *cis*-22a (blue bars) and MRC-130 (red bars). Data shown are mean  $\pm$  SEM ( $n = 2$ ). The data for *cis*-22a was extracted from the ref.<sup>76</sup> The experiments were conducted by Eurofins Cerep SA, France.

### 2.4.3 Antiproliferative activity

We investigated the antiproliferative activities of compound MRC-130 against a panel of six human tumor cells by using XTT assay. *Cis*-22a and doxorubicin (Doxo) were also used for comparison and control, respectively. According to the literature, T47D is highly expressed in TRPV6, whereas in SKOV-3 the channel is supposed to be absent.<sup>76</sup> Comparable to these two cell lines, we decided to use HEK-*h*TRPV6 and HEK-wt to analyze the influence of the channel on cell toxicity. MCF-7 and MDA-MB-231 have shown marginal levels of TRPV6 mRNA and were used as negative control cells.<sup>195</sup> After a 6-day treatment the percentage of viable cells was compared to the blank control (**Table 3**).

**Table 3.** Percentage of viable cells treated with MRC-130, *cis*-22a, and doxorubicin.<sup>a</sup>

Cell line	MRC-130 <sup>b</sup>	<i>cis</i> -22a <sup>b</sup>	Doxo <sup>c</sup>
SKOV-3	101 ± 6	26 ± 1	40 ± 2
T47D	98 ± 3	51 ± 5	35 ± 12
HEK-wt	99 ± 6	49 ± 1	63 ± 5
HEK-TRPV6	107 ± 3	66 ± 5	83 ± 3
MCF-7	95 ± 6	44 ± 10	58 ± 5
MDA-MB-231	101 ± 1	66 ± 29	30 ± 4

<sup>a</sup>Viable cells(%) were analyzed by XTT method after 6-day treatment with the indicated compounds. Medium containing each individual compound was replaced every 48 h. Data shown are mean ± SEM ( $n = 8$ /concentration) for at least 3 independent experiments. <sup>b</sup>Data showed for compounds tested at 100 μM. <sup>c</sup>Tested at 10 μM.

MRC-130 did not induce any changes in cell viability for all the studied cell lines up to 100 μM. Cell morphology was also preserved under MRC-130 treatment (**Figure 24**). On the other hand, *cis*-22a displayed toxicity at high concentrations towards all the cells, especially against SKOV-3 ( $IC_{50} = 36.5 \pm 1.4 \mu\text{M}$ , **Figure S2**). As illustrated in **Table 3**, *cis*-22a also displayed more toxicity towards HEK-wt rather than HEK-*h*TRPV6. Doxo was able to drastically decrease cell growth at 10 μM of SKOV-3, T47D, HEK-wt, MCF-7, and MDA-MB-231 but to a lesser extent towards HEK-*h*TRPV6 cells. This experiment is in line with previous studies in zebrafish<sup>72</sup> and human cell models,<sup>69,70</sup> where the pharmacological block of TRPV6 appears to be ineffective to induce cell death. Moreover, the activities seen for *cis*-22a are believed to be TRPV6-independent once the compound induced more toxicity in TRPV6-negative cells.

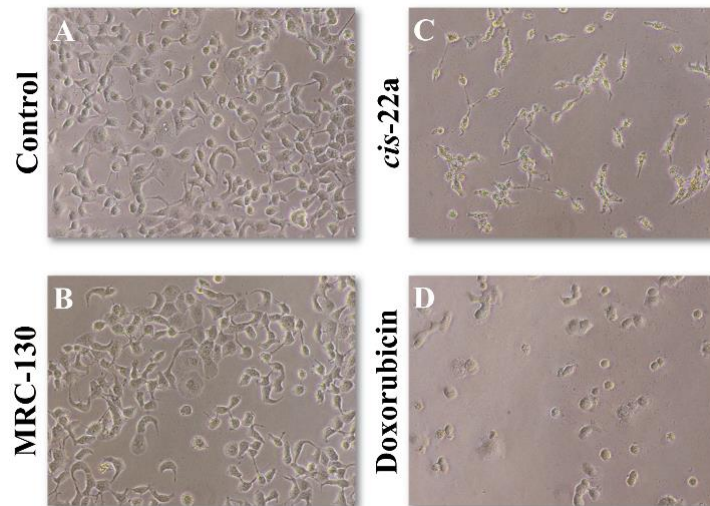


**Figure 24.** Photomicrographs show the morphological aspects of the control cultures of T47D cells (A), and treated with MRC-130 (100 μM, B); *cis*-22a (100 μM, C); doxorubicin (10 μM, D). Cells were imaged at 20X with an inverted microscope (Nikon Eclipse TiU).

### 3. Conclusion and Outlook

A new series of *h*TRPV6 inhibitors was designed by two different approaches. By evaluating their inhibitory activities against the *h*TRPV6, compounds derived from the merged pharmacophores of capsaicin and *cis*-22a, the hybrid capsaicinoids, were able to block the channel at low  $\mu\text{M}$  level. Importantly, the presence of bulky substituents, such as *t*-butyl and phenyl at the *cis*-cyclohexyl moiety is important for TRPV6 potency. The replacement of the vanillin head to the 3-pyridone along with chemical optimization of the hit compound resulted in better ligand affinities and enhanced potency. From a series of hit optimizations, compound **56h**, named MRC-130, arose as a novel potent and selective *h*TRPV6 inhibitor ( $\text{IC}_{50} = 83 \pm 4 \text{ nM}$ ).

The *in vitro* ADMET profiling and poly-pharmacological observations suggest that: MRC-130 is at least 10-fold more metabolically stable relative to the reference compound *cis*-22a in liver microsomes; and possess a much lower affinity for off-targets, such as *h*ERG receptors at  $10 \mu\text{M}$ . MRC-130 was tested continuously at 1200-fold above its  $\text{IC}_{50}$  against a panel of six human cancer cells positive or not for TRPV6, however, we do not observe any morphological changes or reduced cell viability under treatment.

Clearly, the involvement of TRPV6 on cell survival and proliferation must be further studied. The development MRC-130 as a more selective, metabolically stable and non-cytotoxic compound opens new possibilities for probing *h*TRPV6. This compound is currently in a study for the participation of TRPV6 another disease model and will be reported in due time.

## 4. Contributions

The synthesis of bioisosteric capsaicinoids was conducted at LAPESSB. The sulfonylglycine hydrazones (**17a-b**, **18a-b**) were synthesized by the Pharmacy student Caroline Branco, as part of her Scientific Initiation. The synthesis of hybrid capsaicinoids, as well as their optimization, was conducted in the laboratory of Prof. Jean-Louis Reymond, at the Department of Chemistry and Biochemistry, University of Bern. Compound profiling against *hTRPV6*, *hTRPV5*, and *hTRPV1* was measured in collaboration with Dr. Rajesh Bhardwaj in the group of Prof. Matthias Hediger, at the dependencies of the National Competence Center in Research (NCCR) TransCure. The polypharmacology profiling, as well as measurement of the microsomal stability, was done by the company Eurofins Cerep in France.

## 5. Experimental Part

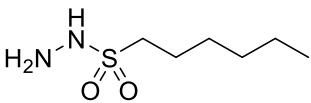
*General Methods.* All commercial reagents were used without further purification. Dry solvents were obtained directly from a drying solvent system. Chromatographic purifications were performed using silica gel (Sigma-Aldrich, 230-400 mesh). Automated chromatographic purification was performed with Puriflash 430 system (Interchim) using Teledyne Isco normal phase RediSepRf cartridge and detection by UV absorption (214 nm). High-resolution mass spectra were obtained electron spray ionization (ESI), positive mode (Thermo Scientific LTQ OrbitrapXL or MicroToF Bruker Daltonics). Preparative RP-HPLC was performed with Waters Prep LC4000 Chromatography System using a Reprospher 100 (C18-DE, 100 mm x 30 mm, particle size 5  $\mu$ M, 100 Å pore size) column from Dr. Maisch GmbH and a Waters 489 Tunable Absorbance Detector operating at 214 nm.  $^1\text{H}$ ,  $^{13}\text{C}$ , and  $^{19}\text{F}$ -NMR spectra were recorded at 300MHz, 75MHz, and 376MHz respectively (Bruker AVANCE III HD 300 or DPX-300). For very small amounts,  $^1\text{H}$  and  $^{13}\text{C}$ -NMR spectra were recorded at 400MHz and 100MHz, respectively (Bruker AVANCE II 400). Chemical shifts are quoted relative to solvent signals. MestreNova was used for further analysis of the spectra. The following abbreviations for multiplicities were used: s = singlet, d = doublet, t = triplet, q = quartet, p = pentet, m = multiplet, dd = doublet of doublets, dt = doublet of triplets, tt = triplet of triplets, and br s = broad singlet. TLC plates (Merck silica gel 60 F<sub>254</sub>) were used to monitor the reaction progress, and spots were visualized under UV (254 nm). The purity of all tested compounds was > 95%. The chromatographic purity of the direct capsaicinoids was determined using a High-Performance Liquid Chromatograph (Shimadzu®-PROMINENCE) coupled with a C18 column (Waters®- $\mu$ Bondpak C18, 3.9 x 300 mm). For the chimeric capsaicinoids the purity was confirmed by analytical RP-UHPLC with detection at 214nm, on a Dionex Ultimate 3000 RSLC System (DAD-3000 RS Photodiode Array Detector) and Dionex Acclaim RSLC 120 column (C18, 3.0 x 50 mm, particle size 2.2  $\mu$ m, 120 Å pore size) at a flow rate of 1.2 mL/min. Data recording and processing was done with Dionex Chromelon Management System (v. 6.8), and Xcalibur (v. 2.2, Thermo Scientific). Eluents for analytical HPLC were as follows: A: miliQ-deionized water with 0.05% TFA and D: HPLC-grade acetonitrile with 0.05% TFA. Conditions for analytical HPLC were as follow: the flow stays in 90% A and 10% D for 4.0 min, then in 25 min from 90% A and 10 % D to 0 % and 100 % D, then staying on 100% D. Eluents for analytical and preparative RP-UHPLC were as follow: A: miliQ-deionized water with 0.05% TFA and D: HPLC-grade

acetonitrile/miliQ-deionized water (9/1) with 0.05% TFA. Conditions for analytical RP-UHPLC were as follow: in 4.5 min from 100% A to 100% D, then staying on 100% D, or in 7.5 min from 100% A to 100% D, then staying on 100% D. Conditions for preparative RP-UHPLC were described after compound characterization. Chemical names were generated using ChemDraw Professional 17.0 (PerkinElmer Informatics).

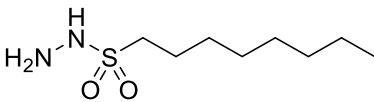
## 5.1 Chemistry

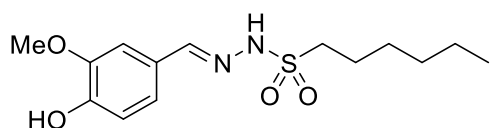
### 5.1.1 Synthesis of the bioisosteric capsaicinoids.

#### Hexane-1-sulfonylhydrazide (**3a**).

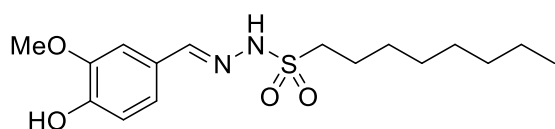
 In a round-bottom flask containing an ice-cold solution of hydrazine hydrate (**2**, 9.4 mL, 10 eq.) in THF (10 mL) was added dropwise a solution of hexane-1-sulfonyl chloride (**1a**, 1.6 mL, 1 eq.) in THF (10 mL). The reaction mixture was stirred for 1 h, at 0 °C, then, it was allowed to warm to r.t. and was stirred for an additional 1 h. The reaction mixture was extracted with EtOAc (5 X 5 mL) and was dried over Na<sub>2</sub>SO<sub>4</sub>. The resulting solution was evaporated and was solubilized in a minimal amount of chloroform. To this solution, hexane was slowly added to precipitate the desired compound as a white solid (1.5 g, 82 %). <sup>1</sup>H NMR (300 MHz, CDCl<sub>3</sub>): δ 5.79 (s, 1H), 3.82 (s, 2H), 3.09 (t, *J* = 8.0 Hz, 2H), 1.79 (p, *J* = 7.7 Hz, 2H), 1.42-1.30 (m, 6H), 0.88 (t, *J* = 6.0 Hz, 3H). <sup>13</sup>C NMR (75 MHz, CDCl<sub>3</sub>): δ 49.4, 31.3, 28.0, 23.2, 22.4, 14.0.

#### Octane-1-sulfonylhydrazide (**3b**).

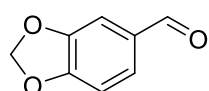
 In a round-bottom flask containing an ice-cold solution **2** (9.4 mL, 10 eq.) in THF (10 mL) was added dropwise a solution of octane-1-sulfonyl chloride (**1b**, 2 mL, 1 eq.) in THF (10 mL). The reaction mixture was stirred for 1 h, at 0 °C, then, it was allowed to warm to r.t. and was stirred for an additional 1 h. The reaction mixture was extracted with EtOAc (5 X 5 mL) and was dried over Na<sub>2</sub>SO<sub>4</sub>. The resulting solution was evaporated and was solubilized in a minimal amount of chloroform. To this solution, hexane was slowly added to precipitate the desired compound as a white solid (1.3 g, 60 %). <sup>1</sup>H NMR (300 MHz, CDCl<sub>3</sub>): δ 6.07 (s, 1H), 3.78 (s, 1H), 3.09 (t, *J* = 7.8 Hz, 2H), 1.78 (p, *J* = 7.4 Hz, 2H), 1.39-1.26 (m, 10H), 0.86 (t, *J* = 5.7 Hz, 3H). <sup>13</sup>C NMR (75 MHz, CDCl<sub>3</sub>): δ 49.2, 31.8, 29.1, 29.0, 23.2, 22.6, 14.1.

**(E)-N'-(4-hydroxy-3-methoxybenzylidene)hexane-1-sulfonohydrazide (5a).**

General procedure B: In a round-bottom flask containing a solution of **3a** (270 mg, 1 eq.) in MeOH (30 mL), was added dropwise a solution of the 4-hydroxy-3-methoxybenzaldehyde (**4**, 228 mg, 1 eq.). The reaction mixture was stirred for 5 h, under reflux. Under completion (TLC), the reaction mixture was evaporated and column chromatographed (hexanes:EtOAc, 50:50) to yield the desired compound as a yellow sticky oil (419 mg, 89 %). <sup>1</sup>H NMR (300 MHz, CDCl<sub>3</sub>): δ 7.95 (s, 1H), 7.76 (s, 1H), 7.29 (d, *J* = 1.7 Hz, 1H), 7.02 (dd, *J*<sup>1</sup> = 1.7 Hz, *J*<sup>2</sup> = 8.4 Hz, 1H), 6.89 (d, *J* = 8.1 Hz, 1H), 5.90 (s, 1H), 3.92 (s, 3H), 3.28 (t, *J* = 8.0 Hz, 2H), 1.85 (p, *J* = 7.7 Hz, 2H), 1.43 (p, *J* = 3.6 Hz, 2H), 1.30-1.25 (m, 4H), 0.85 (t, *J* = 6.9 Hz, 3H). <sup>13</sup>C NMR (75 MHz, CDCl<sub>3</sub>): δ 148.0, 146.8, 125.5, 122.8, 114.0, 107.6, 55.9, 50.9, 31.0, 27.7, 22.9, 22.0, 13.7. HRMS *m/z* calculated for C<sub>14</sub>H<sub>23</sub>N<sub>2</sub>O<sub>4</sub>S: 315.1373 [M+H]<sup>+</sup>; found, 315.1366.

**(E)-N'-(4-hydroxy-3-methoxybenzylidene)octane-1-sulfonohydrazide (5b).**

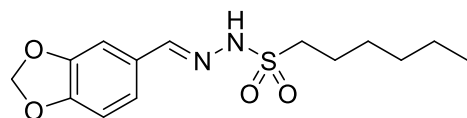
**5b** was synthesized from **3b** (313 mg, 1 eq.) and **4** (228 mg, 1 eq.) following general procedure A and was obtained as a yellow sticky oil (478 mg, 93 %). <sup>1</sup>H NMR (300 MHz, CDCl<sub>3</sub>): δ 8.00 (s, 1H), 7.77 (s, 1H), 7.29 (d, *J* = 1.5 Hz, 1H), 7.03 (dd, *J*<sup>1</sup> = 1.8 Hz, *J*<sup>2</sup> = 8.1 Hz, 1H), 6.90 (d, *J* = 8.4 Hz, 1H), 5.91 (s, 1H), 3.93 (s, 3H), 3.28 (t, *J* = 8.0 Hz, 2H), 1.86 (p, *J* = 7.7 Hz, 2H), 1.45-1.38 (m, 2H), 1.27-1.24 (m, 8H), 0.85 (t, *J* = 6.8 Hz, 3H). <sup>13</sup>C NMR (75 MHz, CDCl<sub>3</sub>): δ 148.4, 148.2, 147.0, 125.8, 123.0, 114.3, 107.9, 56.1, 51.1, 31.7, 29.0, 28.9, 28.2, 23.1, 22.5, 14.0. HRMS *m/z* calculated for C<sub>16</sub>H<sub>27</sub>N<sub>2</sub>O<sub>4</sub>S: 343.1686 [M+H]<sup>+</sup>; found, 343.1680.

**Benzo[d][1,3]dioxole-5-carbaldehyde (7).**

In a round-bottom flask containing a solution of **6** (1.5 g, 1 eq.) in DCM (250 mL), was added MnO<sub>2</sub> (13 g, 15 eq.). The reaction was stirred at r.t., for 4h until complete consumption of the alcohol (TLC). Then, the reaction mixture was filtered through Celite and mixed with activated charcoal. The resulting solution was filtered and evaporated under vacuum. The column chromatographed (hexanes:EtOAc, 50:50) to yield the desired compound as a crystalline solid. <sup>1</sup>H NMR (300 MHz, DMSO-*d*<sub>6</sub>): δ 9.79 (s, 1H), 7.53 (dd, *J*<sup>1</sup> = 8.0 Hz, *J*<sup>2</sup> = 1.6 Hz, 1H), 7.31 (d, *J* = 1.5 Hz, 1H), 7.12

(d,  $J = 8.0$  Hz, 1H), 6.15 (s, 2H).  $^{13}\text{C}$  NMR (75 MHz, DMSO- $d_6$ ):  $\delta$  190.9, 152.7, 148.3, 131.5, 128.5, 108.5, 106.2, 102.3.

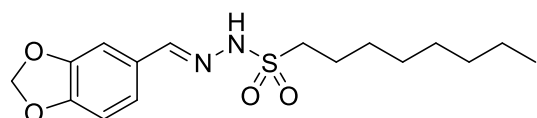
**(*E*)-N'-(benzo[d][1,3]dioxol-5-ylmethylene)hexane-1-sulfonohydrazide (8a).**



**8a** was synthesized from **1a** (270 mg, 1 eq.) and **7** (225 mg, 1 eq.) following general procedure A and was obtained as a white powder (323 mg, 69 %).

$^1\text{H}$  NMR (300 MHz, DMSO- $d_6$ ):  $\delta$  8.09 (s, 1H), 7.76 (s, 1H), 7.27 (s, 1H), 7.00 (d,  $J = 8.0$  Hz, 1H), 6.79 (d,  $J = 8.0$  Hz, 1H), 6.00 (s, 2H), 3.28 (t,  $J = 8.0$  Hz, 2H), 1.85 (qi,  $J = 7.8$  Hz, 2H), 1.45-1.39 (m, 2H), 1.31-1.29 (m, 4H), 0.87 (t,  $J = 6.5$  Hz, 3H).  $^{13}\text{C}$  NMR (75 MHz, DMSO- $d_6$ ):  $\delta$  149.8, 148.3, 147.6, 127.7, 123.7, 108.2, 105.8, 101.5, 51.1, 31.1, 27.9, 23.1, 22.3, 13.9. HRMS  $m/z$  calculated for  $\text{C}_{14}\text{H}_{21}\text{N}_2\text{O}_4\text{S}$ : 313.3915  $[\text{M}+\text{H}]^+$ ; found, 313.1216.

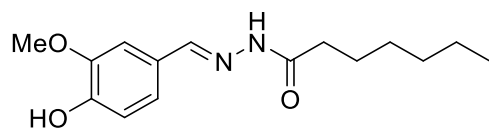
**(*E*)-N'-(benzo[d][1,3]dioxol-5-ylmethylene)octane-1-sulfonohydrazide (8b).**



**8b** was synthesized from **1b** (313 mg, 1 eq.) and **7** (225 mg, 1 eq.) following general procedure A and was obtained as a white powder (310 mg, 61 %).

$^1\text{H}$  NMR (300 MHz,  $\text{CDCl}_3$ ):  $\delta$  8.14 (s, 1H), 7.76 (s, 1H), 7.27 (d,  $J = 1.5$  Hz, 1H), 7.00 (dd,  $J^1 = 1.4$  Hz,  $J^2 = 8.1$  Hz, 1H), 6.79 (d,  $J = 8.0$ , 1H), 6.00 (s, 2H), 3.28 (t,  $J = 8.0$  Hz, 2H), 1.85 (qi,  $J = 7.7$  Hz, 2H), 1.44-1.37 (m, 2H), 1.26-1.23 (m, 8H), 0.86 (t,  $J = 6.6$  Hz, 3H).  $^{13}\text{C}$  NMR (75 MHz,  $\text{CDCl}_3$ ):  $\delta$  149.8, 148.3, 147.6, 127.7, 123.7, 108.2, 105.8, 101.5, 51.1, 31.7, 29.0, 28.9, 28.2, 23.1, 22.5, 14.0. HRMS  $m/z$  calculated for  $\text{C}_{16}\text{H}_{25}\text{N}_2\text{O}_4\text{S}$ : 341.4455  $[\text{M}+\text{H}]^+$ ; found, 341.1527.

**(*E*)-N'-(4-hydroxy-3-methoxybenzylidene)heptanehydrazide (11a).**

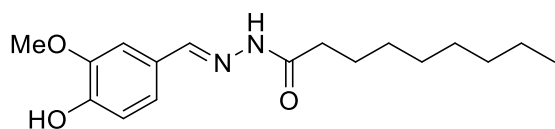


General procedure B: In a round-bottom flask containing an ice-cold solution of **2** (1 mL, 10 eq.) in DCM (6 mL), was added dropwise a solution of

heptanoyl chloride (**9a**, 310  $\mu\text{L}$ , 1 eq.) in DCM (6 mL). The reaction mixture was stirred for 1 h, at 0  $^\circ\text{C}$ , then, it was allowed to warm to r.t. and was stirred for additional 1 h. The reaction mixture was quenched by the addition of  $\text{H}_2\text{O}$  (10 mL). The solution was transferred to a funnel and an aqueous solution of HCl 5% (5 mL) was added. The mixture was extracted and the aqueous phase was re-extracted with DCM (2 X 15 mL). The organic phase was collected, dried over  $\text{MgSO}_4$  and evaporated. The resulting residue was solubilized in a minimal amount of DCM and was precipitated as a white solid (**10a**, 144

mg, 50 %) by the addition of hexane. The compound was used in the next step without further purification. Compound **10a** (144 mg, 1 eq.) was solubilized in EtOH (5 mL) and was added dropwise to a solution of **4** (152 mg, 1 eq.) in EtOH (5 mL), followed by AcOH (2 drops), and the reaction mixture was stirred at r.t., for 2 h. The reaction was quenched by the addition of cold H<sub>2</sub>O until precipitation. The solids were filtered off and dried under vacuum. The crude was then, column chromatographed (hexanes:EtOAc, 1:2) to afford the desired as a white solid (137 mg, 25 %). <sup>1</sup>H NMR (300 MHz, CDCl<sub>3</sub>): δ 9.84 (s, 0.3H), 8.71 (s, 0.5H), 7.64 (s, 1H), 7.42 (s, 1H), 7.07 (dd, *J* = 12.3, 9.1 Hz, 1H), 6.93 (d, *J* = 7.0 Hz, 1H), 3.97 (d, *J* = 5.7 Hz, 3H), 2.74 (t, *J* = 7.3 Hz, 1H), 2.26 (t, *J* = 7.7 Hz, 1H), 1.76-1.67 (m, 2H), 1.33 (brs, 7H), 0.89 (s, 3H). <sup>13</sup>C NMR (75 MHz, CDCl<sub>3</sub>): δ 175.8, 148.0, 147.1, 143.2, 127.6, 122.4, 114.7, 108.0, 33.0, 31.8, 29.3, 24.9, 22.7, 14.2. HRMS *m/z* calculated for C<sub>15</sub>H<sub>23</sub>N<sub>2</sub>O<sub>3</sub>: 279.1703 [M+H]<sup>+</sup>; found, 279.1710.

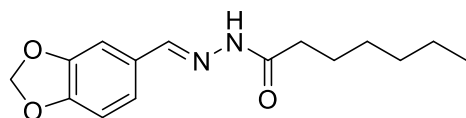
**(*E*)-N'-(4-hydroxy-3-methoxybenzylidene)nonanehydrazide (**11b**).**



**11b** was synthesized from **2** (0.68 μL, 10 eq.) and nonanoyl chloride (**9b**, 252 μL, 1 eq.) following general procedure B and was

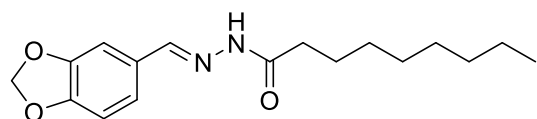
obtained as white solid (129 mg, 31 %). <sup>1</sup>H NMR (300 MHz, DMSO-*d*<sub>6</sub>): δ 11.10 (s, 0.5H), 11.00 (s, 0.5H), 9.60 (s, 0.1H), 9.42 (d, *J* = 6.1 Hz, 1H), 8.03 (s, 0.5H), 7.85 (s, 0.5H), 7.22 (d, *J* = 12.7 Hz, 1H), 7.03 (d, *J* = 8.1 Hz, 1H), 6.80 (dd, *J* = 8.1, 1.3 Hz, 1H), 3.80 (d, *J* = 2.9 Hz, 3H), 2.58 (t, *J* = 7.3 Hz, 1H), 2.16 (t, *J* = 7.3 Hz, 1H), 1.57 (dd, *J* = 13.4, 6.6 Hz, 2H), 1.25 (s, 11H), 0.86–0.81 (m, 2H). <sup>13</sup>C NMR (75 MHz, CDCl<sub>3</sub>): δ 176.3, 147.9, 147.1, 143.6, 126.6, 122.3, 114.7, 108.1, 56.1, 32.9, 32.0, 29.6, 29.5, 29.3, 25.0, 22.8, 14.2. HRMS *m/z* calculated for C<sub>17</sub>H<sub>27</sub>N<sub>2</sub>O<sub>3</sub>: 307.2016 [M+H]<sup>+</sup>; found, 307.2025.

**(*E*)-N'-(benzo[d][1,3]dioxol-5-ylmethylene)heptanehydrazide (**12a**).**

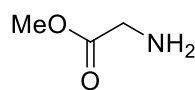


**12a** was synthesized from **2** (1 mL, 10 eq.), **9a** (310 μL, 1 eq.), and **7** (150 mg, 1 eq.) following general procedure B and was obtained as white solid (186

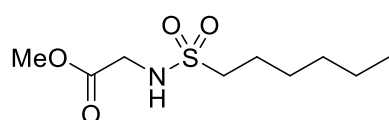
mg, 34 %). <sup>1</sup>H NMR (300 MHz, DMSO-*d*<sub>6</sub>): δ 9.91 (s, 1H), 7.72 (s, 1H), 7.27 (s, 1H), 7.01 (d, *J* = 8.0 Hz, 1H), 6.81 (d, *J* = 8.0 Hz, 1H), 6.00 (s, 2H), 2.73 (t, *J* = 7.5 Hz, 2H), 1.75-1.67 (m, 2H), 1.43-1.32 (m, 6H), 0.89 (t, *J* = 6.5 Hz, 3H). <sup>13</sup>C NMR (75 MHz, DMSO-*d*<sub>6</sub>): δ 176.7, 149.5, 148.5, 143.2, 128.8, 123.4, 108.4, 105.6, 101.6, 32.9, 31.7, 29.2, 25.0, 22.7, 14.2. HRMS *m/z* calculated for C<sub>15</sub>H<sub>20</sub>N<sub>2</sub>O<sub>3</sub>: 277.3435 [M+H]<sup>+</sup>; found, 277.1542.

**(E)-N'-(benzo[d][1,3]dioxol-5-ylmethylene)nonanehydrazide (12b).**

**12b** was synthesized from **2** (1 mL, 10 eq.), **9b** (252  $\mu$ L, 1 eq.), and **7** (150 mg, 1 eq.) following general procedure B and was obtained as white solid (162 mg, 40 %).  $^1\text{H}$  NMR (300 MHz, DMSO- $d_6$ ):  $\delta$  11.20 (s, 0.4H), 11.07 (s, 0.6H), 8.10 (s, 0.4H), 7.90 (s, 0.6H), 7.25 (s, 1H), 7.11 (dd,  $J$  = 14.4, 8.1 Hz, 1H), 6.97 (dd,  $J$  = 7.9, 4.4 Hz, 1H), 6.09 (d,  $J$  = 2.1 Hz, 2H), 2.60 (t,  $J$  = 7.4 Hz, 1H), 2.19 (t,  $J$  = 7.3 Hz, 1H), 1.59 (brs, 2H), 1.28 (s, 11H), 0.87 (d,  $J$  = 3.5 Hz, 1H).  $^{13}\text{C}$  NMR (75 MHz, DMSO- $d_6$ ):  $\delta$  176.5, 149.5, 148.5, 143.1, 128.7, 123.4, 108.4, 105.7, 101.6, 32.9, 32.0, 29.6, 29.5, 29.3, 25.0, 22.8, 14.2. HRMS  $m/z$  calculated for  $\text{C}_{17}\text{H}_{25}\text{N}_2\text{O}_3$ : 305.3975  $[\text{M}+\text{H}]^+$ ; found, 305.1865.

**Methyl glycinate hydrochloride salt (14).**

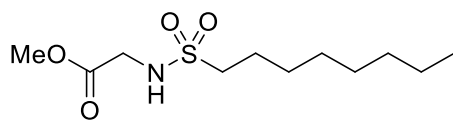
In a round-bottom flask containing an ice-cold solution of **13** (751 mg, 1 eq.) in MeOH (4 mL), was added dropwise a solution thionyl chloride (218  $\mu$ L, 3 eq.). After addition, the reaction mixture was stirred for 12 h, under reflux. Under completion (TLC), the reaction mixture was evaporated the solids were collected and washed thoroughly with EtOAc to afford the desired compound as a white powder (791 mg, 63 %).  $^1\text{H}$  NMR (300 MHz,  $\text{D}_2\text{O}$ ):  $\delta$  4.79 (s, 3H), 4.04 (s, 2H), 3.94 (s, 3H).  $^{13}\text{C}$  NMR (75 MHz,  $\text{D}_2\text{O}$ ):  $\delta$  171.3, 56.0, 42.7.

**Methyl (hexylsulfonyl)glycinate (15a).**

In a round-bottom flask containing a solution of **14** (226 mg, 1 eq.) in DCM (2.5 mL), was added  $\text{Et}_3\text{N}$  (753  $\mu$ L, 3 eq.). The reaction mixture was stirred at 0  $^\circ\text{C}$  for 10 min, followed by the dropwise addition of **1a** (300  $\mu$ L, 1 eq.) in DCM (2.5 mL). The reaction mixture was allowed to warm up to r.t. and was stirred for an additional 6 h. Under completion (TLC), the reaction mixture was extracted with  $\text{H}_2\text{O}$  (3 X 10 mL) and the organic phase was collected and dried over  $\text{MgSO}_4$ . The solvent was removed under vacuum until a minimal amount of DCM was enough to solubilize all the solids. Then, cold hexane was slowly added to precipitate the desired compound as a white solid (192 mg, 45 %).  $^1\text{H}$  NMR (300 MHz,  $\text{CDCl}_3$ ):  $\delta$  4.96 (s, 1H), 3.94 (d,  $J$  = 5.6 Hz, 2H), 3.78 (s, 3H), 3.78 (d,  $J$  = 2.5 Hz, 3H), 3.05 (t,  $J$  = 7.9 Hz, 2H), 1.81 (p,  $J$  = 5.8 Hz, 2H), 1.49-1.24 (m,

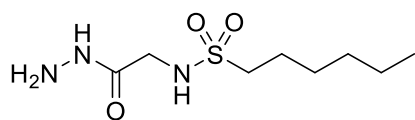
6H), 0.88 (s, 3H).  $^{13}\text{C}$  NMR (75 MHz,  $\text{CDCl}_3$ ):  $\delta$  170.3, 53.9, 52.7, 44.3, 31.4, 28.0, 23.6, 22.4, 14.04.

### Methyl (octylsulfonyl)glycinate (**15b**).



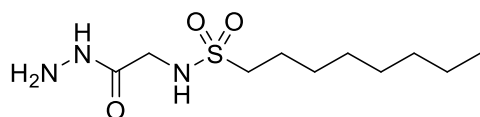
In a round-bottom flask containing a solution of **14** (112 mg, 1 eq.) in DCM (1.2 mL), was added  $\text{Et}_3\text{N}$  (418  $\mu\text{L}$ , 3 eq.). The reaction mixture was stirred at 0  $^\circ\text{C}$  for 10 min, followed by the dropwise addition of **1b** (196  $\mu\text{L}$ , 1.1 eq.) in DCM (1.2 mL). The reaction mixture was allowed to warm up to r.t. and was stirred for an additional 6 h. Under completion (TLC), the reaction mixture was extracted with  $\text{H}_2\text{O}$  (3 X 10 mL) and the organic phase was collected and dried over  $\text{MgSO}_4$ . The solvent was removed under vacuum until a minimal amount of DCM was enough to solubilize all the solids. Then, cold hexane was slowly added to precipitate the desired compound as a white solid (122 mg, 52 %).  $^1\text{H}$  NMR (300 MHz,  $\text{CDCl}_3$ ):  $\delta$  5.00 (t,  $J = 5.2$  Hz, 1H), 3.92 (d,  $J = 5.7$  Hz, 2H), 3.77 (d,  $J = 5.0$  Hz, 3H), 3.04 (t,  $J = 7.9$  Hz, 2H), 1.86-1.74 (m, 2H), 1.42-1.27 (m, 10H), 0.86 (t,  $J = 6.1$  Hz, 3H).  $^{13}\text{C}$  NMR (75 MHz,  $\text{CDCl}_3$ ):  $\delta$  170.6, 53.8, 52.6, 44.2, 31.8, 29.1, 29.0, 28.4, 23.6, 22.7, 14.1.

### N-(2-hydrazineyl-2-oxoethyl)hexane-1-sulfonamide (**16a**).



In a round-bottom flask containing a solution of **15a** (177 mg, 1 eq.) in MeOH (185  $\mu\text{L}$ ), was added **2** (185  $\mu\text{L}$ ). The reaction mixture was stirred at r.t. for 3 h. Under completion (TLC), the solvents were removed under vacuum and the residue was solubilized in a minimal amount of EtOH. Hexane was added to the previous solution until precipitation of the desired compound as a white solid (131 mg, 75 %).  $^1\text{H}$  NMR (300 MHz,  $\text{CDCl}_3$ ):  $\delta$  3.79 (s, 2H), 3.06 (t,  $J = 7.4$  Hz, 2H), 1.80-1.73 (m, 2H), 1.46-1.25 (m, 9H), 0.86 (s, 3H).  $^{13}\text{C}$  NMR (75 MHz,  $\text{CDCl}_3$ ):  $\delta$  169.5, 53.1, 44.9, 31.4, 28.1, 23.6, 22.5, 14.1.

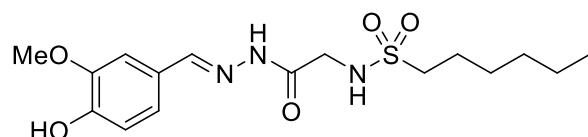
### N-(2-hydrazineyl-2-oxoethyl)octane-1-sulfonamide (**16b**).



In a round-bottom flask containing a solution of **15b** (88 mg, 1 eq.) in MeOH (825  $\mu\text{L}$ ), was added **2** (825  $\mu\text{L}$ ). The reaction mixture was stirred at r.t. for 3 h. Under completion (TLC), the solvents were removed under vacuum and the residue was solubilized in a minimal amount of EtOH. Hexane was added to the previous solution until precipitation of the desired compound as a white solid (87 mg, 99 %).  $^1\text{H}$  NMR (300

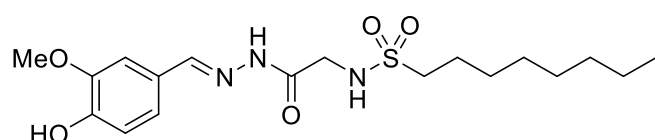
MHz, DMSO-d<sub>6</sub>):  $\delta$  9.04 (s, 1H), 7.17 (s, 1H), 4.23 (s, 2H), 3.54 (s, 2H), 3.01 (t,  $J$  = 7.7 Hz, 2H), 1.65 (q,  $J$  = 6.9 Hz, 2H), 1.33-1.25 (m, 10H), 0.86 (d,  $J$  = 6.3 Hz, 3H). <sup>13</sup>C NMR (75 MHz, DMSO-d<sub>6</sub>):  $\delta$  170.7, 53.7, 45.1, 32.9, 30.2, 30.1, 29.3, 24.6, 23.6, 14.3.

**(*E*)-N-(2-(2-(4-hydroxy-3-methoxybenzylidene)hydrazineyl)-2-oxoethyl)hexane-1-sulfonamide (17a).**



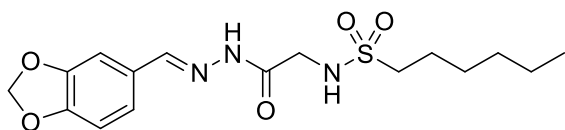
General procedure C: In a round-bottom flask containing a solution of **16a** (47 mg, 1 eq.) in EtOH (1 mL), was added **4** (30 mg, 1 eq.) and AcOH (1 drop) in EtOH (1 mL). The reaction mixture was stirred at r.t. for 24 h. Under completion (TLC), the solvents were removed under vacuum and the residue was column chromatographed (hexanes:EtOAc, 75:25) to afford the desired compound as a white solid (65 mg, 87 %). <sup>1</sup>H NMR (300 MHz, CDCl<sub>3</sub>):  $\delta$  9.13 (s, 1H), 7.69 (s, 1H), 7.24 (s, 1H), 7.08 (d,  $J$  = 8.4 Hz, 1H), 6.94 (d,  $J$  = 8.1 Hz, 1H), 5.93 (s, 1H), 5.19 (t,  $J$  = 5.1 Hz, 1H), 4.40 (d,  $J$  = 5.1 Hz, 2H), 3.95 (d,  $J$  = 13.8 Hz, 3H), 3.08 (t,  $J$  = 8.0 Hz, 2H), 1.87 (p,  $J$  = 7.8 Hz, 2H), 1.44-1.25 (m, 6H), 1.62 (s, 1H), 0.87 (t,  $J$  = 6.5 Hz, 3H). <sup>13</sup>C NMR (75 MHz, DMSO-d<sub>6</sub>):  $\delta$  169.8, 149.0, 148.7, 148.0, 147.9, 125.4, 125.3, 122.0, 121.2, 115.5, 115.4, 109.6, 109.1, 55.5, 52.4, 52.2, 43.3, 30.7, 27.2, 23.0, 21.8, 13.8. HRMS  $m/z$  calculated for C<sub>16</sub>H<sub>25</sub>N<sub>2</sub>O<sub>5</sub>S: 372.1588 [M+H]<sup>+</sup>; found, 372.1582.

**(*E*)-N-(2-(2-(4-hydroxy-3-methoxybenzylidene)hydrazineyl)-2-oxoethyl)octane-1-sulfonamide (17b).**



**17b** was synthesized from **16b** (133 mg, 1 eq.) and **4** (76 mg, 1 eq.) following the general procedure C and was obtained as a white solid (178 mg, 89 %). <sup>1</sup>H NMR (300 MHz, CDCl<sub>3</sub>):  $\delta$  9.85 (s, 0.1H), 9.69 (s, 1H), 8.03 (s, 0.1H), 7.72 (s, 1H), 7.37 (s, 0.1H), 7.22 (s, 1H), 7.09 (d,  $J$  = 8.1 Hz, 1H), 7.01 (d,  $J$  = 8.1 Hz, 0.1H), 6.93 (d,  $J$  = 8.1 Hz, 1H), 6.85 (d,  $J$  = 8.0 Hz, 0.1H), 5.98 (s, 1H), 5.79 (t,  $J$  = 6.1 Hz, 0.1H), 5.34 (t,  $J$  = 5.1 Hz, 1H), 4.38 (d,  $J$  = 5.1 Hz, 2H), 3.95 (s, 3H), 3.85 (s, 0.4H), 3.07 (t,  $J$  = 7.78 Hz, 2H), 1.85 (p,  $J$  = 7.5 Hz, 2H), 1.40-1.26 (m, 10H), 0.86 (t,  $J$  = 6.0 Hz, 3H). <sup>13</sup>C NMR (75 MHz, CDCl<sub>3</sub>):  $\delta$  170.3, 148.5, 147.1, 146.3, 125.5, 123.0, 114.5, 108.0, 56.2, 53.2, 44.3, 31.7, 29.1, 29.0, 28.4, 23.6, 22.6, 14.0. HRMS  $m/z$  calculated for C<sub>18</sub>H<sub>30</sub>N<sub>2</sub>O<sub>5</sub>S: 400.1901 [M+H]<sup>+</sup>; found, 400.1891.

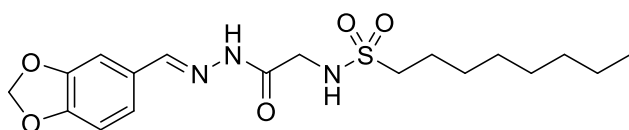
**(E)-N-(2-(2-(benzo[d][1,3]dioxol-5-ylmethylene)hydrazineyl)-2-oxoethyl)hexane-1-sulfonamide (18a).**



**18a** was synthesized from **16a** (69 mg, 1 eq.) and **7** (45 mg, 1 eq.) following the general procedure C and was obtained as a

white solid (93 mg, 84 %).  $^1\text{H}$  NMR (300 MHz,  $\text{CDCl}_3$ ):  $\delta$  9.43 (s, 1H), 7.70 (s, 1H), 7.25 (d,  $J = 1.2$  Hz, 1H), 7.03 (dd,  $J^1 = 1.2$  Hz,  $J^2 = 7.8$  Hz, 1H), 6.83 (d,  $J = 8.1$  Hz, 1H), 6.02 (s, 2H), 5.23 (t,  $J = 5.0$  Hz, 1H), 4.37 (d,  $J = 4.8$  Hz, 2H), 3.07 (t,  $J = 8.0$  Hz, 2H), 1.86 (qi,  $J = 7.4$  Hz, 2H), 1.42 (q,  $J = 6.8$  Hz, 2H), 1.32-1.25 (m, 4H), 0.87 (t,  $J = 6.4$  Hz, 3H).  $^{13}\text{C}$  NMR (75 MHz,  $\text{CDCl}_3$ ):  $\delta$  170.5, 150.2, 148.6, 145.8, 127.6, 124.1, 108.4, 105.7, 101.8, 53.4, 44.3, 31.4, 28.1, 23.6, 22.5, 14.0. HRMS  $m/z$  calculated for  $\text{C}_{16}\text{H}_{24}\text{N}_3\text{O}_5\text{S}$ : 370.4435  $[\text{M}+\text{H}]^+$ ; found, 370.1430.

**(E)-N-(2-(2-(benzo[d][1,3]dioxol-5-ylmethylene)hydrazineyl)-2-oxoethyl)octane-1-sulfonamide (18b).**

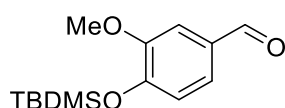


**18b** was synthesized from **16b** (75 mg, 1 eq.) and **7** (133 mg, 1 eq.) following the general procedure C and was

obtained as a white solid (147 mg, 74 %).  $^1\text{H}$  NMR (300 MHz,  $\text{CDCl}_3$ ):  $\delta$  9.90 (s, 1H), 8.05 (s, 0.1H), 7.74 (s, 1H), 7.29 (s, 0.1H), 7.24 (s, 1H), 7.03 (d,  $J = 7.9$  Hz, 1H), 6.81 (d,  $J = 8.0$  Hz, 1H), 6.72 (d,  $J = 7.9$  Hz, 0.1H), 6.00 (s, 2H), 5.93 (s, 0.2H), 5.44 (t,  $J = 4.7$  Hz, 1H), 4.36 (d,  $J = 5.0$  Hz, 2H), 3.97 (d,  $J = 5.4$  Hz, 0.2H), 3.08 (t,  $J = 7.9$  Hz, 2H), 1.85 (qi,  $J = 7.4$  Hz, 2H), 1.40-1.26 (m, 10H), 0.86 (t,  $J = 5.9$  Hz, 3H).  $^{13}\text{C}$  NMR (75 MHz,  $\text{CDCl}_3$ ):  $\delta$  170.7, 150.1, 148.6, 145.9, 127.8, 12.1, 108.4, 105.7, 101.7, 53.4, 44.3, 31.8, 29.2, 29.1, 28.4, 23.7, 22.7, 14.2. HRMS  $m/z$  calculated for  $\text{C}_{18}\text{H}_{28}\text{N}_3\text{O}_5\text{S}$ : 398.4975  $[\text{M}+\text{H}]^+$ ; found, 398.1747.

### 5.1.2 Synthesis of the hybrid capsaicinoids.

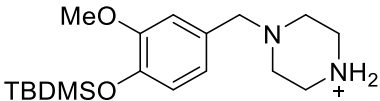
**4-((tert-butyldimethylsilyl)oxy)-3-methoxybenzaldehyde (19).**



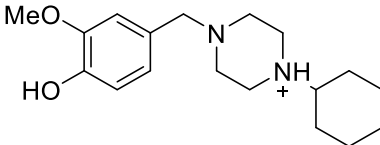
In a round-bottom flask containing a solution of **4** (2.1 g, 1 eq.), imidazole (1.9 g, 2 eq.), and DMAP (84.3 mg, 0.05 eq.) in DCM (50 mL) was added dropwise a solution of tert-butyldimethylsilyl chloride (2.5 g, 1.2 eq.) in DCM (50 mL). The reaction mixture was stirred for 2 h, at r.t. The reaction was quenched by the addition of a saturated solution of  $\text{NH}_4\text{Cl}$  (50.0 mL). The organic phase was

extracted. Another 50.0 mL of a saturated solution of  $\text{NH}_4\text{Cl}$  was added and extracted. The organic phase was washed with Brine (2 x 50.0 mL) and water (2 x 50.0 mL) and dried over  $\text{MgSO}_4$ . The solvent was evaporated under vacuum and the crude was column chromatographed (hexanes:EtOAc, 9:1) to afford the desired compound as a colorless oil (3.7 g, quant.).  $^1\text{H}$  NMR (300 MHz,  $\text{CDCl}_3$ ):  $\delta$  9.65 (s, 1H), 7.21 (d,  $J = 1.9$  Hz, 1H), 7.17 (dd,  $J = 8.0, 1.9$  Hz, 1H), 6.77 (d,  $J = 7.9$  Hz, 1H), 3.67 (s, 3H), 0.81 (s, 9H), -0.00 (s, 6H).  $^{13}\text{C}$  NMR (75 MHz,  $\text{CDCl}_3$ ):  $\delta$  191.1, 151.8, 151.5, 131.1, 126.3, 120.8, 110.2, 55.5, 25.7, 18.6, -4.5.

#### 1-(4-((tert-butyldimethylsilyl)oxy)-3-methoxybenzyl)piperazine (22).

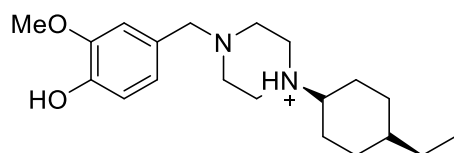
 In a round-bottom flask containing a solution of **19** (2.7 g, 1 eq.),  $\text{N}_1$ -Boc-piperazine (**20**, 2 g, 1.1 eq.) and AcOH (100  $\mu\text{L}$ ) in dry DCE (50 mL) was added  $\text{NaBH}(\text{OAc})_3$  (2.8 g, 1.3 eq.) and the reaction mixture was stirred for 48 h, at r.t. After completion (TLC), the reaction mixture was evaporated under vacuum. The crude was re-suspended in DCM for silica loading. Column chromatography (hexanes:EtOAc, 9:1 to 5:5 + 0.5%  $\text{Et}_3\text{N}$ ) afforded **21**, used in the next step without further purification. The intermediate **21** was then solubilized in a mixture of DCM/TFA (1:1; 40 mL) and was stirred for 90 min, at r.t. The solvents were removed under vacuum. The crude compound was solubilized in EtOAc and precipitated by the addition of dry  $\text{Et}_2\text{O}$  to afford the desired compound as a white solid (2.5 g, 45 %).  $^1\text{H}$  NMR (300 MHz,  $\text{CD}_3\text{OD}$ ):  $\delta$  7.12 (d,  $J = 1.2$  Hz, 1H), 6.95 (dd,  $J = 8.0, 1.4$  Hz, 1H), 6.89 (d,  $J = 8.0$  Hz, 1H), 4.25 (s, 2H), 3.83 (s, 3H), 3.48 (dd,  $J = 27.9, 4.1$  Hz, 8H), 1.00 (s, 9H), 0.15 (s, 6H).  $^{13}\text{C}$  NMR (75 MHz,  $\text{CDCl}_3$ ):  $\delta$  152.8, 147.8, 124.9, 124.1, 122.1, 115.5, 61.9, 55.9, 42.4, 26.1, 19.3, -4.5.

#### 4-((4-cyclohexylpiperazin-1-yl)methyl)-2-methoxyphenol (24c).

 General procedure D: In a round-bottom flask containing a solution of **22** (311 mg, 1.1 eq.) in dry DCE (5 mL) was added  $\text{Et}_3\text{N}$  (280  $\mu\text{L}$ , 4 eq.). After 15 min, cyclohexanone (**23c**, 52  $\mu\text{L}$ , 1 eq.) and  $\text{NaBH}(\text{OAc})_3$  (144 mg, 1.3 eq.) were added, and the mixture was stirred for 24 h, at r.t. The reaction mixture was evaporated under vacuum. The crude was re-suspended in DCM and was column chromatographed (hexanes:EtOAc, 5:5 + 0.5%  $\text{Et}_3\text{N}$ ) afforded the protected intermediate, used in the next step without further purification. To the previously obtained compound, a solution of TBAF (in THF, 1.1 mL, 1 M) was

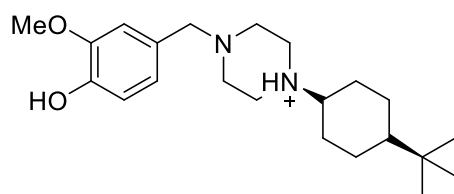
added dropwise, and the reaction was stirred for 3 h, at r.t. Upon completion, the reaction was quenched by the addition of saturated solution of NaHCO<sub>3</sub> (3.0 mL) and was extracted with EtOAc (2 x 10.0 mL). The collected organic phase was washed with Brine (2 x 10.0 mL) and water (2 x 10.0 mL), and dried over Na<sub>2</sub>SO<sub>4</sub>. The solvent was removed under vacuum. After work-up, the crude was solubilized in MeOH/HCl (3.0 M) and was precipitated by the addition of dry Et<sub>2</sub>O as a white powder (140 mg, 37 %). <sup>1</sup>H NMR (300 MHz, D<sub>2</sub>O): δ 7.15 (d, *J* = 1.5 Hz, 1H), 7.02 (m, 2H), 4.39 (s, 2H), 3.90 (s, 3H), 3.44 (m, 9H), 2.12 (d, *J* = 11.1 Hz, 2H), 1.92 (d, *J* = 12.9 Hz, 2H), 1.67 (m, 1H), 1.42 (m, 4H), 1.15 (m, 1H). <sup>13</sup>C NMR (75 MHz, D<sub>2</sub>O): δ 147.8, 146.8, 124.8, 119.8, 115.9, 114.9, 66.3, 60.4, 56.0, 48.1, 45.5, 26.5, 24.3, 24.2. HRMS *m/z* calculated for C<sub>18</sub>H<sub>29</sub>N<sub>2</sub>O<sub>2</sub>: 305.2224 [M+H]<sup>+</sup>; found, 305.2220.

#### 4-((4-((1*S*,4*S*)-4-ethylcyclohexyl)piperazin-1-yl)methyl)-2-methoxyphenol (24d).



**24d** was synthesized by **22** (311 mg, 1.1 eq.) and 4-ethyl-cyclohexanone (**23d**, 71 μL, 1 eq.) following the general procedure D and was obtained as a white powder (119 mg, 59 %). <sup>1</sup>H NMR (300 MHz, CD<sub>3</sub>OD): δ 7.15 (d, *J* = 2.0 Hz, 1H), 6.90 (dd, *J* = 8.1, 2.0 Hz, 1H), 6.77 (d, *J* = 8.1 Hz, 1H), 4.29 (s, 2H), 3.82 (s, 3H), 3.76-3.49 (m, 9H), 2.47 (d, *J* = 2.6 Hz, 4H), 1.85-1.47 (m, 9H), 1.33 (p, *J* = 7.3 Hz, 2H), 0.82 (t, *J* = 7.4 Hz, 3H). <sup>13</sup>C NMR (75 MHz, D<sub>2</sub>O): δ 147.8, 146.8, 124.8, 119.8, 115.9, 114.9, 66.3, 60.4, 56.0, 48.0, 45.8, 33.2, 27.0, 23.3, 21.7, 11.3. HRMS *m/z* calculated for C<sub>20</sub>H<sub>33</sub>N<sub>2</sub>O<sub>2</sub>: 333.2537 [M+H]<sup>+</sup>; found, 333.2532.

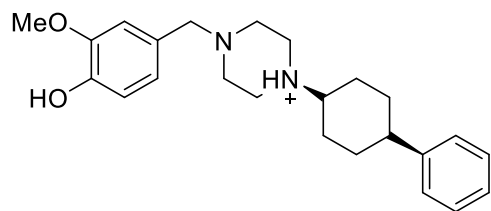
#### 4-((4-((1*S*,4*S*)-4-(tert-butyl)cyclohexyl)piperazin-1-yl)methyl)-2-methoxyphenol (24e).



**24e** was synthesized by **22** (311 mg, 1.1 eq.) and 4-tert-butyl-cyclohexanone (**23e**, 77 mg, 1 eq) following general procedure D and was purified by RP-UHPLC (from 75%A25%D to 65%A35%D in 30 min; RT<sub>7min</sub>: 2.33 min) to be afforded as white powder (89 mg, 30 %). <sup>1</sup>H NMR (300 MHz, C<sub>6</sub>D<sub>6</sub>): δ 7.03 (d, *J* = 8.0 Hz, 1H), 6.88 (d, *J* = 1.7 Hz, 1H), 6.81 (dd, *J* = 8.0, 1.8 Hz, 1H), 3.34 (s, 2H), 3.19 (s, 3H), 2.45 (s, 8H), 2.08 (t, *J* = 8.0 Hz, 1H), 1.95 (d, *J* = 14.6 Hz, 2H), 1.54-1.34 (m, 4H), 1.19 (tt, *J* = 13.4, 2.9 Hz, 2H), 1.04 (tt, *J* = 11.7, 3.7 Hz, 1H), 0.92 (s, 9H). <sup>13</sup>C NMR (75 MHz, C<sub>6</sub>D<sub>6</sub>): δ 147.1, 145.7, 130.8, 122.5, 114.4, 111.8, 63.5, 58.4, 55.2,

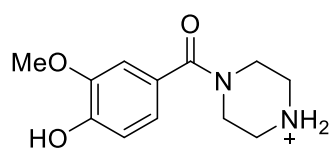
54.1, 50.5, 48.8, 32.8, 29.6, 27.8, 21.6. HRMS  $m/z$  calculated for  $C_{22}H_{37}N_2O_2$ : 361.2850  $[M+H]^+$ ; found, 361.2843.

**2-methoxy-4-((4-((1*S*,4*S*)-4-phenylcyclohexyl)piperazin-1-yl)methyl)phenol (24f).**

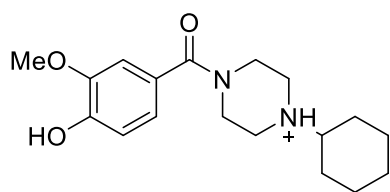


**24f** was synthesized by **22** (311 mg, 1.1 eq.) and 4-phenyl-cyclohexanone (**23f**, 87 mg, 1 eq.) following general procedure D, and was purified by RP-UHPLC (from 75%A25%D to 65%A35%D in 30 min;  $RT_{7min}$ : 3.66 min) to be afforded as a white powder (151 mg, 50 %).  $^1H$  NMR (300 MHz,  $C_6D_6$ ):  $\delta$  7.25 (ddd,  $J = 15.0, 10.7, 4.7$  Hz, 4H), 7.10 (tt,  $J = 7.0$  Hz, 1H), 7.04 (d,  $J = 8.0$  Hz, 1H), 6.89 (d,  $J = 1.7$  Hz, 1H), 6.82 (dd,  $J = 8.0, 1.7$  Hz, 1H), 3.37 (s, 2H), 3.20 (s, 3H), 2.51-2.45 (m, 9H), 2.11 (t,  $J = 2.9$  Hz, 1H), 2.05-1.87 (m, 4H), 1.55-1.50 (m, 2H), 1.35-1.25 (m, 2H).  $^{13}C$  NMR (75 MHz,  $C_6D_6$ ):  $\delta$  147.9, 147.1, 145.8, 130.7, 128.7, 127.4, 126.2, 122.5, 114.5, 111.8, 63.5, 58.8, 55.2, 54.1, 50.4, 44.4, 28.9, 28.7. HRMS  $m/z$  calculated for  $C_{24}H_{33}N_2O_2$ : 381.2537  $[M+H]^+$ ; found, 381.2526.

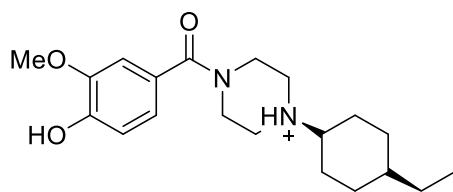
**(4-hydroxy-3-methoxyphenyl)(piperazin-1-yl)methanone (27).**



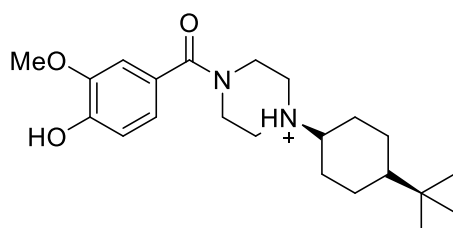
A round-bottom flask was added 4-hydroxy-3-methoxybenzoic acid (**25**, 841 mg, 1 eq.), **20** (1 g, 1.1 eq), EDCI (1 g, 1.1 eq) and DMAP (672 mg, 1.1 eq.) in DCM (50 mL). The mixture was stirred for 17 h at r.t. until all the reagents were solubilized. Upon completion, the reaction mixture was evaporated under vacuum and the crude was re-suspended in DCM for silica loading. Column chromatography (Hexanes:EtOAc, 5:5) afforded the intermediate **26**, used in the next step without further purification Compound **26** (1 g, 1 eq.) was added to a round-bottom flask and was suspended in an aqueous solution of HCl (1 M). The suspension was refluxed for 2 h, then the solvent was removed under vacuum. The gummy residue was solubilized in a minimal amount of water and lyophilized to afford the desired compound as a white powder (822 mg, 60%).  $^1H$  NMR (300 MHz,  $D_2O$ ):  $\delta$  7.06 (d,  $J = 1.5$  Hz, 1H), 6.98-6.90 (m, 2H), 3.84 (s, 7H), 3.58 (s, 2H), 3.31 (s, 4H).  $^{13}C$  NMR (75 MHz,  $D_2O$ ):  $\delta$  172.5, 147.4, 147.4, 125.3, 120.9, 115.3, 111.4, 56.0, 43.0, 40.3.

**(4-cyclohexylpiperazin-1-yl)(4-hydroxy-3-methoxyphenyl)methanone (28c).**

General procedure E: In a round-bottom flask containing a solution of **27** (108 mg, 1.1 eq.) in dry DCE (5 mL) was added Et<sub>3</sub>N (195 μL, 4 eq.). After 15 min, **23c** (37 μL, 1 eq.) and NaBH(OAc)<sub>3</sub> (101 mg, 1.3 eq.) were added, and the mixture was stirred for 48 h, at r.t. Upon completion, the solvent was removed under vacuum. The compound was purified by RP-UHPLC (from 90%A10%D to 60%A40%D in 20 min; RT<sub>7min</sub>: 1.47 min) and was afforded as a white powder (54 mg, 31 %). <sup>1</sup>H NMR (300 MHz, D<sub>2</sub>O): δ 7.09 (s, 1H), 7.01-6.95 (m, 2H), 4.12 (bs, 1H), 3.86 (s, 3H), 3.54-3.18 (m, 7H), 2.08 (d, *J* = 10.9 Hz, 2H), 1.90 (d, *J* = 12.8 Hz, 2H), 1.66 (d, *J* = 12.6 Hz, 1H), 1.52-1.26 (m, 4H), 1.21-1.08 (m, 1H). <sup>13</sup>C NMR (75 MHz, D<sub>2</sub>O): δ 172.3, 147.5, 125.1, 121.0, 115.3, 111.5, 66.1, 56.0, 48.0, 26.6, 24.4. HRMS *m/z* calculated for C<sub>18</sub>H<sub>27</sub>N<sub>2</sub>O<sub>3</sub>: 319.2016 [M+H]<sup>+</sup>; found, 319.2022.

**(4-((1*S*,4*S*)-4-ethylcyclohexyl)piperazin-1-yl)(4-hydroxy-3-methoxyphenyl)methanone (28d).**

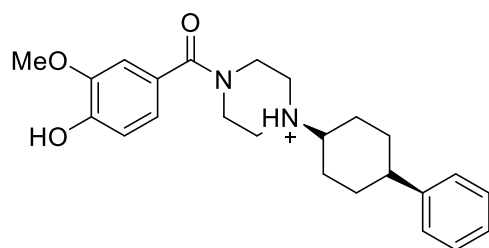
**28d** was synthesized **27** (150 mg, 1.1 eq.) and **23d** (71 μL, 1 eq.) following general procedure E, and was obtained as a white powder (41 mg, 21 %). <sup>1</sup>H NMR (300 MHz, CD<sub>3</sub>OD): δ 7.09 (d, *J* = 1.9 Hz, 1H), 7.00 (dd, *J* = 8.1, 1.9 Hz, 1H), 6.87 (d, *J* = 8.1 Hz, 1H), 4.42 (s, 2H), 3.89 (s, 3H), 3.61 (d, *J* = 12.4 Hz, 2H), 3.50 (t, *J* = 13.0 Hz, 2H), 3.20 (ddd, *J* = 24.4, 11.7, 3.1 Hz, 3H), 1.95-1.91 (m, 2H), 1.83-1.58 (m, 7H), 1.44 (q<sub>i</sub>, *J* = 7.3 Hz, 2H), 0.93 (t, *J* = 7.4 Hz, 3H). <sup>13</sup>C NMR (75 MHz, CD<sub>3</sub>OD): δ 172.7, 150.5, 149.2, 126.1, 122.2, 116.1, 112.6, 67.5, 56.6, 35.1, 28.9, 24.7, 23.0, 12.4. HRMS *m/z* calculated for C<sub>20</sub>H<sub>31</sub>N<sub>2</sub>O<sub>3</sub>: 347.2329 [M+H]<sup>+</sup>; found, 347.2316.

**(4-((1*S*,4*S*)-4-(tert-butyl)cyclohexyl)piperazin-1-yl)(4-hydroxy-3-methoxyphenyl)methanone (28e).**

**28e** was synthesized from **27** (150 mg, 1.1 eq.) and **23e** (77 mg, 1 eq.) following general procedure E, as was obtained a white powder (53 mg, 26 %). <sup>1</sup>H NMR (300 MHz, CD<sub>3</sub>OD): δ 7.10 (d, *J* = 1.8 Hz, 1H), 7.00 (dd, *J* = 8.1, 1.9 Hz, 1H), 6.87 (d, *J* = 8.1

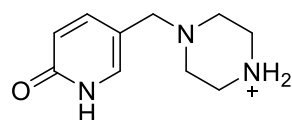
Hz, 1H), 4.35 (s, 2H), 3.89 (s, 3H), 3.76-3.63 (m, 4H), 3.40 (t,  $J = 3.5$  Hz, 1H), 3.15 (td,  $J = 12.0, 3.0$  Hz, 2H), 2.28 (d,  $J = 14.0$  Hz, 2H), 1.82-1.72 (m, 4H), 1.48-1.34 (m, 2H), 1.23 (tt,  $J = 11.2, 3.1$  Hz, 1H), 0.92 (s, 9H).  $^{13}\text{C}$  NMR (75 MHz,  $\text{CD}_3\text{OD}$ ):  $\delta$  172.7, 150.6, 149.2, 126.1, 122.2, 116.1, 112.6, 65.0, 56.6, 51.2, 33.5, 28.0, 26.8, 22.6. HRMS  $m/z$  calculated for  $\text{C}_{22}\text{H}_{35}\text{N}_2\text{O}_3$ : 375.2642  $[\text{M}+\text{H}]^+$ ; found, 375.2626.

**(4-hydroxy-3-methoxyphenyl)(4-((1*S*,4*S*)-4-phenylcyclohexyl)piperazin-1-yl)methanone (28f).**



**28f** was synthesized from **27** (150 mg, 1.1 eq.) and **23f** (87 mg, 1 eq.) following general procedure E, and was obtained as a white powder (52 mg, 24 %).  $^1\text{H}$  NMR (300 MHz,  $\text{CD}_3\text{OD}$ ):  $\delta$  7.40 (d,  $J = 7.5$  Hz, 2H), 7.31 (t,  $J = 7.6$  Hz, 2H), 7.18 (t,  $J = 7.2$  Hz, 1H), 7.08 (d,  $J = 1.7$  Hz, 1H), 6.99 (dd,  $J = 8.1, 1.8$  Hz, 1H), 6.86 (d,  $J = 8.1$  Hz, 1H), 4.37 (s, 2H), 3.88 (s, 3H), 3.67-3.53 (m, 4H), 3.42 (s, 1H), 3.15 (td,  $J = 12.1, 3.0$  Hz, 2H), 2.98 (s, 1H), 2.34-2.26 (m, 2H), 2.06-1.85 (m, 6H).  $^{13}\text{C}$  NMR (75 MHz,  $\text{CD}_3\text{OD}$ ):  $\delta$  172.7, 150.5, 149.1, 144.9, 129.6, 128.3, 127.1, 126.1, 122.2, 116.1, 112.6, 66.4, 56.6, 49.6, 39.3, 29.1, 25.0. HRMS  $m/z$  calculated for  $\text{C}_{24}\text{H}_{31}\text{N}_2\text{O}_3$ : 395.2329  $[\text{M}+\text{H}]^+$ ; found, 395.2312.

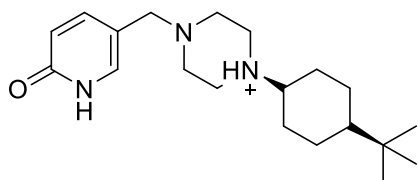
**5-(piperazin-1-ylmethyl)pyridin-2(1H)-one (31).**



In a round-bottom flask containing a solution of 6-hydroxynicotinaldehyde (**29**, 616 mg, 1 eq.) in dry DCE (50 mL) was added **20** (1 g, 1.1 eq.). After 5 min stirring,  $\text{NaBH}(\text{OAc})_3$  (1.3 g, 1.3 eq.) was added, and the mixture was stirred for 48 h, at r.t. Upon completion, the reaction mixture was diluted with DCM (25 mL) and was extracted with an aqueous solution of HCl (3 x 25mL; 1.0 M). The collected aqueous phase was basified with an aqueous saturated solution of  $\text{NaHCO}_3$  and extracted with EtOAc (2 x 25.0 mL). The organic phase was dried over  $\text{Na}_2\text{SO}_4$  and evaporated under vacuum to yield the intermediate **30** as white solids, used in the next step without further purification. Compound **30** (1.1 g, 1 eq.) was solubilized in a mixture of DCM: TFA (1:1, 20 mL) and was stirred at r.t. for 90 min. The reaction mixture was then evaporated and the residue was solubilized in water (50.0 mL) and lyophilized to afford the desired compound as a white powder (1.6 g, 78 %).  $^1\text{H}$  NMR (300 MHz,  $\text{D}_2\text{O}$ ):  $\delta$  7.82-7.78 (m, 1H), 6.72 (dd,  $J = 2.0,$

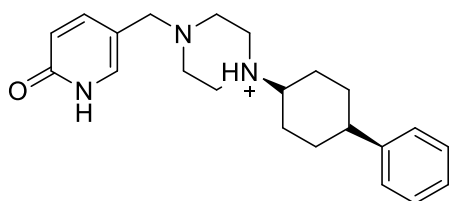
4.1, 10.2 Hz, 2H), 4.37 (s, 2H), 3.64 (s, 8H), 3.60 (s, 1H).  $^{13}\text{C}$  NMR (75 MHz,  $\text{D}_2\text{O}$ ):  $\delta$  164.5, 144.8, 138.8, 120.0, 117.5, 108.7, 57.1, 47.7, 40.7, 40.3.

**5-((4-((1*S*,4*S*)-4-(tert-butyl)cyclohexyl)piperazin-1-yl)methyl)pyridin-2(1H)-one (32e).**



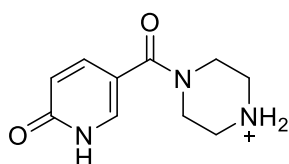
**32e** was synthesized from **31** (147 mg, 1.2 eq.) and **23e** (77 mg, 1 eq.) following the general procedure E, and was purified by RP-UHPLC (from 75%A25%D to 70%A30%D in 30 min;  $\text{RT}_{7\text{min}}$ : 1.61 min) to be afforded as a white powder (43 mg, 15 %).  $^1\text{H}$  NMR (300 MHz,  $\text{C}_6\text{D}_6$ ):  $\delta$  7.19 (d,  $J = 2.3$  Hz, 1H), 6.92 (s, 1H), 6.59 (d,  $J = 9.3$  Hz, 1H), 2.76 (s, 2H), 2.43 (s, 4H), 2.19 (s, 4H), 2.05 (d,  $J = 7.2$  Hz, 2H), 1.94 (d,  $J = 14.1$  Hz, 2H), 1.51-1.36 (m, 4H), 1.21 (t,  $J = 13.0$  Hz, 1H), 1.09-1.00 (m, 1H), 0.92 (s, 9H).  $^{13}\text{C}$  NMR (75 MHz,  $\text{C}_6\text{D}_6$ ):  $\delta$  165.7, 143.4, 133.9, 120.2, 117.2, 58.9, 58.3, 53.6, 50.3, 48.7, 32.8, 29.5, 27.8, 21.6. HRMS  $m/z$  calculated for  $\text{C}_{20}\text{H}_{34}\text{N}_3\text{O}$ : 332.2696  $[\text{M}+\text{H}]^+$ ; found, 332.2682.

**5-((4-((1*S*,4*S*)-4-phenylcyclohexyl)piperazin-1-yl)methyl)pyridin-2(1H)-one (32f).**



**32f** was synthesized from **31** (147 mg, 1.2 eq.) and **23f** (87 mg, 1 eq.) following general procedure E, and was obtained as a white powder (95 mg, 45 %).  $^1\text{H}$  NMR (300 MHz,  $\text{C}_6\text{D}_6$ ):  $\delta$  14.26 (s, 1H), 7.30-7.18 (m, 5H), 7.10 (tt,  $J = 7.0, 1.5$  Hz, 1H), 6.89 (d,  $J = 2.0$  Hz, 1H), 6.61 (d,  $J = 9.3$  Hz, 1H), 2.77 (s, 2H), 2.54 (tt,  $J = 11.0, 3.6$  Hz, 1H), 2.33 (s, 4H), 2.20 (s, 4H), 2.09 (s, 1H), 2.05-1.87 (m, 4H), 1.57-1.52 (m, 2H), 1.32 (t,  $J = 12.9$  Hz, 2H).  $^{13}\text{C}$  NMR (75 MHz,  $\text{C}_6\text{D}_6$ ):  $\delta$  165.8, 147.8, 143.2, 134.1, 128.7, 127.3, 126.2, 120.4, 116.9, 59.1, 58.7, 53.6, 50.3, 44.3, 28.9, 28.7. HRMS  $m/z$  calculated for  $\text{C}_{22}\text{H}_{30}\text{N}_3\text{O}$ : 352.2383  $[\text{M}+\text{H}]^+$ ; found, 352.2372.

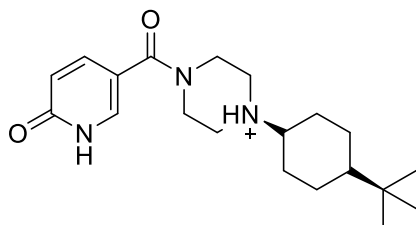
**5-(piperazine-1-carbonyl)pyridin-2(1H)-one (35).**



A round-bottom flask was added 6-hydroxynicotinic acid (**33**, 696 mg, 1 eq.), **20** (1 g, 1.1 eq), EDCI (1 g, 1.1 eq) and DMAP (672 mg, 1.1 eq.) in DCM (50 mL). The mixture was stirred for 17 h at r.t. until all the reagents were solubilized. Upon completion, the reaction mixture was washed with an aqueous solution of HCl (3 x 254 mL; 1.0 M). The resulting organic phase was dried over  $\text{MgSO}_4$  and evaporated. The obtained intermediate **34** was used in the next step without further purification. Compound **34** (1 g, 1 eq.) was

dissolved in a mixture of DCM (25.0 mL) and TFA (25.0 mL) and was stirred at r.t., for 90 min. The reaction mixture was cooled in an ice bath and H<sub>2</sub>O (50.0 mL) was added to it. The aqueous phase was extracted and washed with DCM (2 x 50.0 mL). The collected aqueous phase was partially evaporated under vacuum and was lyophilized to yield the desired compound as a white powder (1.1 g, 70%). <sup>1</sup>H NMR (300 MHz, D<sub>2</sub>O): δ 7.81 (d, *J* = 2.2 Hz, 1H), 7.72 (dd, *J* = 9.4, 2.6 Hz, 1H), 6.65 (d, *J* = 9.4 Hz, 1H), 3.88 (t, *J* = 10.6, 5.2 Hz, 4H), 3.32 (t, *J* = 10.6, 5.2 Hz, 4H). <sup>13</sup>C NMR (75 MHz, D<sub>2</sub>O): δ 168.6, 164.5, 141.7, 136.7, 119.2, 114.6, 42.8.

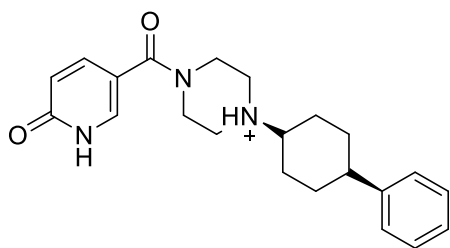
**5-(4-((1*S*,4*S*)-4-(tert-butyl)cyclohexyl)piperazine-1-carbonyl)pyridin-2(1H)-one (36e).**



**36e** was synthesized from **35** (177 mg, 1.1 eq.) and **23e** (77 mg, 1 eq.) following general procedure E, and was purified by RP-UHPLC (from 75%A25%D to 60%A40%D in 30 min; RT<sub>7min</sub>: 1.70 min) to be afforded as a white powder (16 mg, 6 %). <sup>1</sup>H NMR (300 MHz,

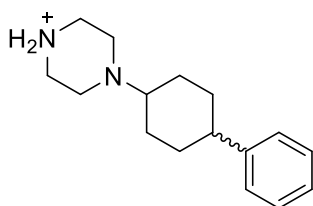
CD<sub>3</sub>OD): δ 7.78 (d, *J* = 2.1 Hz, 1H), 7.70 (dd, *J* = 9.5, 2.6 Hz, 1H), 6.56 (d, *J* = 9.4 Hz, 1H), 4.31 (s, 2H), 3.67 (d, *J* = 45.8 Hz, 4H), 3.36 (t, *J* = 3.5 Hz, 1H), 3.13 (s, 2H), 2.28 (d, *J* = 15.5 Hz, 2H), 1.77 (dd, *J* = 21.9, 8.9 Hz, 4H), 1.43-1.17 (m, 3H), 0.90 (s, 9H). <sup>13</sup>C NMR (75 MHz, CD<sub>3</sub>OD): δ 168.9, 165.2, 142.1, 138.6, 120.7, 114.9, 65.0, 51.1, 33.5, 27.9, 26.8, 22.5. HRMS *m/z* calculated for C<sub>20</sub>H<sub>32</sub>N<sub>3</sub>O<sub>2</sub>: 346.2489 [M+H]<sup>+</sup>; found, 346.2490.

**5-(4-((1*S*,4*S*)-4-phenylcyclohexyl)piperazine-1-carbonyl)pyridin-2(1H)-one (36f).**

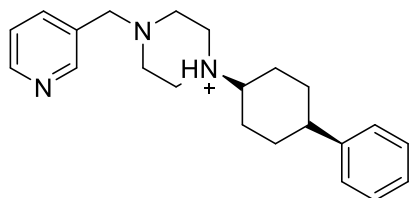


**36f** was synthesized from **35** (177 mg, 1.1 eq.) and **23f** (87 mg, 1 eq.) following general procedure E, and was purified by RP-UHPLC (from 75%A25%D to 60%A40%D in 30 min; RT<sub>7min</sub>: 1.62 min) to be afforded as a white powder (96 mg, 23 %). <sup>1</sup>H NMR

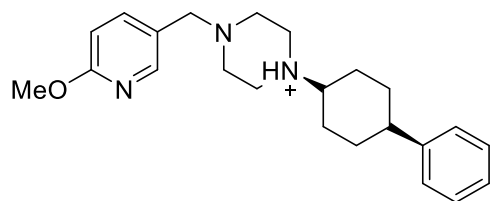
(300 MHz, D<sub>2</sub>O): δ 7.84 (d, *J* = 2.1 Hz, 1H), 7.75 (dd, *J* = 9.4, 2.5 Hz, 1H), 7.47-7.40 (m, 4H), 7.30 (dt, *J* = 8.4, 2.1 Hz, 1H), 6.69 (d, *J* = 9.5 Hz, 1H), 4.36 (s, 2H), 3.68-3.46 (m, 5H), 3.18 (dt, *J* = 12.3, 3.3 Hz, 2H), 3.03 (s, 1H), 2.25-2.15 (m, 2H), 2.01-1.81 (m, 6H). <sup>13</sup>C NMR (75 MHz, D<sub>2</sub>O): δ 168.5, 164.6, 144.1, 141.6, 136.9, 128.7, 127.3, 126.2, 119.4, 117.5, 114.4, 65.2, 48.6, 37.1, 27.3, 23.2. HRMS *m/z* calculated for C<sub>22</sub>H<sub>28</sub>N<sub>3</sub>O<sub>2</sub>: 366.2176 [M+H]<sup>+</sup>; found, 366.2184.

**1-(4-phenylcyclohexyl)piperazine (38f).**

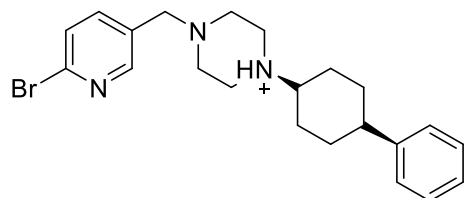
In a round-bottom flask containing a solution of **23f** (1.7 g, 1 eq.) and **20** (2.1 g, 1.1 eq.) in dry DCE (20.0 mL), was added AcOH (100  $\mu$ L). After 15 min, NaBH(OAc)<sub>3</sub> (287 g, 1.3 eq.) was added and the mixture was stirred for 48 h at r.t. The reaction was quenched by addition of saturated aqueous solution of NaHCO<sub>3</sub> (20 mL). The mixture was extracted with DCM (3 x 20.0 mL). The organic phase was collected and extracted with an aqueous solution of HCl (1 M; 3 x 20 mL) and was washed with H<sub>2</sub>O (1 x 20 mL). The resulting organic phase was dried in Na<sub>2</sub>SO<sub>4</sub>, and the solvent was removed by vacuum to afford the desired intermediate **37f** used in the next step without further purification. Compound **37f** (3 g, 1 eq.) was suspended in an aqueous HCl solution (2 M; 35 mL) and was refluxed for 90 min. The solvent was partially removed by vacuum. The resulting solution was diluted with H<sub>2</sub>O (10.0 mL) and lyophilized to afford the mixture of diastereomers as a white powder (2.8 g, 88 %). <sup>1</sup>H-NMR (300 MHz, D<sub>2</sub>O,  $\delta$  = ppm):  $\delta$  7.37-7.24 (m, 5H), 3.74-3.43 (m, 9H), 2.84 (s, 1H), 2.25-1.30 (m, 8H). <sup>13</sup>C-NMR (75 MHz, CDCl<sub>3</sub>,  $\delta$  = ppm):  $\delta$  145.8, 144.3, 128.7, 127.4, 126.9, 126.2, 65.8, 65.4, 46.0, 45.5, 41.0, 40.5, 37.9, 31.6, 27.3, 26.4, 23.5.

**1-((1*S*,4*S*)-4-phenylcyclohexyl)-4-(pyridin-3-ylmethyl)piperazine (42f).**

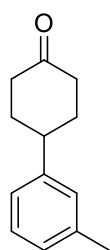
**42f** was synthesized from **38f** (169 mg, 1.1 eq.) and nicotinaldehyde (**39**, 47  $\mu$ L, 1 eq.) following general procedure E, and was purified by RP-UHPLC (from 75%A25%D to 60%A40%D in 20 min; RT<sub>7min</sub>: 1.56 min) to be afforded as a white powder (193 mg, 68 %). <sup>1</sup>H NMR (300 MHz, C<sub>6</sub>D<sub>6</sub>):  $\delta$  8.73 (d,  $J$  = 1.6 Hz, 1H), 8.53 (dd,  $J$  = 4.7, 1.6 Hz, 1H), 7.38 (dt,  $J$  = 7.7, 1.9 Hz, 1H), 7.29-7.36 (m, 4H), 7.10 (dt,  $J$  = 6.9, 1.7 Hz, 1H), 6.79 (dd,  $J$  = 7.7, 4.7 Hz, 1H), 3.14 (s, 2H), 2.52 (tt,  $J$  = 11.1, 3.9 Hz, 1H), 2.28 (s, 8H), 2.09-2.06 (m, 1H), 2.02-1.83 (m, 4H), 1.55-1.49 (m, 2H), 1.34-1.24 (m, 2H). <sup>13</sup>C NMR (75 MHz, CDCl<sub>3</sub>):  $\delta$  151.1, 149.1, 147.9, 136.1, 134.3, 128.7, 127.3, 126.2, 123.2, 60.4, 58.7, 53.9, 50.3, 44.3, 28.9, 28.7. HRMS  $m/z$  calculated for C<sub>22</sub>H<sub>30</sub>N<sub>3</sub>: 336.2434 [M+H]<sup>+</sup>; found, 336.2435.

**1-((6-methoxypyridin-3-yl)methyl)-4-((1*S*,4*S*)-4-phenylcyclohexyl)piperazine (43f).**

**43f** was synthesized from **38f** (169 mg, 1.1 eq.) and 6-methoxynicotinaldehyde (**40**, 69 mg, 1 eq.) following general procedure E, and was afforded as a white powder (94 mg, 43 %). <sup>1</sup>H NMR (300 MHz, D<sub>2</sub>O): δ 8.25 (d, *J* = 2.2 Hz, 1H), 7.98 (dd, *J* = 8.8, 2.5 Hz, 1H), 7.44-7.38 (m, 4H), 7.29 (ddd, *J* = 8.5, 5.6, 3.0 Hz, 1H), 7.08 (d, *J* = 8.8 Hz, 1H), 4.38 (s, 2H), 3.99 (s, 3H), 3.58 (s, 8H), 2.99 (s, 1H), 2.16 (dd, *J* = 13.2, 10.9 Hz, 2H), 1.94 (ddd, *J* = 16.2, 15.7, 8.3 Hz, 6H). <sup>13</sup>C NMR (75 MHz, D<sub>2</sub>O): δ 164.5, 147.8, 144.1, 143.7, 128.7, 127.2, 126.2, 118.6, 111.2, 65.3, 57.0, 55.0, 48.0, 46.7, 37.5, 27.2, 23.4. HRMS *m/z* calculated for C<sub>23</sub>H<sub>32</sub>N<sub>3</sub>O: 366.2540 [M+H]<sup>+</sup>; found, 366.2521.

**1-((6-bromopyridin-3-yl)methyl)-4-((1*S*,4*S*)-4-phenylcyclohexyl)piperazine (44f).**

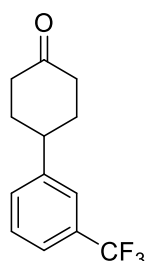
**44f** was synthesized from **38f** (337 mg, 1.2 eq.) and 6-bromo-nicotinaldehyde (**41**, 186 mg, 1 eq.) following general procedure E, and was obtained as a white powder (294 mg, 60 %). <sup>1</sup>H NMR (300 MHz, C<sub>6</sub>D<sub>6</sub>): δ 8.19 (d, *J* = 1.4 Hz, 1H), 7.29-7.20 (m, 4H), 7.10 (dt, *J* = 7.0, 1.7 Hz, 1H), 7.03-6.96 (m, 2H), 2.91 (s, 2H), 2.53 (tt, *J* = 11.0, 3.8 Hz, 1H), 2.3 (s, 4H), 2.2 (2, 4H), 2.07 (t, *J* = 3.0 Hz, 1H), 2.02-1.84 (m, 4H), 1.56-1.51 (m, 2H), 1.37-1.24 (m, 2H). <sup>13</sup>C NMR (75 MHz, C<sub>6</sub>D<sub>6</sub>): δ 150.9, 147.8, 141.3, 138.9, 133.8, 128.7, 127.8, 127.3, 126.3, 59.3, 58.67, 53.8, 50.2, 44.3, 28.8, 28.7. HRMS *m/z* calculated for C<sub>22</sub>H<sub>29</sub>BrN<sub>3</sub>: 414.1539 [M+H]<sup>+</sup>; found, 414.1526.

**4-(*m*-tolyl)cyclohexan-1-one (50g).**

General procedure F: A dry three-neck round-bottom flask equipped with a condenser was charged with Mg (342 mg, 1.4 eq.) and dry THF (1.0 mL) under Argon atmosphere. To this suspension, a solution of 1-Bromo-3-methyl-benzene (**45g**, 1.2 mL, 1.2 eq.) in dry THF (0.4 mL) was added dropwise using an addition funnel. The reaction mixture was stirred under reflux and Argon atmosphere for 30 min. The obtained Grignard-reagent was used *in situ*, without purification. After cooling the previous mixture to r.t., a solution of 1,4-dioxaspiro[4.5]decan-8-one (**46**, 1.6 g, 1 eq.) in dry THF (1 mL) was added dropwise and the reaction was stirred for another 30 min, under reflux and Argon atmosphere. The reaction was quenched by the addition of an

aqueous saturated solution of  $\text{NH}_4\text{Cl}$  (6 mL) and was extracted with  $\text{Et}_2\text{O}$  (3 x 50 mL). The combined organic phase was dried over  $\text{MgSO}_4$  and evaporated under vacuum. The obtained residue column chromatographed (hexanes:EtOAc, 95:05 to 75:25) to yield the intermediate **47g** used in the next step without further purification. Compound **47g** was dissolved in dry toluene (44 mL) and added to a new round-bottom flask. To this solution,  $\text{TsOH}\cdot\text{H}_2\text{O}$  (177 mg, 0.1 eq.) was added and the reaction mixture was stirred under reflux and Argon atmosphere for 4 h. The reaction mixture then was cooled to r.t. and was washed with an aqueous saturated solution of  $\text{NaHCO}_3$  (3 x 50 mL), was dried over  $\text{MgSO}_4$  and was evaporated under vacuum. The obtained intermediate **48g** (yellow oil) was used in the next step without further purification. To a two-neck round-bottom flask, was added a solution of **48g** in EtOAc (20 mL). To the stirring solution, Pd/C (229 mg, 0.3 eq.) was added and the system was purged with Argon, followed by  $\text{H}_2$ . The reaction was stirred at r.t., under an  $\text{H}_2$  atmosphere for 16 h. Upon completion (TLC), the reaction mixture was filtered over a pad of Celite (washed thoroughly 3 X 50 mL of EtOAc) to remove the catalyst. The solvent was removed under vacuum and the crude **49g** was used in the next step without further purification. The intermediate was dissolved in a mixture of acetone and  $\text{H}_2\text{O}$  (1:1, 40 mL). To this solution, pyridinium *p*-toluene sulfonate (PPTS, 4.6 g, 2.0 eq.) was added and the mixture was stirred at 60 °C for 6 h. The organic solvent was removed under vacuum and the resulting aqueous phase was extracted with EtOAc (3 x 50 mL). The collected organic phase was dried over  $\text{Na}_2\text{SO}_4$  and evaporated. The crude was column chromatographed (hexane:EtOAc, 9:1), to yield the desired ketone as a colorless oil (1.1 g, 57 %).  $^1\text{H}$  NMR (300 MHz,  $\text{CDCl}_3$ ):  $\delta$  7.25-7.19 (m, 1H), 7.05 (d,  $J = 7.5$  Hz, 3H), 2.99 (tt,  $J = 12.1, 3.4$  Hz, 1H), 2.58-2.48 (m, 4H), 2.36 (s, 3H), 2.25-2.18 (m, 2H), 2.02-1.87 (m, 2H).  $^{13}\text{C}$  NMR (75 MHz,  $\text{CDCl}_3$ ):  $\delta$  211.4, 144.9, 138.3, 128.6, 127.6, 127.4, 123.8, 42.9, 41.5, 34.1, 21.6.

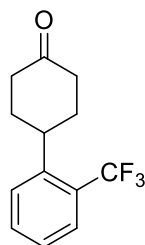
#### 4-(3-(trifluoromethyl)phenyl)cyclohexan-1-one (**50h**).



**50h** was synthesized from 1-Bromo-3-trifluoromethyl-benzene (**45h**, 1.7 mL, 1.2 eq.) and **46** (1.6 g, 1 eq.) following general procedure F and was obtained as pale yellow solids (1.6 g, 68 %).  $^1\text{H}$  NMR (300 MHz,  $\text{C}_6\text{D}_6$ ):  $\delta$  7.27 (d,  $J = 7.3$  Hz, 2H), 6.93 (t,  $J = 7.7$  Hz, 1H), 6.82 (d,  $J = 7.7$  Hz, 1H), 2.23-2.15 (m, 3H), 1.86 (td,  $J = 14.2, 6.0$  Hz, 2H), 1.47 (ddd,  $J = 12.0, 5.8, 2.9$  Hz, 2H), 1.25 (qd,  $J = 13.3, 4.1$  Hz, 2H).  $^{13}\text{C}$  NMR (75 MHz,  $\text{C}_6\text{D}_6$ ):  $\delta$  207.7, 146.4, 130.9 (q,  $J =$

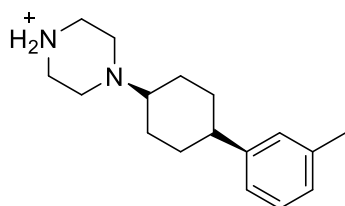
31.7 Hz), 130.2, 129.2, 126.9, 123.9 (q,  $J = 3.8$  Hz), 123.5 (q,  $J = 3.8$  Hz), 123.3, 119.7, 42.3, 41.0, 33.4.  $^{19}\text{F}$  NMR (376 MHz,  $\text{C}_6\text{D}_6$ ): -62.1.

#### 4-(2-(trifluoromethyl)phenyl)cyclohexan-1-one (**50i**).



**50i** was synthesized from 1-Bromo-2-trifluoromethyl-benzene (**45i**, 1.6 mL, 1.2 eq.) and **46** (1.6 g, 1 eq.) following general procedure F and was obtained as pale yellow solids (460 mg, 19 %).  $^1\text{H}$  NMR (300 MHz,  $\text{C}_6\text{D}_6$ ):  $\delta$  7.45 (d,  $J = 8.0$  Hz, 1H), 7.07 (q,  $J = 7.2$  Hz, 1H), 6.88 (ddd,  $J = 23.0, 14.9, 7.2$  Hz, 2H), 5.35 (t,  $J = 3.7$  Hz, 0.45H), 3.27 (t,  $J = 12.0$  Hz, 0.55H), 2.63 (dd,  $J = 3.6, 1.8$  Hz, 1H), 2.34-2.26 (m, 2H), 2.22 (ddd,  $J = 12.6, 4.5, 2.3$  Hz, 1H), 2.02 (td,  $J = 14.3, 6.0$  Hz, 1H), 1.76 (dq,  $J = 15.2, 6.0, 3.0$  Hz, 1H), 1.50 (qd,  $J = 13.2, 4.2$  Hz, 1H).  $^{13}\text{C}$  NMR (75 MHz,  $\text{C}_6\text{D}_6$ ):  $\delta$  207.3, 206.2, 144.7 (d,  $J = 1.4$  Hz), 142.4 (d,  $J = 2.1$  Hz), 137.6, 132.2, 132.2, 131.7, 130.4, 127.7, 127.4, 126.8, 126.6, 126.4 (q,  $J = 5.3$  Hz), 126.2 (q,  $J = 5.9$  Hz), 124.7 (d,  $J = 1.8$  Hz), 124.1, 123.7, 121.4, 121.0, 41.2, 39.7, 38.8, 38.7, 38.6, 34.1, 31.2, 31.2.  $^{19}\text{F}$  NMR (376 MHz,  $\text{C}_6\text{D}_6$ ): -58.4, -58.7.

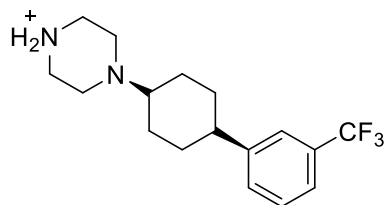
#### 1-((1*S*,4*S*)-4-(*m*-tolyl)cyclohexyl)piperazine (**52g**).



General procedure G: In a round-bottom flask containing a solution of **50g** (378 mg, 1 eq.) and benzylpiperazine (**51**, 416  $\mu\text{L}$ , 1.2 eq.) in dry DCE (10 mL), was added AcOH (100  $\mu\text{L}$ ). After 15 min,  $\text{NaBH}(\text{OAc})_3$  (593 mg, 1.4 eq.) was added and the mixture was stirred for 48 h at r.t. The solvent was removed under vacuum and the crude was purified by column chromatography (hexanes:EtOAc, 9:1 + 0.5 %  $\text{Et}_3\text{N}$ ). The obtained intermediate was dissolved in  $\text{Et}_2\text{O}$  and was precipitated by the addition of a methanol solution of HCl (3.0 M). The collected solids were washed with  $\text{Et}_2\text{O}$  and hexanes and were used in the next step without further purification. The previously obtained compound was dissolved in a mixture of methanol (27 mL) and AcOH (106  $\mu\text{L}$ , 2 eq.). To this stirring solution, Pd/C (30 mg, 0.3 eq.) was added and the reactional mixture was stirred for 16 h, at r.t., under  $\text{H}_2$  atmosphere. The reaction mixture was filtered through a pad of Celite to remove the catalyst (washed with MeOH, 3 x 50 mL). The solvent was removed under vacuum and the compound was purified by RP-UHPLC (from 100%A0%D to 80%A20%D, in 20 min;  $\text{RT}_{5\text{min}}$ : 1.58 min). The desired compound was obtained as white powder (385 mg, 38 %).  $^1\text{H}$ -NMR (300 MHz,  $\text{D}_2\text{O}$ ,  $\delta = \text{ppm}$ ):  $\delta$  7.23 (dt,  $J = 18.3, 7.7$  Hz, 3H), 7.09 (d,  $J = 7.4$  Hz, 1H), 3.85-3.35 (m, 9H), 2.90 (d,  $J = 3.2$  Hz, 1H), 2.30 (s, 3H),

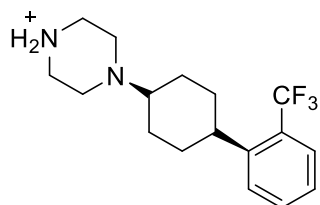
2.10 (dd,  $J = 17.0, 6.9$  Hz, 2H), 2.00-1.78 (m, 6H).  $^{13}\text{C}$ -NMR (75 MHz,  $\text{D}_2\text{O}$ ,  $\delta = \text{ppm}$ ):  $\delta$  144.2, 138.8, 128.7, 127.8, 126.8, 124.1, 65.5, 45.9, 40.5, 37.4, 27.1, 23.3, 20.4.

### 1-((1*S*,4*S*)-4-(3-(trifluoromethyl)phenyl)cyclohexyl)piperazine (52h).



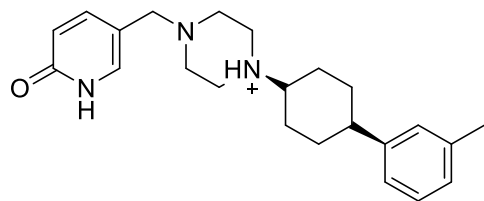
**52h** was synthesized from **50h** (488 mg, 1 eq.) and **51** (416  $\mu\text{L}$ , 1.2 eq.) following general procedure G and was obtained as white solids (311 mg, 28 %).  $^1\text{H}$  NMR (300 MHz,  $\text{D}_2\text{O}$ ):  $\delta$  7.71 (s, 1H), 7.65-7.52 (m, 3H), 3.89-3.54 (m, 9H), 3.06 (t,  $J = 5.5, 2.4$  Hz, 1H), 2.21-2.10 (m, 2H), 2.06-1.84 (m, 6H).  $^{13}\text{C}$  NMR (75 MHz,  $\text{D}_2\text{O}$ ):  $\delta$  144.9, 131.0, 130.3, 129.9, 129.2, 123.8 (q,  $J = 3.8$  Hz), 122.9 (q,  $J = 3.7$  Hz), 117.5, 65.3, 46.0, 40.6, 37.5, 26.9, 23.2.  $^{19}\text{F}$  NMR (376 MHz,  $\text{D}_2\text{O}$ ): -62.3, -75.6.

### 1-((1*S*,4*S*)-4-(2-(trifluoromethyl)phenyl)cyclohexyl)piperazine (52i).



**52i** was synthesized from **50i** (364 mg, 1 eq.) and **51** (312  $\mu\text{L}$ , 1.2 eq.) following general procedure GG and was obtained as white solids (215 mg, 27 %).  $^1\text{H}$  NMR (300 MHz,  $\text{D}_2\text{O}$ ):  $\delta$  7.74-7.60 (m, 3H), 7.40 (t,  $J = 7.4$  Hz, 1H), 4.07-3.50 (m, 9H), 3.19-3.12 (m, 1H), 2.38 (d,  $J = 16.5$  Hz, 1H), 2.03 (tt,  $J = 16.5, 3.8$  Hz, 1H), 1.87-1.68 (m, 4H).  $^{13}\text{C}$  NMR (75 MHz,  $\text{D}_2\text{O}$ ):  $\delta$  144.5, 132.5, 128.0, 127.4, 127.0, 126.6, 126.4, 126.0 (q,  $J = 6.1$  Hz), 63.9, 47.0, 40.2, 38.0, 26.9, 25.0.  $^{19}\text{F}$  NMR (376 MHz,  $\text{D}_2\text{O}$ ): -58.8, -75.6.

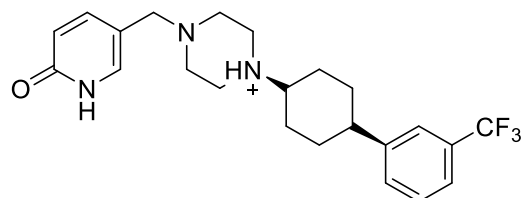
### 5-((4-((1*S*,4*S*)-4-(*m*-tolyl)cyclohexyl)piperazin-1-yl)methyl)pyridin-2(1*H*)-one (53g).



General procedure H: In a round-bottom flask containing a solution of **52g** (195 mg, 1.1 eq.) and **29** (45 mg, 1 eq.) in dry DCE (4 mL), was added  $\text{Et}_3\text{N}$  (223  $\mu\text{L}$ , 1.4 eq.). After 15 min,  $\text{NaBH}(\text{OAc})_3$  (110 mg, 1.3 eq.) was added and the mixture was stirred for 24 h at r.t. The solvent was removed under vacuum and the crude was purified by RP-UHPLC (from 80%A20%D to 60%A40%D, in 20 min;  $\text{RT}_{5\text{min}}$ : 1.61 min). The desired compound was obtained as white powder (181 mg, 76 %).  $^1\text{H}$ -NMR (300 MHz,  $\text{CD}_3\text{CN}:\text{D}_2\text{O}$ , 3:1,  $\delta = \text{ppm}$ ):  $\delta$  7.57 (d,  $J = 7.7$  Hz, 1H), 7.16 (t,  $J = 7.5$  Hz, 1H), 7.08 (d,  $J = 9.7$  Hz, 1H), 6.99 (d,  $J = 7.3$  Hz, 1H), 6.50 (d,  $J = 10.0$  Hz, 1H), 4.04 (s, 2H), 3.50 (s, 12H), 3.36 (dd,  $J = 10.2, 5.0$  Hz, 1H), 2.82-2.76 (m, 1H), 2.27 (s, 3H), 2.04-1.88 (m, 7H), 1.79-1.71 (m, 2H).  $^{13}\text{C}$ -NMR (75 MHz,  $\text{CD}_3\text{CN}:\text{D}_2\text{O}$ , 3:1,  $\delta = \text{ppm}$ ):  $\delta$  164.5, 145.6, 144.9, 139.3, 139.1, 129.4, 128.8, 127.7, 125.1,

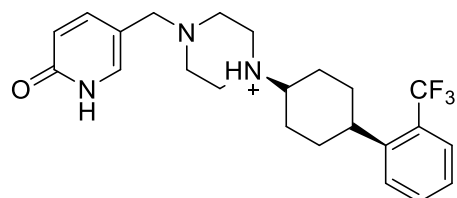
121.2, 118.8, 109.5, 65.5, 57.4, 48.7, 48.0, 39.9, 28.4, 25.0, 21.5. HRMS  $m/z$  calculated for  $C_{23}H_{32}N_3O$ : 366.2540  $[M+H]^+$ ; found, 366.2552.

**5-((4-((1*S*,4*S*)-4-(3-(trifluoromethyl)phenyl)cyclohexyl)piperazin-1-yl)methyl)pyridin-2(1H)-one (53h).**

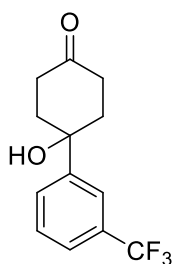


**53h** was synthesized from **52h** (270 mg, 1.1 eq.) and **29** (56 mg, 1 eq.) following general procedure H and was obtained as white powder (284 mg, 81 %).  $^1H$ -NMR (300 MHz,  $CD_3CN:D_2O$ , 3:1,  $\delta = ppm$ ):  $\delta$  7.60-7.55 (m, 4H), 7.52-7.45 (m, 2H), 4.07 (s, 2H), 3.52 (s, 8H), 2.96-2.89 (m, 1H), 2.04 (ddd,  $J = 11.7, 10.4, 5.2$  Hz, 2H), 1.96-1.90 (m, 5H), 1.84-1.75 (m, 2H).  $^{13}C$ -NMR (75 MHz,  $CD_3CN:D_2O$ , 3:1,  $\delta = ppm$ ):  $\delta$  164.3, 147.0, 144.8, 139.5, 132.1, 131.2, 130.7, 130.3, 127.4, 125.0, 124.8 (q,  $J = 3.8$  Hz), 123.9 (q,  $J = 3.8$  Hz), 121.3, 119.5, 118.7, 109.1, 65.2, 57.4, 48.6, 48.1, 40.1, 28.1, 25.1.  $^{19}F$  NMR (376 MHz,  $CD_3CN:D_2O$ , 3:1,  $\delta = ppm$ ):  $\delta$  -62.9, -76.0. HRMS  $m/z$  calculated for  $C_{23}H_{29}F_3N_3O$ : 420.2257  $[M+H]^+$ ; found, 420.2265.

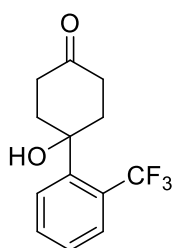
**5-((4-((1*S*,4*S*)-4-(2-(trifluoromethyl)phenyl)cyclohexyl)piperazin-1-yl)methyl)pyridin-2(1H)-one (53i).**



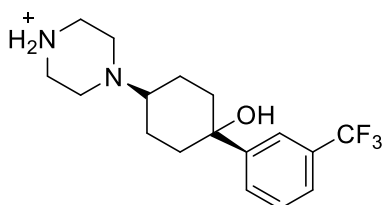
**53i** was synthesized from **52i** (215 mg, 1.1 eq.) and **29** (45 mg, 1 eq.) following general procedure H and was obtained as white powder (186 mg, 72 %).  $^1H$ -NMR (300 MHz,  $CD_3CN:D_2O$ , 3:1,  $\delta = ppm$ ):  $\delta$  7.80 (d,  $J = 7.9$  Hz, 1H), 7.64 (d,  $J = 9.2$  Hz, 3H), 7.50 (t,  $J = 7.5$  Hz, 1H), 7.34 (t,  $J = 7.6$  Hz, 1H), 6.56 (d,  $J = 9.8$  Hz, 1H), 4.10 (s, 2H), 3.69 (s, 8H), 3.37 (s, 1H), 3.04 (t,  $J = 8.5$  Hz, 1H), 2.34 (t,  $J = 13.4$  Hz, 2H), 2.00-1.82 (m, 5H), 1.67 (d,  $J = 10.1$  Hz, 2H).  $^{13}C$ -NMR (75 MHz,  $CD_3CN:D_2O$ , 3:1,  $\delta = ppm$ ):  $\delta$  163.8, 161.6 (q,  $J = 35.7$  Hz), 145.4, 139.6, 133.4, 129.8, 128.2, 127.8, 127.7, 127.5, 126.5 (q,  $J = 6.0$  Hz), 124.1, 120.8, 119.4, 118.3, 115.6, 109.7, 64.2, 57.0, 49.0, 48.1, 39.8, 28.0, 26.6.  $^{19}F$  NMR (376 MHz,  $CD_3CN:D_2O$ , 3:1,  $\delta = ppm$ ):  $\delta$  -59.3, -76.1. HRMS  $m/z$  calculated for  $C_{23}H_{29}F_3N_3O$ : 420.2257  $[M+H]^+$ ; found, 420.2270.

**4-hydroxy-4-(3-(trifluoromethyl)phenyl)cyclohexan-1-one (54h).**

In a round-bottom flask containing a solution of **47g** (605 mg, 1 eq.) was dissolved in a mixture of acetone and H<sub>2</sub>O (1:1, 20 mL). To this solution, PPTS (1 g, 2.0 eq.) was added and the mixture was stirred at 60 °C for 6 h. The organic solvent was removed under vacuum and the resulting aqueous phase was extracted with EtOAc (3 x 50 mL). The collected organic phase was dried over Na<sub>2</sub>SO<sub>4</sub> and evaporated. The crude was column chromatographed (hexanes:EtOAc, 9:1) to yield the desired ketone as a white powder (465 mg, 56 %). <sup>1</sup>H NMR (300 MHz, C<sub>6</sub>D<sub>6</sub>, δ = ppm): δ 7.62 (s, 1H), 7.29 (d, *J* = 7.7 Hz, 1H), 7.07 (d, *J* = 8.0 Hz, 1H), 6.93 (t, *J* = 7.8 Hz, 1H), 2.49 (td, *J* = 14.0, 6.6 Hz, 2H), 2.09 (dd, *J* = 4.7, 2.1 Hz, 1H), 2.05 (dd, *J* = 4.7, 2.1 Hz, 1H), 1.51 (td, *J* = 13.7, 4.7 Hz, 2H), 1.42-1.33 (m, 2H). <sup>13</sup>C NMR (75 MHz, C<sub>6</sub>D<sub>6</sub>, δ = ppm): δ 208.2, 149.2, 130.8 (q, *J* = 31.9 Hz), 129.0, 128.3, 124.1 (q, *J* = 3.7 Hz), 121.7 (q, *J* = 3.8 Hz), 71.6, 38.1, 37.1. <sup>19</sup>F NMR (376 MHz, C<sub>6</sub>D<sub>6</sub>, δ = ppm): δ -62.1.

**4-hydroxy-4-(2-(trifluoromethyl)phenyl)cyclohexan-1-one (54i).**

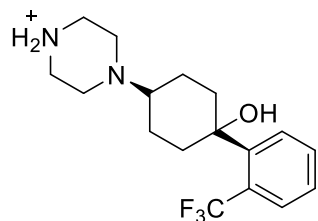
In a round-bottom flask containing a solution of **47i** (471 mg, 1 eq.) was dissolved in a mixture of acetone and H<sub>2</sub>O (1:1, 20 mL). To this solution, PPTS (1 g, 2.0 eq.) was added and the mixture was stirred at 60 °C for 6 h. The organic solvent was removed under vacuum and the resulting aqueous phase was extracted with EtOAc (3 x 50 mL). The collected organic phase was dried over Na<sub>2</sub>SO<sub>4</sub> and evaporated. The crude was column chromatographed (hexanes:EtOAc, 9:1) to yield the desired ketone as a white powder (292 mg, 38 %). <sup>1</sup>H NMR (300 MHz, C<sub>6</sub>D<sub>6</sub>, δ = ppm): δ 7.61 (dd, *J* = 7.9, 0.9 Hz, 1H), 6.96 (td, *J* = 7.9, 1.1 Hz, 1H), 6.82 (dd, *J* = 16.5, 8.0 Hz, 2H), 2.61-2.50 (m, 2H), 2.09 (d, *J* = 2.1 Hz, 1H), 2.05 (dd, *J* = 4.2, 2.1 Hz, 1H), 1.77-1.62 (m, 4H), 1.52 (s, 1H). <sup>13</sup>C NMR (75 MHz, C<sub>6</sub>D<sub>6</sub>, δ = ppm): δ 208.6, 147.3, 131.5, 128.5, 127.6, 127.4, 123.8, 73.0, 38.6, 38.6, 37.1. <sup>19</sup>F NMR (376 MHz, C<sub>6</sub>D<sub>6</sub>, δ = ppm): δ -53.4.

**(1*S*,4*S*)-4-(piperazin-1-yl)-1-(3-(trifluoromethyl)phenyl)cyclohexan-1-ol (55h).**

**55h** was synthesized from **54h** (465 mg, 1 eq.) and **51** (372 μL, 1.2 eq.) following general procedure G and was obtained as white powder (112 mg, 9 %). <sup>1</sup>H NMR (300 MHz, D<sub>2</sub>O): δ 7.90 (s, 1H), 7.84 (d, *J* = 7.8 Hz, 1H), 7.72

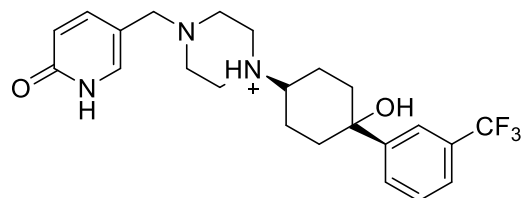
(d,  $J = 7.7$  Hz, 1H), 7.64 (t,  $J = 7.8$  Hz, 1H), 3.59 (s, 9H), 2.69 (d,  $J = 14.0$  Hz, 2H), 2.24 (d,  $J = 10.2$  Hz, 2H), 1.95-1.85 (m, 2H), 1.56 (q,  $J = 10.8$  Hz, 2H).  $^{13}\text{C}$  NMR (75 MHz,  $\text{D}_2\text{O}$ ):  $\delta$  162.9 (q,  $J = 35.3$  Hz), 143.0, 130.7 (t,  $J = 31.9$  Hz), 129.8, 129.7, 129.6, 124.9 (q,  $J = 3.6$  Hz), 122.9 (q,  $J = 3.8$  Hz), 116.4 (q,  $J = 301.5$  Hz), 71.8, 64.7, 45.9, 40.7, 34.0, 23.3.  $^{19}\text{F}$  NMR (376 MHz,  $\text{D}_2\text{O}$ ,  $\delta = \text{ppm}$ ): -62.3, -75.6.

**(1*S*,4*S*)-4-(piperazin-1-yl)-1-(2-(trifluoromethyl)phenyl)cyclohexan-1-ol (55i).**



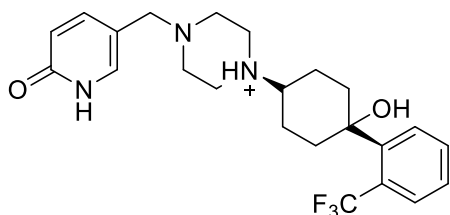
**55i** was synthesized from **54i** (292 mg, 1 eq.) and **51** (235  $\mu\text{L}$ , 1.2 eq.) following general procedure G and was obtained as white powder (113 mg, 19%).  $^1\text{H}$  NMR (300 MHz,  $\text{D}_2\text{O}$ ):  $\delta$  7.90 (d,  $J = 7.8$  Hz, 1H), 7.75 (d,  $J = 7.8$  Hz, 1H), 7.65 (t,  $J = 7.3$  Hz, 1H), 7.51 (t,  $J = 7.2$  Hz, 1H), 3.63 (s, 8H), 3.52 (s, 1H), 2.45 (t,  $J = 9.5$  Hz, 2H), 2.26 (d,  $J = 10.0$  Hz, 2H), 1.97 (t,  $J = 17.4$  Hz, 4H).  $^{13}\text{C}$  NMR (75 MHz,  $\text{D}_2\text{O}$ ):  $\delta$  144.3, 132.1, 128.8 (q,  $J = 7.2$  Hz), 128.3, 127.9, 127.6, 127.2, 126.7, 123.0, 72.9, 63.6, 46.5, 40.9, 34.0, 22.4.  $^{19}\text{F}$  NMR (376 MHz,  $\text{D}_2\text{O}$ ,  $\delta = \text{ppm}$ ): -53.8.

**5-((4-((1*S*,4*S*)-4-hydroxy-4-(3-(trifluoromethyl)phenyl)cyclohexyl)piperazin-1-yl)methyl)pyridin-2(1*H*)-one (56h).**



**56h** was synthesized from **55h** (113 mg, 1.1 eq.) and **29** (23 mg, 1 eq.) following general procedure H and was obtained as white powder (21 mg, 17%).  $^1\text{H}$ -NMR (400 MHz,  $\text{D}_2\text{O}$ ,  $\delta = \text{ppm}$ ):  $\delta$  7.90 (s, 1H), 7.85 (d,  $J = 7.9$  Hz, 1H), 7.76-7.73 (m, 2H), 7.65 (t,  $J = 7.8$  Hz, 1H), 6.70 (dd,  $J = 10.4, 2.2$  Hz, 1H), 4.26 (s, 2H), 3.60-3.58 (m, 9H), 2.69 (d,  $J = 14.1$  Hz, 1H), 2.26-2.23 (m, 2H), 1.94-1.87 (m, 2H), 1.56 (q,  $J = 10.7$  Hz, 2H).  $^{13}\text{C}$ -NMR (100 MHz,  $\text{D}_2\text{O}$ ,  $\delta = \text{ppm}$ ):  $\delta$  164.5, 162.9 (q,  $J = 35.4$  Hz), 144.8, 143.0, 138.5, 130.5 (q,  $J = 32.0$  Hz), 129.9, 129.7, 128.2, 125.5, 124.9 (q,  $J = 3.8$  Hz), 122.9 (q,  $J = 3.7$  Hz), 122.8, 120.0, 116.3 (q,  $J = 291.8$  Hz), 109.2, 71.8, 64.5, 56.7, 48.0, 46.4, 34.0, 23.5.  $^{19}\text{F}$  NMR (376 MHz,  $\text{D}_2\text{O}$ ,  $\delta = \text{ppm}$ ):  $\delta$  -62.3, -75.6. HRMS  $m/z$  calculated for  $\text{C}_{23}\text{H}_{28}\text{F}_3\text{N}_3\text{O}_2$ : 436.2206  $[\text{M}+\text{H}]^+$ ; found, 436.2207.

**5-((4-((1*S*,4*S*)-4-hydroxy-4-(2-(trifluoromethyl)phenyl)cyclohexyl)piperazin-1-yl)methyl)pyridin-2(1*H*)-one (56i).**



**56i** was synthesized from **55i** (113 mg, 1.1 eq.) and **29** (28 mg, 1 eq.) following general procedure H and was obtained as white powder (91 mg, 60 %). <sup>1</sup>H-NMR (400 MHz, D<sub>2</sub>O, δ = ppm): δ 7.90 (dd, *J* = 7.9, 0.8 Hz, 1H), 7.79-7.76 (m, 2H), 7.71 (d, *J* = 7.9 Hz, 1H), 7.66-7.62 (m, 1H), 7.51 (t, *J* = 7.6 Hz, 1H), 6.71 (d, *J* = 10.2, 4.5 Hz, 1H), 4.33 (s, 2H), 3.67-3.62 (m, 9H), 2.41 (dd, *J* = 18.1, 8.9 Hz, 2H), 2.31 (dd, *J* = 13.7, 7.3 Hz, 2H), 2.00-1.93 (m, 4H). <sup>13</sup>C-NMR (100 MHz, D<sub>2</sub>O, δ = ppm): δ 164.5, 162.9 (q, *J* = 35.4 Hz), 144.8, 144.2, 138.6, 132.1, 128.9 (q, *J* = 7.4 Hz), 128.2, 128.0, 127.5 (q, *J* = 30.9 Hz), 126.2, 123.5, 120.1, 116.4 (q, *J* = 291.9 Hz), 109.0, 72.7, 63.9, 56.7, 47.8, 47.0, 33.9, 22.3. <sup>19</sup>F NMR (376 MHz, D<sub>2</sub>O, δ = ppm): δ -53.9, -75.6. HRMS *m/z* calculated for C<sub>23</sub>H<sub>28</sub>F<sub>3</sub>N<sub>3</sub>O<sub>2</sub>: 436.2206 [M+H]<sup>+</sup>; found, 436.2209.

## 5.2 Biology

### 5.2.1 TRPV FLIPR assay.

Calcium-5 was bought from Molecular Devices LLC. All other chemicals were purchased from Sigma-Aldrich.

*h*TRPV6 activity was measured using the HEK293 cell line stably overexpressing human TRPV6 as previously reported.<sup>76,179</sup> Stable cells were trypsinized and plated at 7.5 x 10<sup>4</sup> cells/well onto poly-D-lysine coated 96-well black plates with clear bottom using 100 μL DMEM supplemented with 10% FBS and 2 mM glutamine without antibiotics or phenol-red. After 16 h the medium was replaced with 90 μL of nominally calcium-free (NCF) loading buffer (modified Krebs buffer containing 117 mM NaCl, 4.8 mM KCl, 1 mM MgCl<sub>2</sub>, 5mM D-glucose, 10 mM HEPES, and calcium-5 fluorescence dye (50 μL/mL loading buffer)). Cells were incubated in the NCF-loading buffer at 37 °C for 1 h. Fluorescence Cd<sup>2+</sup> measurements were carried out using FLIPR<sub>TETRA</sub> high throughput (Molecular Devices, LLC), fluorescence microplate reader. Cells were excited using a 470-495 nm LED module, and the emitted fluorescence signal was filtered with a 515-575 nm emission filter (manufacturer's guidelines). Stable Ca<sup>2+</sup>-free baselines were established for 60 seconds before 10 μL of a 10X compound was added to the cells. Cells were incubated at 37 °C and fluorescence was monitored in the presence of compound for an additional 5 minutes before administration of 100 μL of CdCl<sub>2</sub> (final concentration: 50 μM). The activity of TRPV6 was measured by calculating the area under the curve of the Cd<sup>2+</sup> entry traces.

hTRPV5 activity was measured in a similar experiment as described above.<sup>196</sup> Briefly, HEK293 cells were trypsinized and plated at  $1.5 \times 10^4$  cells/well onto Corning® 96-well black polystyrene clear bottom microplates (CLS3603 Sigma-Aldrich) coated with 100  $\mu\text{g}/\text{mL}$  poly-D-lysine (P6407 Sigma-Aldrich) using 100  $\mu\text{L}$  phenol-red free DMEM with 10% FBS and 2mM glutamine without antibiotics. Cells were incubated at 37 °C for 24 h. on the following day, transfection was performed using 200 ng of pTagRFP-C1-hTRPV5 and 0.6  $\mu\text{L}$  Lipofectamine 2000 reagent/well. Fluorescent ion measurements using FLIPR<sub>TETRA</sub> were carried out 24h post-transfection. The FLIPR protocol for measuring hTRPV5 activity was identical to the one described for hTRPV6.

hTRPV1 activity was measured using HEK293 cells transiently overexpressing TRPV1, as previously reported.<sup>164</sup> Briefly, HEK293 cells were trypsinized and plated at  $2.7 \times 10^4$  cells/well onto Corning® 96-well black polystyrene clear bottom microplates coated with 100  $\mu\text{g}/\text{mL}$  poly-D-lysine using 100  $\mu\text{L}$  phenol-red free DMEM with 10% FBS and 2mM glutamine without antibiotics. Cells were incubated at 37 °C for 24 h. on the following day, transfection was performed using 200 ng of hTRPV1-pcDNA 3.1 and 0.6  $\mu\text{L}$  Lipofectamine 2000 reagent/well. Fluorescent ion measurements using FLIPR<sub>TETRA</sub> were carried out 24h post-transfection. The medium was replaced with 90  $\mu\text{L}$  of NCF. Cells were incubated in the loading buffer at 37 °C for 1 h in dark. Stable baselines were established for 50 s before 10  $\mu\text{L}$  of a 10X compound prepared in 1.8mM  $\text{CaCl}_2$ -containing Krebs buffer was robotically administered to the cells. Cells were incubated and fluorescence was monitored in the presence of compound for an additional 5 min before administration of 100  $\mu\text{L}$  of a 200 nM solution of capsaicin 1.8mM  $\text{CaCl}_2$ -containing Krebs buffer (final concentration of capsaicin = 100 nM).

Screening experiments were done with 3 to 6 repeats per group at 50  $\mu\text{M}$  (direct capsaicinoids) or 10  $\mu\text{M}$  (chimeric capsaicinoids). Fluorescence signals were analyzed using the ScreenWorks 3.1.1.8 software (Molecular Devices). Dose-response curves were generated (9-point curve, 6 repeats/concentration, 2-fold serial dilution starting at 10  $\mu\text{M}$ ), and the  $\text{IC}_{50}$  values were extrapolated from these plots for each compound (GraphPad® Prism, v. 5.0, San Diego, CA, US). Inhibition curves were obtained by non-linear regression using the built-in log(inhibitor) vs. response-variable slope function (four parameters).

### 5.2.2 Confocal imaging.

HEK-hTRPV6 were trypsinized and plated at  $1 \times 10^4$  cells/well onto poly-D-lysine coated Nunc Lab-Tek II 8-well chambered coverglass plates (Faust Laborbedarf AG,

Schaffhausen) using 100  $\mu$ L DMEM supplemented with 10% FBS and 2 mM glutamine without antibiotics or phenol-red. After 24 h of incubation at 37 °C, the medium was replaced by 200  $\mu$ L/well of a mixture of Leadmium Green (final concentration: 5 ng/ $\mu$ L), Hoechst 33258 (final concentration: 1 ng/ $\mu$ L) and Alexa Fluor 298 (final concentration: 5 ng/ $\mu$ L) in NCF buffer.<sup>191,192</sup> The chamber was covered with aluminum foil and was incubated at 37 °C for 30 min. Then, the buffer was removed, cells were washed twice with fresh NCF buffer (2 x 200  $\mu$ L) and another 190  $\mu$ L of NCF containing 10X of MRC-130 was added. For control cells, 200  $\mu$ L of NCF was added after washing. The chamber was mounted in the confocal microscope and 10  $\mu$ L of CdCl<sub>2</sub> (final concentration: 50  $\mu$ M) was added right after the start of imaging (total duration: 30 min).

The cells were imaged at 100X lenses with a confocal, laser scanning microscope setup using a Nikon Eclipse TE2000-E fully automatized inverted, epifluorescence microscope outfitted with Nikon D-Eclipse C1 laser confocal optics. The system equipped with a violet-diode (405 nm) and a multiline Argon (457-515 nm) from Melles Griot, and a Helium/Neon (594 nm) lasers from JDS Uniphase. Nikon EZ-C1 3.6 confocal imaging software installed on an HP xw4400 workstation was used for image acquisition. Brightness and contrast were adjusted with ImageJ.

### **5.2.3 *In vitro* Polypharmacology and metabolism**

Activities of MRC-130 against ion channels and metabolism in liver microsomes were measured at 10  $\mu$ M in accordance with Eurofins Cerep's validation Standard Operating Procedure (Eurofins Cerep, Celle L'Evescault, France; <https://www.eurofins.com/>). Reference compounds were tested in each experiment concurrently with the test compounds, and the data were compared with historical values determined at Cerep.

### **5.2.4 Antiproliferative activity.**

Unless specified cell culture reagents were obtained from Gibco, Life Technology, Switzerland. MCF-7 (human mammary adenocarcinoma), MDA-MB-231 (human mammary adenocarcinoma), and T47D (human mammary ductal carcinoma) cell lines were obtained from NIH cell collection and were grown in RPMI medium complemented with 10% FBS, 2mM L-Glutamine, 100 U/ml Penicillin and 100  $\mu$ g/ml Streptomycin (Sigma) and 1% non-essential amino acids (Bioconcept, Switzerland). HEK293 (human embryonic kidney) and SKOV-3 (human ovary adenocarcinoma) cell lines were obtained from the ATCC cell bank. Along with the HEK-hTRPV6, HEK293 and SKOV-3 were

grown in DMEM medium supplemented with 10% FBS, 2mM L-Glutamine, 100 U/ml Penicillin and 100 µg/ml Streptomycin (Sigma) and 1% non-essential amino acids (Bioconcept, Switzerland).

The XTT assay was used to evaluate cell proliferation. Cells were plated at a density of  $5 \times 10^3$  cells/well in 96-well plates and were incubated at 37 °C for 24 h. On the following day, the medium was carefully aspirated and replaced with 100 µL of MRC-130 or *cis*-22a at concentrations ranging from 100 µM to 0.4 µM. Doxorubicin (10 µM) and DMSO (0.01 %) were used as positive and negative controls, respectively. All the treatments used the original cell medium (RPMI or DMEM), depending on the cell line. Cells were incubated for a total of 6 days at 37 °C with the medium (treatment and controls) being replaced by a freshly prepared solution every 48 h. Then, 25 µL of XTT (with 1.25 % of PMS) was added to each well and incubated at 37 °C for 2 h. Subsequently, the absorbance was read at 650 nm and subtracted from the absorbance of 450 nm by spectrophotometry ( $V_{\max}$  Kinetic Microplate Reader, Molecular Devices LLC). The resulting subtracted absorbance for each compound concentration ( $A_t$ ) was expressed as a percentage of viable cells relative to the negative control ( $A_b$ ).

$$\% \text{ viable cells} = \frac{A_t}{A_b} \times 100$$

Where  $A_t$ : treatment absorbance;  $A_b$ : negative control absorbance.

For the treatment with *cis*-22a which the % of viable cells was  $\leq 50$  % at 100 µM,  $A_t$  was plotted and the inhibition curves obtained by non-linear regression using the built-in log(inhibitor) vs. response-variable slope function (GraphPad® Prism, v. 5.0, San Diego, CA, US).

### 5.3 Purity

**Table S1.** Analytical RP-HPLC purity of direct capsaicinoids

<b>Compound</b>	<b>HPLC Purity (%)<sup>a</sup></b>
<b>5a</b>	98%
<b>5b</b>	96%
<b>8a</b>	> 99%
<b>8b</b>	> 99%
<b>11a</b>	95%
<b>11b</b>	97%
<b>12a</b>	98%
<b>12b</b>	99%
<b>17a</b>	98%
<b>17b</b>	97%
<b>18a</b>	99%
<b>18b</b>	98%

<sup>a</sup>HPLC. Shimadzu<sup>®</sup>-PROMINENCE system; Column, Waters<sup>®</sup>- $\mu$ Bondpak C18, 3.9 x 300 mm. UV Detection, Shimadzu<sup>®</sup> SPD-M10A VP Photodiode array detector. Eluents, A: water with 0.05% TFA and B: Acetonitrile with 0.05% TFA.

**Table S2.** Analytical RP-UHPLC purity of chimeric capsaicinoids

<b>Compound</b>	<b>UPLC Purity (%)<sup>a</sup></b>
<b>24c</b>	99%
<b>24d</b>	96%
<b>24e</b>	> 99%
<b>24f</b>	99%
<b>28c</b>	> 99%
<b>28d</b>	> 99%
<b>28e</b>	> 99%
<b>28f</b>	99%
<b>32e</b>	> 99%
<b>32f</b>	> 99%
<b>36e</b>	99%
<b>36f</b>	> 99%
<b>42f</b>	> 99%
<b>43f</b>	98%
<b>44f</b>	96%
<b>53g</b>	> 99%
<b>53h</b>	99%
<b>53i</b>	99%
<b>56h</b>	> 99%
<b>56i</b>	> 99%

<sup>a</sup>UHPLC. Dionex ULTIMATE 3000 RSLC chromatography system; Column, Dionex Acclaim<sup>®</sup> RSLC 120 C18, 3.0 x 50 mm, particle size 2.2  $\mu$ m, 120 Å pore size; UV Detection, ULTIMATE 3000 RS Photo diode array detector. Eluents, A: water with 0.05% TFA and D: Acetonitrile/water (9/1) with 0.05% TFA.

## 6. References

- (1) COSENS, D. J.; MANNING, A. *Nature* **1969**, 224 (5216), 285–287.
- (2) Montell, C.; Rubin, G. M. *Neuron* **1989**, 2 (4), 1313–1323.
- (3) Zhu, X.; Chu, P. B.; Peyton, M.; Birnbaumer, L. *FEBS Lett.* **1995**, 373 (3), 193–198.
- (4) Wes, P. D.; Chevesich, J.; Jeromin, A.; Rosenberg, C.; Stetten, G.; Montell, C. *Proc. Natl. Acad. Sci.* **1995**, 92 (21), 9652–9656.
- (5) Rodrigues, T.; Sieglitz, F.; Bernardes, G. J. L. *Chem. Soc. Rev.* **2016**, 45 (22), 6130–6137.
- (6) Nilius, B.; Owsianik, G. *Genome Biol.* **2011**, 12 (3), 218.
- (7) Liao, M.; Cao, E.; Julius, D.; Cheng, Y. *Nature* **2013**, 504 (7478), 107–112.
- (8) Yang, F.; Xiao, X.; Cheng, W.; Yang, W.; Yu, P.; Song, Z.; Yarov-Yarovoy, V.; Zheng, J. *Nat. Chem. Biol.* **2015**, 11 (7), 518–526.
- (9) Hoenderop, J. G. J.; Nilius, B.; Bindels, R. J. M. *Eur. J. Physiol.* **2003**, 446 (3), 304–308.
- (10) Nilius, B.; Szallasi, A. *Pharmacol. Rev.* **2014**, 66 (3), 676–814.
- (11) Baylie, R. L.; Brayden, J. E. *Acta Physiol.* **2011**, 203 (1), 99–116.
- (12) Oh, U.; Hwang, S.; Kim, D. *J. Neurosci.* **1996**, 16 (5), 1659–1667.
- (13) Wood, J.; Winter, J.; James, I.; Rang, H.; Yeats, J.; Bevan, S. *J. Neurosci.* **1988**, 8 (9), 3208–3220.
- (14) Bevan, S.; Szolcsányi, J. *Trends Pharmacol. Sci.* **1990**, 11 (8), 331–333.
- (15) Szallasi, A.; Blumberg, P. M. *Brain Res.* **1990**, 524 (1), 106–111.
- (16) Biró, T.; Maurer, M.; Modarres, S.; Lewin, N. E.; Brodie, C.; Ács, G.; Ács, P.; Paus, R.; Blumberg, P. M. *Blood* **1998**, 91 (4), 1332–1340.
- (17) Caterina, M. J.; Schumacher, M. A.; Tominaga, M.; Rosen, T. A.; Levine, J. D.; Julius, D. *Nature* **1997**, 389 (6653), 816–824.
- (18) Lukacs, V.; Rives, J.-M.; Sun, X.; Zakharian, E.; Rohacs, T. *J. Biol. Chem.* **2013**, 288 (49), 35003–35013.
- (19) Sun, X.; Zakharian, E. *J. Biol. Chem.* **2015**, 290 (8), 4741–4747.
- (20) Caterina, M. J. *Pain* **2003**, 105 (1), 5–9.
- (21) Peier, A. M. *Science (80-. )*. **2002**, 296 (5575), 2046–2049.
- (22) Xu, H.; Zhao, H.; Tian, W.; Yoshida, K.; Rouillet, J.-B.; Cohen, D. M. *J. Biol. Chem.* **2003**, 278 (13), 11520–11527.
- (23) Peng, J.-B.; Chen, X.-Z.; Berger, U. V.; Vassilev, P. M.; Tsukaguchi, H.; Brown, E. M.; Hediger, M. A. *J. Biol. Chem.* **1999**, 274 (32), 22739–22746.
- (24) Chung, M.-K.; Lee, H.; Mizuno, A.; Suzuki, M.; Caterina, M. J. *J. Biol. Chem.* **2004**, 279 (20), 21569–21575.
- (25) Vriens, J.; Watanabe, H.; Janssens, A.; Droogmans, G.; Voets, T.; Nilius, B. *Proc. Natl. Acad. Sci.* **2004**, 101 (1), 396–401.
- (26) Chung, M.-K.; Lee, H.; Caterina, M. J. *J. Biol. Chem.* **2003**, 278 (34), 32037–32046.
- (27) Muraki, K.; Iwata, Y.; Katanosaka, Y.; Ito, T.; Ohya, S.; Shigekawa, M.; Imaizumi, Y. *Circ. Res.* **2003**, 93 (9), 829–838.
- (28) Gunthorpe, M. J.; Benham, C. D.; Randall, A.; Davis, J. B. *Trends Pharmacol. Sci.* **2002**, 23 (4), 183–191.
- (29) Smith, G. D.; Gunthorpe, M. J.; Kelsell, R. E.; Hayes, P. D.; Reilly, P.; Facer, P.; Wright, J. E.; Jerman, J. C.; Walhin, J.-P.; Ooi, L.; Egerton, J.; Charles, K. J.; Smart, D.; Randall, A. D.; Anand, P.; Davis, J. B. *Nature* **2002**, 418 (6894), 186–190.
- (30) Hoenderop, J. G. J.; van der Kemp, A. W. C. M.; Hartog, A.; van de Graaf, S. F. J.; van Os, C. H.; Willems, P. H. G. M.; Bindels, R. J. M. *J. Biol. Chem.* **1999**, 274 (13), 8375–8378.
- (31) Peng, J.-B.; Chen, X.-Z.; Berger, U. V.; Weremowicz, S.; Morton, C. C.; Vassilev, P. M.; Brown, E. M.; Hediger, M. A. *Biochem. Biophys. Res. Commun.* **2000**, 278 (2), 326–332.
- (32) Singh, A. K.; Saotome, K.; Sobolevsky, A. I. *Sci. Rep.* **2017**, 7 (1), 10669.
- (33) Chang, Q.; Gyftogianni, E.; van de Graaf, S. F. J.; Hoefs, S.; Weidema, F. A.; Bindels, R. J. M.; Hoenderop, J. G. J. *J. Biol. Chem.* **2004**, 279 (52), 54304–54311.
- (34) Rutter, A. R.; Ma, Q.-P.; Leveridge, M.; Bonnert, T. P. *Neuroreport* **2005**, 16 (16), 1735–1739.
- (35) Schaefer, M. *Pflügers Arch. - Eur. J. Physiol.* **2005**, 451 (1), 35–42.
- (36) Hoenderop, J. G. J. *EMBO J.* **2003**, 22 (4), 776–785.
- (37) Erler, I.; Hirnet, D.; Wissenbach, U.; Flockerzi, V.; Niemeyer, B. A. *J. Biol. Chem.* **2004**, 279 (33), 34456–34463.
- (38) Al-Ansary, D.; Bogeski, I.; Disteldorf, B. M. J.; Becherer, U.; Niemeyer, B. A. *FASEB J.* **2010**, 24 (2), 425–435.
- (39) Becker, D.; Müller, M.; Leuner, K.; Jendrach, M. *Mol. Membr. Biol.* **2008**, 25 (2), 139–151.

- (40) Gao, Y.; Cao, E.; Julius, D.; Cheng, Y. *Nature* **2016**, *534* (7607), 347–351.
- (41) Huynh, K. W.; Cohen, M. R.; Jiang, J.; Samanta, A.; Lodowski, D. T.; Zhou, Z. H.; Moiseenkova-Bell, V. Y. *Nat. Commun.* **2016**, *7* (1), 11130.
- (42) Zubcevic, L.; Herzik, M. A.; Wu, M.; Borschel, W. F.; Hirschi, M.; Song, A. S.; Lander, G. C.; Lee, S.-Y. *Nat. Commun.* **2018**, *9* (1), 4773.
- (43) Deng, Z.; Paknejad, N.; Maksaev, G.; Sala-Rabanal, M.; Nichols, C. G.; Hite, R. K.; Yuan, P. *Nat. Struct. Mol. Biol.* **2018**, *25* (3), 252–260.
- (44) Dang, S.; Van Goor, M. K.; Asarnow, D.; Wang, Y. Q.; Julius, D.; Cheng, Y.; van der Wijst, J. *Proc. Natl. Acad. Sci. U. S. A.* **2019**.
- (45) Hughes, T. E. T.; Pumroy, R. A.; Yazici, A. T.; Kasimova, M. A.; Fluck, E. C.; Huynh, K. W.; Samanta, A.; Molugu, S. K.; Zhou, Z. H.; Carnevale, V.; Rohacs, T.; Moiseenkova-Bell, V. Y. *Nat. Commun.* **2018**, *9* (1), 4198.
- (46) McGoldrick, L. L.; Singh, A. K.; Saotome, K.; Yelshanskaya, M. V.; Twomey, E. C.; Grassucci, R. A.; Sobolevsky, A. I. *Nature* **2018**, *553* (7687), 233–237.
- (47) Vennekens, R.; Hoenderop, J. G. J.; Prenen, J.; Stuiver, M.; Willems, P. H. G. M.; Droogmans, G.; Nilius, B.; Bindels, R. J. M. *J. Biol. Chem.* **2000**, *275* (6), 3963–3969.
- (48) Fecher-Trost, C.; Lux, F.; Busch, K.-M.; Raza, A.; Winter, M.; Hielscher, F.; Belkacemi, T.; van der Eerden, B.; Boehm, U.; Freichel, M.; Weissgerber, P. *J. Bone Miner. Res.* **2019**, *34* (4), e3646.
- (49) Lehen'kyi, V.; Raphaël, M.; Oulidi, A.; Flourakis, M.; Khalimonchuk, S.; Kondratskyi, A.; Gordienko, D. V.; Mauroy, B.; Bonnal, J.-L.; Skryma, R.; Prevarskaya, N. *PLoS One* **2011**, *6* (2), e16856.
- (50) van de Graaf, S. F. J.; Boullart, I.; Hoenderop, J. G. J.; Bindels, R. J. M. *J. Steroid Biochem. Mol. Biol.* **2004**, *89–90*, 303–308.
- (51) Nilius, B.; Prenen, J.; Hoenderop, J. G. J.; Vennekens, R.; Hoefs, S.; Weidema, A. F.; Droogmans, G.; Bindels, R. J. M. *J. Biol. Chem.* **2002**, *277* (34), 30852–30858.
- (52) den Dekker, E.; Hoenderop, J. G. J.; Nilius, B.; Bindels, R. J. M. *Cell Calcium* **2003**, *33* (5–6), 497–507.
- (53) Niemeyer, B. A.; Bergs, C.; Wissenbach, U.; Flockerzi, V.; Trost, C. *Proc. Natl. Acad. Sci.* **2001**, *98* (6), 3600–3605.
- (54) Singh, A. K.; McGoldrick, L. L.; Twomey, E. C.; Sobolevsky, A. I. *Sci. Adv.* **2018**, *4* (8), eaau6088.
- (55) Fecher-Trost, C.; Wissenbach, U.; Weissgerber, P. *Cell Calcium* **2017**, *67*, 116–122.
- (56) Thyagarajan, B.; Benn, B. S.; Christakos, S.; Rohacs, T. *Mol. Pharmacol.* **2009**, *75* (3), 608–616.
- (57) Thyagarajan, B.; Lukacs, V.; Rohacs, T. *J. Biol. Chem.* **2008**, *283* (22), 14980–14987.
- (58) Rohacs, T.; Nilius, B. *Pflügers Arch. - Eur. J. Physiol.* **2007**, *455* (1), 157–168.
- (59) Velisetty, P.; Borbiro, I.; Kasimova, M. A.; Liu, L.; Badheka, D.; Carnevale, V.; Rohacs, T. *Sci. Rep.* **2016**, *6* (1), 27652.
- (60) Nijenhuis, T.; Hoenderop, J. G. J.; Nilius, B.; Bindels, R. J. M. *Pflügers Arch. - Eur. J. Physiol.* **2003**, *446* (4), 401–409.
- (61) Haustrate, A.; Hantute-Ghesquier, A.; Prevarskaya, N.; Lehen'kyi, V. *Cell Calcium* **2019**, *80*, 117–124.
- (62) Chen, F.; Ni, B.; Yang, Y. O.; Ye, T.; Chen, A. *Cell. Physiol. Biochem.* **2014**, *33* (3), 796–809.
- (63) Suzuki, Y.; Chitayat, D.; Sawada, H.; Deardorff, M. A.; McLaughlin, H. M.; Begtrup, A.; Millar, K.; Harrington, J.; Chong, K.; Roifman, M.; Grand, K.; Tominaga, M.; Takada, F.; Shuster, S.; Obara, M.; Mutoh, H.; Kushima, R.; Nishimura, G. *Am. J. Hum. Genet.* **2018**, *102* (6), 1104–1114.
- (64) Yamashita, S.; Mizumoto, H.; Sawada, H.; Suzuki, Y.; Hata, D. *J. Endocr. Soc.* **2019**, *3* (3), 602–606.
- (65) Suzuki, Y.; Pasch, A.; Bonny, O.; Mohaupt, M. G.; Hediger, M. A.; Frey, F. J. *Hum. Mol. Genet.* **2008**, *17* (11), 1613–1618.
- (66) Zhuang, L.; Peng, J.-B.; Tou, L.; Takanaga, H.; Adam, R. M.; Hediger, M. A.; Freeman, M. R. *Lab. Invest.* **2002**, *82* (12), 1755–1764.
- (67) Peng, J.-B.; Zhuang, L.; Berger, U. V.; Adam, R. M.; Williams, B. J.; Brown, E. M.; Hediger, M. A.; Freeman, M. R. *Biochem. Biophys. Res. Commun.* **2001**, *282* (3), 729–734.
- (68) Lehen'kyi, V.; Raphaël, M.; Prevarskaya, N. *J. Physiol.* **2012**, *590* (6), 1369–1376.
- (69) Schwarz, E. C.; Wissenbach, U.; Niemeyer, B. A.; Strauß, B.; Philipp, S. E.; Flockerzi, V.; Hoth, M. *Cell Calcium* **2006**, *39* (2), 163–173.
- (70) Lehen'kyi, V.; Flourakis, M.; Skryma, R.; Prevarskaya, N. *Oncogene* **2007**, *26* (52), 7380–7385.
- (71) Bolanz, K. A.; Hediger, M. A.; Landowski, C. P. *Mol. Cancer Ther.* **2008**, *7* (2), 271–279.
- (72) Dai, W.; Bai, Y.; Hebda, L.; Zhong, X.; Liu, J.; Kao, J.; Duan, C. *Cell Death Differ.* **2014**.
- (73) Fu, S.; Hirte, H.; Welch, S.; Ilenchuk, T. T.; Lutes, T.; Rice, C.; Fields, N.; Nemet, A.; Dugourd, D.; Piha-Paul, S.; Subbiah, V.; Liu, L.; Gong, J.; Hong, D.; Stewart, J. M. *Invest. New Drugs* **2017**,

- 35 (3), 324–333.
- (74) Franzius, D.; Hoth, M.; Penner, R. *Pflügers Arch. - Eur. J. Physiol.* **1994**, *428* (5–6), 433–438.
- (75) Hughes, T. E. T.; Lodowski, D. T.; Huynh, K. W.; Yazici, A.; Del Rosario, J.; Kapoor, A.; Basak, S.; Samanta, A.; Han, X.; Chakrapani, S.; Zhou, Z. H.; Filizola, M.; Rohacs, T.; Han, S.; Moiseenkova-Bell, V. Y. *Nat. Struct. Mol. Biol.* **2018**, *25* (1), 53–60.
- (76) Simonin, C.; Awale, M.; Brand, M.; Van Deursen, R.; Schwartz, J.; Fine, M.; Kovacs, G.; Häfliger, P.; Gyimesi, G.; Sithampari, A.; Charles, R. P.; Hediger, M. A.; Reymond, J. L. *Angew. Chemie - Int. Ed.* **2015**, *54* (49), 14748–14752.
- (77) Haverstick, D. M.; Heady, T. N.; Macdonald, T. L.; Gray, L. S. *Cancer Res.* **2000**, *60* (4), 1002–1008.
- (78) Landowski, C. P.; Bolanz, K. A.; Suzuki, Y.; Hediger, M. A. *Pharm. Res.* **2011**, *28* (2), 322–330.
- (79) Kovacs, G.; Montalbetti, N.; Simonin, A.; Danko, T.; Balazs, B.; Zsembergy, A.; Hediger, M. A. *Cell Calcium* **2012**, *52* (6), 468–480.
- (80) Singh, A. K.; McGoldrick, L. L.; Sobolevsky, A. I. *Nat. Struct. Mol. Biol.* **2018**, *25* (9), 805–813.
- (81) Singh, A. K.; Saotome, K.; McGoldrick, L. L.; Sobolevsky, A. I. *Nat. Commun.* **2018**, *9* (1), 2465.
- (82) Hu, H.-Z.; Gu, Q.; Wang, C.; Colton, C. K.; Tang, J.; Kinoshita-Kawada, M.; Lee, L.-Y.; Wood, J. D.; Zhu, M. X. *J. Biol. Chem.* **2004**, *279* (34), 35741–35748.
- (83) Li, M.; Jiang, J.; Yue, L. *J. Gen. Physiol.* **2006**, *127* (5), 525–537.
- (84) Hinman, A.; Chuang, H. -h.; Bautista, D. M.; Julius, D. *Proc. Natl. Acad. Sci.* **2006**, *103* (51), 19564–19568.
- (85) Awale, M.; Reymond, J.-L. *J. Chem. Inf. Model.* **2019**, *59* (1), 10–17.
- (86) Gibbs, H. A. A.; O’Garro, L. W. *HortScience* **2004**, *39* (1), 132–135.
- (87) Yaldiz, G.; Ozguven, M.; Sekeroglu, N. *Ind. Crops Prod.* **2010**, *32* (3), 434–438.
- (88) Thapa, B.; Skalko-Basnet, N.; Takano, A.; Masuda, K.; Basnet, P. *J. Med. Food* **2009**, *12* (4), 908–913.
- (89) Sanatombi, K.; G.J.Sharma. *Not. Bot. Horti Agrobot. Cluj-Napoca* **2008**, *36* (2), 89–90.
- (90) Fusco, B. M.; Alessandri, M. *Anesth. Analg.* **1992**, *74* (3), 375–377.
- (91) McCleane, G. *Br. J. Clin. Pharmacol.* **2001**, *49* (6), 574–579.
- (92) Luo, X.-J. J.; Peng, J.; Li, Y.-J. *J. Eur. J. Pharmacol.* **2011**, *650* (1), 1–7.
- (93) van de Wall, E. H. E. M.; Gram, D. X.; Strubbe, J. H.; Scheurink, A. J. W.; Koolhaas, J. M. *Life Sci.* **2005**, *77* (11), 1283–1292.
- (94) Srinivasan, K. *Crit. Rev. Food Sci. Nutr.* **2015**, 00–00.
- (95) Leung, F. W. In *Capsaicin as a Therapeutic Molecule*; Springer Basel: Basel, 2014; pp 171–179.
- (96) Zheng, J.; Zheng, S.; Feng, Q.; Zhang, Q.; Xiao, X. *Biosci. Rep.* **2017**, *37* (3), BSR20170286.
- (97) Clark, R.; Lee, S. *Anticancer Res.* **2016**, *36*, 837–844.
- (98) Kim, S.; Moon, A. *Arch. Pharm. Res.* **2004**, *27* (8), 845–849.
- (99) Baker, C.; Rodrigues, T.; de Almeida, B. P.; Barbosa-Morais, N. L.; Bernardes, G. J. L. *Bioorg. Med. Chem.* **2019**.
- (100) Ip, S. W.; Lan, S. H.; Huang, A. C.; Yang, J. S.; Chen, Y. Y.; Huang, H. Y.; Lin, Z. P.; Hsu, Y. M.; Yang, M. D.; Chiu, C. F.; Chung, J. G. *Environ. Toxicol.* **2012**, *27* (6), 332–341.
- (101) Ito, K.; Nakazato, T.; Yamato, K.; Miyakawa, Y.; Yamada, T.; Hozumi, N.; Segawa, K.; Ikeda, Y.; Kizaki, M. *Cancer Res.* **2004**, *64* (3), 1071–1078.
- (102) Thoenissen, N. H.; O’Kelly, J.; Lu, D.; Iwanski, G. B.; La, D. T.; Abbassi, S.; Leiter, A.; Karlan, B.; Mehta, R.; Koeffler, H. P. *Oncogene* **2010**, *29* (2), 285–296.
- (103) Batista Fernandes, T.; Alexandre de Azevedo, R.; Yang, R.; Fernandes Teixeira, S.; Henrique Goulart Trossini, G.; Alexandre Marzagao Barbuto, J.; Kleber Ferreira, A.; Parise Filho, R. *Lett. Drug Des. Discov.* **2018**, *15* (1).
- (104) Damião, M. C. F. C. B. Design and synthesis of capsaicin analogues and evaluation of antitumor activity., University of Sao Paulo: São Paulo, 2014.
- (105) Ferreira, A. K.; Tavares, M. T.; Pasqualoto, K. F. M.; de Azevedo, R. A.; Teixeira, S. F.; Ferreira-Junior, W. A.; Bertin, A. M.; de-Sá-Junior, P. L.; Barbuto, J. A. M.; Figueiredo, C. R.; Cury, Y.; Damião, M. C. F. C. B.; Parise-Filho, R. *Tumor Biol.* **2015**.
- (106) De-Sá-Júnior, P. L.; Pasqualoto, K. F. M.; Ferreira, A. K.; Tavares, M. T.; Damião, M. C. F. C. B.; De Azevedo, R. A.; Câmara, D. A. D.; Pereira, A.; De Souza, D. M.; Parise Filho, R. *Toxicol. Appl. Pharmacol.* **2013**, *266* (3), 385–398.
- (107) Cao, E.; Liao, M.; Cheng, Y.; Julius, D. *Nature* **2013**, *504* (7478), 113–118.
- (108) Darré, L.; Domene, C. *Mol. Pharm.* **2015**, *12*, 4454–2265.
- (109) Yang, F.; Zheng, J. *Protein Cell* **2017**, *8* (3), 169–177.
- (110) Lee, J. H.; Lee, Y.; Ryu, H.; Kang, D. W.; Lee, J.; Lazar, J.; Pearce, L. V.; Pavlyukovets, V. A.; Blumberg, P. M.; Choi, S. *J. Comput. Aided. Mol. Des.* **2011**, *25* (4), 317–327.

- (111) Klotz, L.; Venier, N.; Colquhoun, A. J.; Sasaki, H.; Loblaw, D. A.; Fleshner, N.; Venkateswaran, V. *J. Clin. Oncol.* **2011**, *29* (7\_suppl), 23–23.
- (112) Venier, N. A.; Colquhoun, A. J.; Loblaw, A. D.; Fleshner, N. E.; Klotz, L. H.; Venkateswaran, V. In *Proceedings of the 101st Annual Meeting of the American Association for Cancer Research*; American Association for Cancer Research, 2010; Vol. 70, pp 5724–5724.
- (113) Chow, J.; Norng, M.; Zhang, J.; Chai, J. *Biochim. Biophys. Acta (BBA)-Molecular Cell Res.* **2007**, *1773* (4), 565–576.
- (114) Lau, J. K.; Brown, K. C.; Dom, A. M.; Witte, T. R.; Thornhill, B. A.; Crabtree, C. M.; Perry, H. E.; Brown, J. M.; Ball, J. G.; Creel, R. G.; Damron, C. L.; Rollyson, W. D.; Stevenson, C. D.; Hardman, E. E.; Valentovic, M. A.; Carpenter, A. B.; Dasgupta, P. *Apoptosis* **2014**, *19*, 1190–1201.
- (115) Momeni, H. R. *Cell J.* **2011**, *13* (2), 65–72.
- (116) Kubinyi, H. *J. Recept. Signal Transduct.* **1999**, *19* (1–4), 15–39.
- (117) Harvey, A. L.; Clark, R. L.; Mackay, S. P.; Johnston, B. F. *Expert Opin. Drug Discov.* **2010**, *5* (6), 559–568.
- (118) Liu, R.; Li, X.; Lam, K. S. *Curr. Opin. Chem. Biol.* **2017**, *38*, 117–126.
- (119) Chen, H.; Engkvist, O.; Wang, Y.; Olivecrona, M.; Blaschke, T. *Drug Discov. Today* **2018**, *23* (6), 1241–1250.
- (120) Meanwell, N. a. *J. Med. Chem.* **2011**, *54* (8), 2529–2591.
- (121) Guido, R. V. C.; Andricopulo, A. D.; Oliva, G. *Estud. Avançados* **2010**, *24* (70), 81–98.
- (122) Lee, C.-H.; Huang, H.-C.; Juan, H.-F. *Int. J. Mol. Sci.* **2011**, *12* (8), 5304–5318.
- (123) Guido, R. V. C.; Oliva, G.; Andricopulo, A. D. *Pure Appl. Chem.* **2012**, *84* (9), 1857–1866.
- (124) Tan, J. J.; Cong, X. J.; Hu, L. M.; Wang, C. X.; Jia, L.; Liang, X.-J. *Drug Discov. Today* **2010**, *15* (5–6), 186–197.
- (125) Lill, M. A.; Danielson, M. L. *J. Comput. Aided. Mol. Des.* **2011**, *25* (1), 13–19.
- (126) Lu, W.; Zhang, R.; Jiang, H.; Zhang, H.; Luo, C. *Front. Chem.* **2018**, *6*.
- (127) Blundell, T. L. *Nature* **1996**, *384* (6604), 23–26.
- (128) Renaud, J.-P.; Chari, A.; Ciferri, C.; Liu, W.; Rémygy, H.-W.; Stark, H.; Wiesmann, C. *Nat. Rev. Drug Discov.* **2018**, *17* (7), 471–492.
- (129) Montanari, C. A.; Bolzani, V. da S. *Quim. Nova* **2001**, *24* (1).
- (130) Mavromoustakos, T.; Durdagi, S.; Koukoulitsa, C.; Simcic, M.; G. Papadopoulos, M.; Hodoscek, M.; Golic Grdadolnik, S. *Curr. Med. Chem.* **2011**, *18* (17), 2517–2530.
- (131) Sutch, B. T.; Romero, R. M.; Neamati, N.; Haworth, I. S. *J. Chem. Educ.* **2012**, *89* (1), 45–51.
- (132) Ferreira, L.; dos Santos, R.; Oliva, G.; Andricopulo, A. *Molecules* **2015**, *20* (7), 13384–13421.
- (133) Anderson, A. C. *Chem. Biol.* **2003**, *10* (9), 787–797.
- (134) Bacilieri, M.; Moro, S. *Curr. Drug Discov. Technol.* **2006**, *3* (3), 155–165.
- (135) Avery, M. A.; Alvim-Gaston, M.; Rodrigues, C. R.; Barreiro, E. J.; Cohen, F. E.; Sabnis, Y. A.; Woolfrey, J. R. *J. Med. Chem.* **2002**, *45* (2), 292–303.
- (136) Lima, L. M. L.; Barreiro, E. J. *Curr. Med. Chem.* **2005**, *12* (1), 23–49.
- (137) Burger, A. *Prog. Drug Res.* **1991**, *37*, 287–371.
- (138) Brown, N. In *Bioisosteres in Medicinal Chemistry*; Wiley-VCH Verlag GmbH & Co. KGaA: Weinheim, Germany, 2012; pp 1–14.
- (139) Patani, G. A.; LaVoie, E. J. *Chem. Rev.* **1996**, *96* (8), 3147–3176.
- (140) Griffen, E.; Leach, A. G.; Robb, G. R.; Warner, D. J. *J. Med. Chem.* **2011**, *54* (22), 7739–7750.
- (141) Firth, N. C.; Brown, N.; Blagg, J. *J. Chem. Inf. Model.* **2012**, *52* (10), 2516–2525.
- (142) Wirth, M.; Zoete, V.; Michielin, O.; Sauer, W. H. B. *Nucleic Acids Res.* **2013**, *41* (D1), D1137–D1143.
- (143) Walpole, C. S. J.; Wrigglesworth, R.; Bevan, S.; Campbell, E. A.; Dray, A.; James, I. F.; Masdin, K. J.; Perkins, M. N.; Winter, J. *J. Med. Chem.* **1993**, *36* (16), 2373–2380.
- (144) Walpole, C. S. J.; Wrigglesworth, R.; Bevan, S.; Campbell, E. A.; Dray, A.; James, I. F.; Masdin, K. J.; Perkins, M. N.; Winter, J. *J. Med. Chem.* **1993**, *36* (16), 2381–2389.
- (145) Conway, S. J. *Chem. Soc. Rev.* **2008**, *37* (8), 1530.
- (146) Walpole, C. S. J.; Bevan, S.; Bovermann, G.; Boelsterli, J. J.; Breckenridge, R.; Davies, J. W.; Hughes, G. A.; James, I.; Oberer, L.; Winter, J.; Wrigglesworth, R. *J. Med. Chem.* **1994**, *37* (13), 1942–1954.
- (147) Urban, L.; Campbell, E. A.; Panesar, M.; Patel, S.; Chaudhry, N.; Kane, S.; Buchheit, K.-H.; Sandells, B.; James, I. F. *Pain* **2000**, *89* (1), 65–74.
- (148) Claudio Viegas-Junior; Eliezer J. Barreiro; Carlos Alberto Manssour Fraga. *Curr. Med. Chem.* **2007**, *14* (17), 1829–1852.
- (149) Fraga, C. A. M. *Expert Opin. Drug Discov.* **2009**, *4* (6), 605–609.
- (150) Thakur, G. A.; Duclos, R. I.; Makriyannis, A. *Life Sci.* **2005**, *78* (5), 454–466.

- (151) Pertwee, R. G. *Int. J. Obes.* **2006**, *30* (S1), S13–S18.
- (152) Muller, C.; Morales, P.; Reggio, P. H. *Front. Mol. Neurosci.* **2019**, *11*.
- (153) Di Marzo, V.; Griffin, G.; De Petrocellis, L.; Brandi, I.; Bisogno, T.; Williams, W.; Grier, M. C.; Kulasegram, S.; Mahadevan, A.; Razdan, R. K.; Martin, B. R. *J. Pharmacol. Exp. Ther.* **2002**, *300* (3), 984–991.
- (154) Di Marzo, V.; Breivogel, C.; Bisogno, T.; Melck, D.; Patrick, G.; Tao, Q.; Szallasi, A.; Razdan, R. K.; Martin, B. R. *Eur. J. Pharmacol.* **2000**, *406* (3), 363–374.
- (155) Ding, Z.; Cowan, A.; Rawls, S. M. *Brain Res.* **2005**, *1065* (1–2), 147–151.
- (156) Smart, D.; Gunthorpe, M. J.; Jerman, J. C.; Nasir, S.; Gray, J.; Muir, A. I.; Chambers, J. K.; Randall, A. D.; Davis, J. B. *Br. J. Pharmacol.* **2000**, *129* (2), 227–230.
- (157) De Petrocellis, L.; Bisogno, T.; Davis, J. B.; Pertwee, R. G.; Di Marzo, V. *FEBS Lett.* **2000**, *483* (1), 52–56.
- (158) Hayman, M.; Kam, P. C. A. *Curr. Anaesth. Crit. Care* **2008**, *19* (5–6), 338–343.
- (159) Bley, K.; Boorman, G.; Mohammad, B.; McKenzie, D.; Babbar, S. *Toxicol. Pathol.* **2012**, *40* (6), 847–873.
- (160) Thota, S.; Rodrigues, D. A.; Pinheiro, P. de S. M.; Lima, L. M.; Fraga, C. A. M.; Barreiro, E. J. *Bioorg. Med. Chem. Lett.* **2018**, *28* (17), 2797–2806.
- (161) Carneiro Brum, J. de O.; França, T. C. C.; Villar, J. D. F. *Mini-Reviews Med. Chem.* **2019**, *19*.
- (162) Yang, F.; Xiao, X.; Cheng, W.; Yang, W.; Yu, P.; Song, Z.; Yarov-Yarovoy, V.; Zheng, J. *Nat. Chem. Biol.* **2015**, *11*, 518–526.
- (163) Damião, M. C. F. C. B.; Pasqualoto, K. F. M.; Ferreira, A. K.; Teixeira, S. F.; Azevedo, R. a.; Barbuto, J. a. M.; Palace-Berl, F.; Franchi-Junior, G. C.; Nowill, A. E.; Tavares, M. T.; Parise-Filho, R. *Arch. Pharm. (Weinheim)*. **2014**, *347* (12), 885–895.
- (164) Pereira, G. J. V.; Tavares, M. T.; Azevedo, R. A.; Martins, B. B.; Cunha, M. R.; Bhardwaj, R.; Cury, Y.; Zambelli, V. O.; Barbosa, E. G.; Hediger, M. A.; Parise-Filho, R. *Bioorg. Med. Chem.* **2019**, *27* (13), 2893–2904.
- (165) Cunha, M. R.; Tavares, M. T.; Carvalho, C. F.; Silva, N. A. T.; Souza, A. D. F.; Pereira, G. J. V.; Ferreira, F. F.; Parise-Filho, R. *ACS Sustain. Chem. Eng.* **2016**, *4* (4), 1899–1905.
- (166) Kamimura, A.; Komatsu, H.; Moriyama, T.; Nozaki, Y. *Tetrahedron* **2013**, *69* (29), 5968–5972.
- (167) Firouzabadi, H.; Karimi, B.; Abbassi, M. *J. Chem. Res.* **1999**, No. 3, 236–237.
- (168) Silva, T. F.; Bispo Júnior, W.; Alexandre-Moreira, M. S.; Costa, F. N.; Monteiro, C.; Furlan Ferreira, F.; Barroso, R. C. R.; Noël, F.; Sudo, R. T.; Zapata-Sudo, G.; Lima, L. M.; Barreiro, E. *Molecules* **2015**, *20* (2), 3067–3088.
- (169) Tian, B.; He, M.; Tang, S.; Hewlett, I.; Tan, Z.; Li, J.; Jin, Y.; Yang, M. *Bioorg. Med. Chem. Lett.* **2009**, *19* (8), 2162–2167.
- (170) Tian, B.; He, M.; Tan, Z.; Tang, S.; Hewlett, I.; Chen, S.; Jin, Y.; Yang, M. *Chem. Biol. Drug Des.* **2011**, *77* (3), 189–198.
- (171) Lopes, A.; Miguez, E.; Kümmerle, A.; Rumjanek, V.; Fraga, C.; Barreiro, E. *Molecules* **2013**, *18* (10), 11683–11704.
- (172) Bunnell, C. A.; Fuchs, P. L. *J. Org. Chem.* **1977**, *42* (15), 2614–2617.
- (173) Costa, F. N.; Ferreira, F. F.; da Silva, T. F.; Barreiro, E. J.; Lima, L. M.; Braz, D.; Barroso, R. C. *Powder Diffr.* **2013**, *28* (S2), S491–S509.
- (174) Hayakawa, M.; Kawaguchi, K.; Kaizawa, H.; Koizumi, T.; Ohishi, T.; Yamano, M.; Okada, M.; Ohta, M.; Tsukamoto, S.; Raynaud, F. I. *Bioorg. Med. Chem.* **2007**, *15* (17), 5837–5844.
- (175) Novak, I.; Li, W.; Harrison, L. J. *Acta Crystallogr. Sect. E Struct. Reports Online* **2007**, *63* (5), o2599–o2599.
- (176) Kylmälä, T.; Hämäläinen, A.; Kuuloja, N.; Tois, J.; Franzén, R. *Tetrahedron* **2010**, *66* (46), 8854–8861.
- (177) Kylmälä, T.; Udd, S.; Tois, J.; Franzén, R. *Tetrahedron Lett.* **2010**, *51* (28), 3613–3615.
- (178) Zhu, X.-Q.; Mao, S.; Guo, D.-D.; Li, B.; Guo, S.-H.; Gao, Y.-R.; Wang, Y.-Q. *ChemCatChem* **2017**, *9* (6), 1084–1091.
- (179) Cunha, M. R.; Bhardwaj, R.; Lindinger, S.; Butorac, C.; Romanin, C.; Hediger, M. A.; Reymond, J.-L. *ACS Med. Chem. Lett.* **2019**, *10* (9), 1341–1345.
- (180) van Dijken, D. J.; Kovaříček, P.; Ihrig, S. P.; Hecht, S. *J. Am. Chem. Soc.* **2015**, *137* (47), 14982–14991.
- (181) Bai, B.; Zhang, M.; Ji, N.; Wei, J.; Wang, H.; Li, M. *Chem. Commun.* **2017**, *53* (18), 2693–2696.
- (182) Neises, B.; Steglich, W. *Angew. Chemie Int. Ed. English* **1978**, *17* (7), 522–524.
- (183) Abdel-Magid, A. F.; Maryanoff, C. A. In *ACS Symposium Series*; 1996; pp 201–216.
- (184) Hopkins, A. L.; Groom, C. R.; Alex, A. *Drug Discov. Today* **2004**, *9* (10), 430–431.
- (185) Hopkins, A. L.; Keserü, G. M.; Leeson, P. D.; Rees, D. C.; Reynolds, C. H. *Nat. Rev. Drug Discov.*

- 
- 2014, 13 (2), 105–121.
- (186) Bissantz, C.; Kuhn, B.; Stahl, M. *J. Med. Chem.* **2010**, 53 (14), 5061–5084.
- (187) Diana, G. D.; Rudewicz, P.; Pevear, D. C.; Nitz, T. J.; Aldous, S. C.; Aldous, D. J.; Robinson, D. T.; Draper, T.; Dutko, F. J. *J. Med. Chem.* **1995**, 38 (8), 1355–1371.
- (188) Murphy, C. D.; Sandford, G. *Expert Opin. Drug Metab. Toxicol.* **2015**, 11 (4), 589–599.
- (189) Lednicer, D.; Emmert, D. E.; Lahti, R.; Rudzik, A. D. *J. Med. Chem.* **1972**, 15 (12), 1239–1243.
- (190) Miyashita, M.; Yoshikoshi, A.; Grieco, P. A. *J. Org. Chem.* **1977**, 42 (23), 3772–3774.
- (191) Malaiyandi, L. M.; Sharthiya, H.; Dineley, K. E. *BioMetals* **2016**, 29 (4), 625–635.
- (192) Lundberg, P.; Magzoub, M.; Lindberg, M.; Hällbrink, M.; Jarvet, J.; Eriksson, L. E. ; Langel, Ü.; Gräslund, A. *Biochem. Biophys. Res. Commun.* **2002**, 299 (1), 85–90.
- (193) Murayama, N.; Imai, N.; Nakane, T.; Shimizu, M.; Yamazaki, H. *Biochem. Pharmacol.* **2007**, 73 (12), 2020–2026.
- (194) Parikh, A.; Gillam, E. M. J.; Guengerich, F. P. *Nat. Biotechnol.* **1997**, 15 (8), 784–788.
- (195) Bolanz, K. A.; Kovacs, G. G.; Landowski, C. P.; Hediger, M. A. *Mol. Cancer Res.* **2009**, 7 (12), 2000–2010.
- (196) Kovacs, G.; Montalbetti, N.; Franz, M.-C.; Graeter, S.; Simonin, A.; Hediger, M. A. *Cell Calcium* **2013**, 54 (4), 276–286.

## 7. Supplementary Data

### 7.1 Time-course confocal microscopy

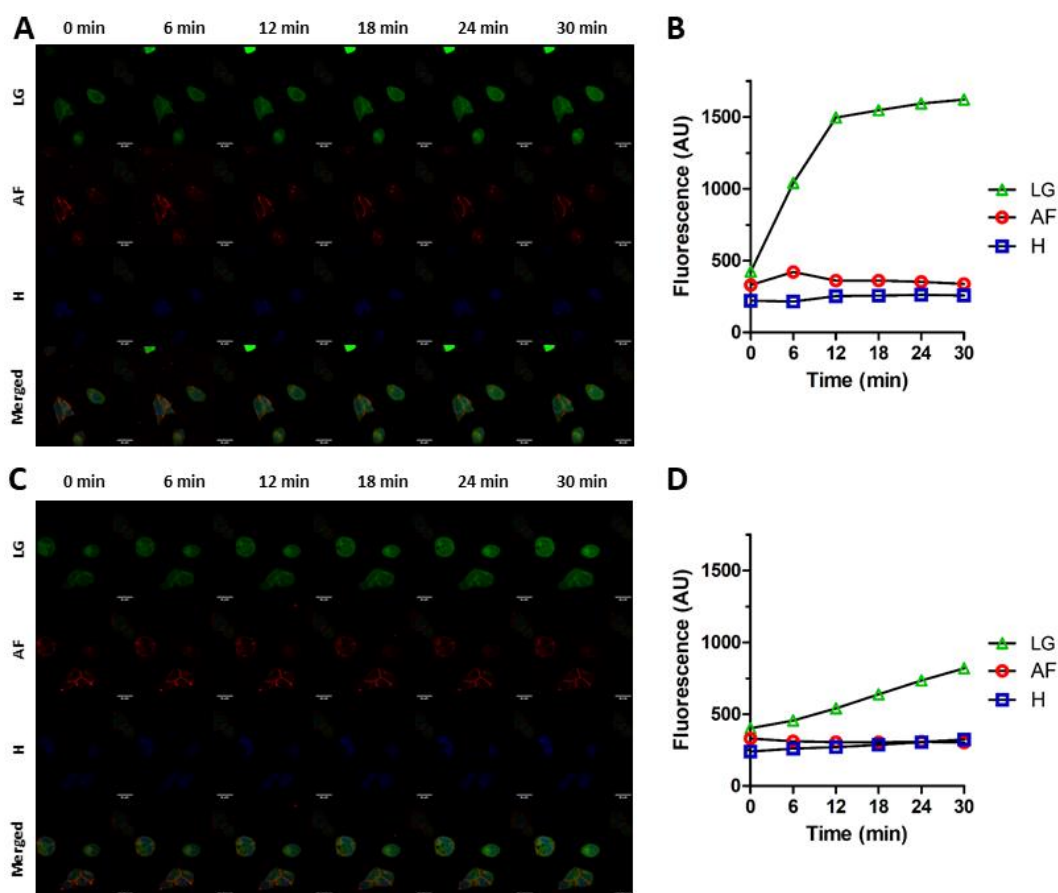


**Figure S1.** Time-course of  $\text{Cd}^{2+}$  uptake in HEK-hTRPV6 cells with Leadmiun Green (LG), Alexa Fluor 298 (AF), and Hoechst 33258 (H) along 30 min. Images were collected using confocal microscopy (Nikon Eclipse TE2000-E, 100X). HEK-hTRPV6 cells were incubated with fluorescent dyes for 30 min at 37 °C. To these cells, DMSO (A) or MRC-130 (10  $\mu\text{M}$ , C) was applied followed by a solution of  $\text{Cd}^{2+}$  (50  $\mu\text{M}$ ). The total fluorescence intensity for each channel was plotted in graphs (B) and (D), respectively for DMSO and compound MRC-130. Images were collected with excitation for LG at  $\lambda_{\text{ex}} = 488$  nm and emission at  $\lambda_{\text{em}} = 520$  nm, H at  $\lambda_{\text{ex}} = 352$  nm and emission at  $\lambda_{\text{em}} = 461$  nm, and AF at  $\lambda_{\text{ex}} = 590$  nm and emission at  $\lambda_{\text{em}} = 617$  nm. White bars denote 20  $\mu\text{m}$ .

## 7.2 Inhibition curves of *cis-22a* against SKOV-3 and HEK-wt

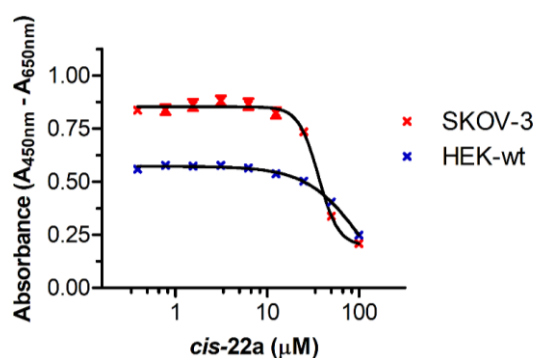


**Figure S2.** XTT cell viability curve of SKOV-3 (human ovary adenocarcinoma) and HEK-wt (human embryonic kidney-wild type) under *cis-22a* treatment. Data shown is mean  $\pm$  SEM ( $n = 6$ /concentration) from 3 independent experiments.

## 7.3 In vitro Polypharmacology and metabolism

**Table S1.** *In vitro* pharmacology profile of MRC-130 and *cis-22a* on several ion channels

Ion Channel ( <i>h</i> )	% of Inhibition at 10 $\mu$ M <sup>a</sup>	
	MRC-130	<i>cis-22a</i> <sup>c</sup>
Adrenergic $\alpha_{1A}$	4.8 $\pm$ 0.2	94.0 $\pm$ 5.0
Dopamine D <sub>1</sub>	2.3 $\pm$ 4.3	63.9 $\pm$ 0.2
Dopamine D <sub>2S</sub> <sup>b</sup>	27.1 $\pm$ 3.2	90.3 $\pm$ 0.6
Dopamine D <sub>4.4</sub>	7.3 $\pm$ 2.3	93.8 $\pm$ 0.5
<i>h</i> ERG	7.7 $\pm$ 0.4	82.3 $\pm$ 4.0
Muscarinic M <sub>1</sub>	15.1 $\pm$ 2.6	74.3 $\pm$ 2.7
Muscarinic M <sub>2</sub>	33.3 $\pm$ 1.9	87.2 $\pm$ 2.7
Opiate $\mu$ <sup>b</sup>	12.2 $\pm$ 2.6	98.1 $\pm$ 0.6
Serotonine 5-HT <sub>1A</sub>	4.8 $\pm$ 0.2	88.5 $\pm$ 4.5

<sup>a</sup>The effect of MRC-130 on voltage- and/or ligand-gated ion channels were measured in radioligand binding assays using an antagonist radioligand. <sup>b</sup>An agonist radioligand was used for the binding competition assay. <sup>c</sup>Values were taken from ref.<sup>76</sup>

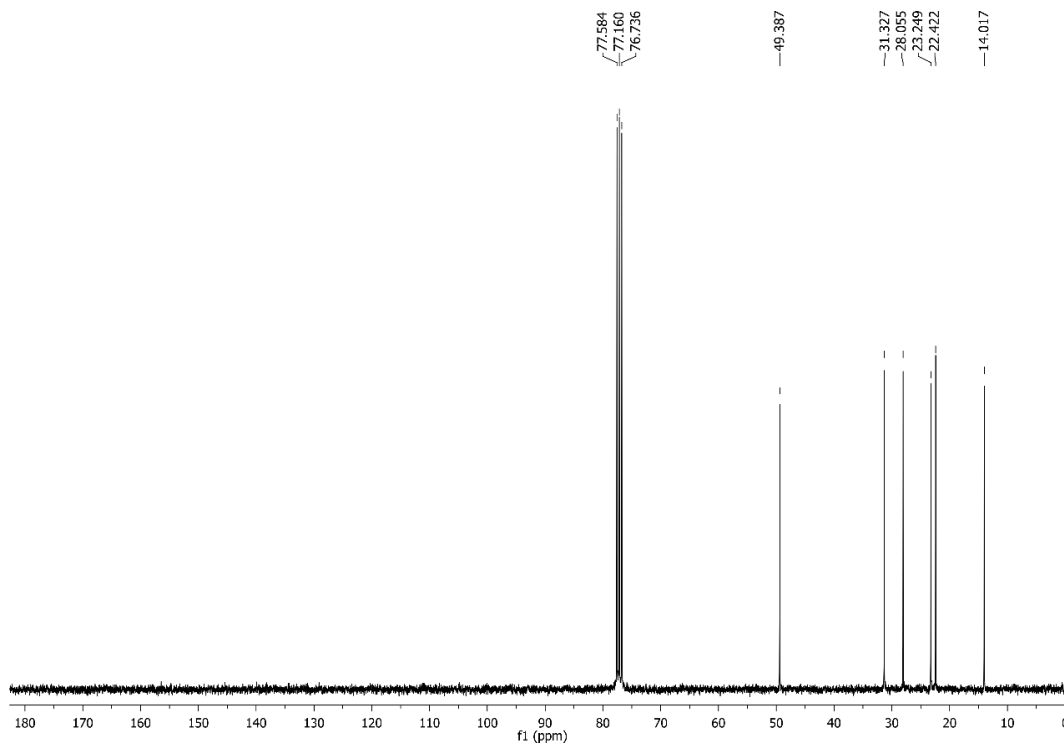
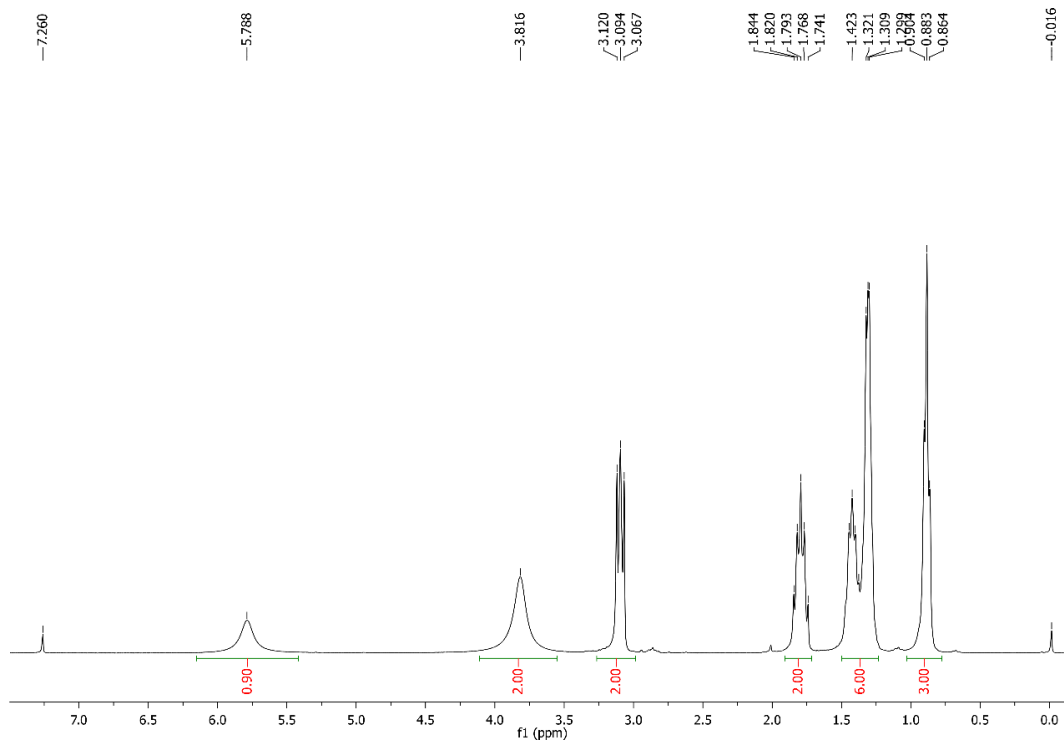
**Table S2.** *In vitro* pharmacology profile of MRC-130 and *cis-22a* on several ion channels

Time (min)	% of the remaining compound	
	MRC-130	<i>cis-22a</i>
0	100	100
15	101.7 $\pm$ 0.8	38.4 $\pm$ 0.5
30	100.4 $\pm$ 0.8	2.9 $\pm$ 0.4
45	98.4 $\pm$ 3.1	3.1 $\pm$ 0.1
60	91.3 $\pm$ 0.2	4.4 $\pm$ 0.4

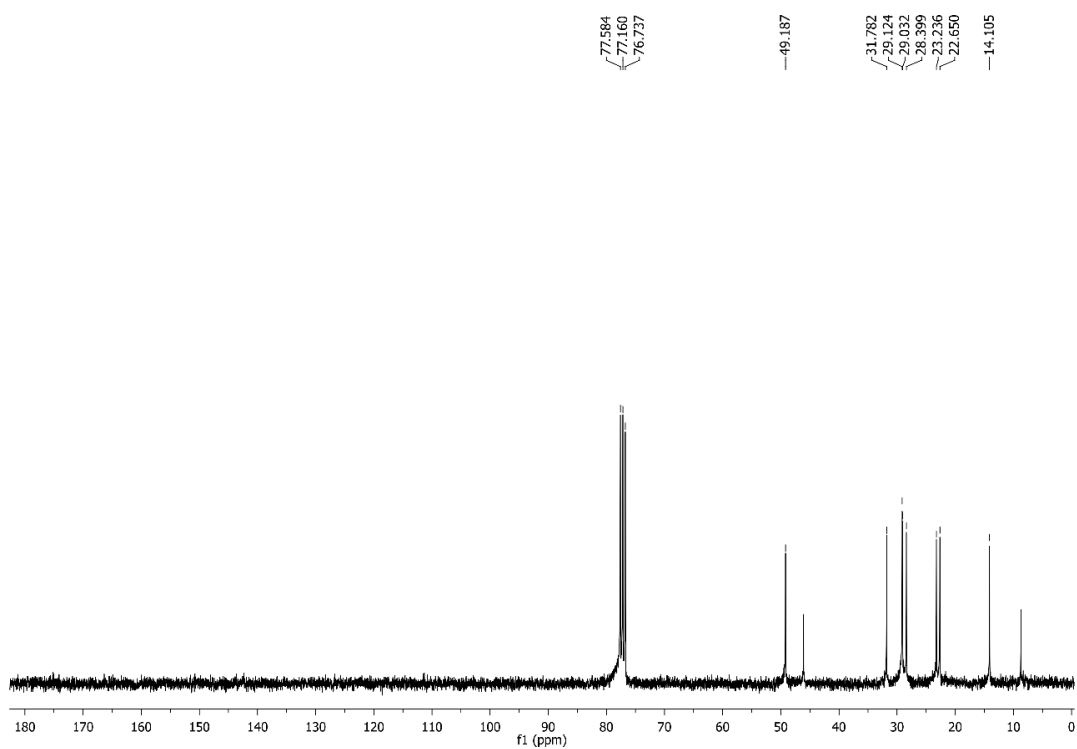
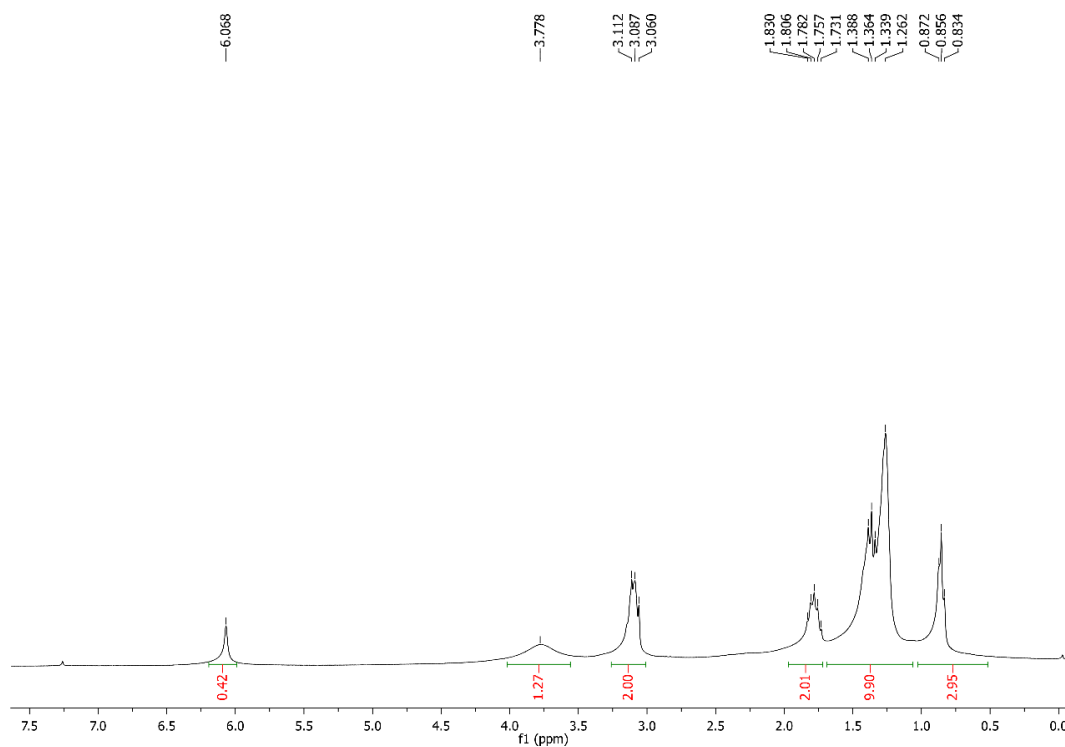
<sup>a</sup>Metabolic stability, expressed as a percent of the parent compound remaining, was calculated by comparing the peak area of the compound at the time point relative to that at time 0 min. The half-life ( $T_{1/2}$ ) was estimated from the slope of the initial linear range of the logarithmic curve of compound remaining (%) vs. time, assuming first-order kinetics.

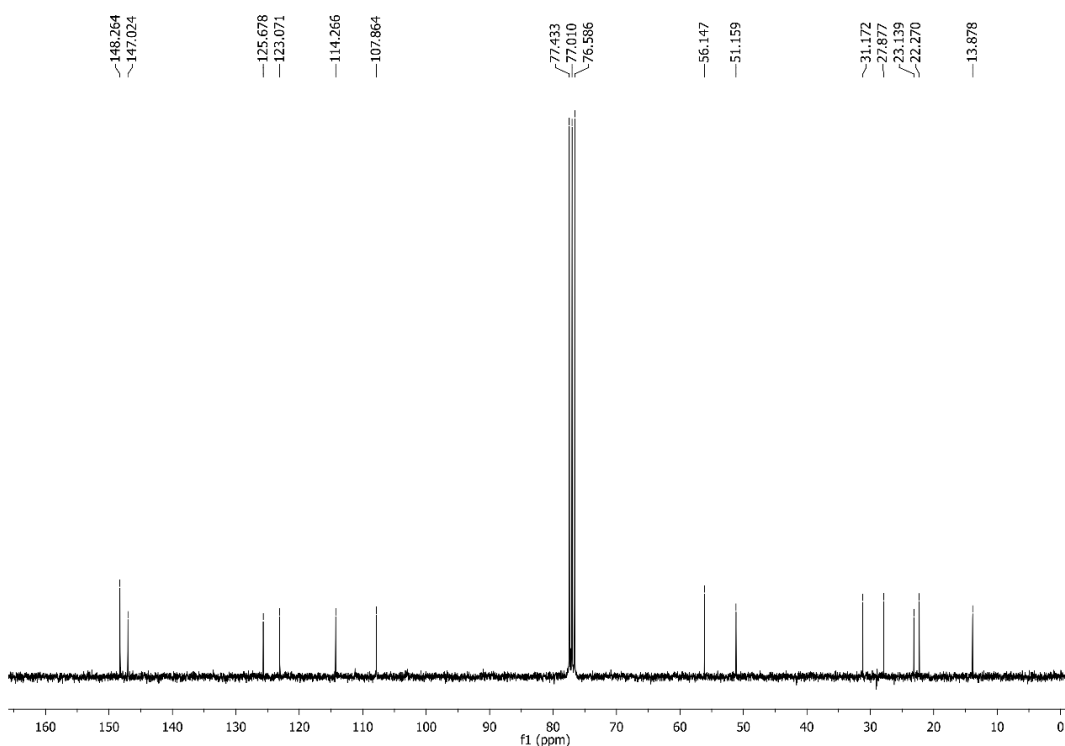
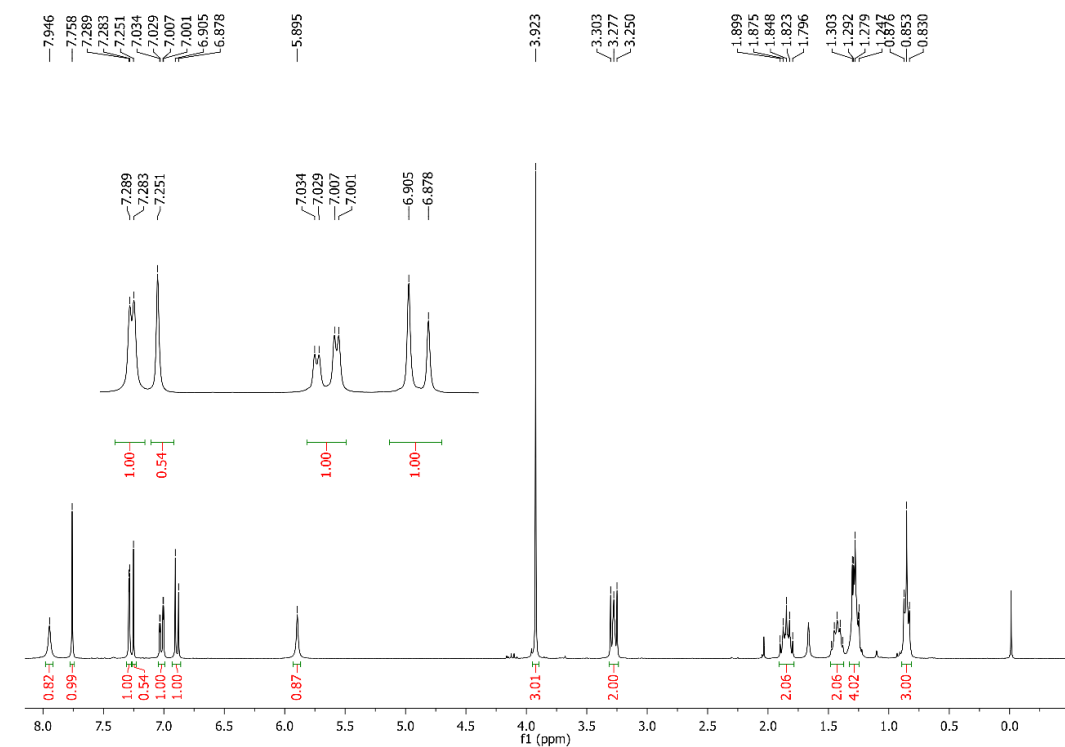
## 7.4 Copy of NMR spectra, ESI-HRMS and HPLC traces

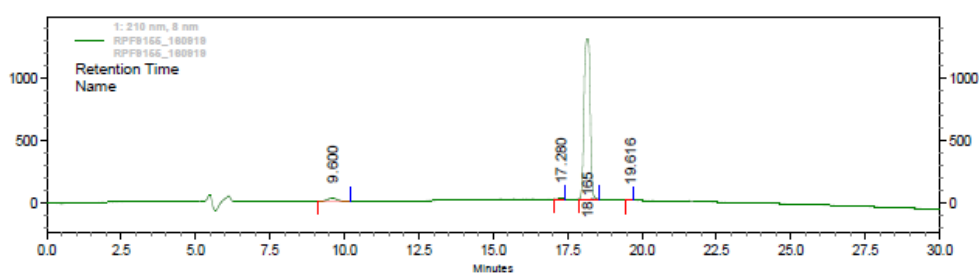
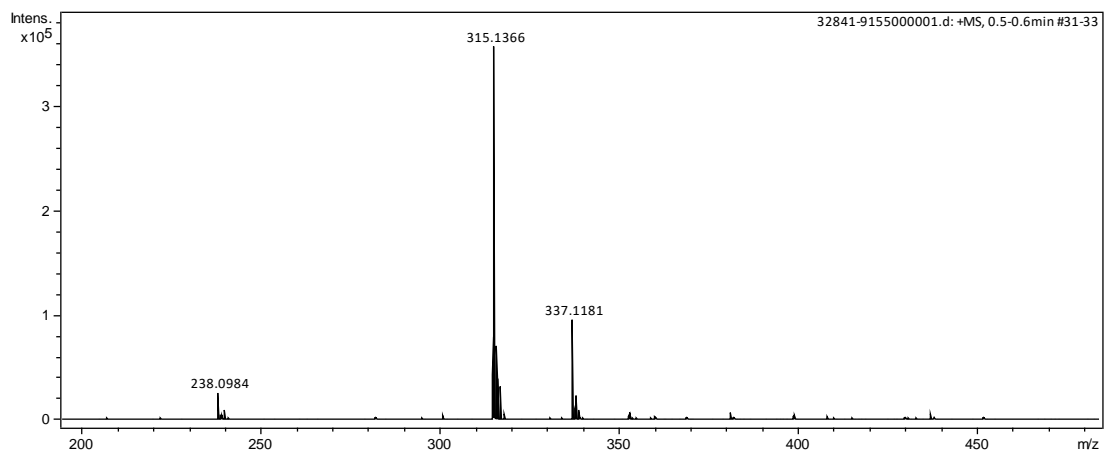
## Hexane-1-sulfonohydrazide (3a).



## Octane-1-sulfonylhydrazide (3b).

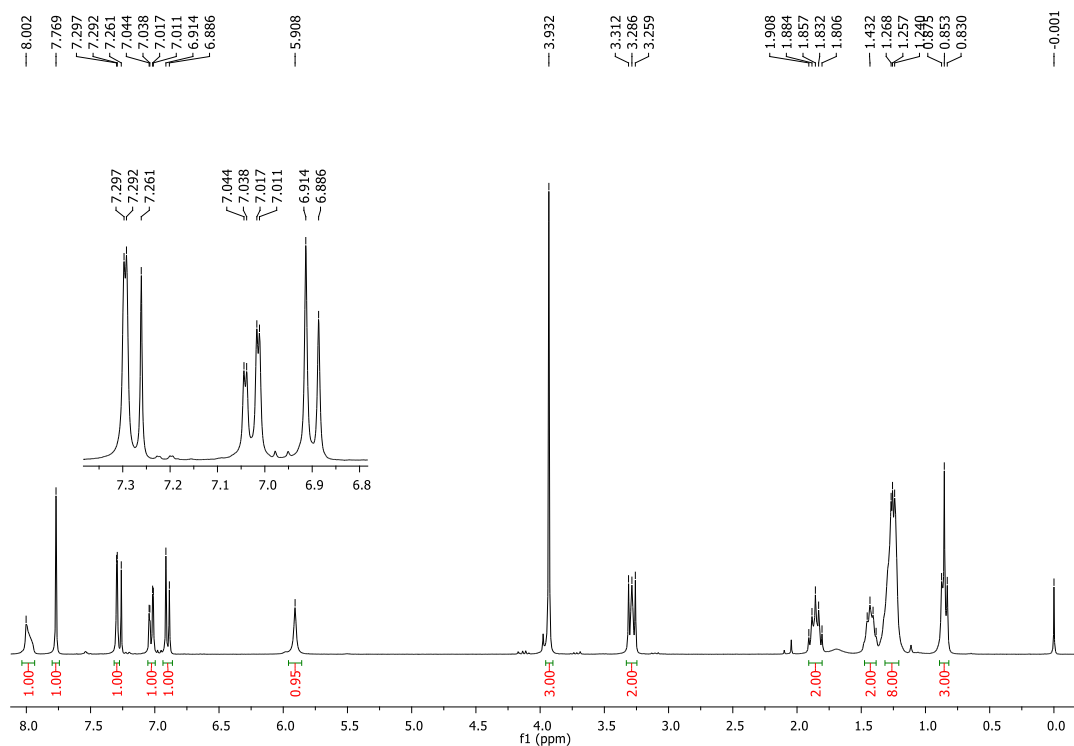


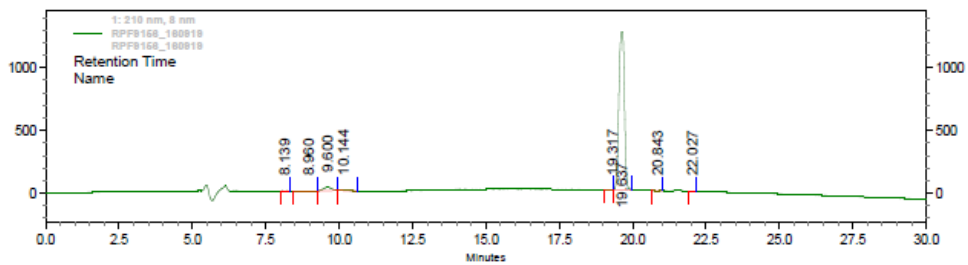
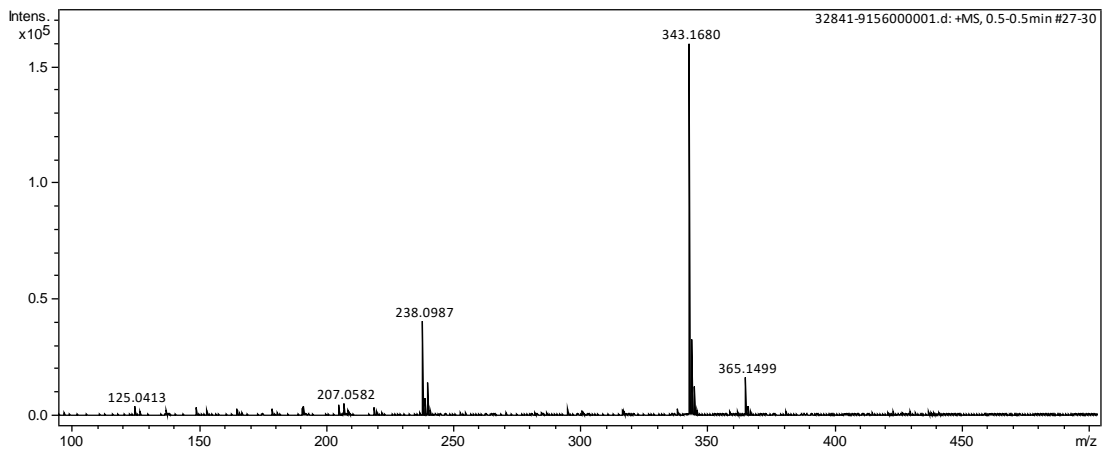
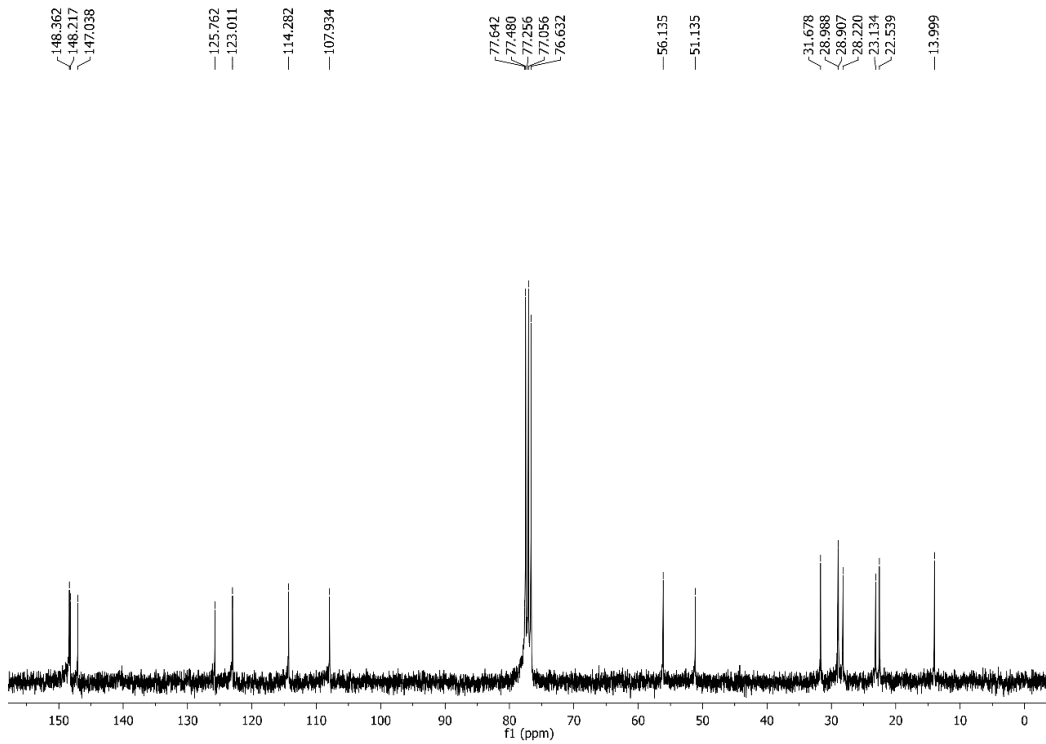
**(E)-N'-(4-hydroxy-3-methoxybenzylidene)hexane-1-sulfonylhydrazide (5a).**



Pk #	Name	Retention Time	Area	Area Percent	Height Percent
1		9.600	535991	2.85	1.88
2		17.280	28022	0.15	0.21
3		18.165	18240399	96.84	97.65
4		19.616	32119	0.17	0.25

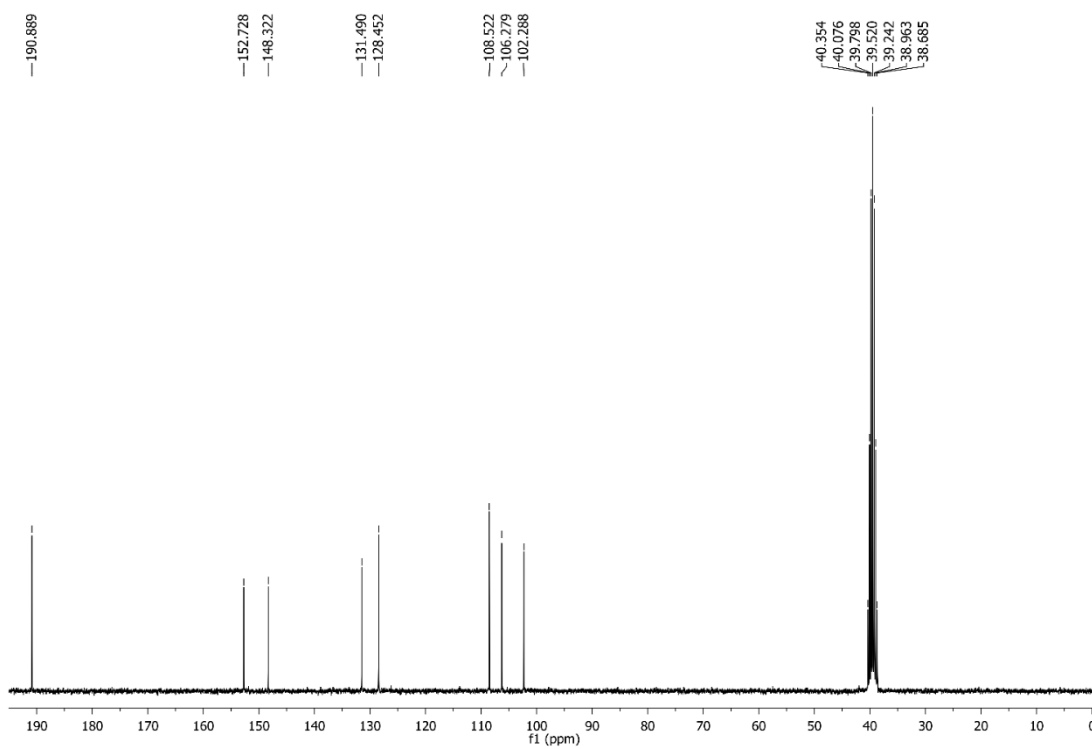
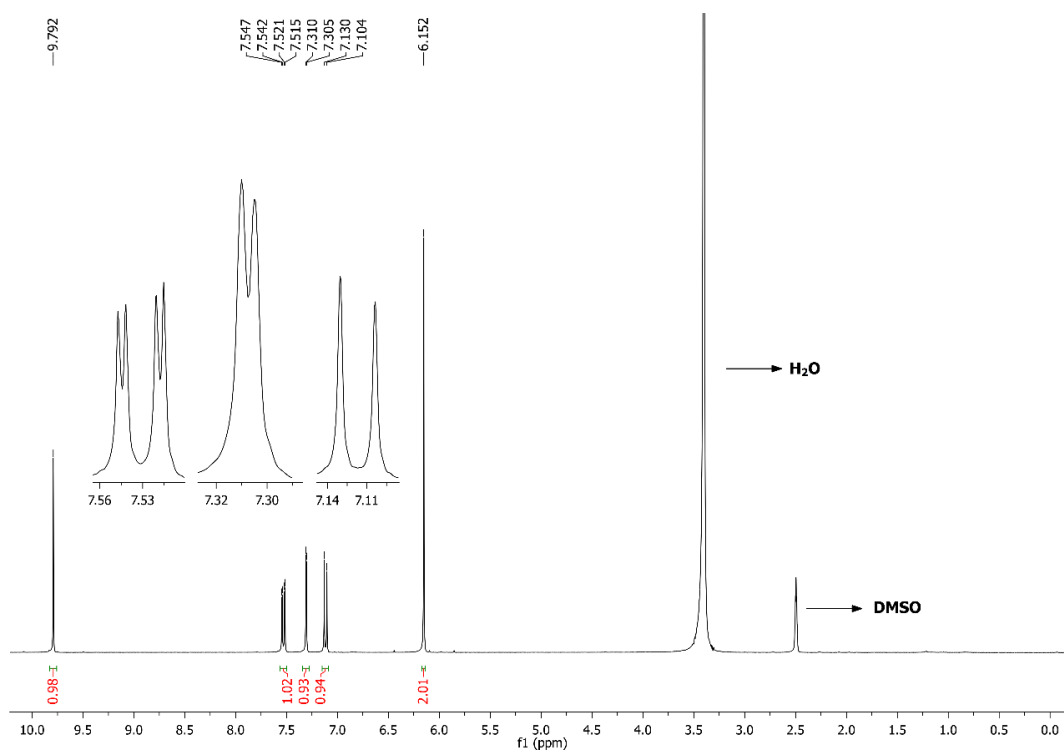
**(E)-N'-(4-hydroxy-3-methoxybenzylidene)octane-1-sulfonohydrazide (5b).**

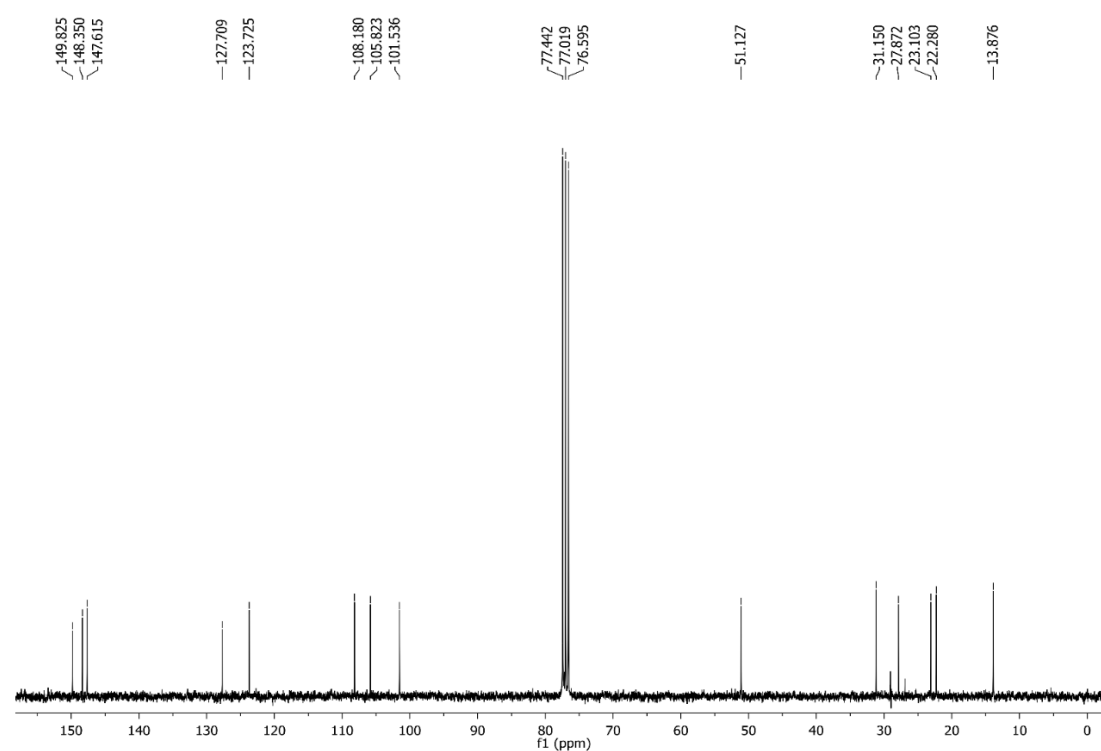
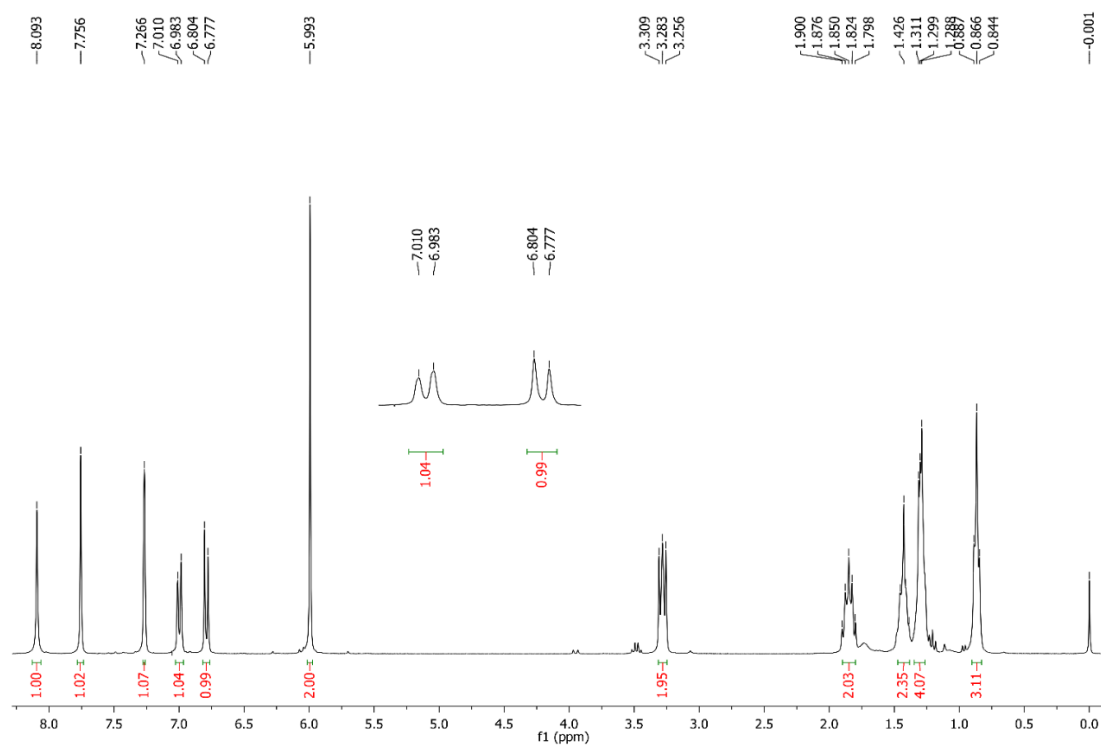


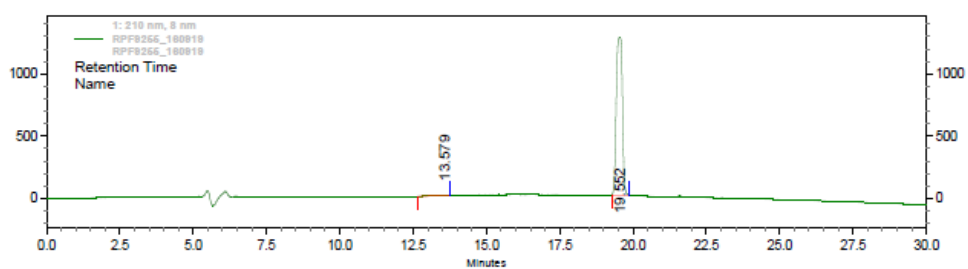
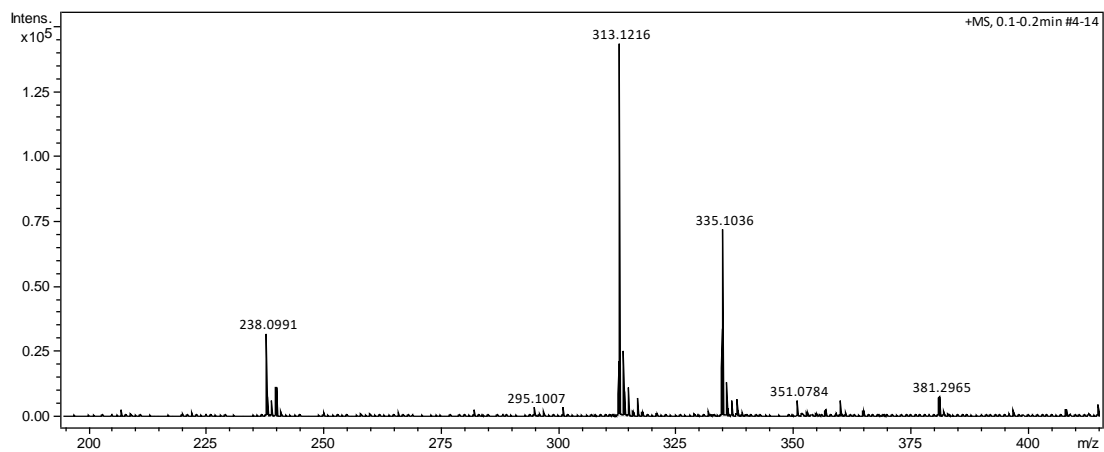


Pk #	Name	Retention Time	Area	Area Percent	Height Percent
1		8.139	19402	0.11	0.13
2		8.960	47178	0.28	0.13
3		9.600	532579	3.13	2.08
4		10.144	63488	0.37	0.25
5		19.317	25180	0.15	0.16
6		19.637	16284702	95.78	97.01
7		20.843	15640	0.09	0.09
8		22.027	14891	0.09	0.14

## Benzo[d][1,3]dioxole-5-carbaldehyde (7).

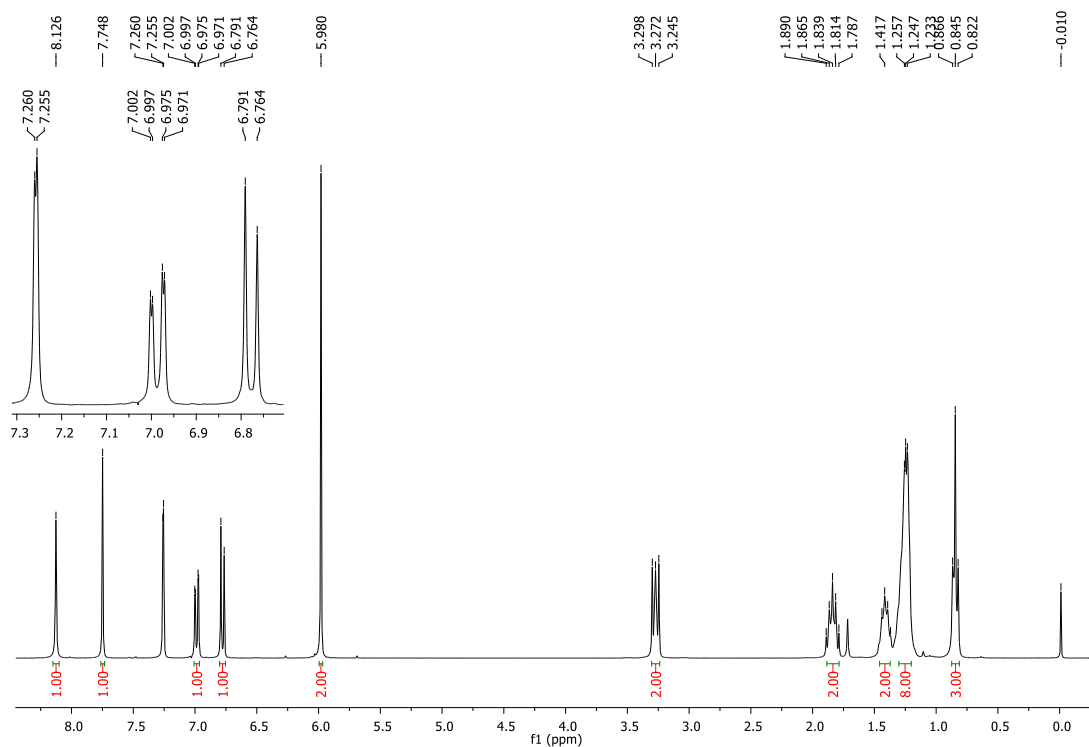


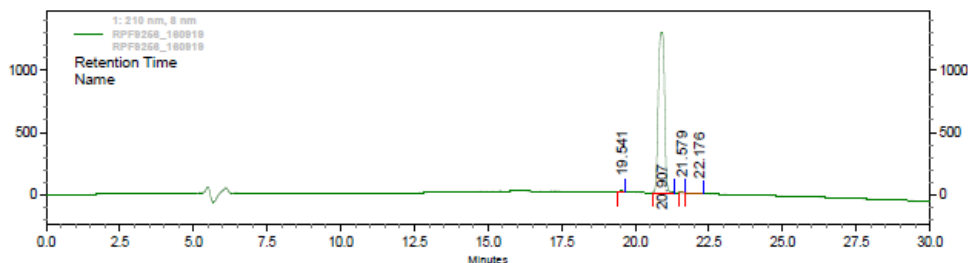
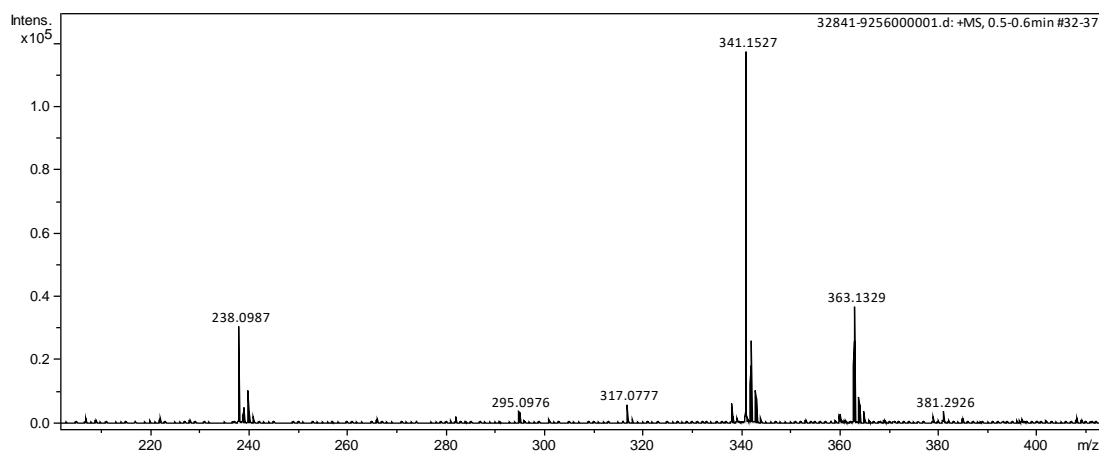
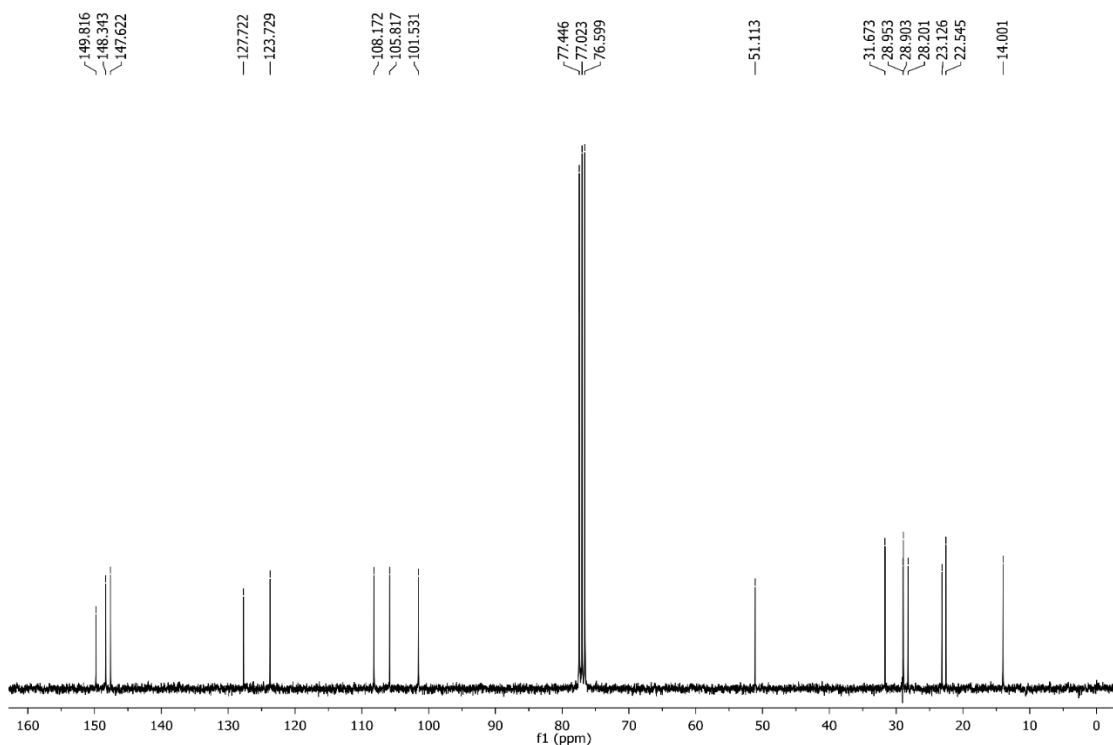
**(E)-N'-(benzo[d][1,3]dioxol-5-ylmethylene)hexane-1-sulfonohydrazide (8a).**



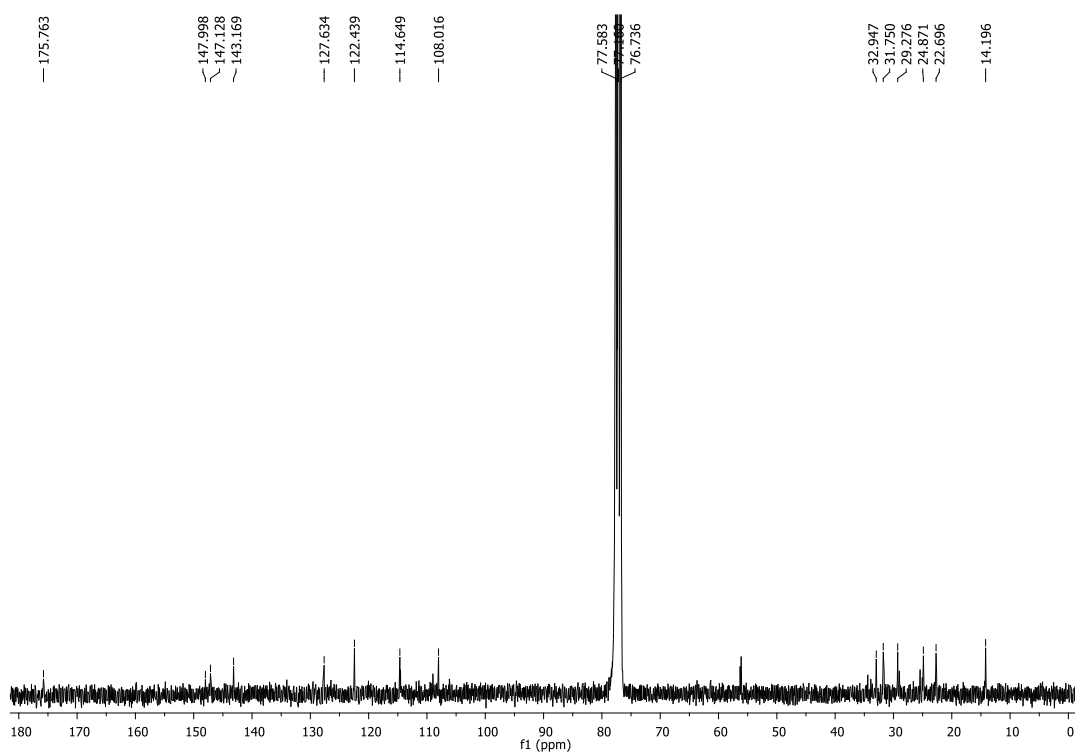
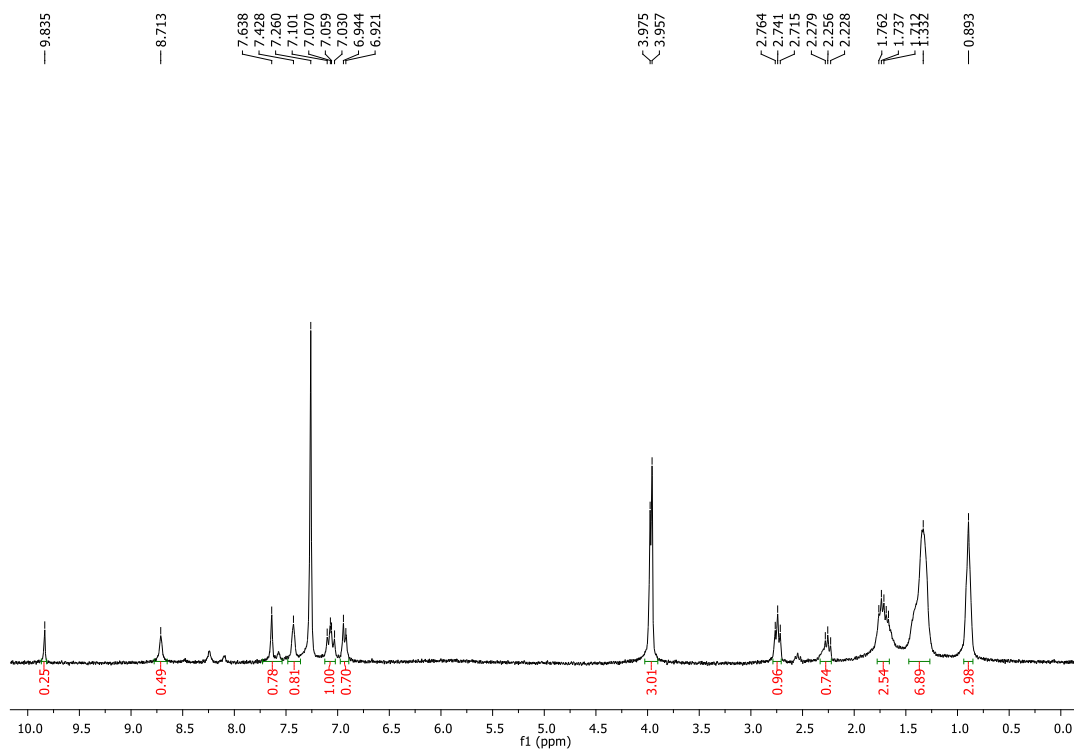
Pk #	Name	Retention Time	Area	Area Percent	Height Percent
1		13.579	69931	0.38	0.18
2		19.552	18220656	99.62	99.82

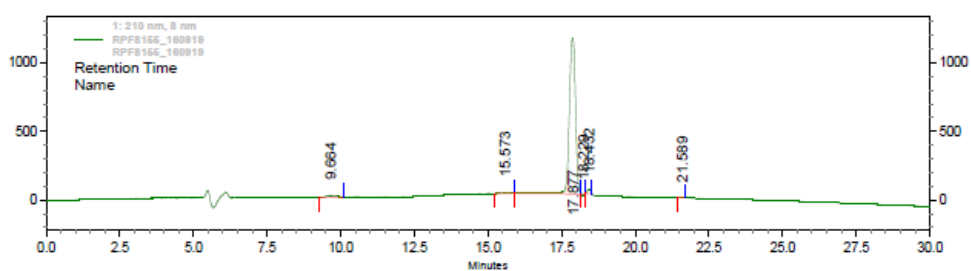
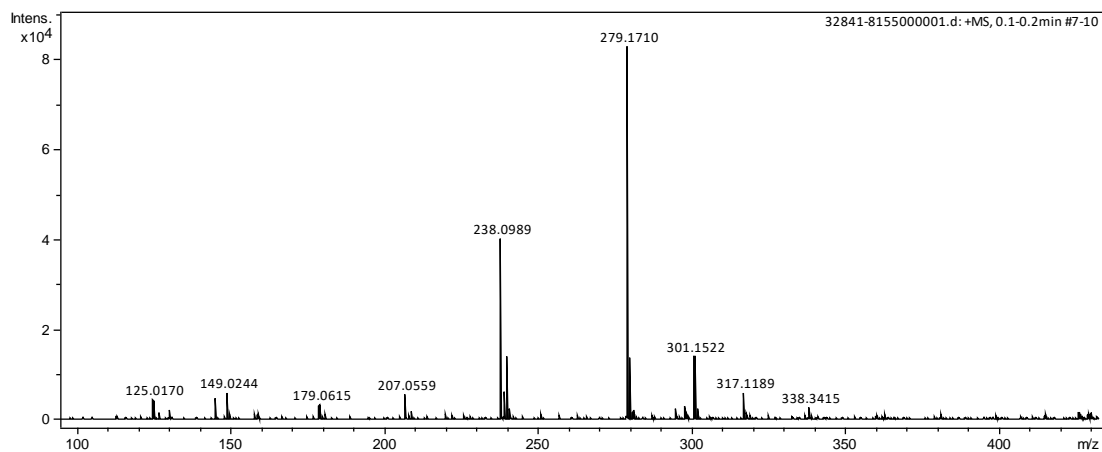
**(E)-N'-(benzo[d][1,3]dioxol-5-ylmethylene)octane-1-sulfonohydraide (8b).**





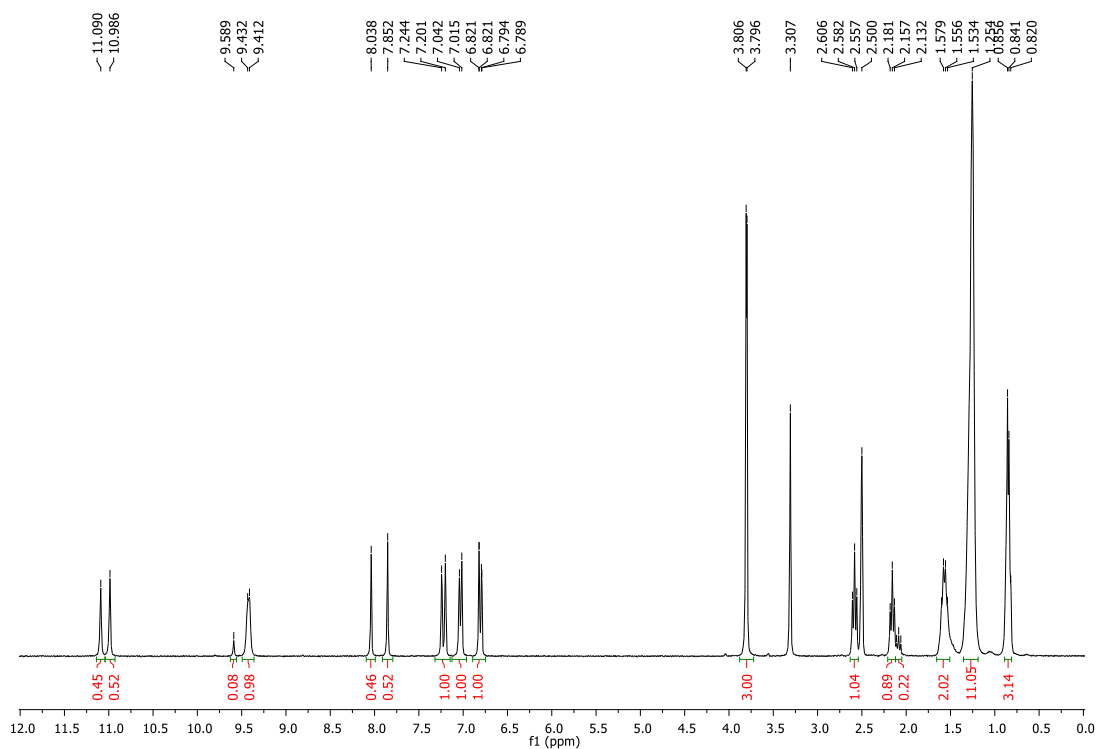
Pk #	Name	Retention Time	Area	Area Percent	Height Percent
1		19.541	87165	0.46	0.73
2		20.907	18682056	98.97	98.89
3		21.579	22143	0.12	0.23
4		22.176	86033	0.46	0.15

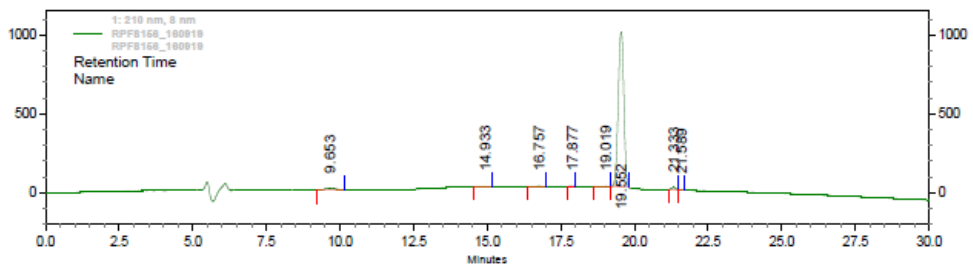
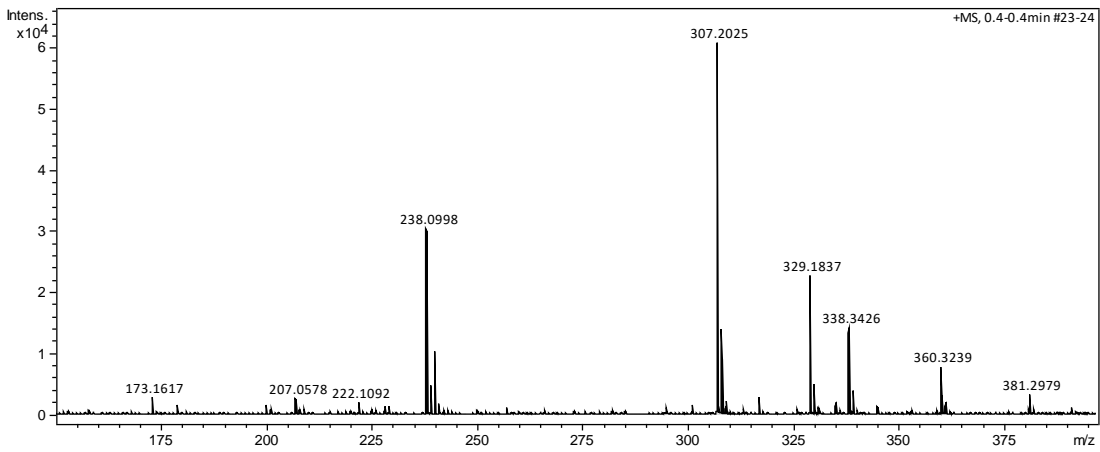
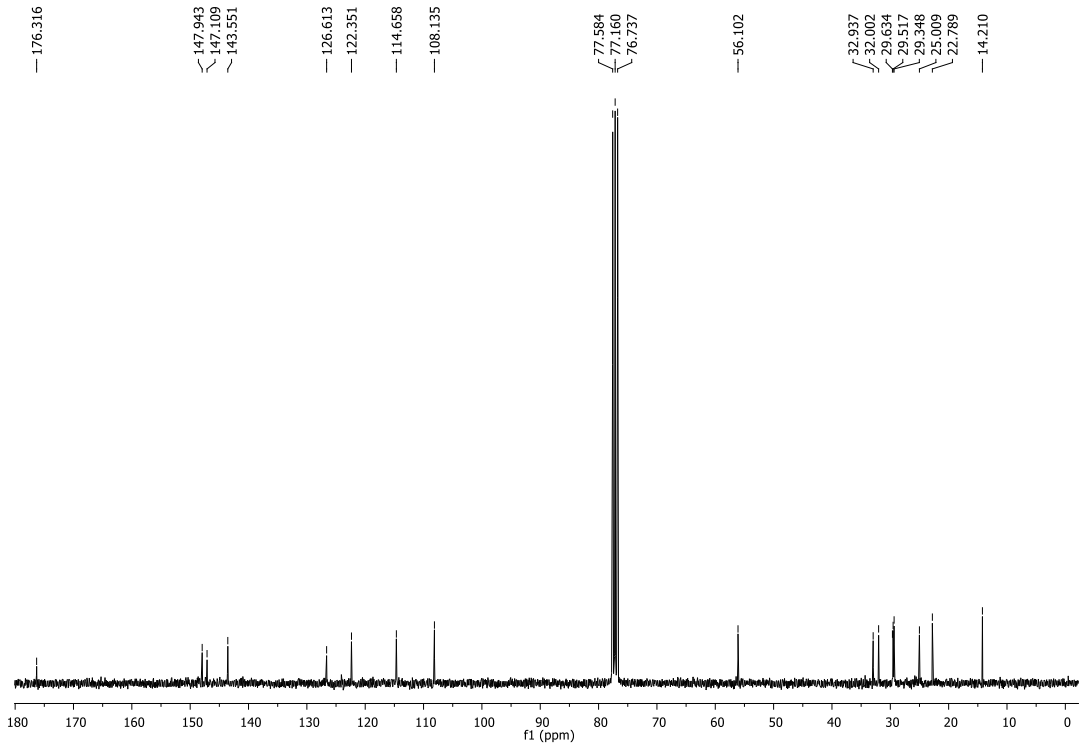
**(E)-N'-(4-hydroxy-3-methoxybenzylidene)heptanehydrazide (11a).**



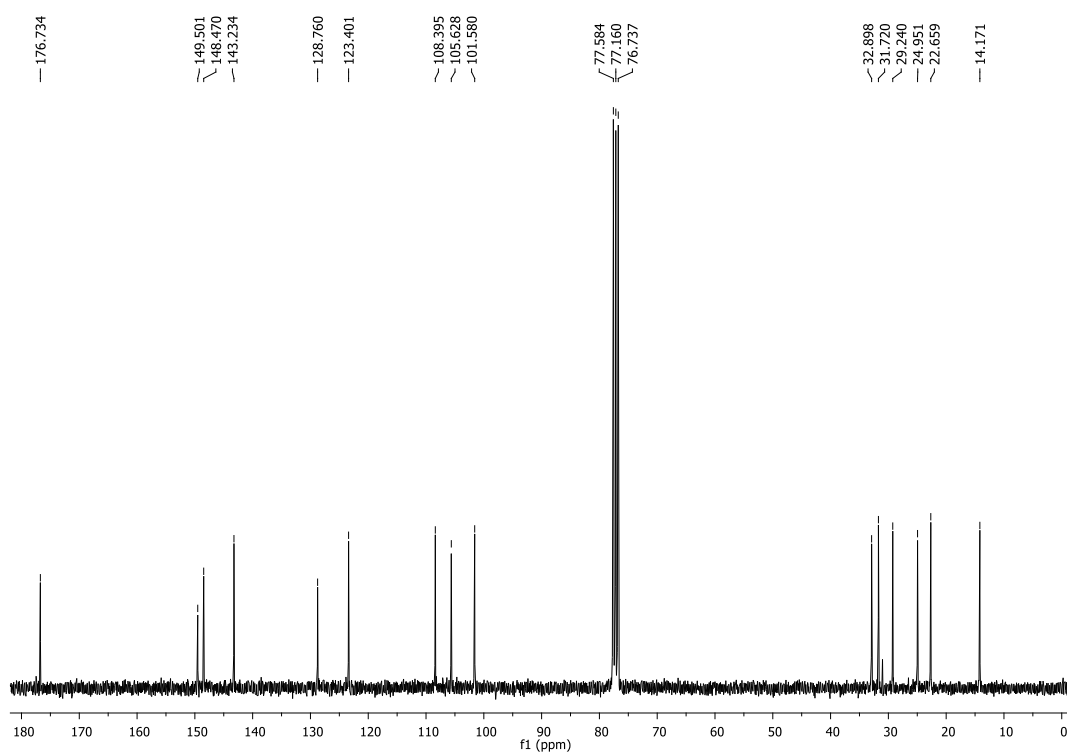
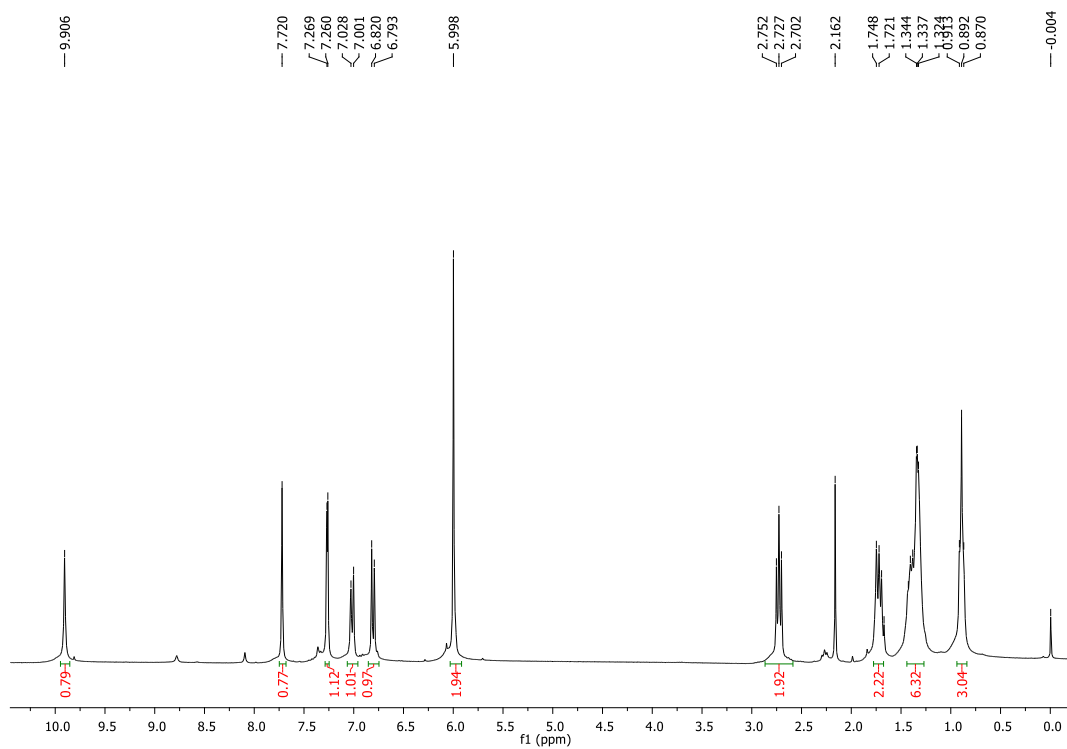
Pk #	Name	Retention Time	Area	Area Percent	Height Percent
1		9.664	318388	1.83	1.24
2		15.573	133326	0.77	0.69
3		17.877	16609269	95.39	94.22
4		18.229	75463	0.43	0.90
5		18.432	238604	1.37	2.62
6		21.589	37677	0.22	0.34

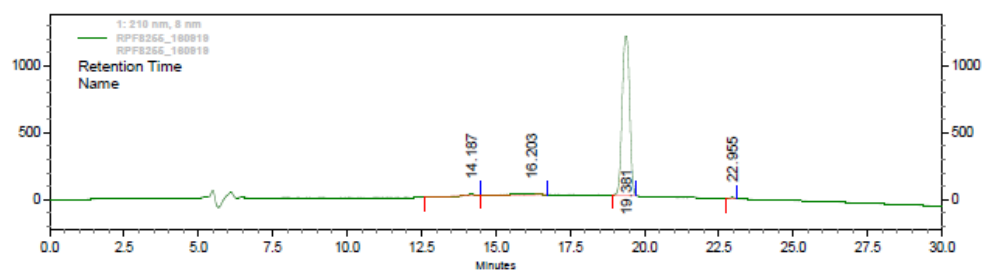
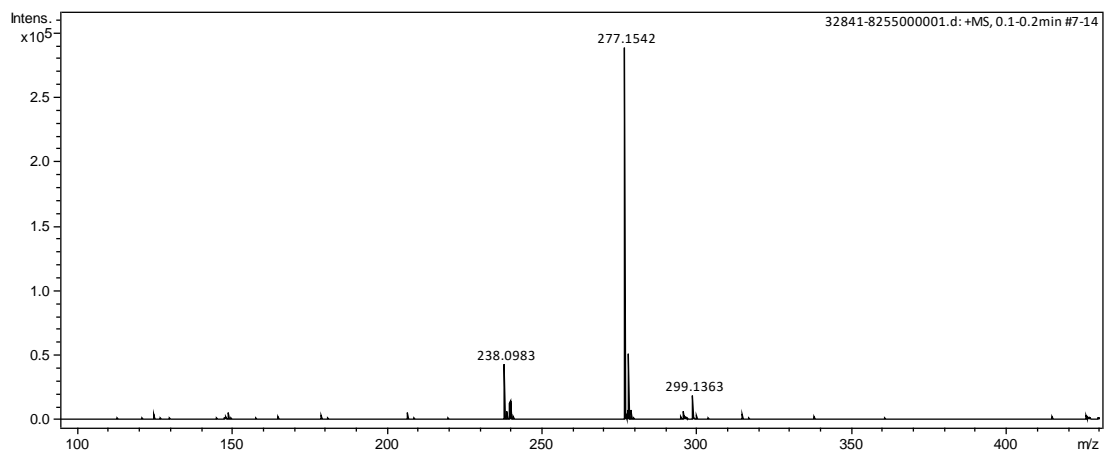
**(E)-N'-(4-hydroxy-3-methoxybenzylidene)nonanehydrazide (11b).**





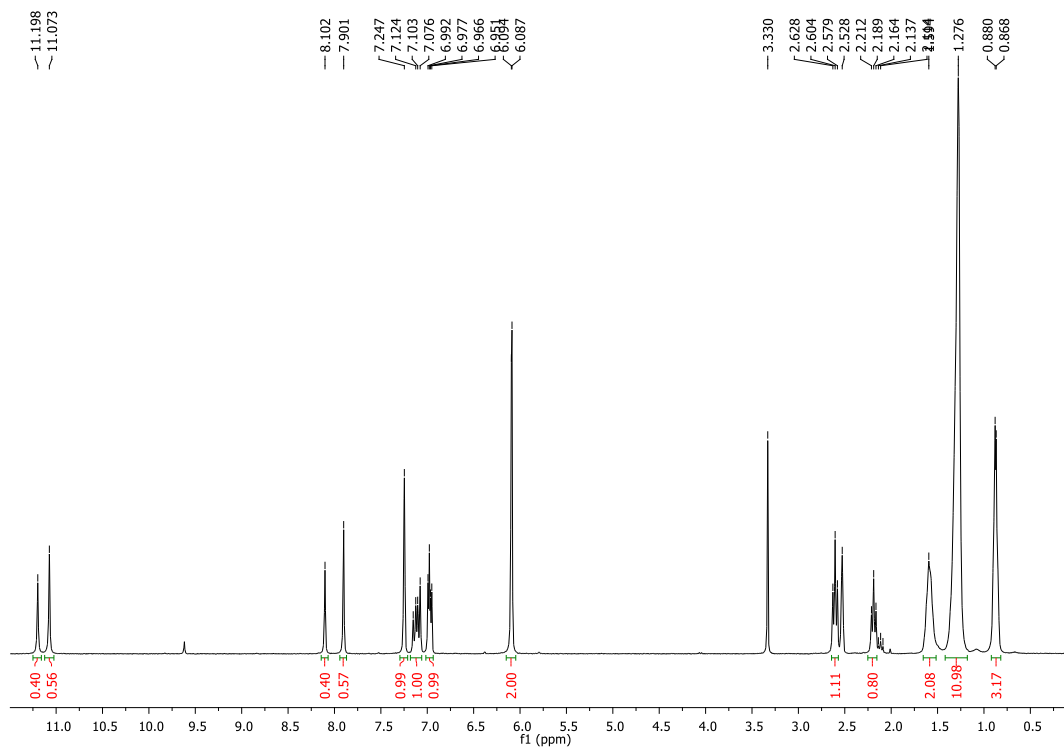
Pk #	Name	Retention Time	Area	Area Percent	Height Percent
1		9.653	257097	1.93	1.18
2		14.933	22220	0.17	0.11
3		16.757	17125	0.13	0.08
4		17.877	10676	0.08	0.14
5		19.019	13062	0.10	0.11
6		19.552	12866990	96.50	96.86
7		21.333	132014	0.99	1.33
8		21.589	14613	0.11	0.21

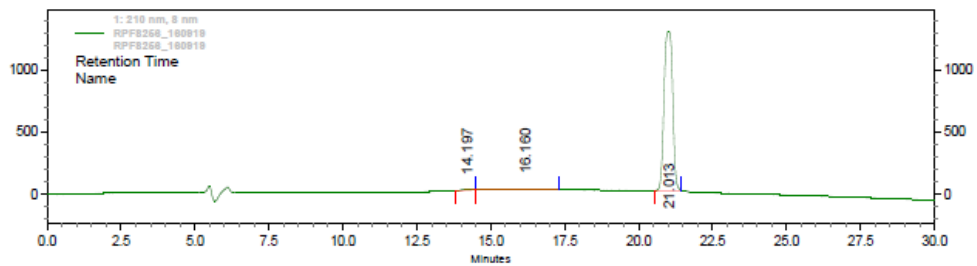
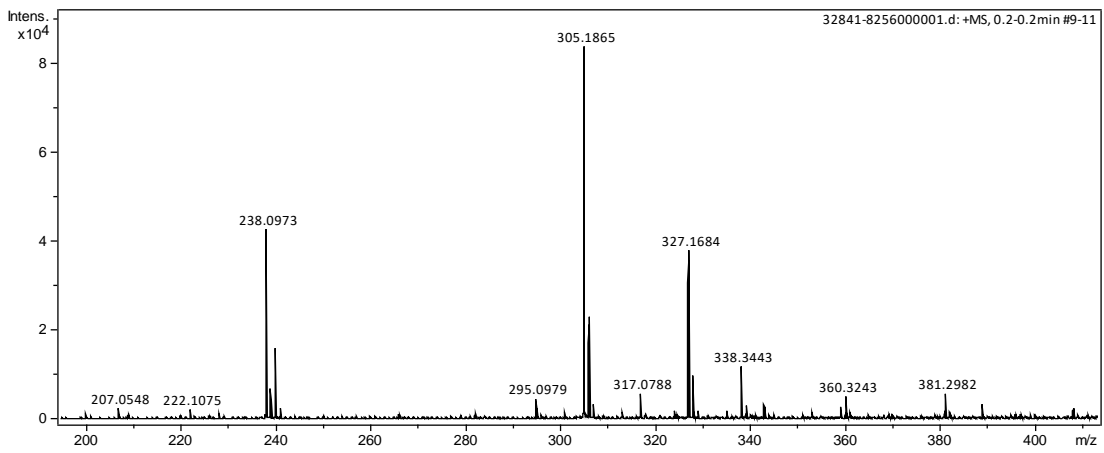
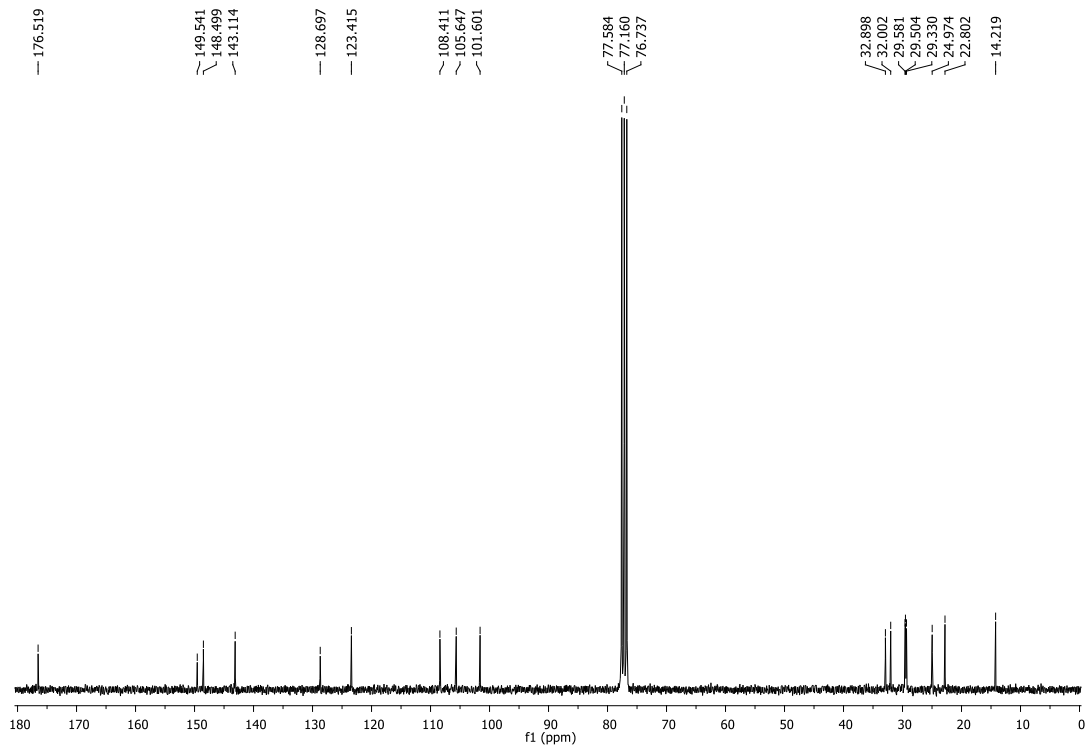
**(E)-N'-(benzo[d][1,3]dioxol-5-ylmethylene)heptanehydrazide (12a).**



Pk #	Name	Retention Time	Area	Area Percent	Height Percent
1		14.187	130493	0.62	0.63
2		16.203	248322	1.18	0.25
3		19.381	20663848	97.81	98.44
4		22.955	84609	0.40	0.68

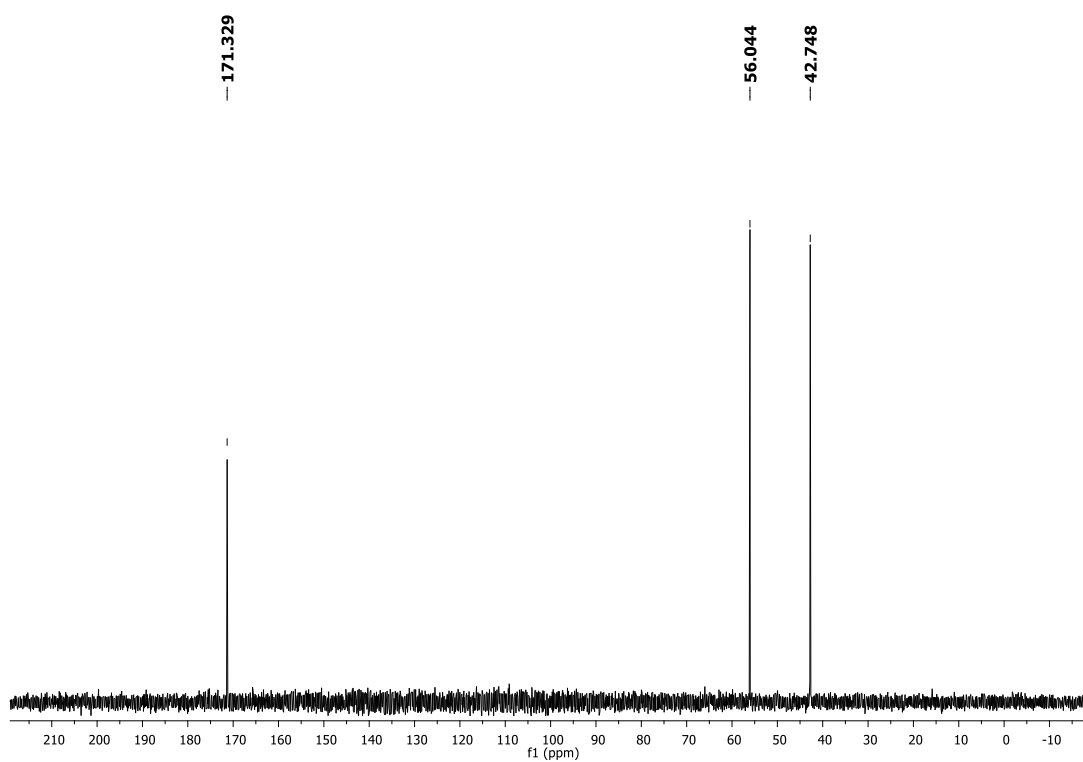
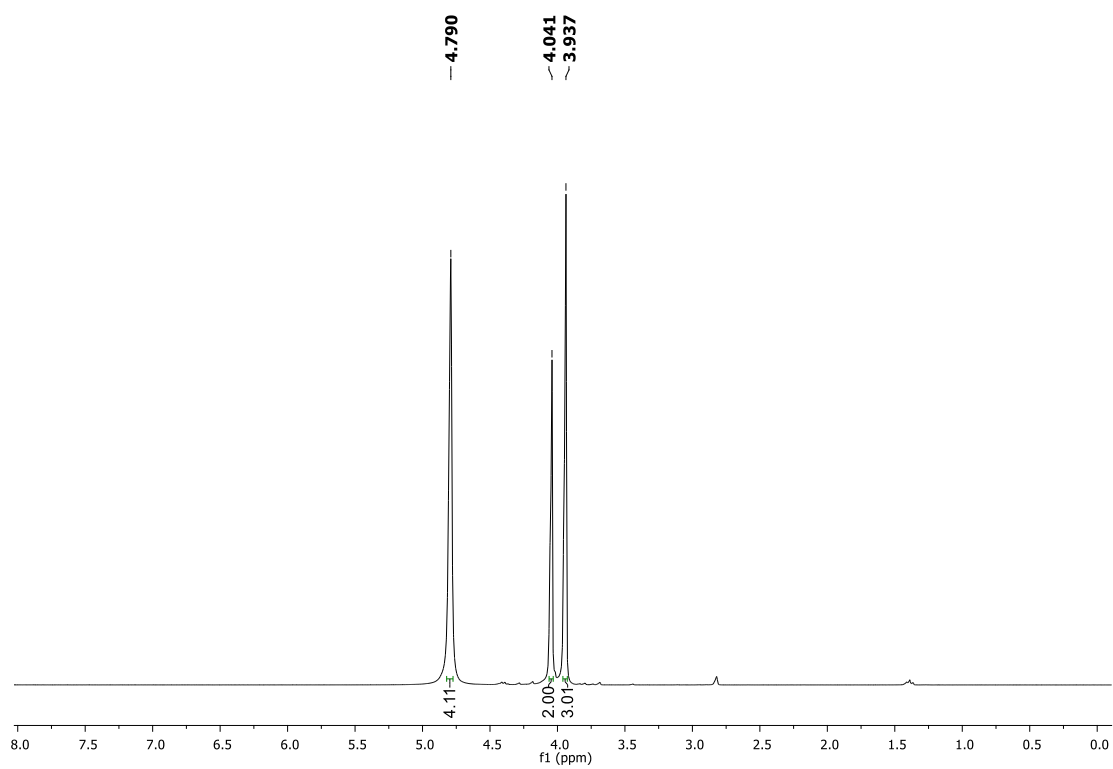
**(E)-N'-(benzo[d][1,3]dioxol-5-ylmethylene)nonanehydrazide (12b).**



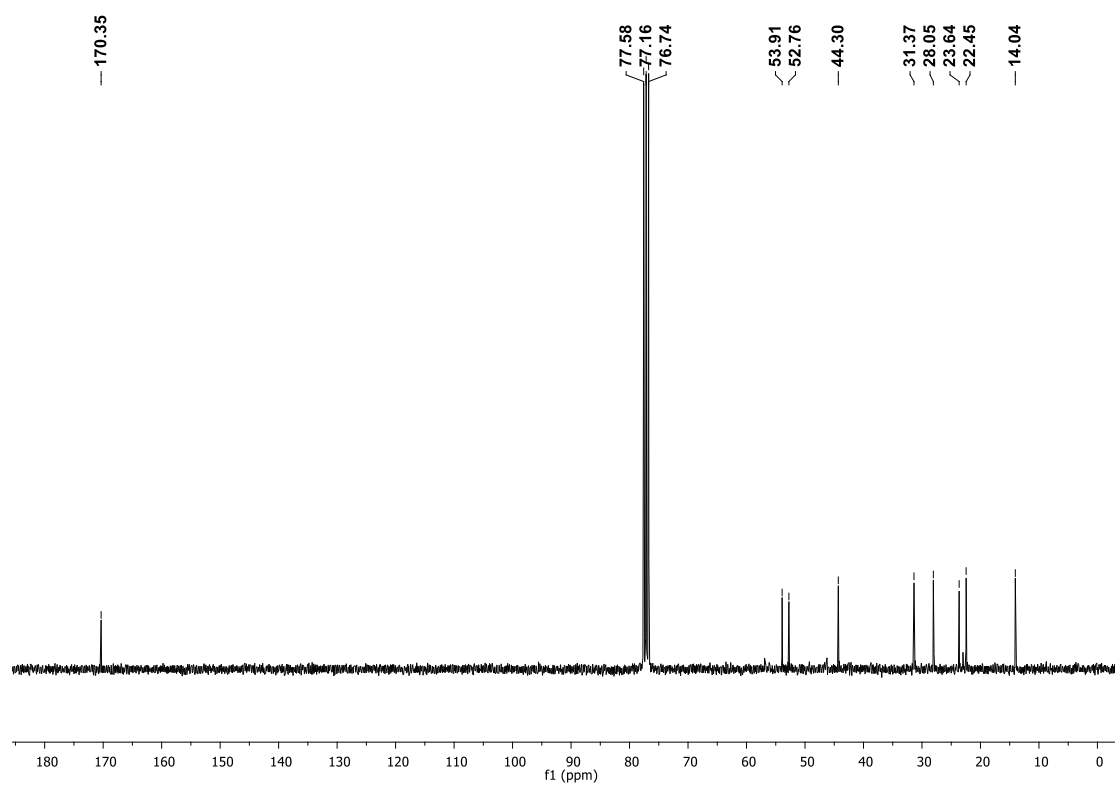
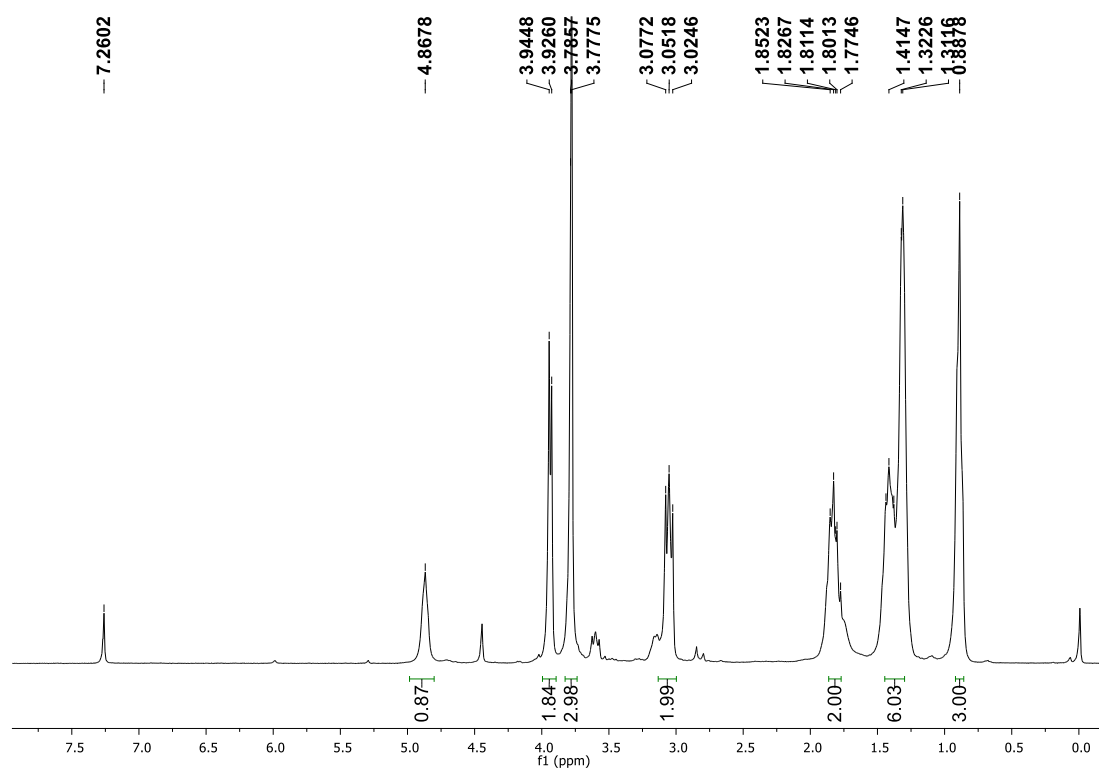


PK #	Name	Retention Time	Area	Area Percent	Height Percent
1		14.197	173480	0.66	0.72
2		16.160	543427	2.05	0.46
3		21.013	25754780	97.29	98.82

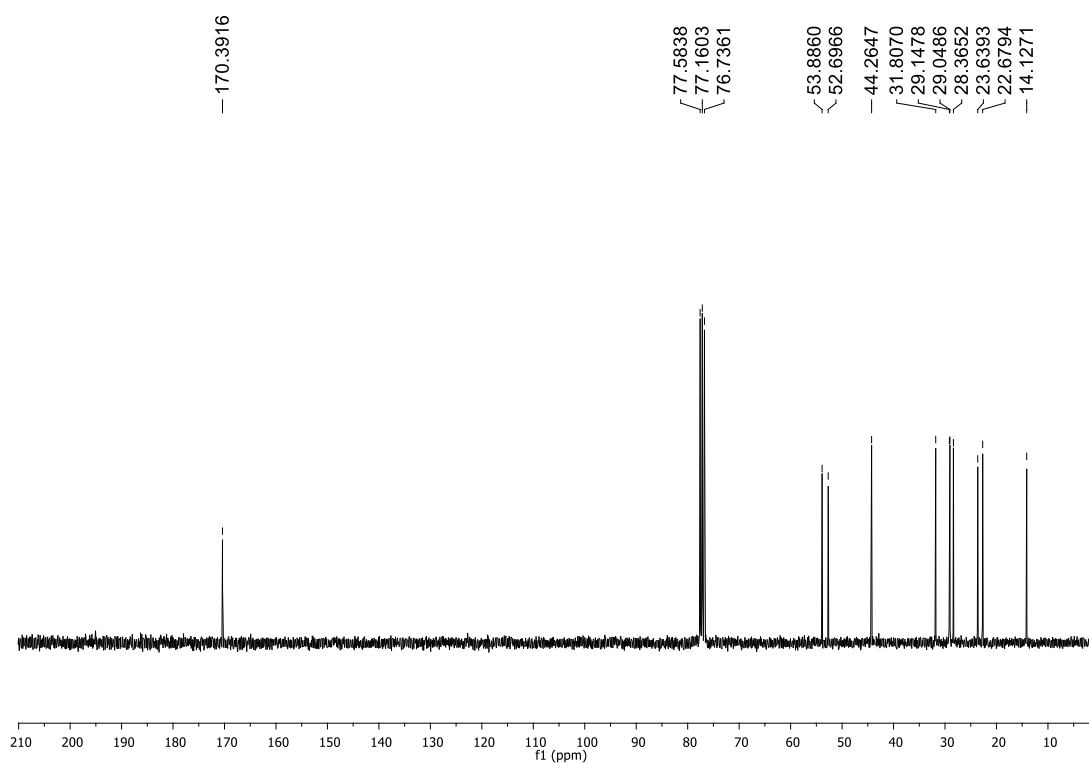
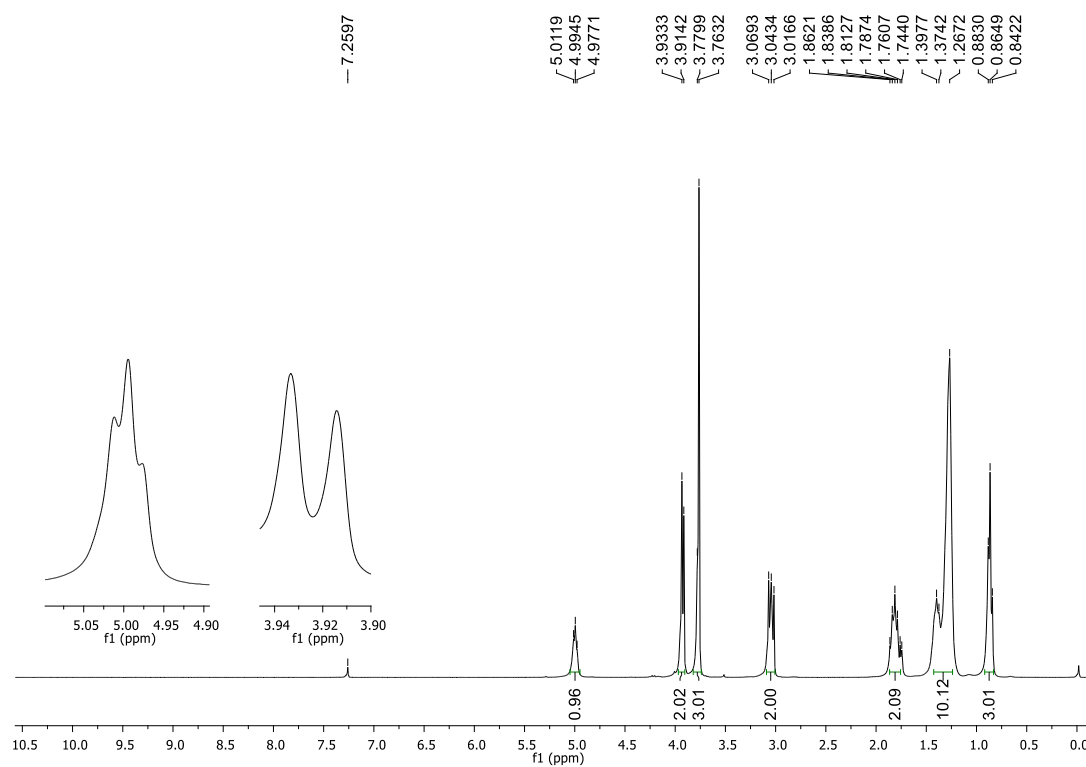
## Methyl glycinate hydrochloride salt (14).

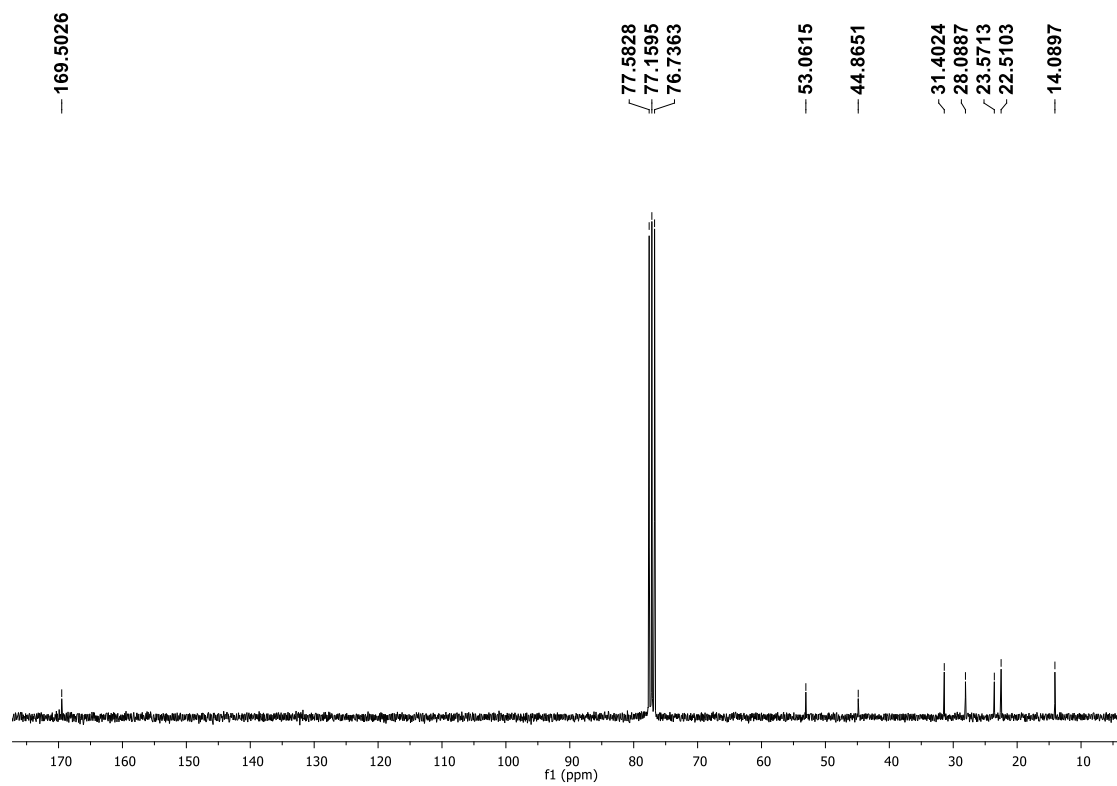
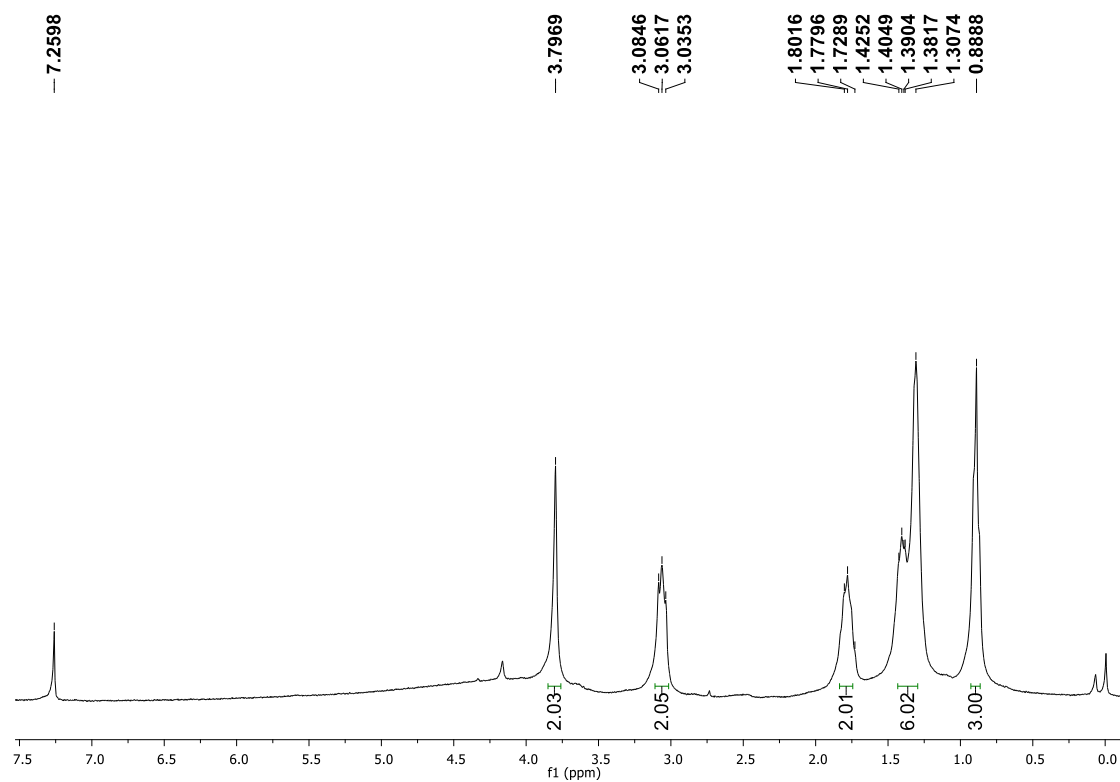


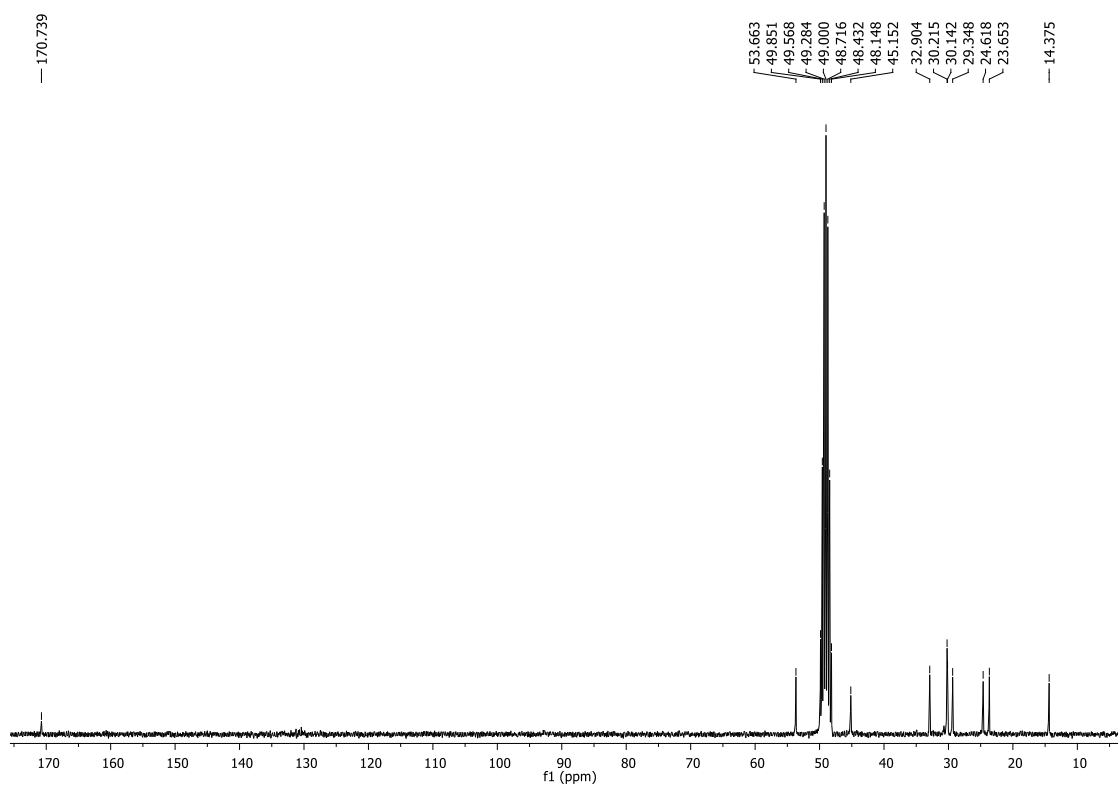
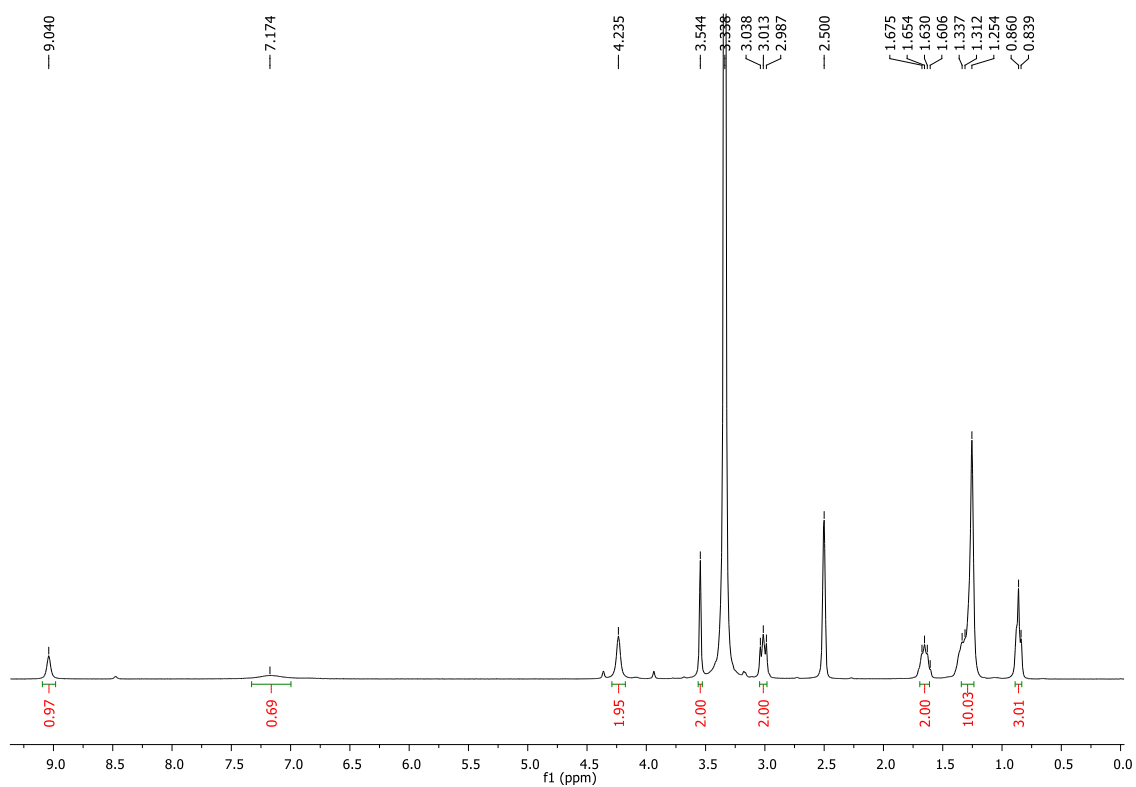
## Methyl (hexylsulfonyl)glycinate (15a).



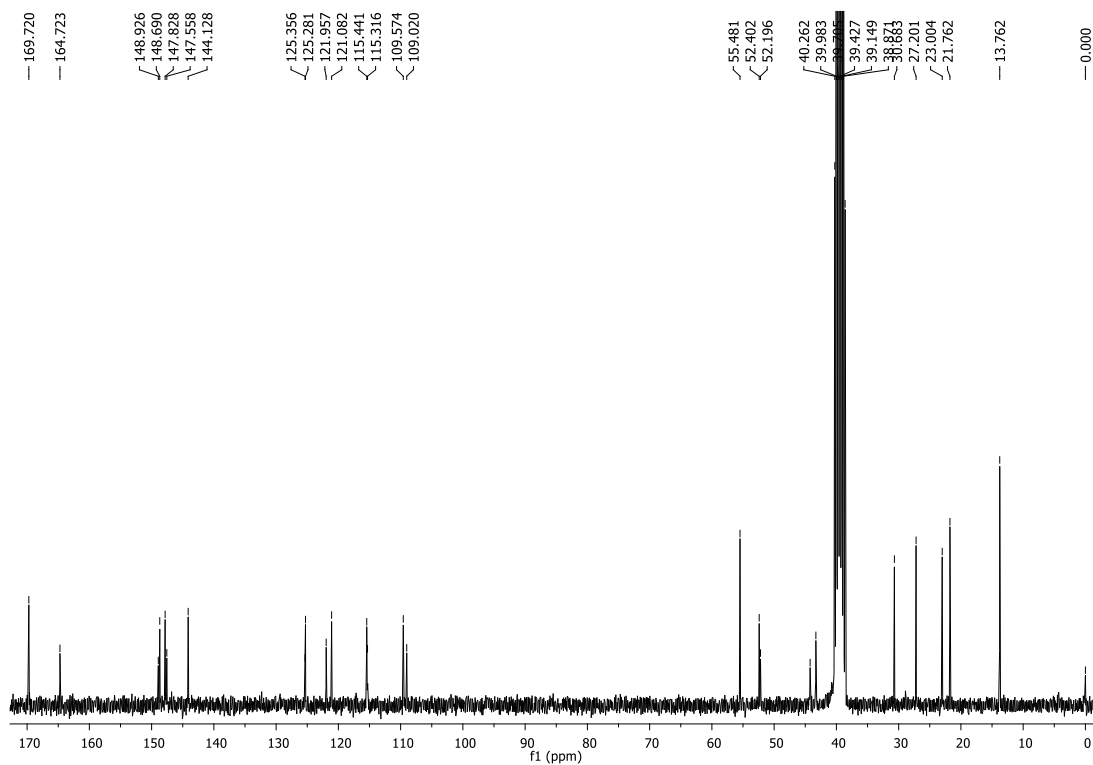
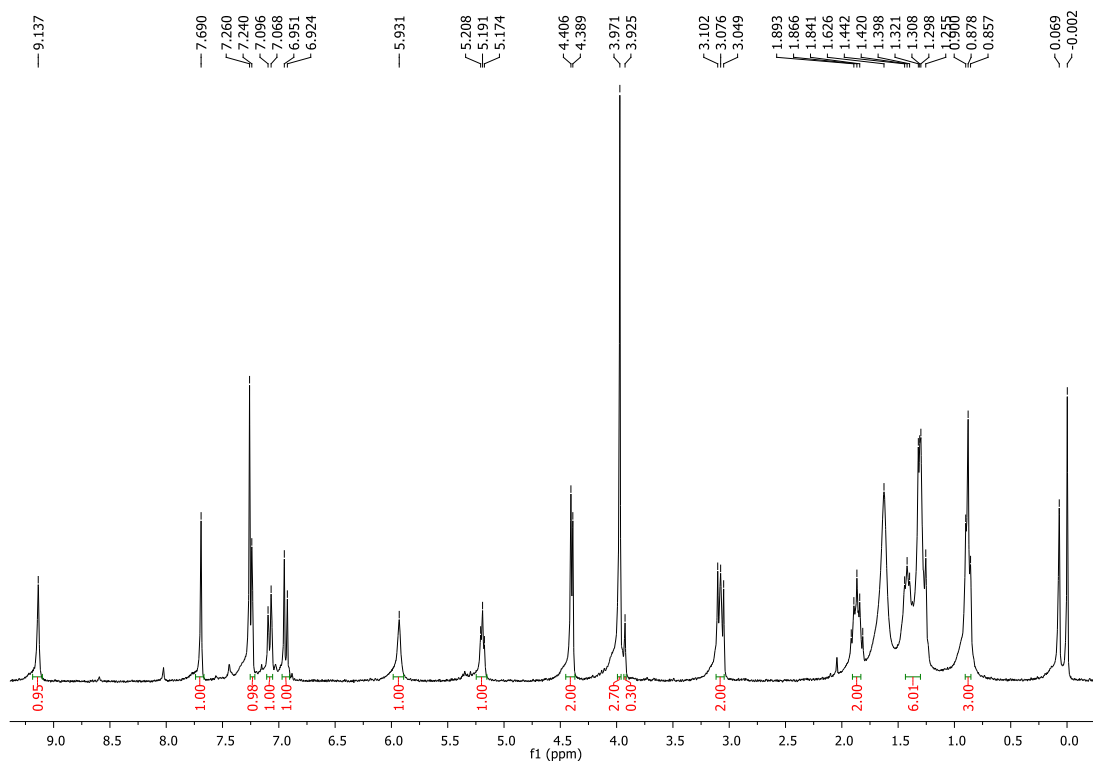
## Methyl (octylsulfonyl)glycinate (15b).

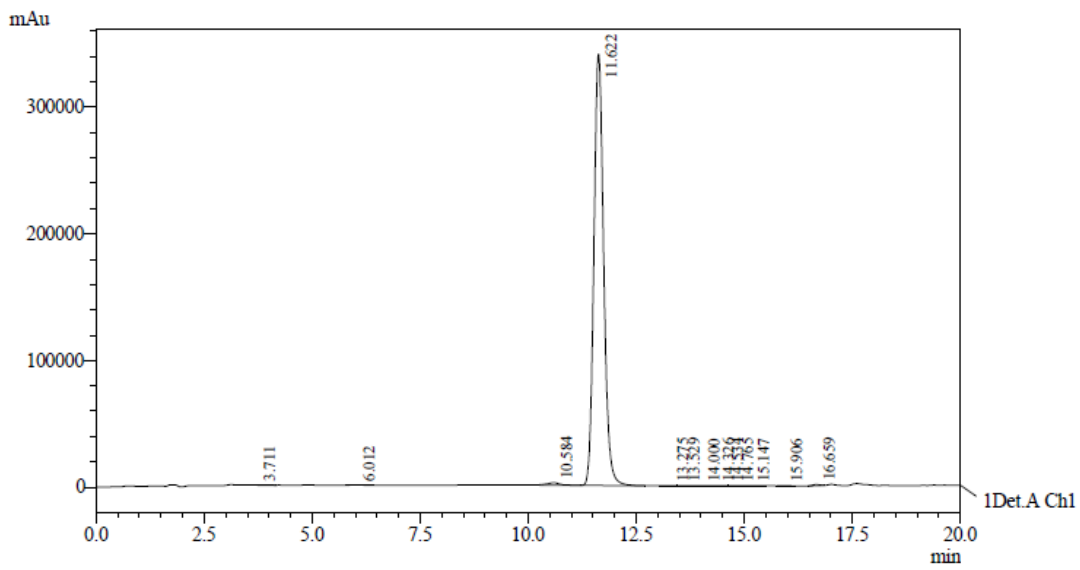
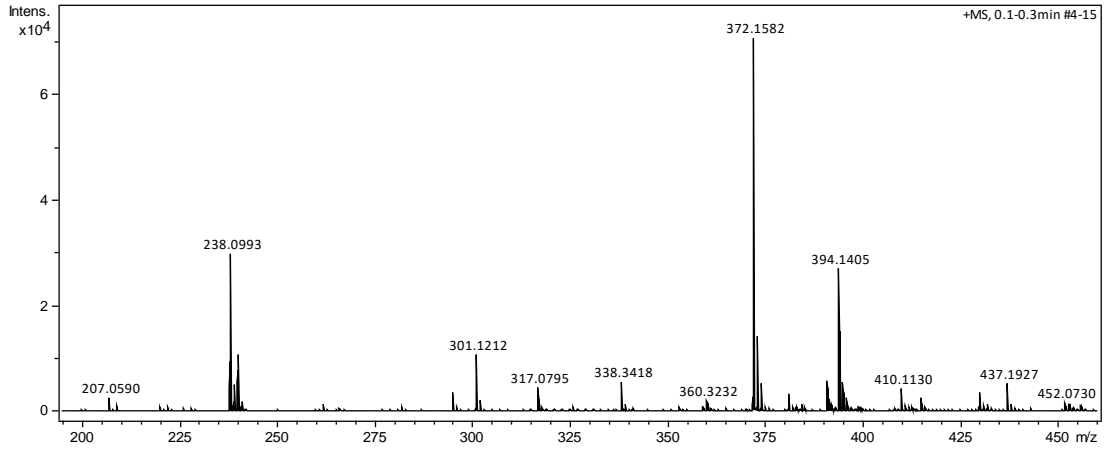


**N-(2-hydrazineyl-2-oxoethyl)hexane-1-sulfonamide (16a).**

**N-(2-hydrazineyl-2-oxoethyl)octane-1-sulfonamide (16b).**

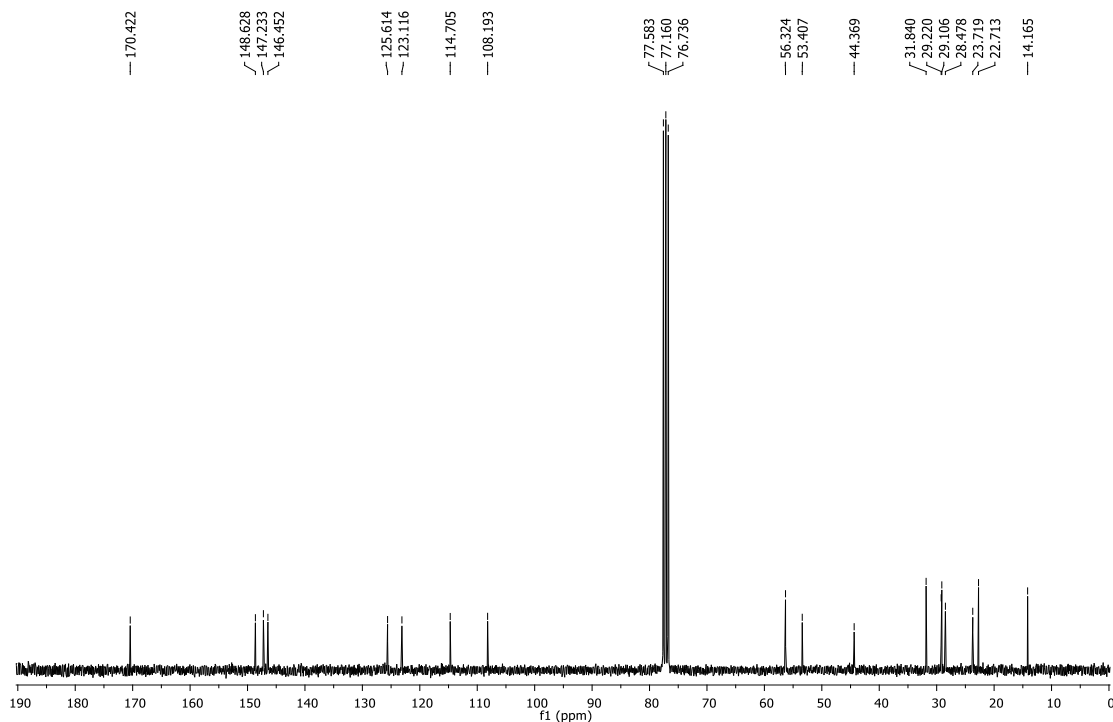
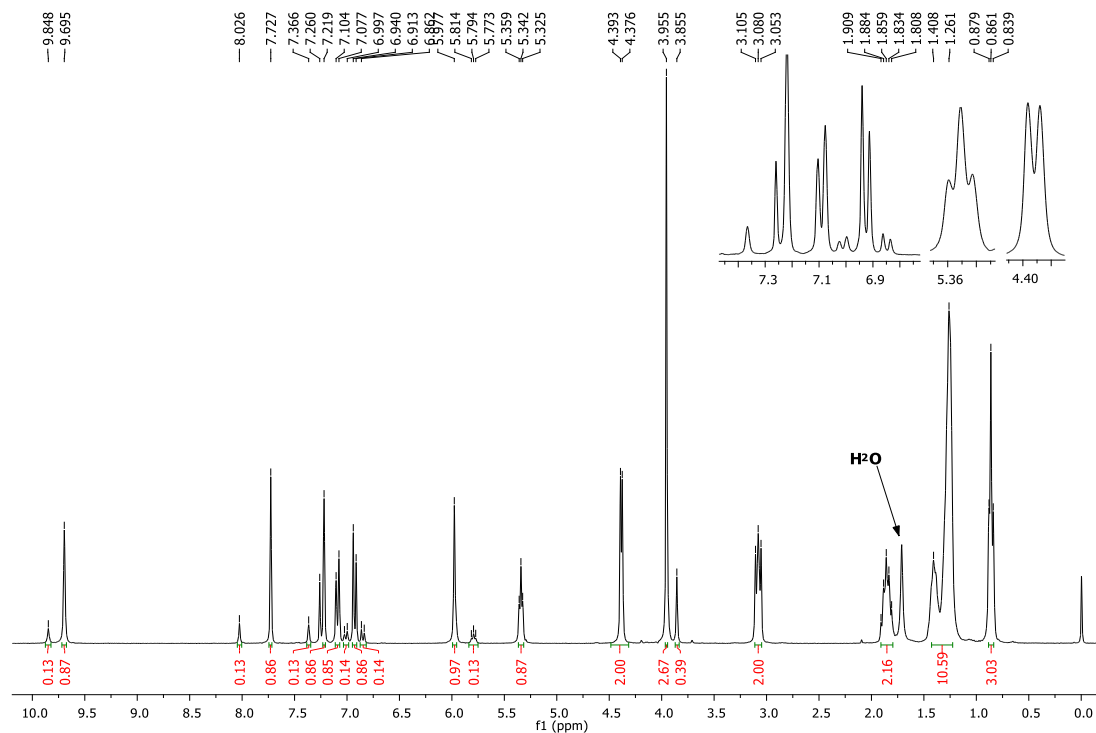
**(E)-N-(2-(2-(4-hydroxy-3-methoxybenzylidene)hydrazineyl)-2-oxoethyl)hexane-1-sulfonamide (17a).**

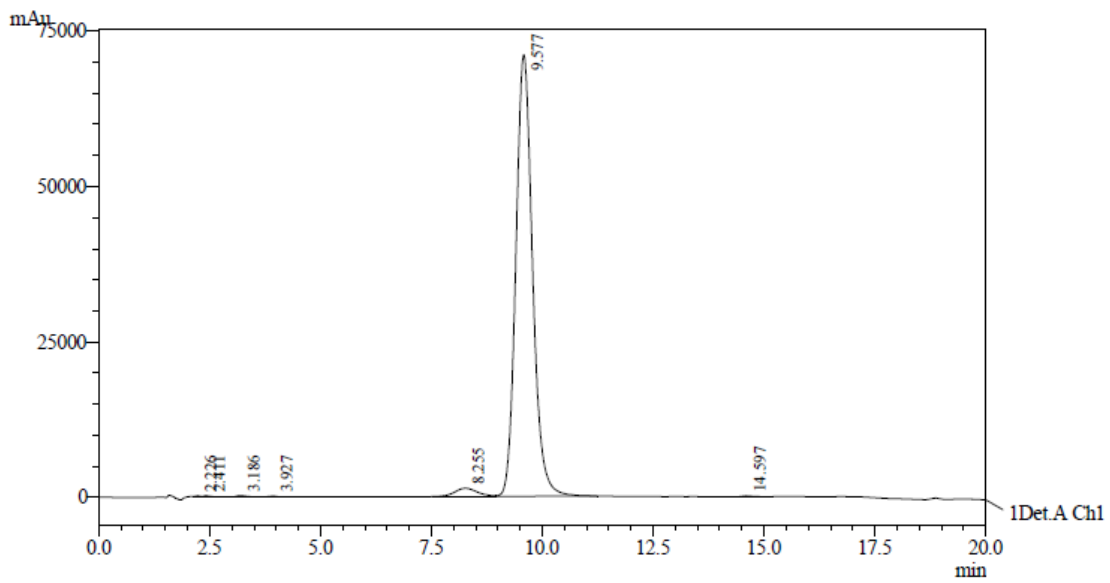
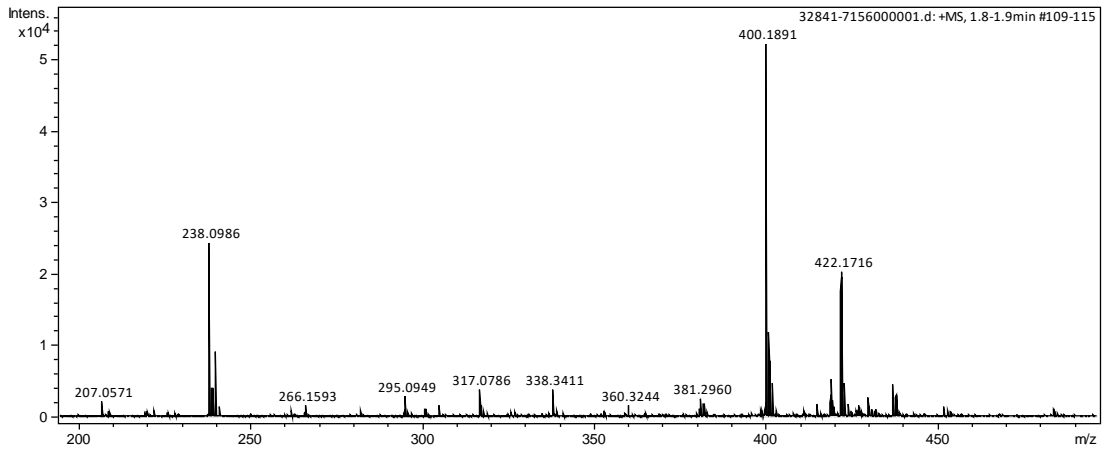




Peak#	Ret. Time	Area	Resolution	Area %	Conc.
1	3.711	1571	0.000	0.029	0.029
2	6.012	1822	5.563	0.033	0.033
3	10.584	44267	9.253	0.812	0.812
4	11.622	5367746	2.178	98.448	98.448
5	13.275	3439	1.751	0.063	0.063
6	13.529	3486	0.193	0.064	0.064
7	14.000	1654	0.498	0.030	0.030
8	14.326	3218	0.420	0.059	0.059
9	14.534	2656	0.234	0.049	0.049
10	14.765	7579	0.320	0.139	0.139
11	15.147	2512	0.556	0.046	0.046
12	15.906	1768	1.222	0.032	0.032
13	16.659	10657	2.300	0.195	0.195
Total		5452377		100.000	

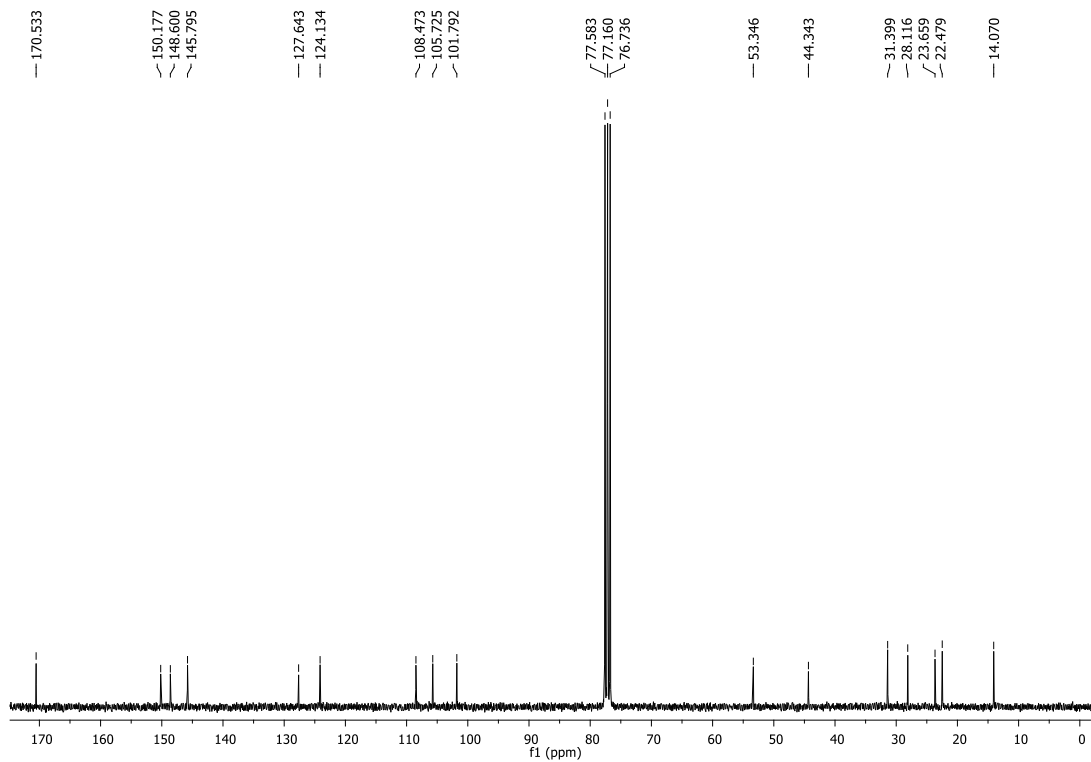
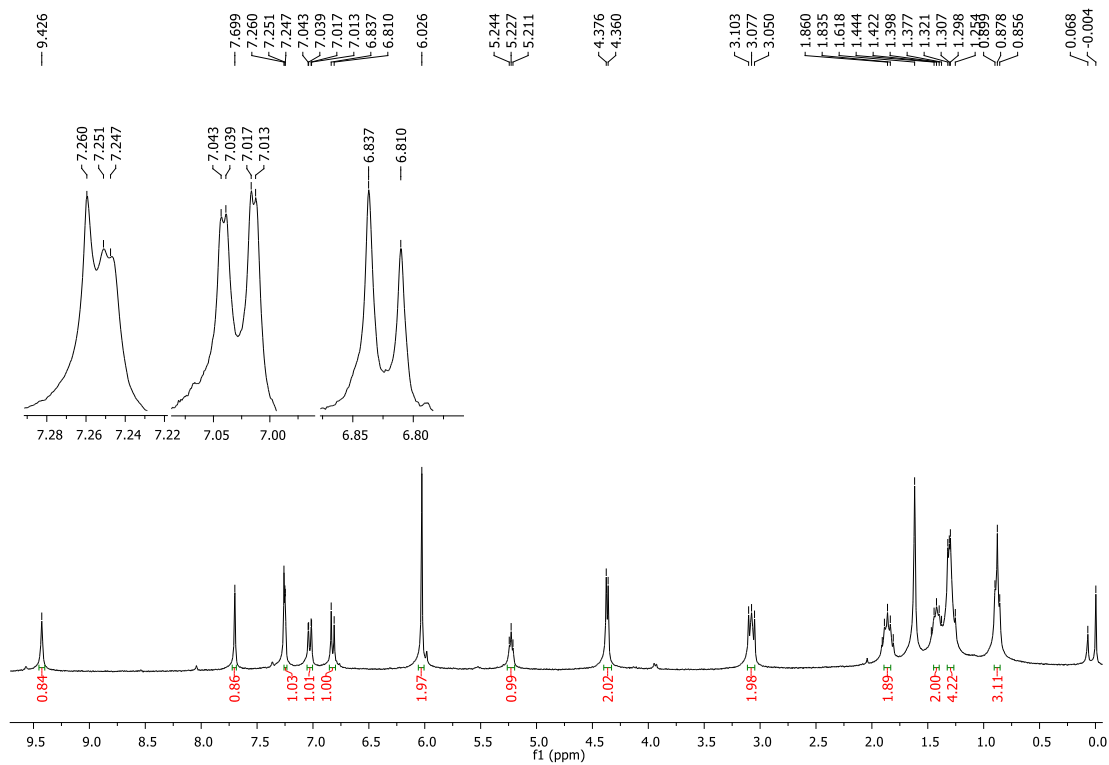
**(E)-N-(2-(2-(4-hydroxy-3-methoxybenzylidene)hydrazineyl)-2-oxoethyl)octane-1-sulfonamide (17b).**

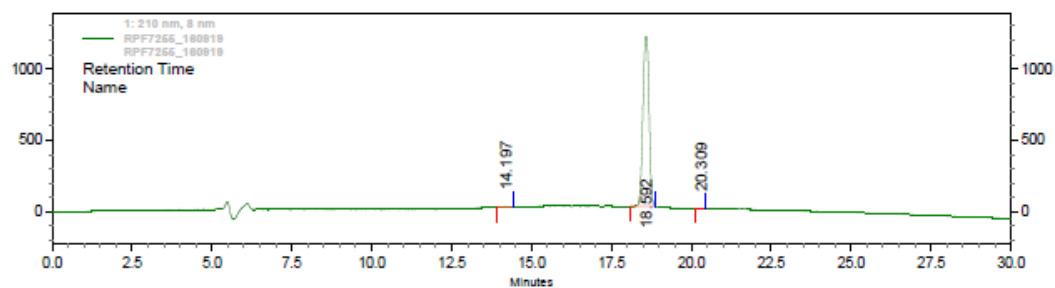
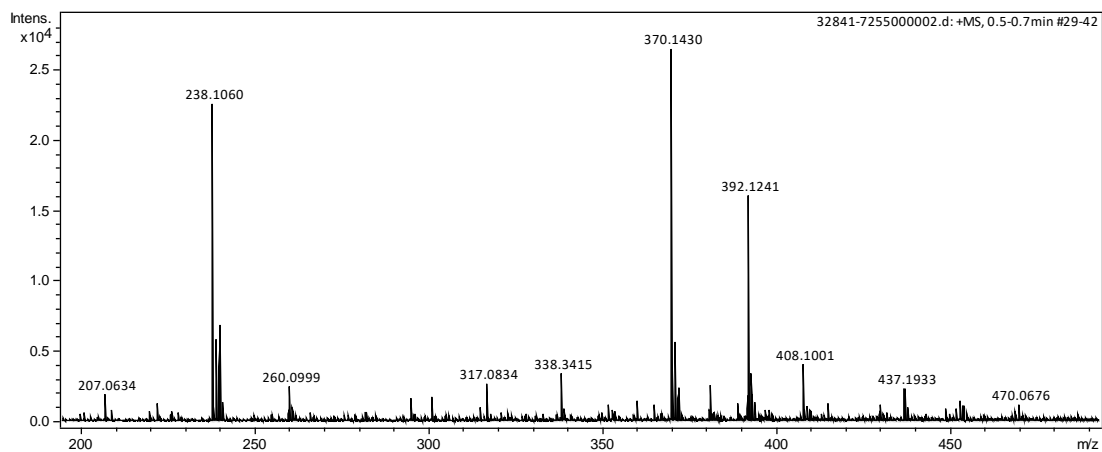




Peak#	Ret. Time	Area	Resolution	Area %	Conc.
1	2.226	1077	0.000	0.056	0.056
2	2.411	1426	0.722	0.075	0.075
3	3.186	2461	2.576	0.129	0.129
4	3.927	1186	2.153	0.062	0.062
5	8.255	45932	6.904	2.402	2.402
6	9.577	1858995	1.660	97.199	97.199
7	14.597	1480	9.549	0.077	0.077
Total		1912557		100.000	

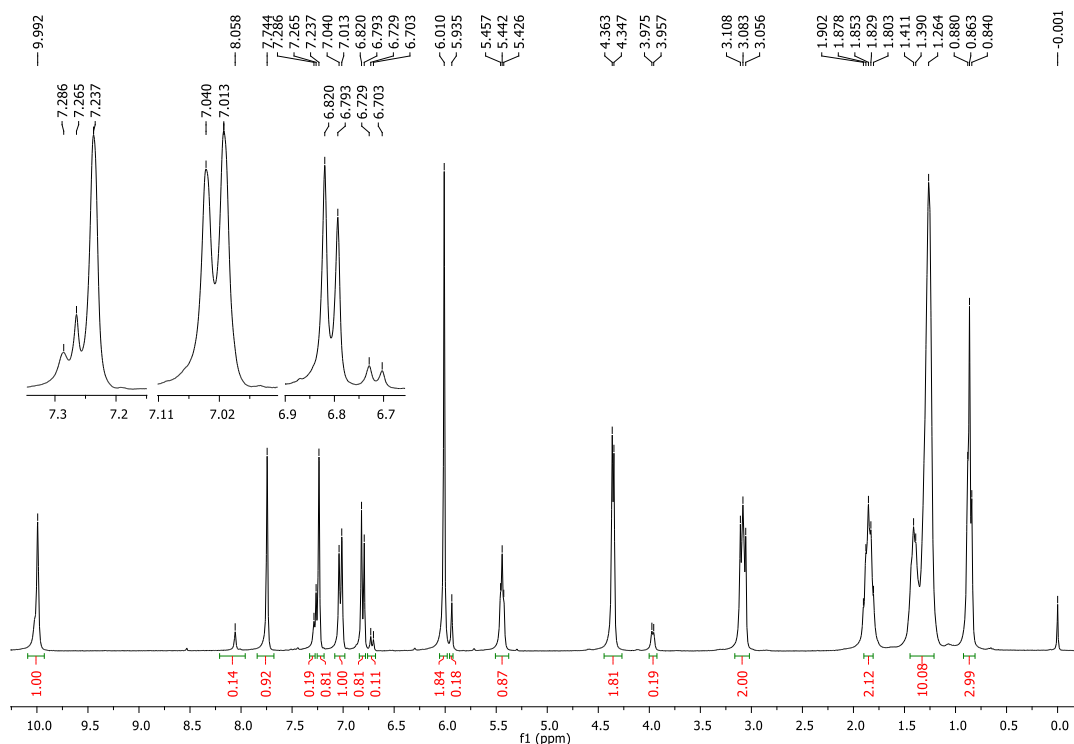
**(E)-N-(2-(2-(benzo[d][1,3]dioxol-5-ylmethylene)hydrazineyl)-2-oxoethyl)hexane-1-sulfonamide (18a).**

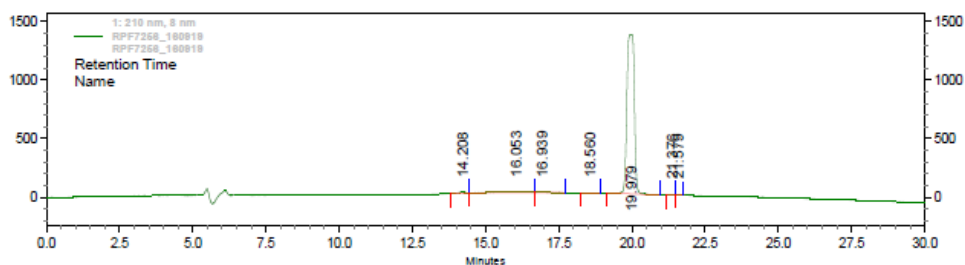
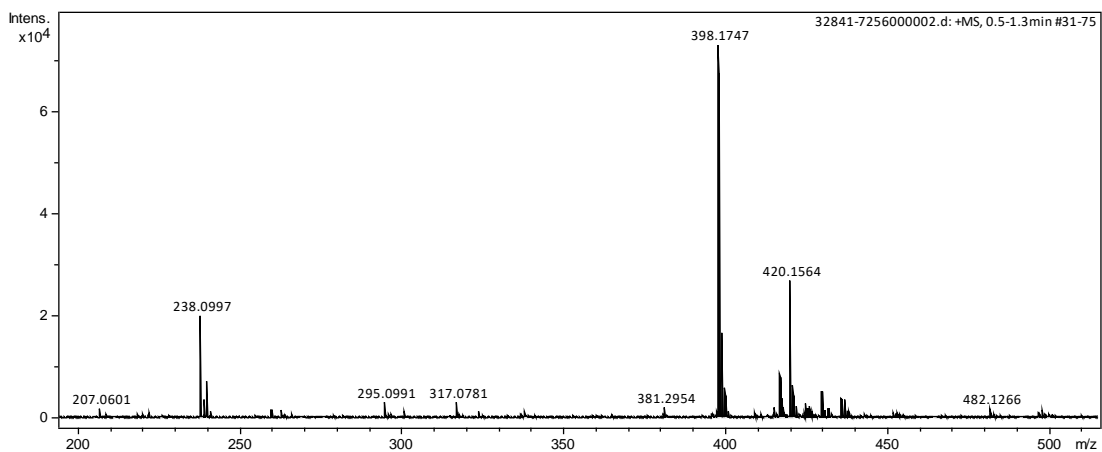
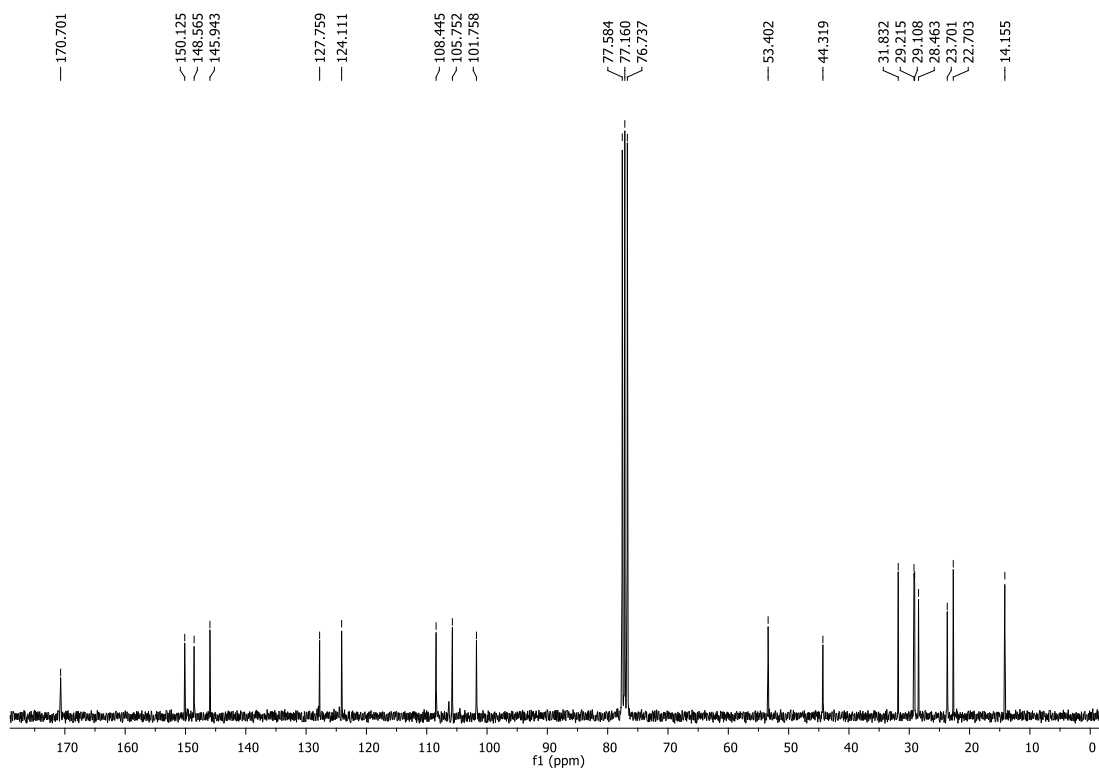




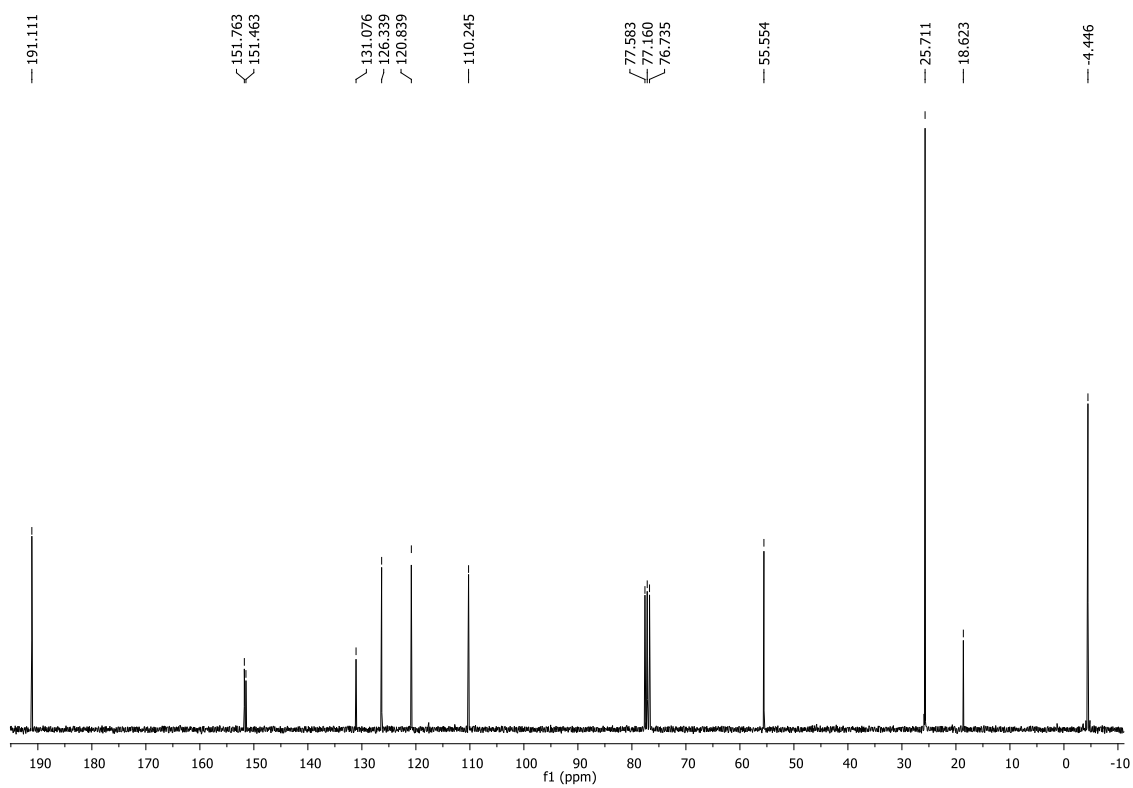
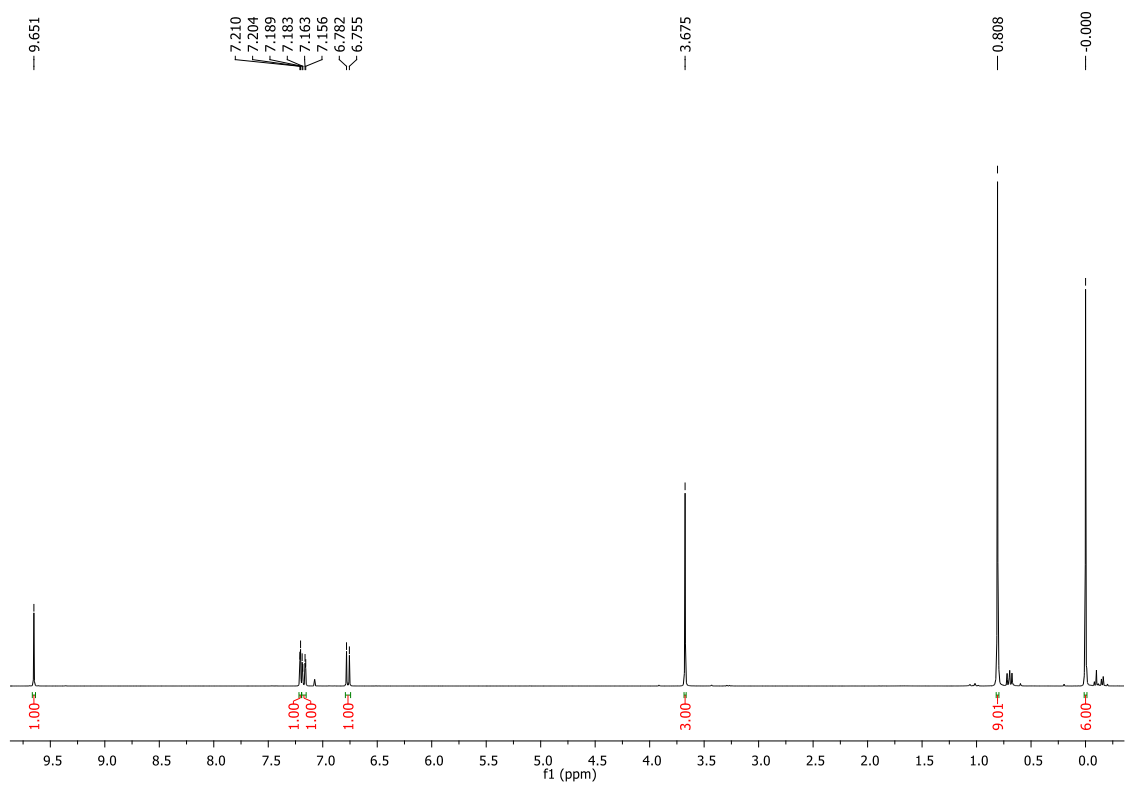
Pk #	Name	Retention Time	Area	Area Percent	Height Percent
1		14.197	68990	0.43	0.35
2		18.592	15917825	99.47	99.50
3		20.309	15116	0.09	0.15

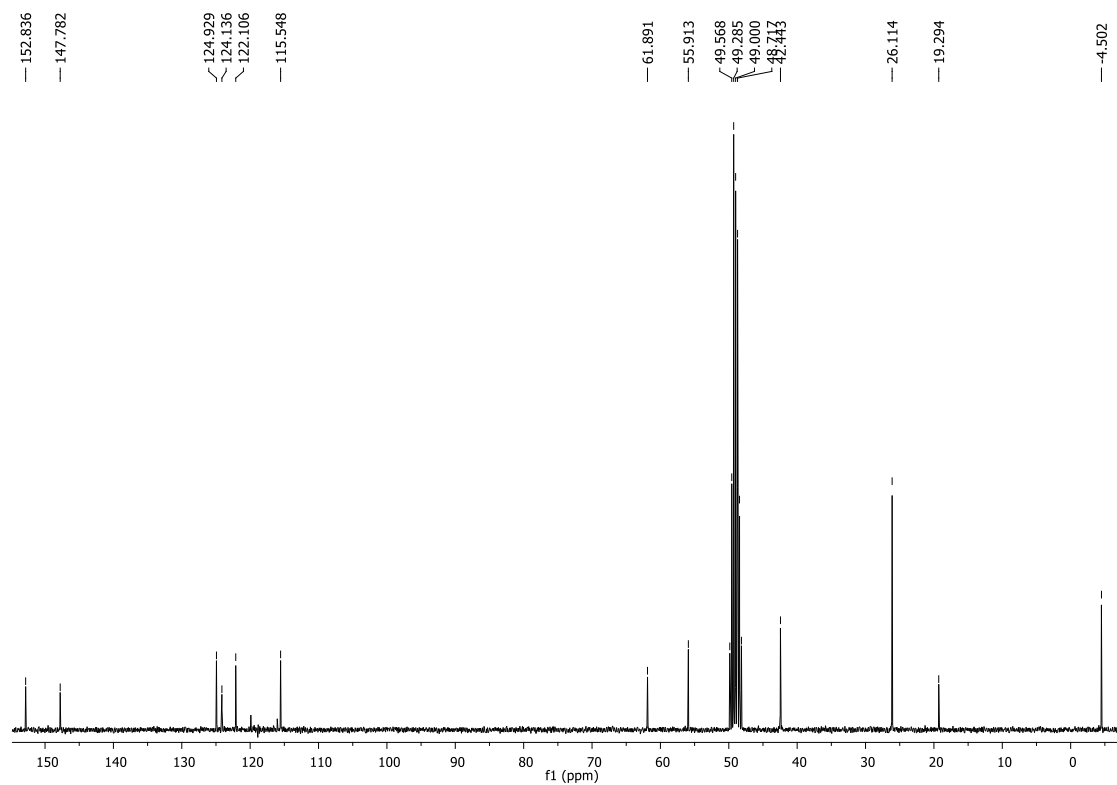
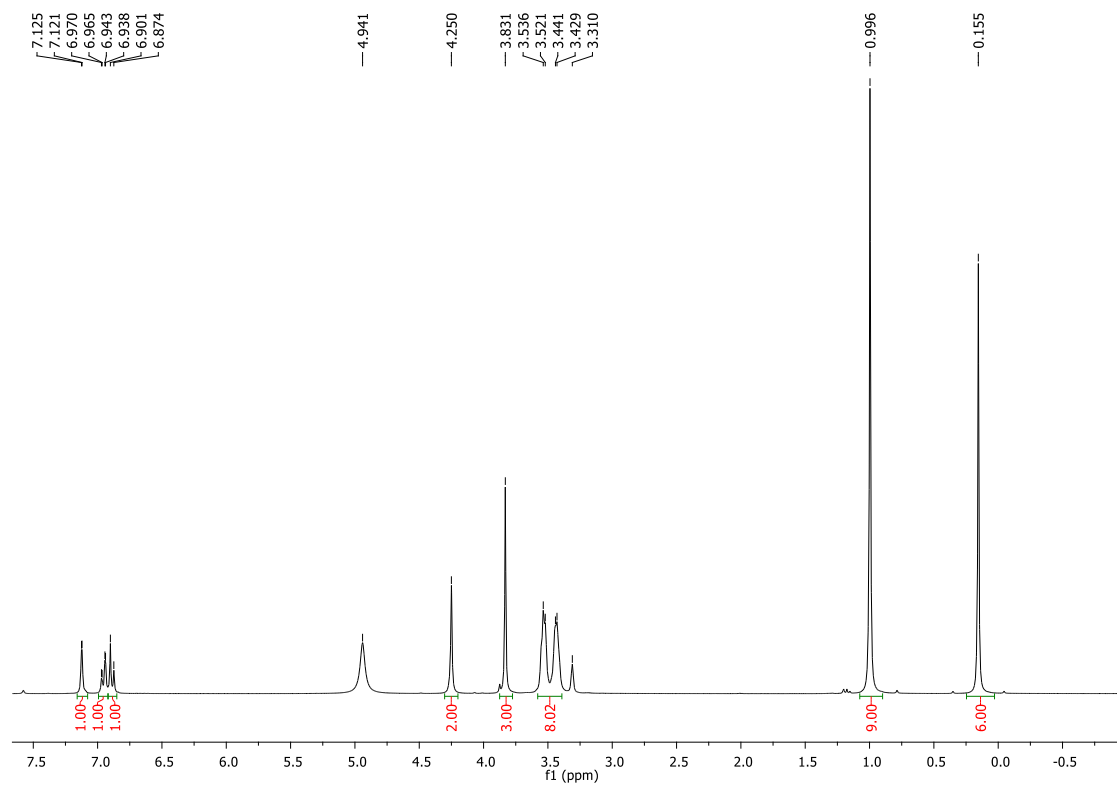
**(E)-N-(2-(2-(benzo[d][1,3]dioxol-5-ylmethylene)hydrazineyl)-2-oxoethyl)octane-1-sulfonamide (18b).**

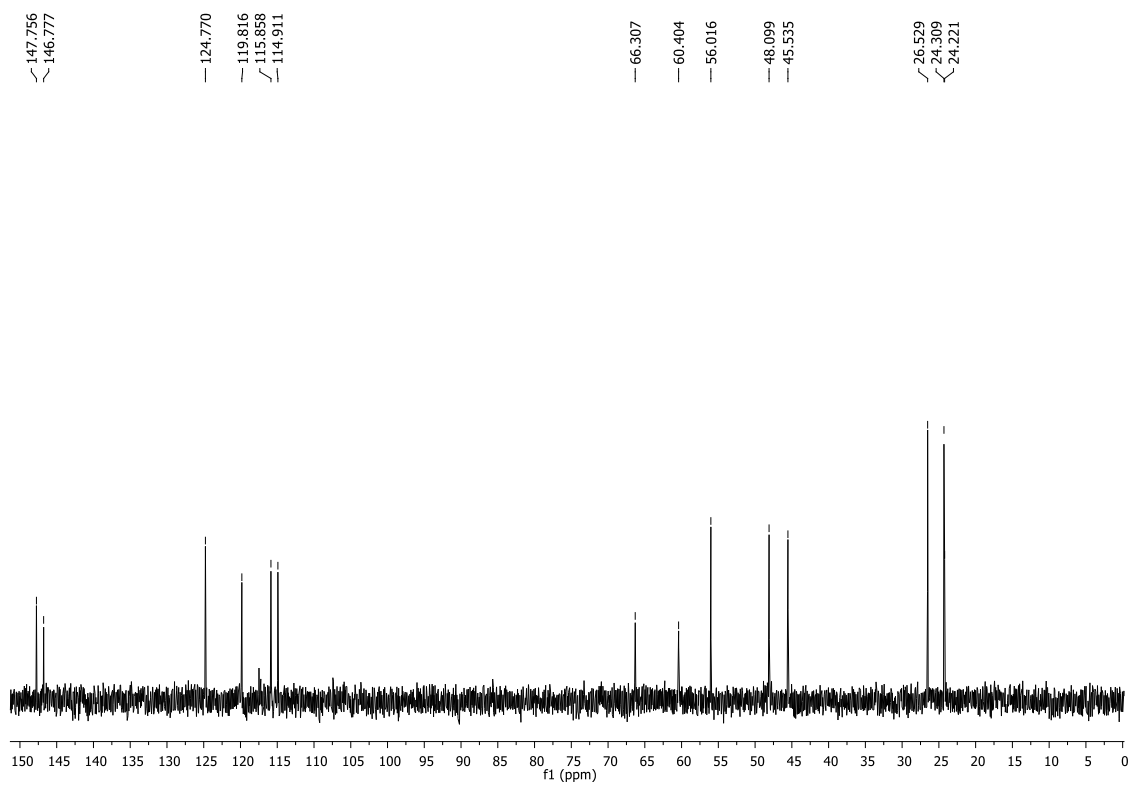
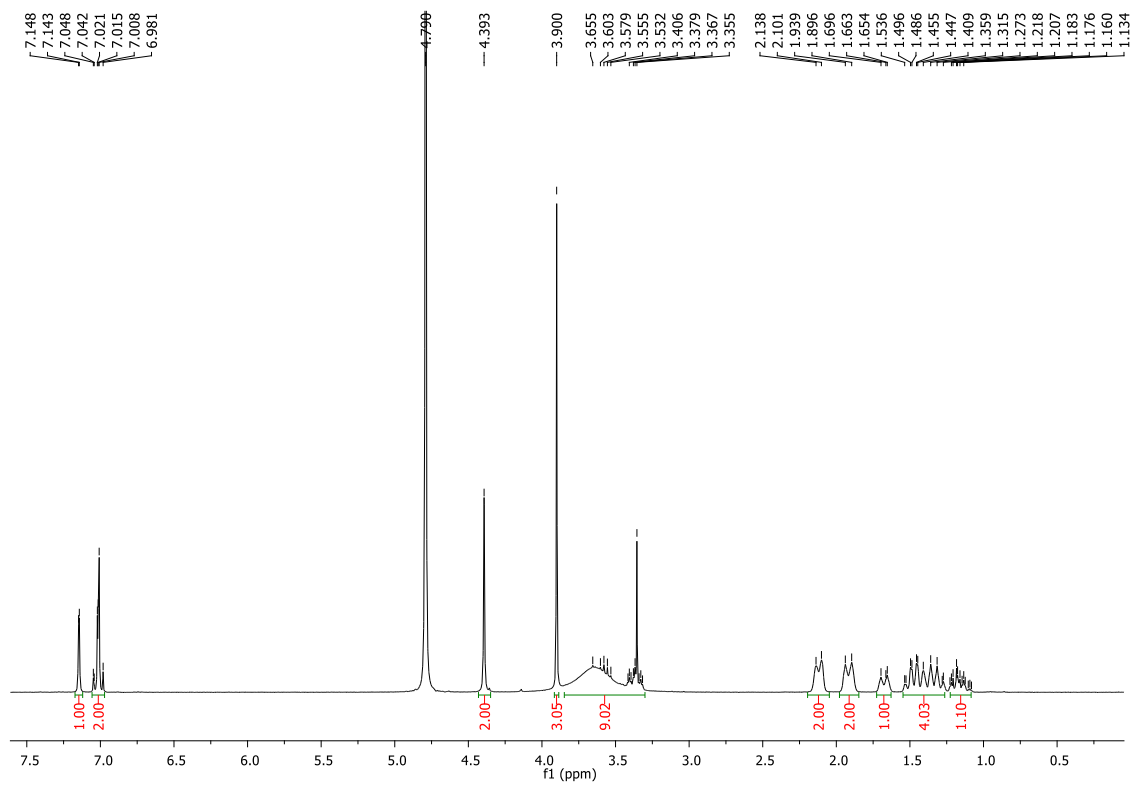


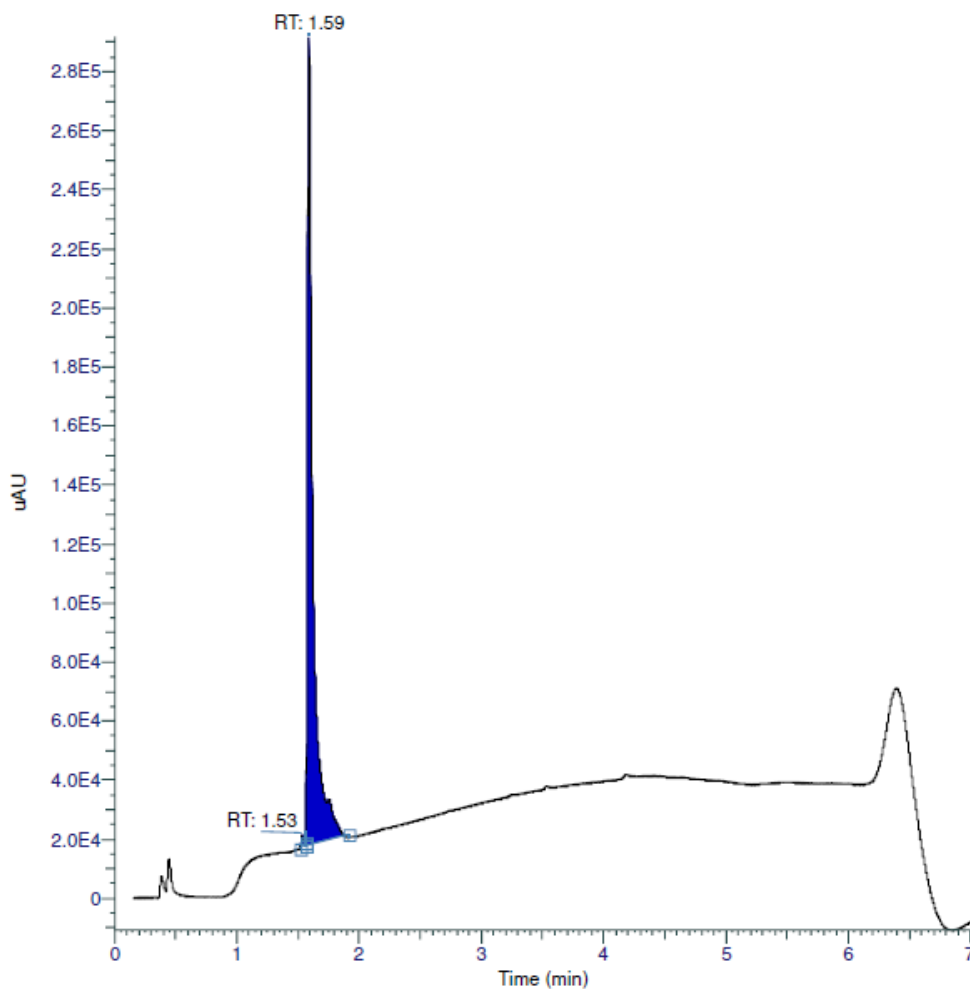
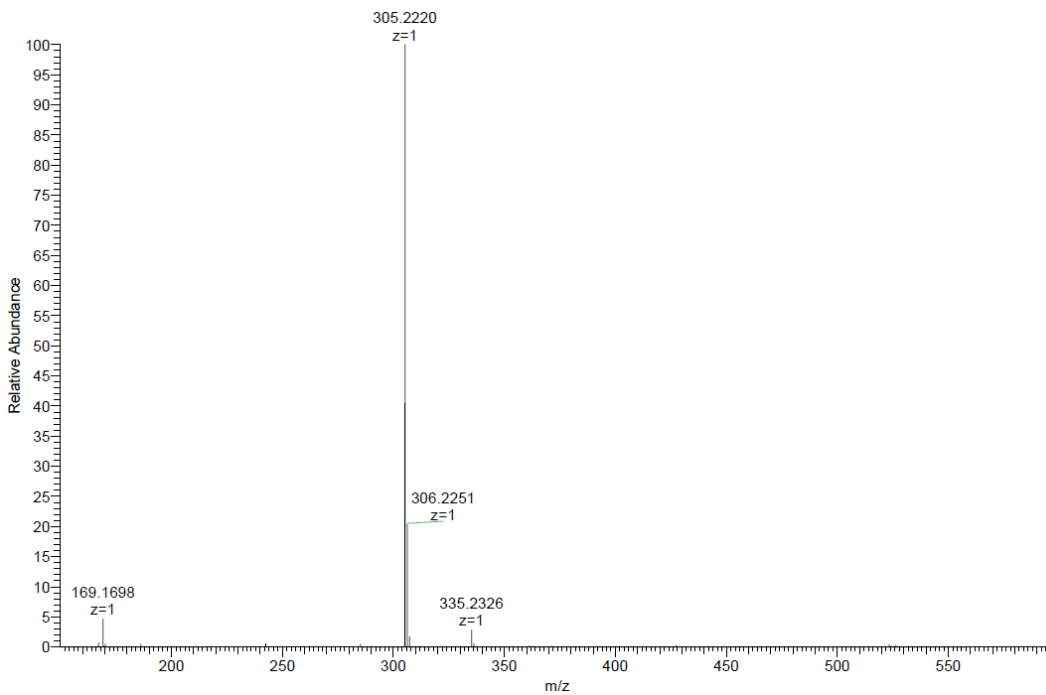


PK #	Name	Retention Time	Area	Area Percent	Height Percent
1		14.208	121991	0.50	0.49
2		16.053	348109	1.43	0.33
3		16.939	71636	0.29	0.26
4		18.560	13917	0.06	0.07
5		19.979	23784113	97.54	98.48
6		21.376	21880	0.09	0.18
7		21.579	23290	0.10	0.18

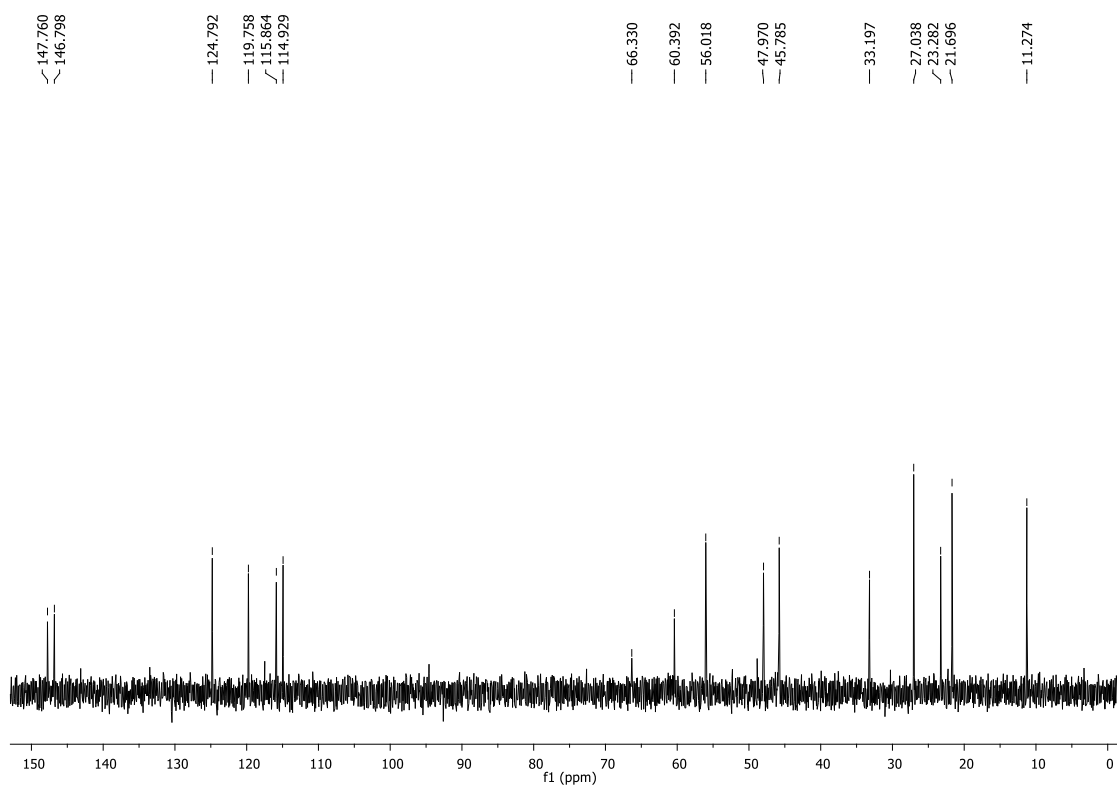
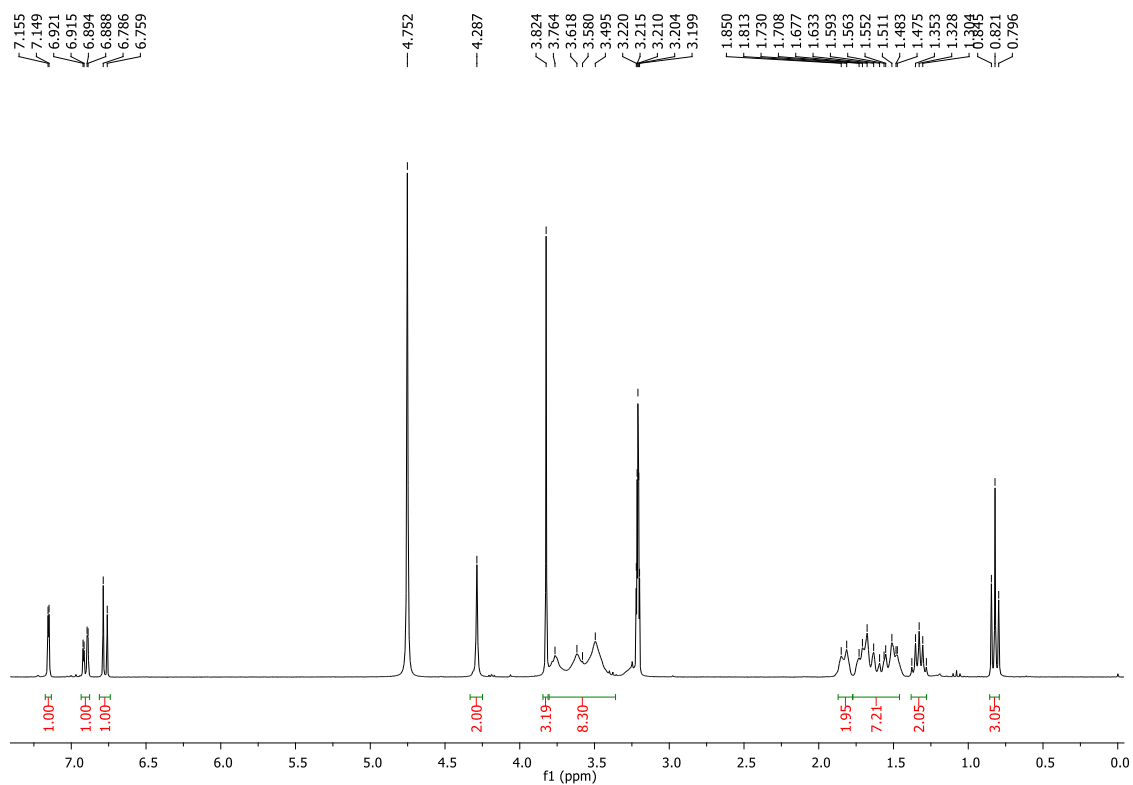
**4-((tert-butyl dimethylsilyl)oxy)-3-methoxybenzaldehyde (19).**

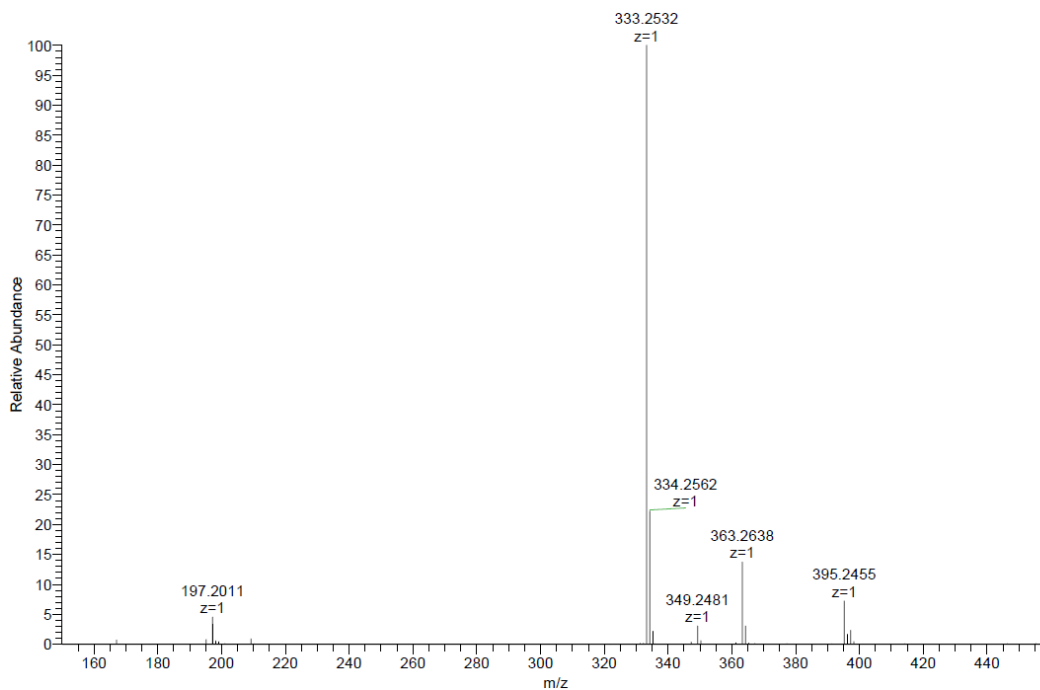
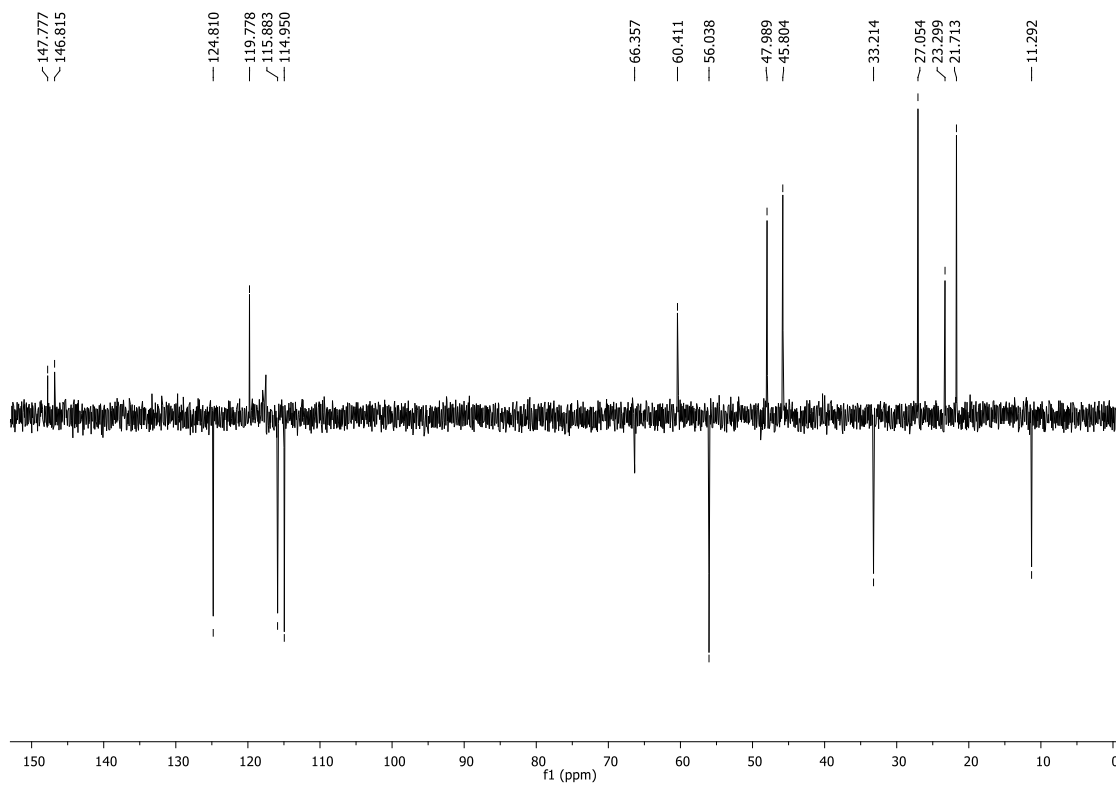
**1-(4-((tert-butyldimethylsilyl)oxy)-3-methoxybenzyl)piperazine (22).**

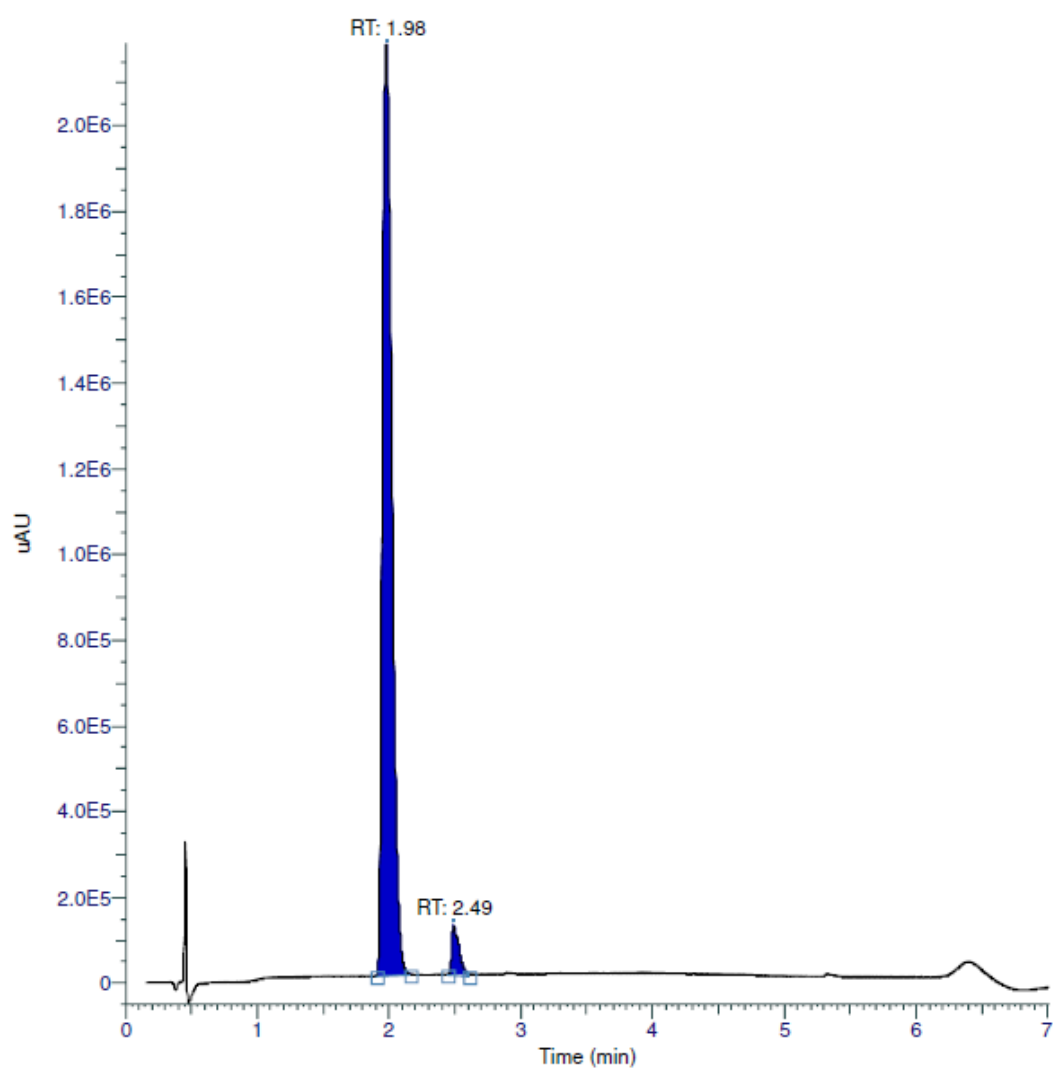
**4-((4-cyclohexylpiperazin-1-yl)methyl)-2-methoxyphenol (24c).**



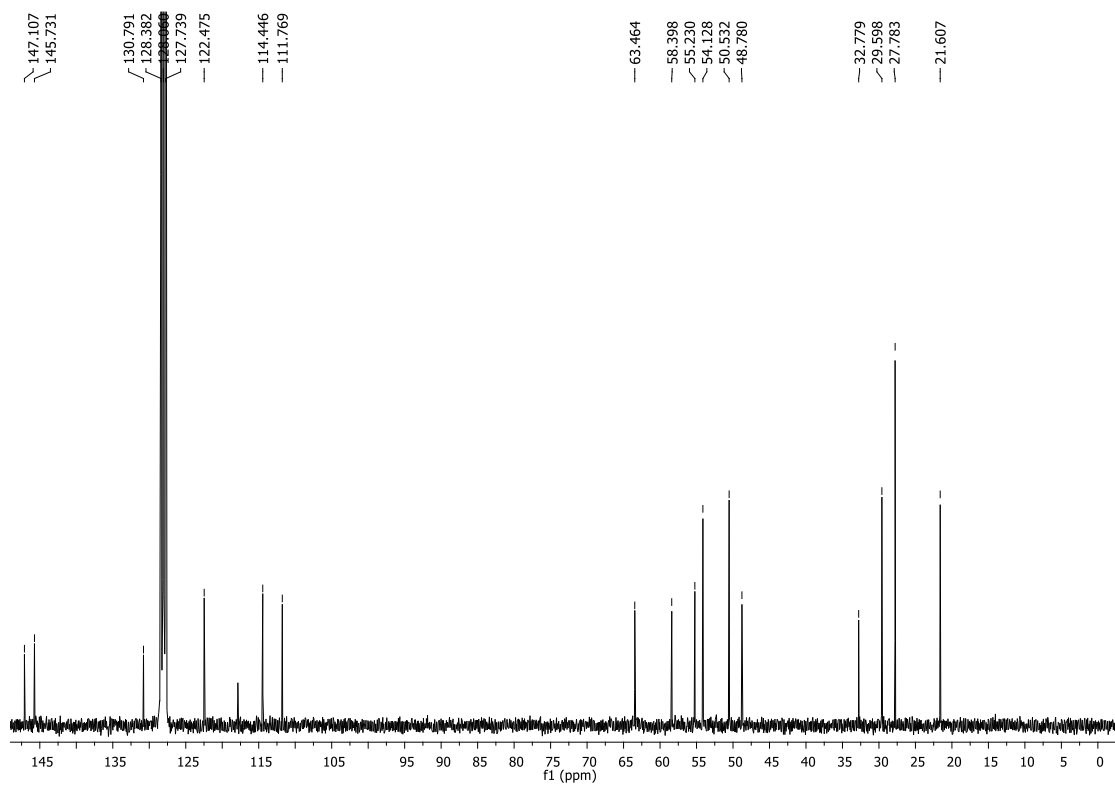
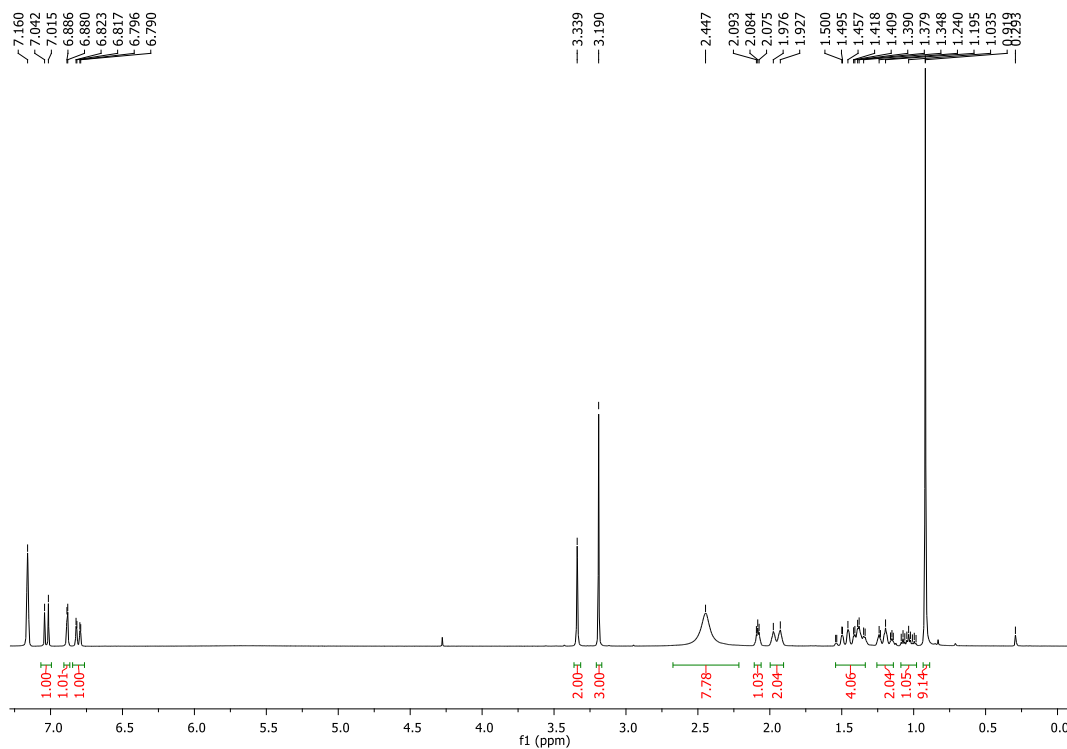
RT (Min)	% Area
1.5885	99.42
1.53183333333333	0.58

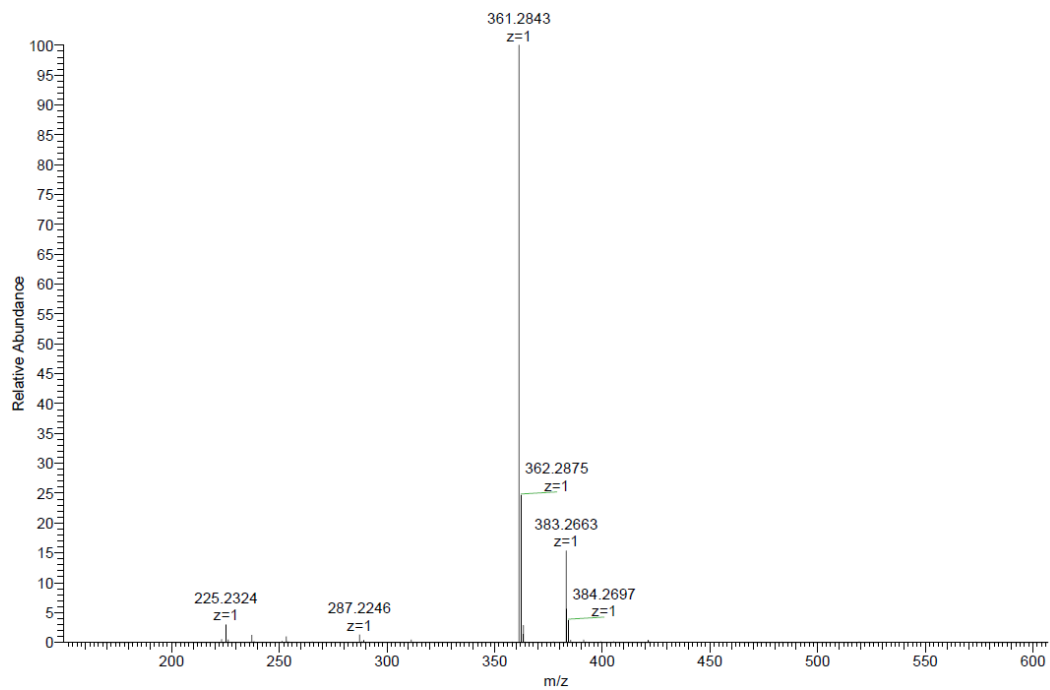
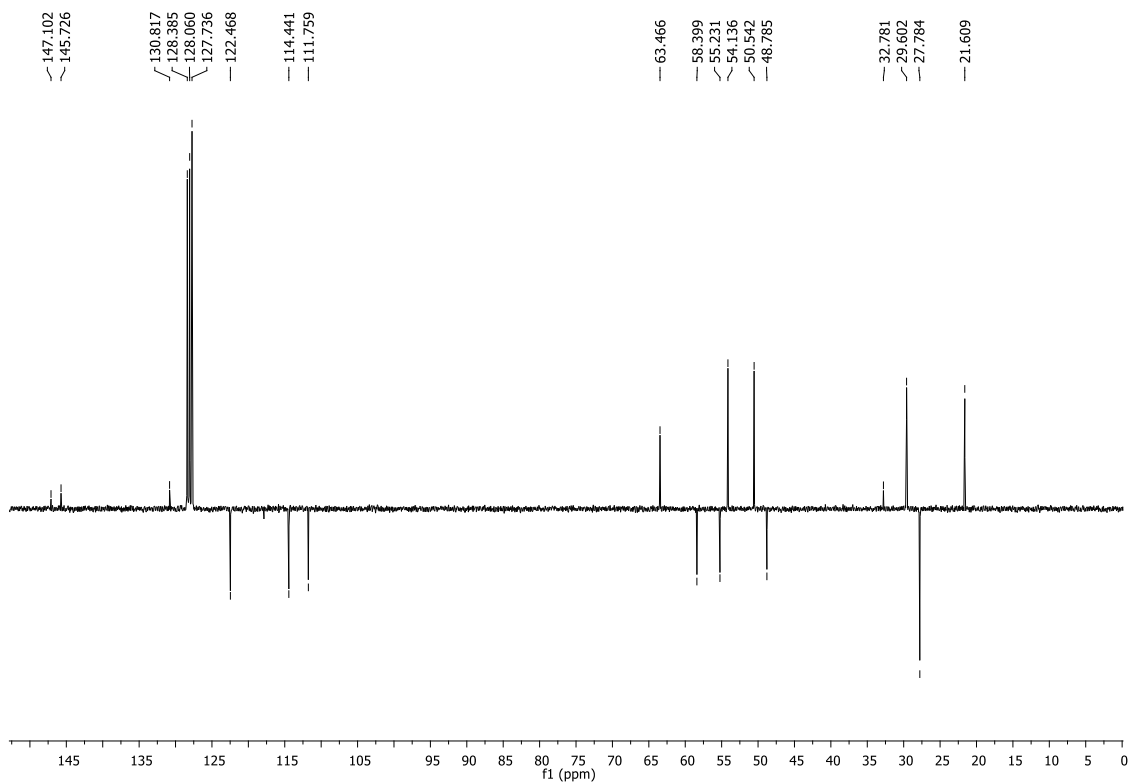
**4-((4-((1*S*,4*S*)-4-ethylcyclohexyl)piperazin-1-yl)methyl)-2-methoxyphenol (24d).**

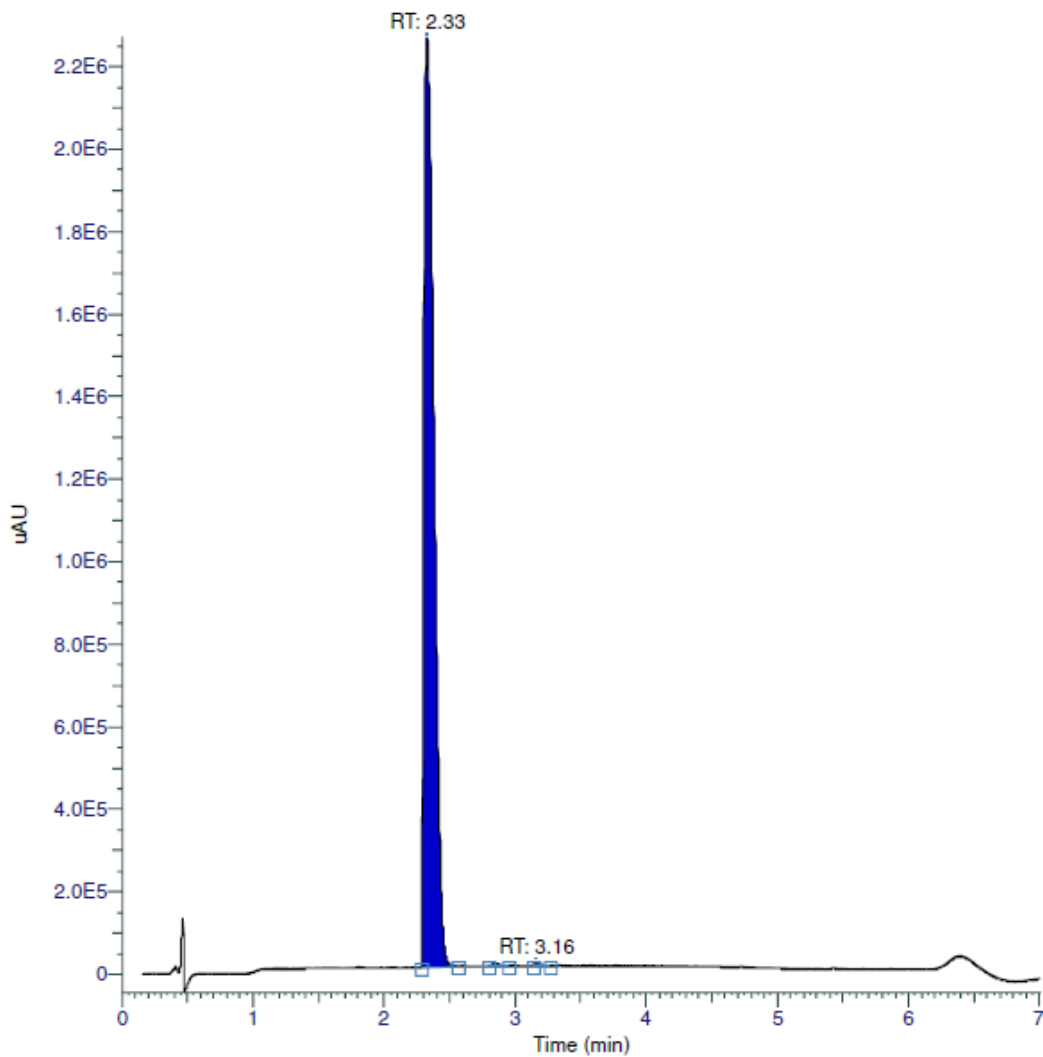




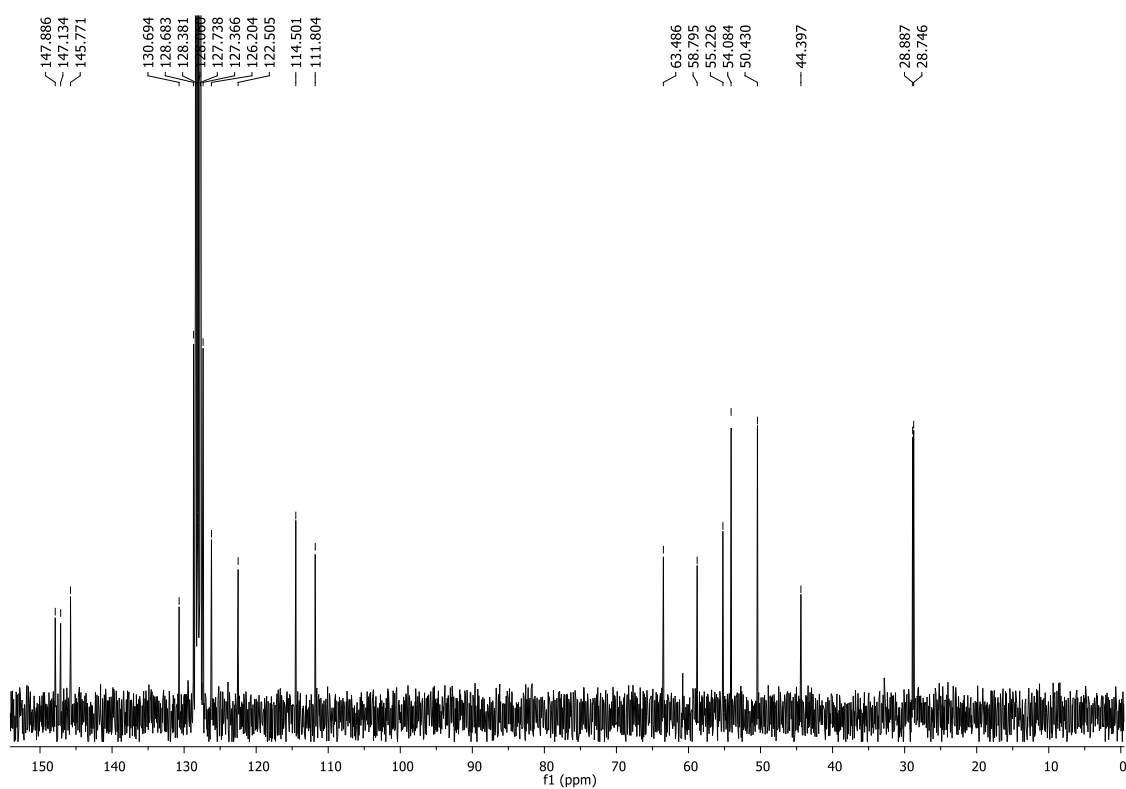
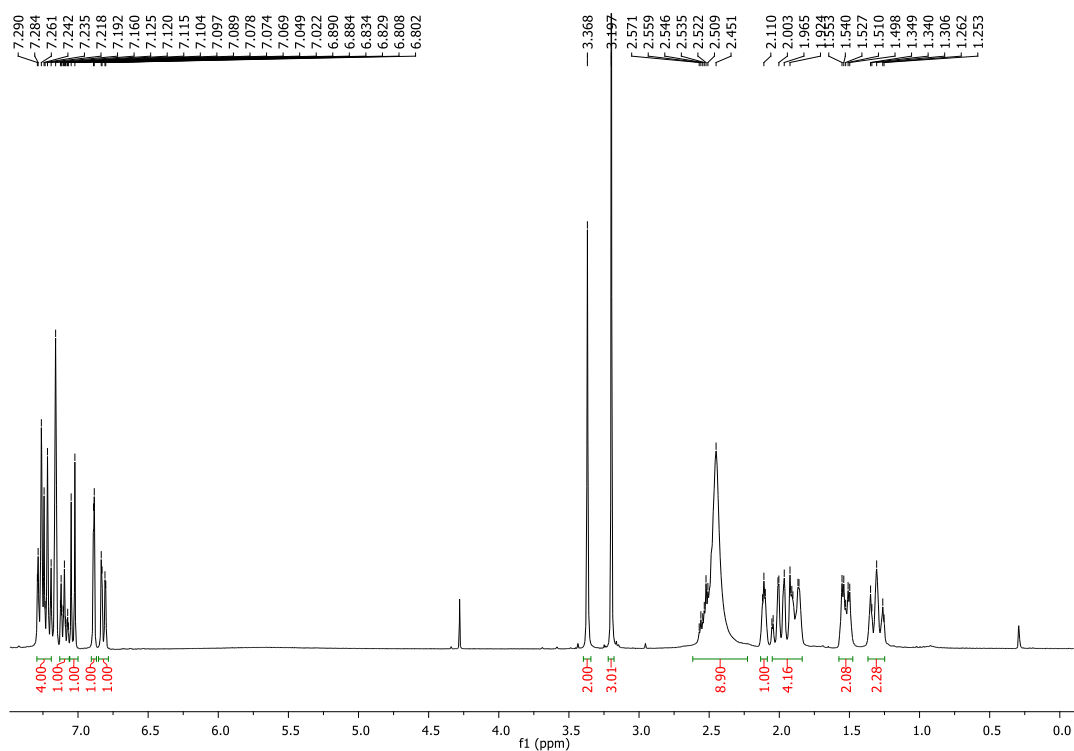
RT (Min)	% Area
1.9785	96.25
2.4885	3.75

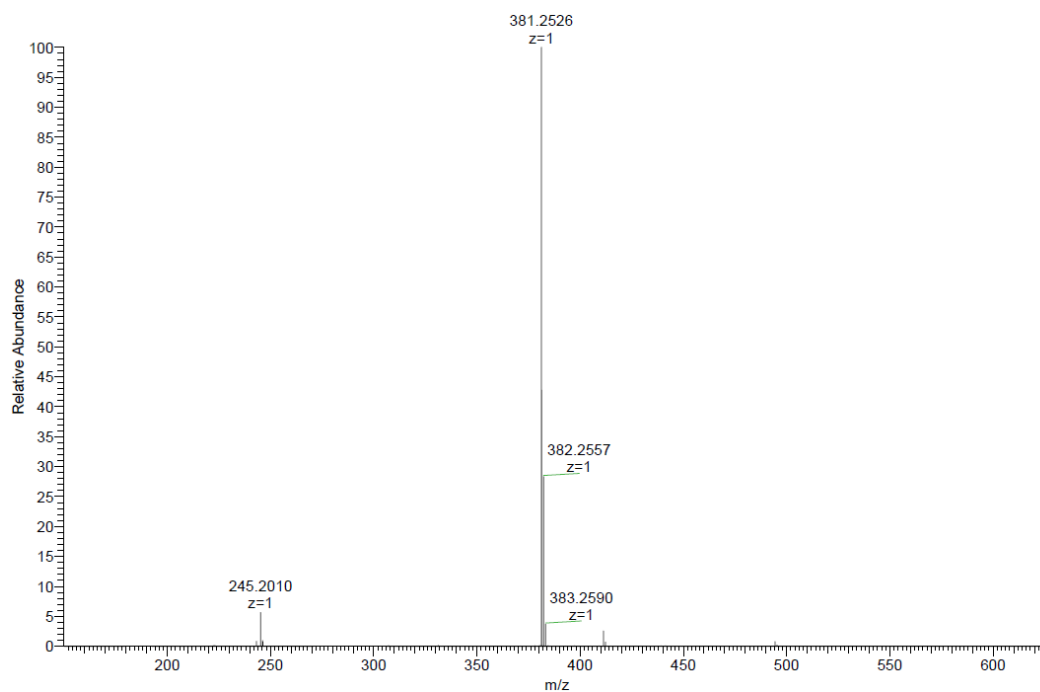
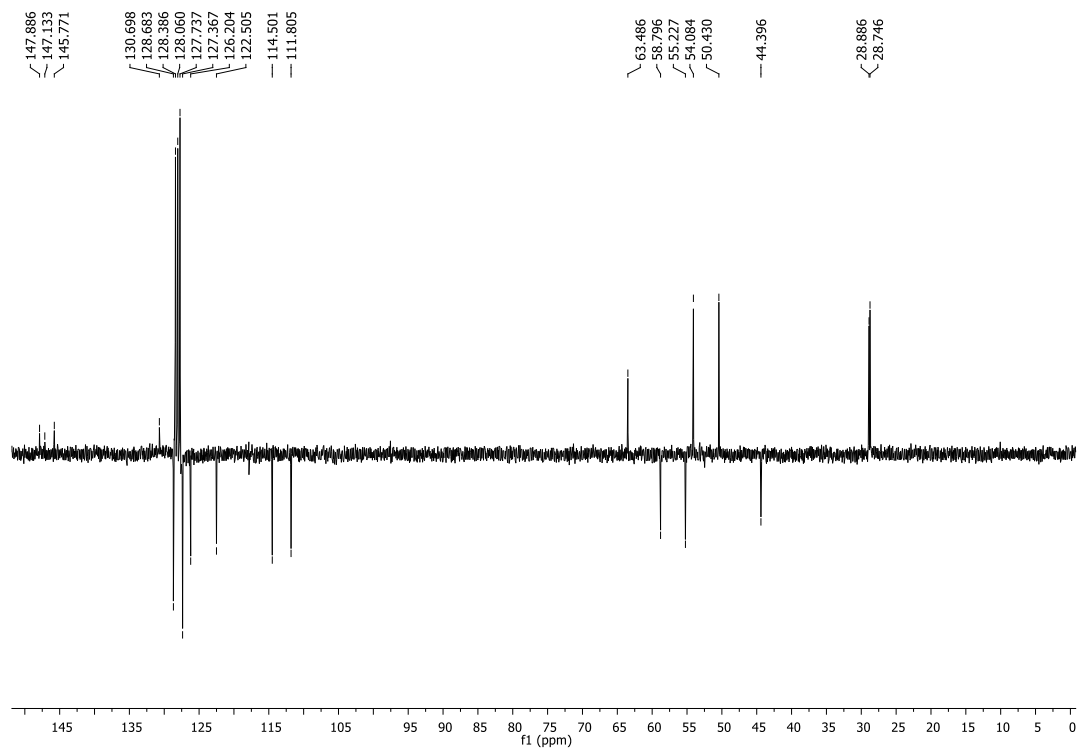
**4-((4-((1*S*,4*S*)-4-(tert-butyl)cyclohexyl)piperazin-1-yl)methyl)-2-methoxyphenol (24e).**

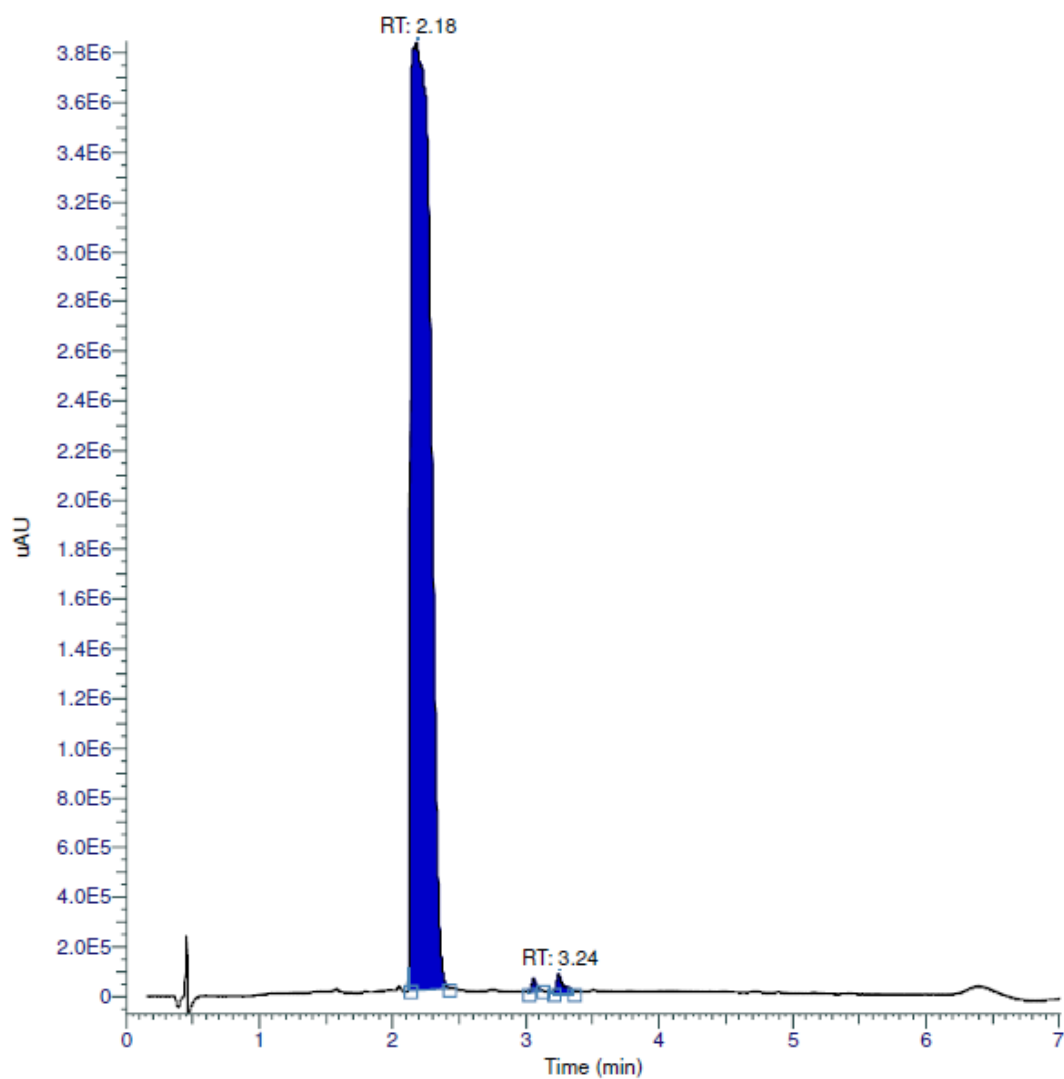




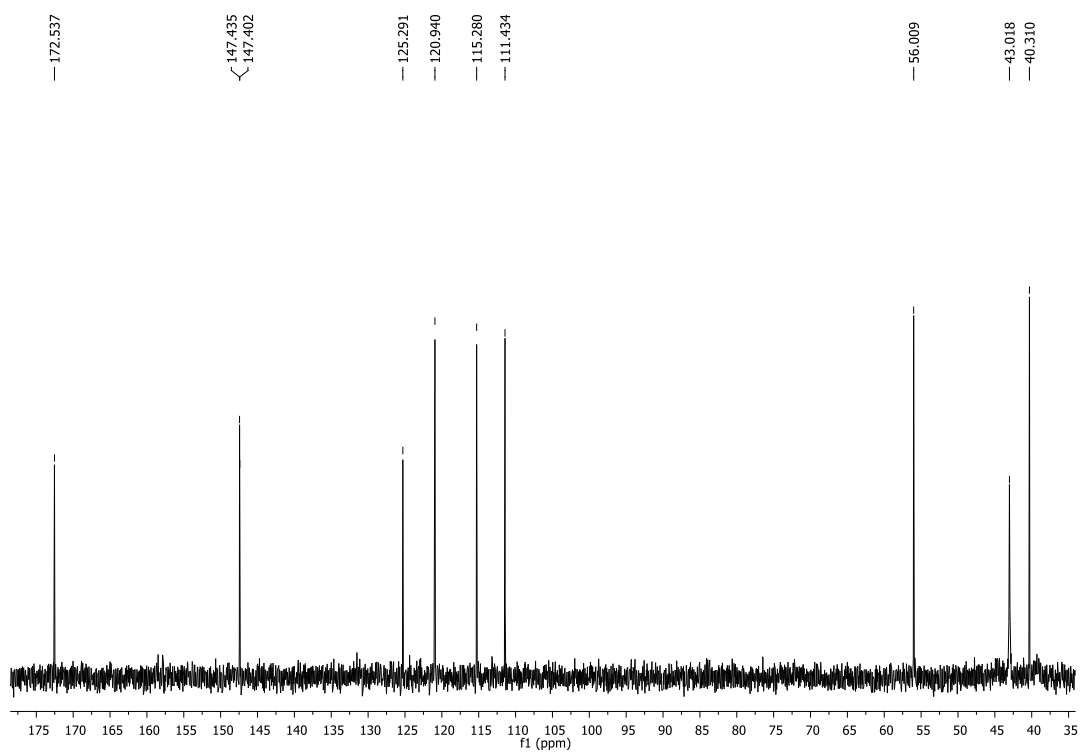
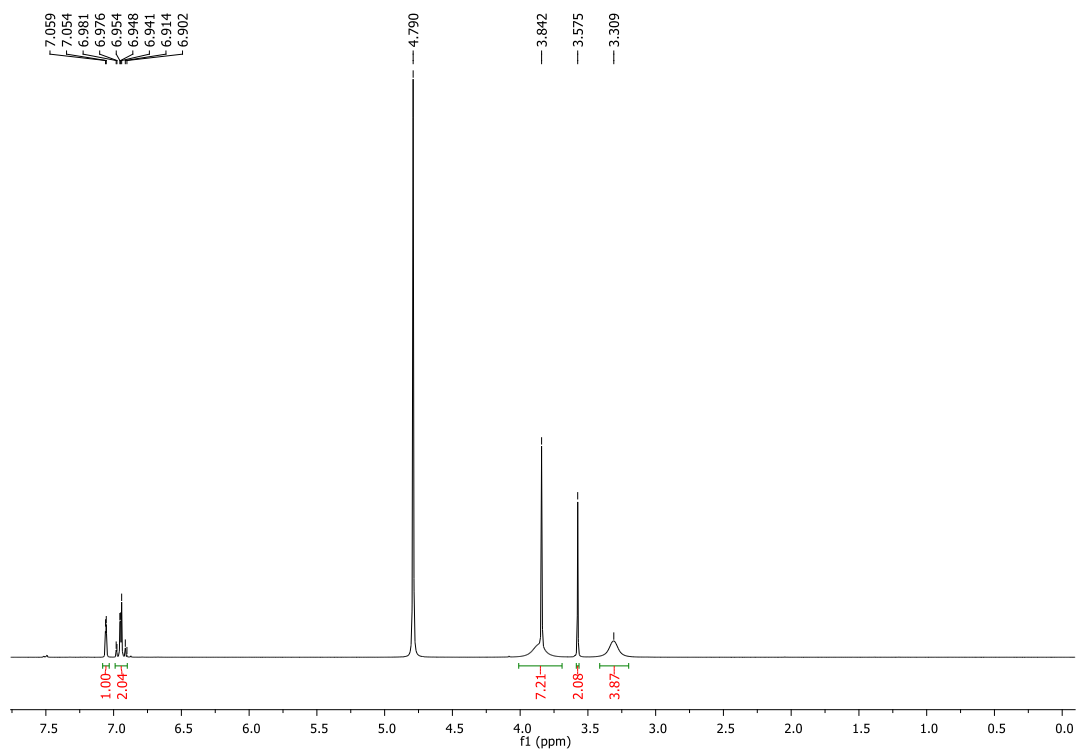
RT (Min)	% Area
2.326833333333333	99.59
2.836833333333333	0.2
3.1585	0.21

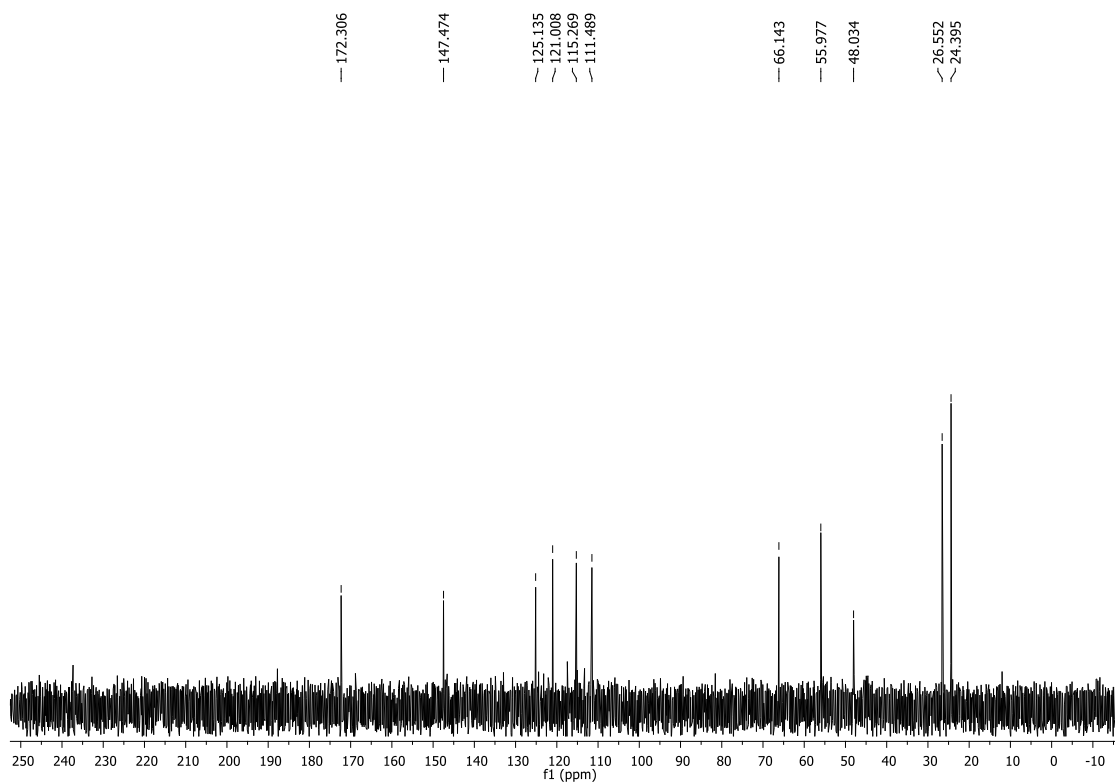
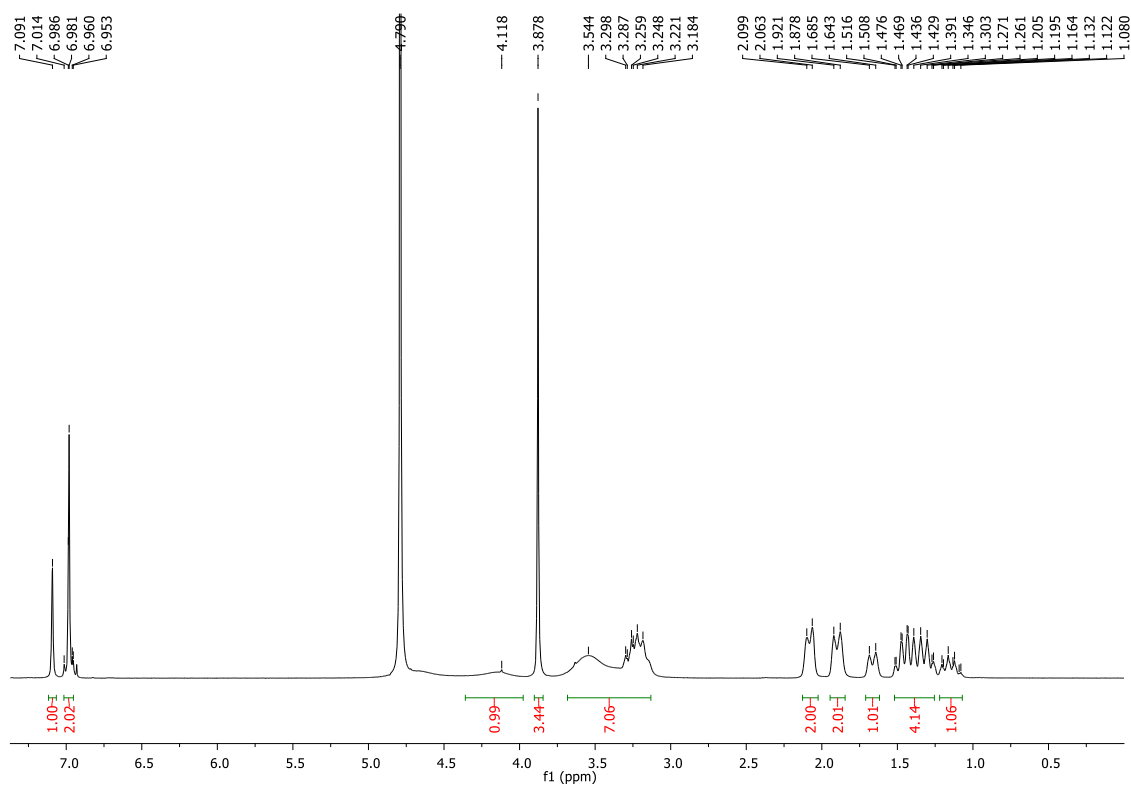
**2-methoxy-4-((4-((1*S*,4*S*)-4-phenylcyclohexyl)piperazin-1-yl)methyl)phenol (24f).**

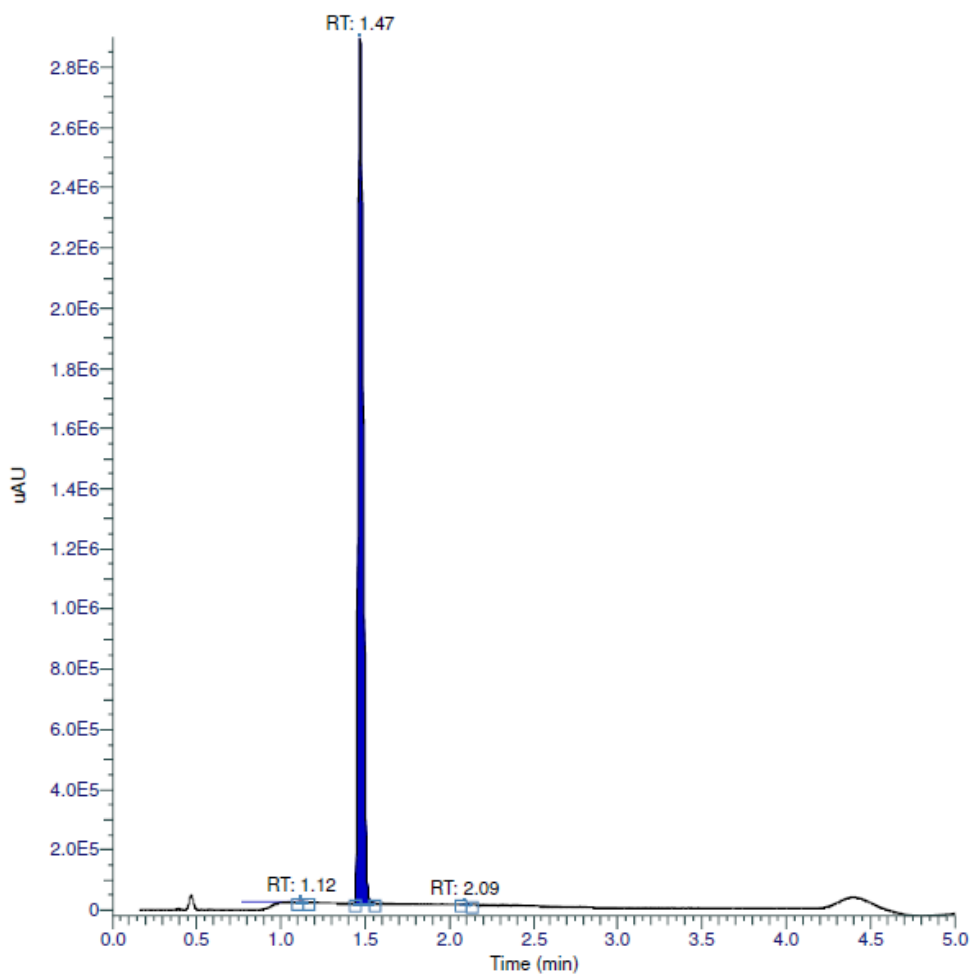
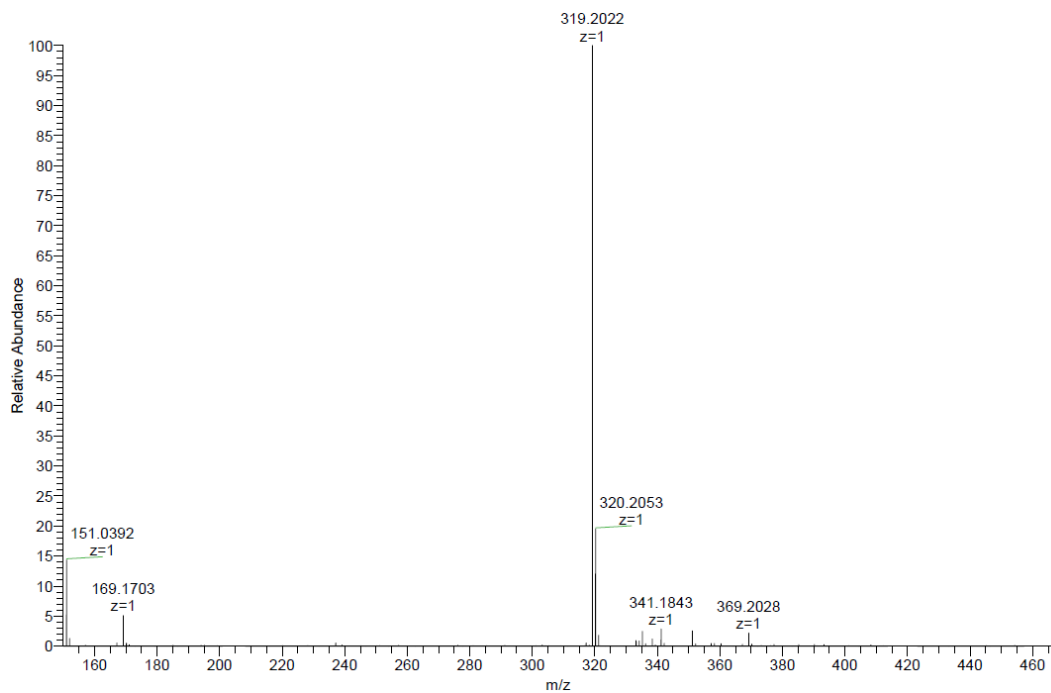




RT (Min)	% Area
2.18016666666667	98.96
3.05683333333333	0.33
3.2435	0.71

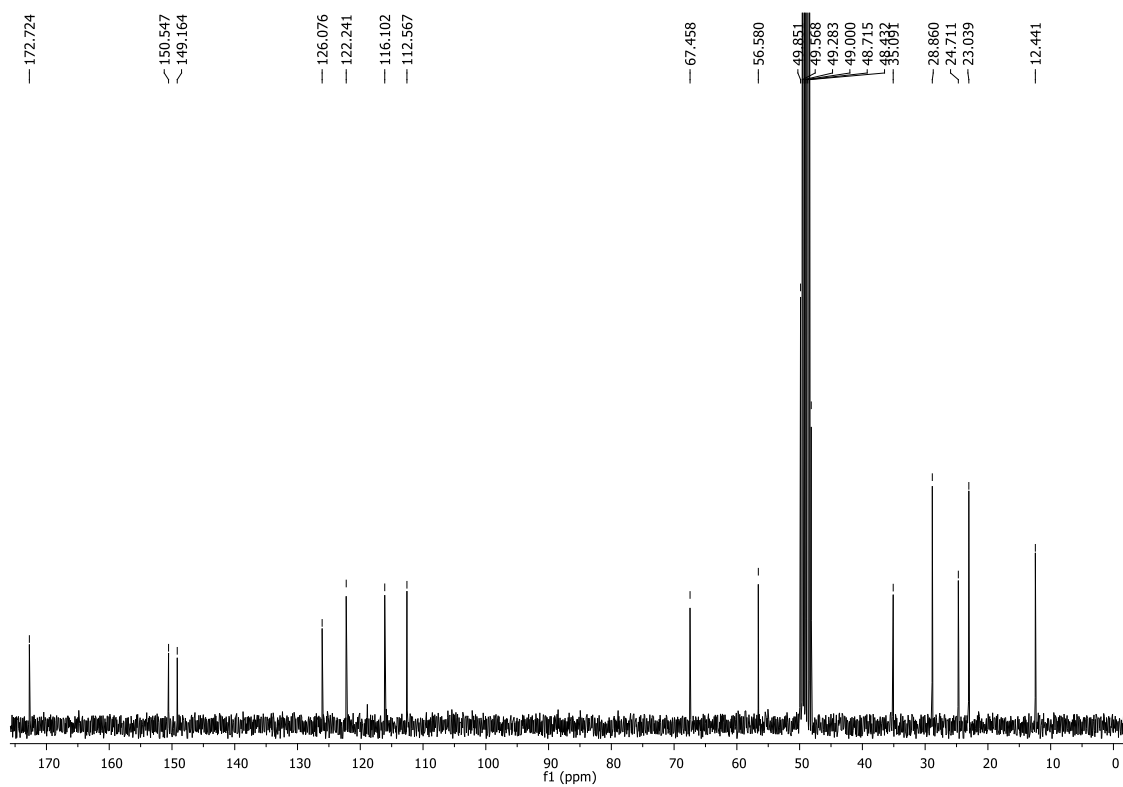
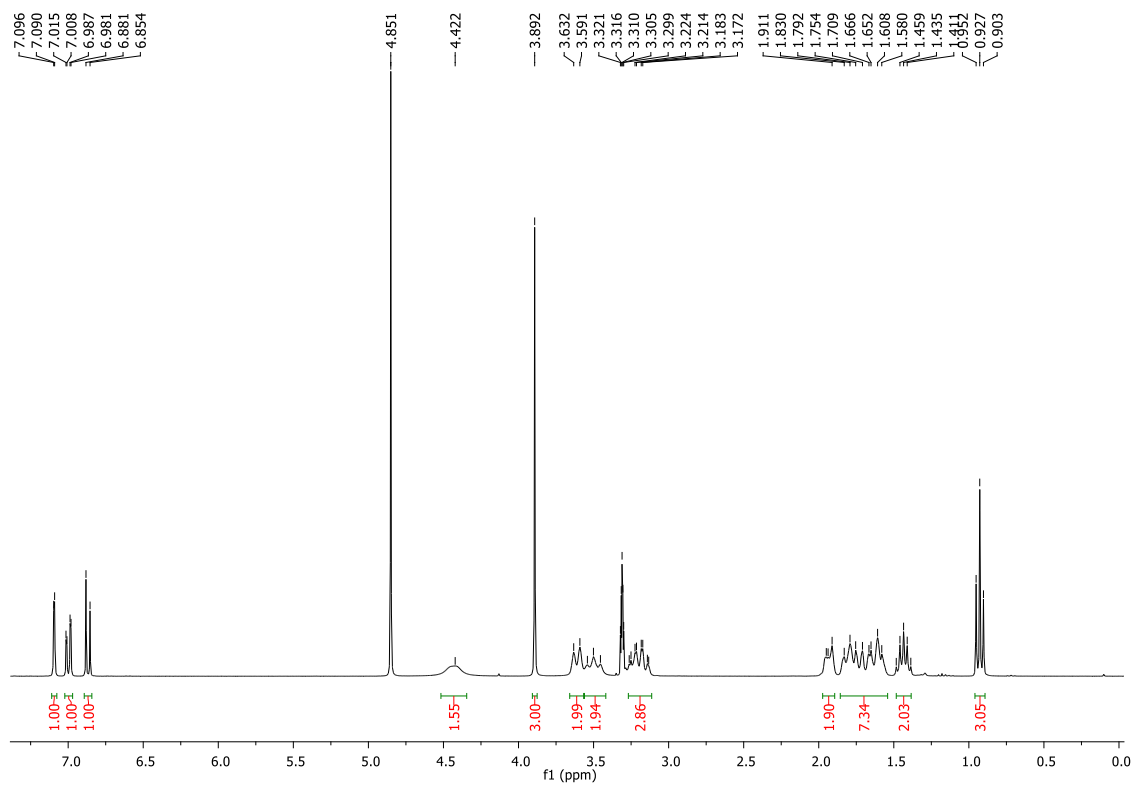
**(4-hydroxy-3-methoxyphenyl)(piperazin-1-yl)methanone (27).**

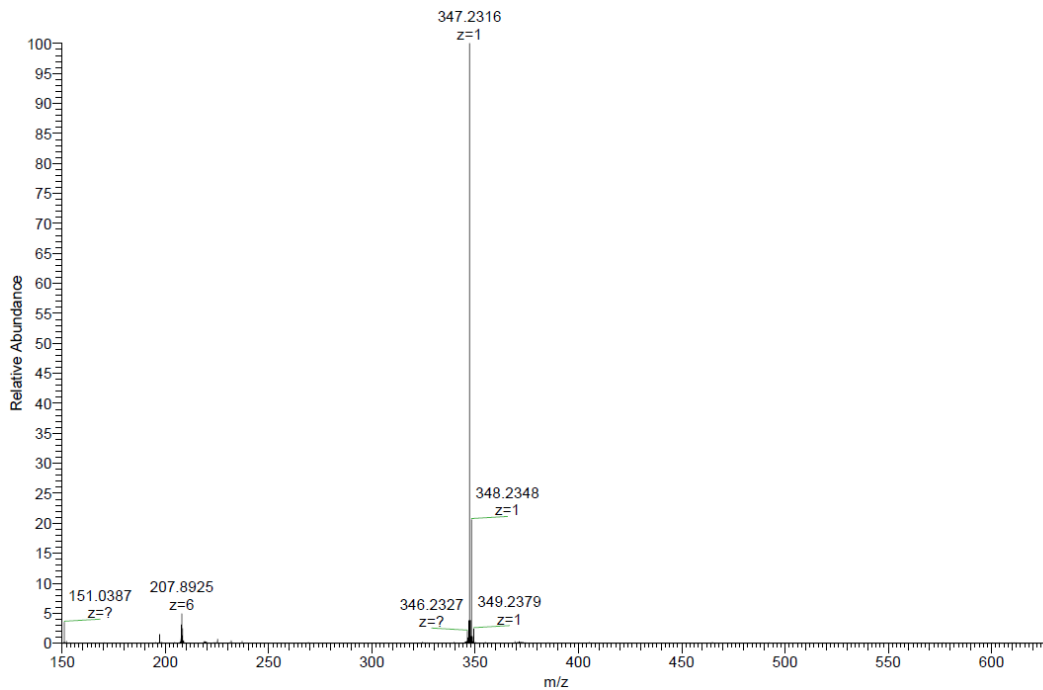
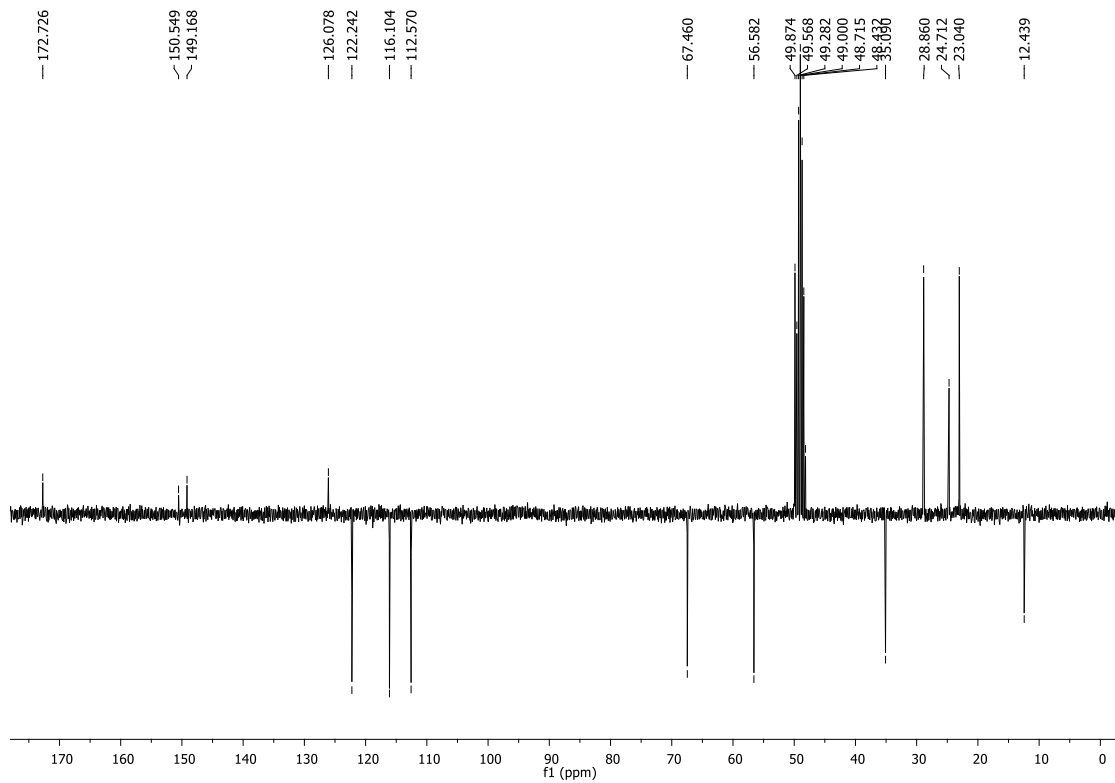
**(4-cyclohexylpiperazin-1-yl)(4-hydroxy-3-methoxyphenyl)methanone (28c).**

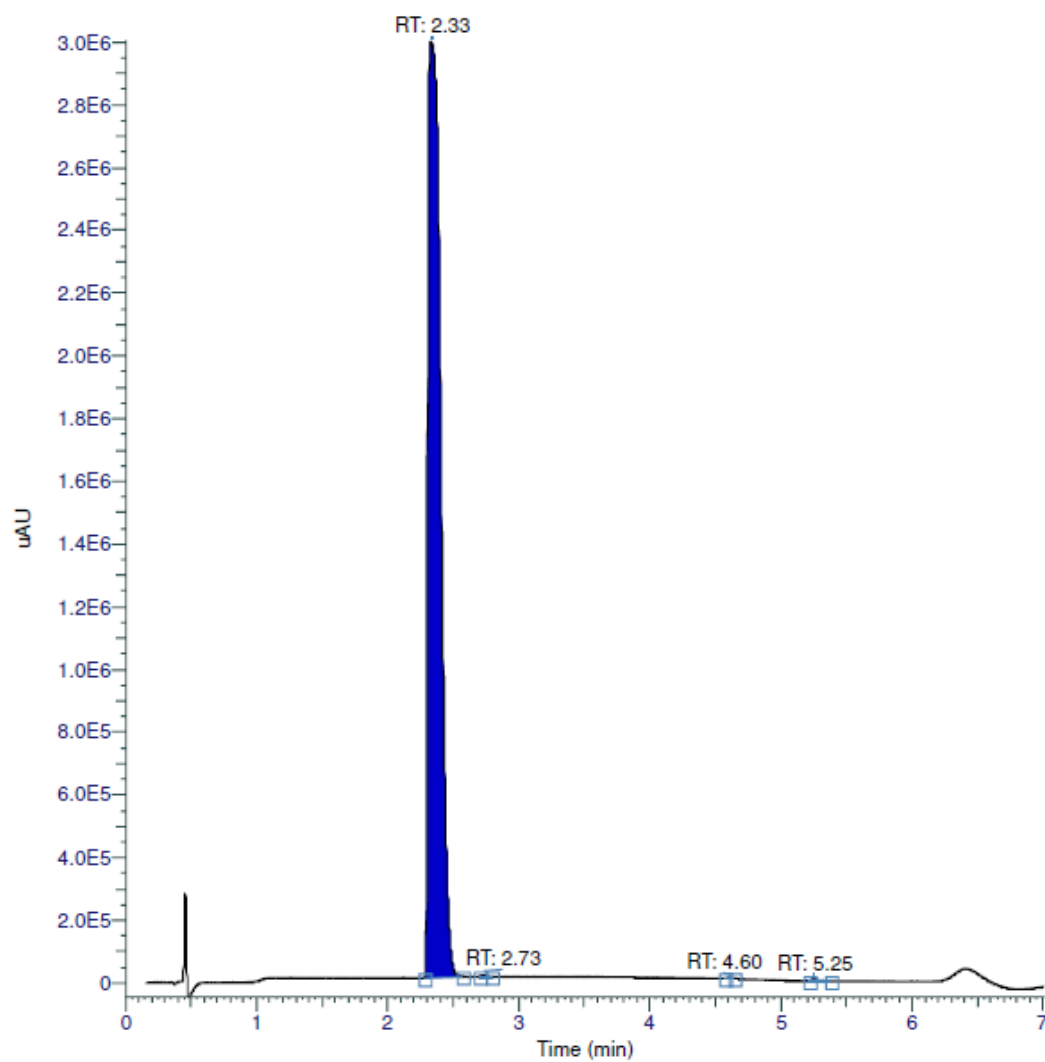


RT (Min)	% Area
1.1183333333333333	0.08
1.47	99.88
2.086666666666667	0.04

**(4-((1*S*,4*S*)-4-ethylcyclohexyl)piperazin-1-yl)(4-hydroxy-3-methoxyphenyl)methanone (28d).**

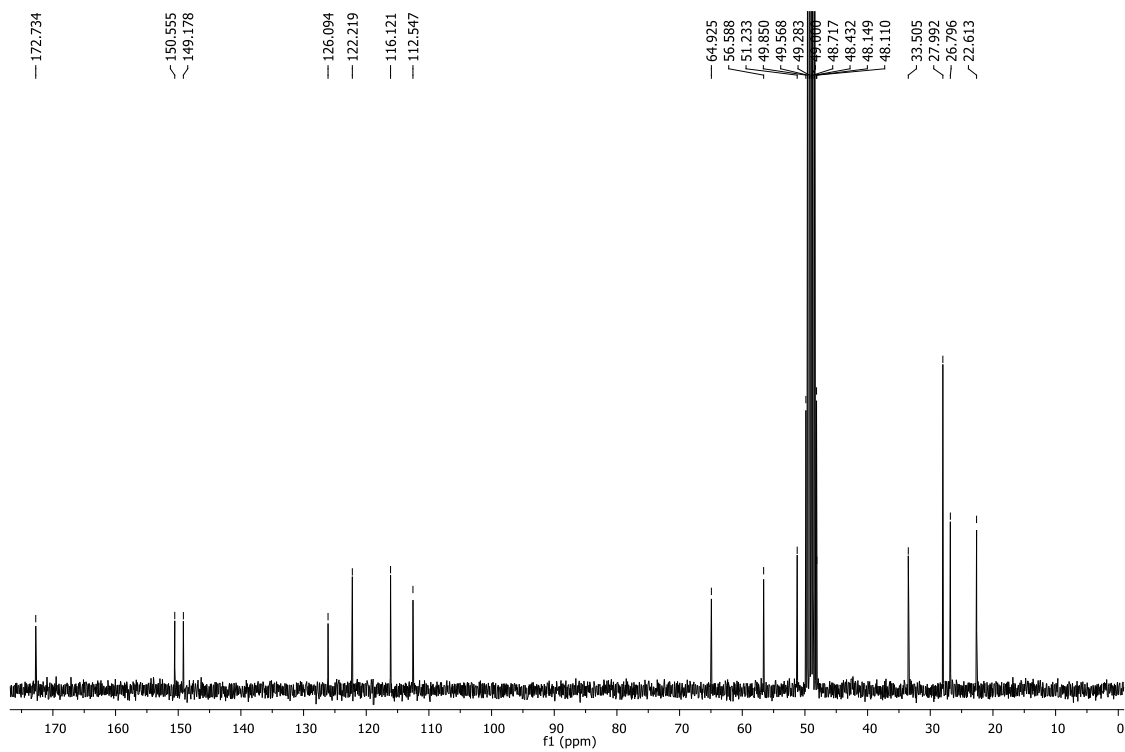
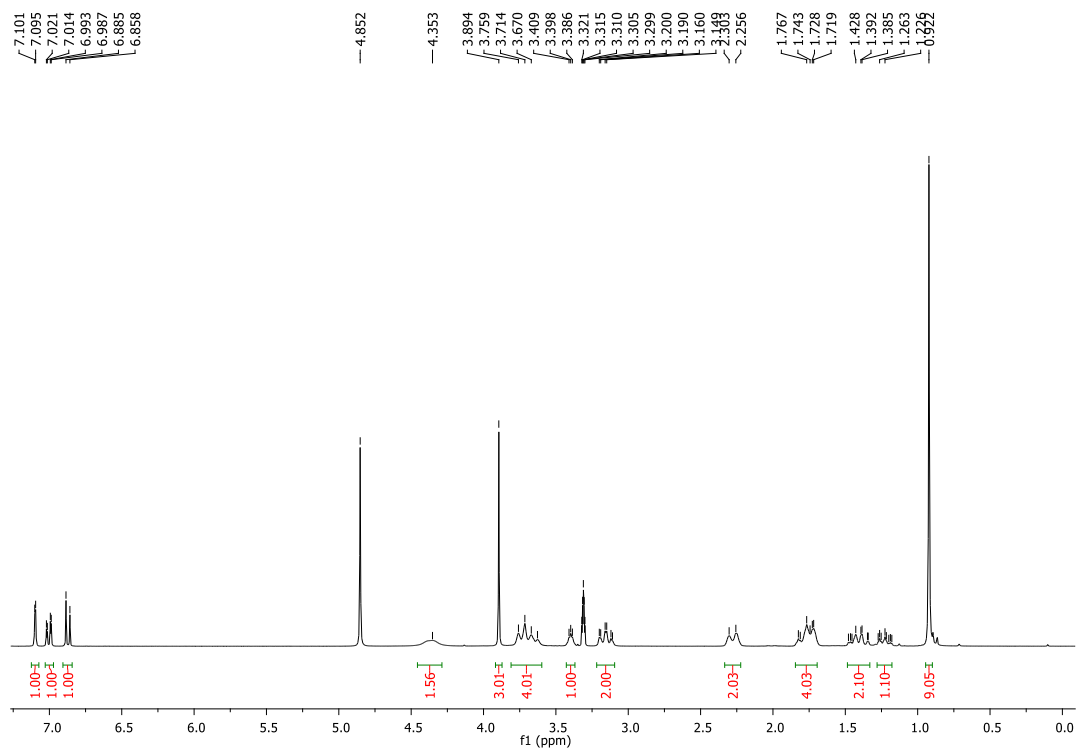


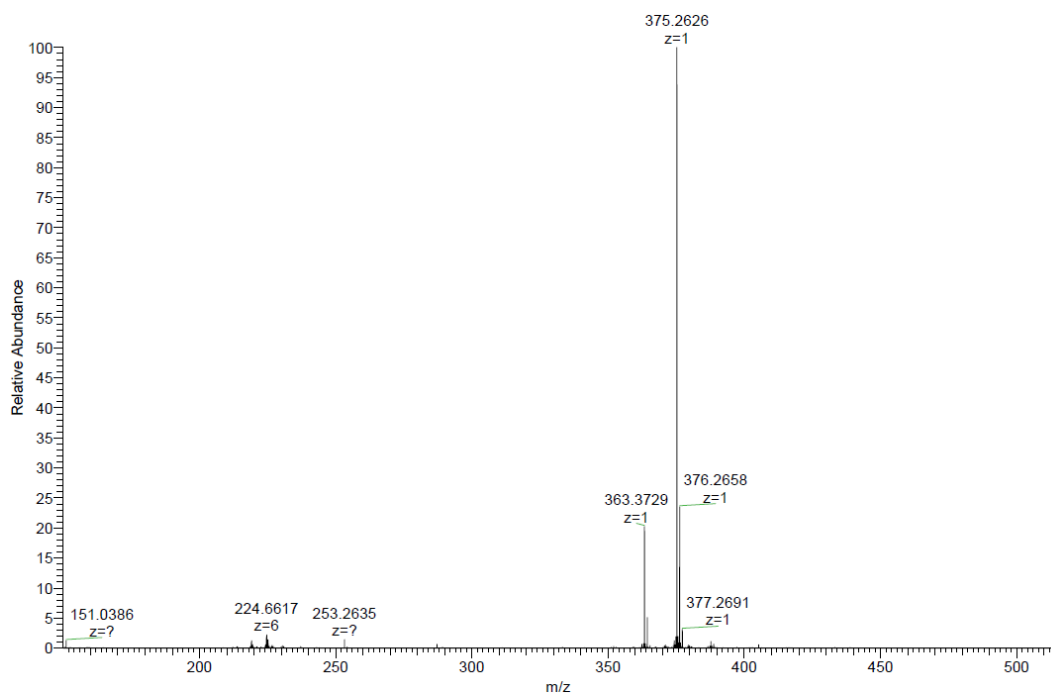
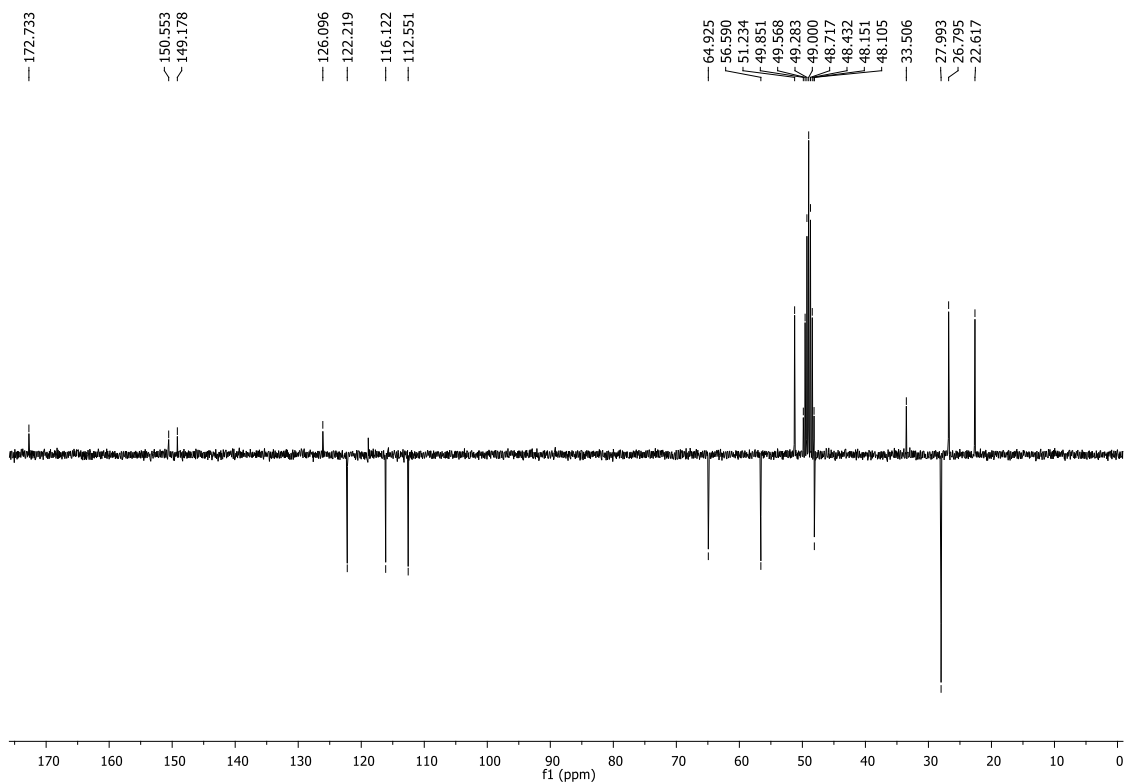


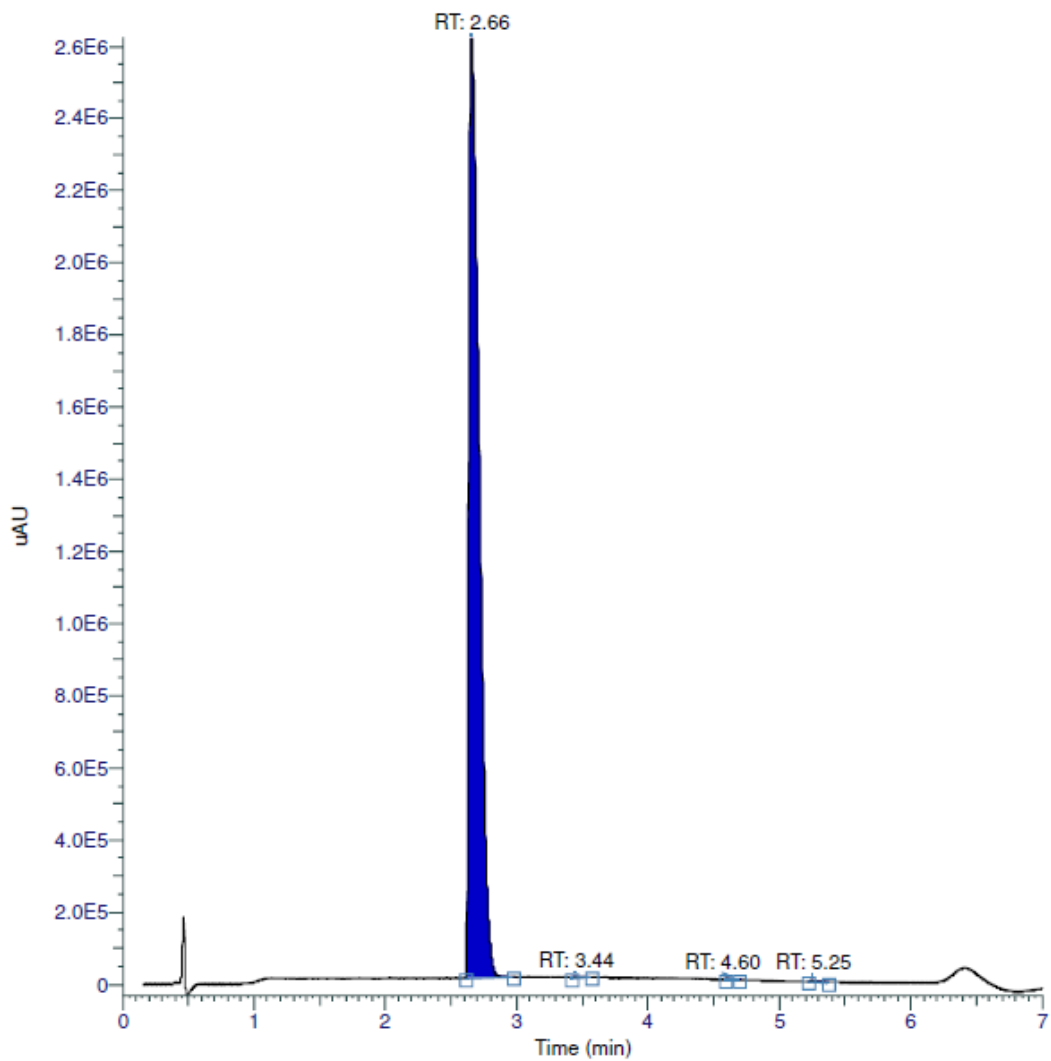


RT (Min)	% Area
2.33183333333333	99.8
2.73183333333333	0.04
4.6035	0.03
5.25016666666667	0.12

**(4-((1*S*,4*S*)-4-(tert-butyl)cyclohexyl)piperazin-1-yl)(4-hydroxy-3-methoxyphenyl)methanone (28e).**

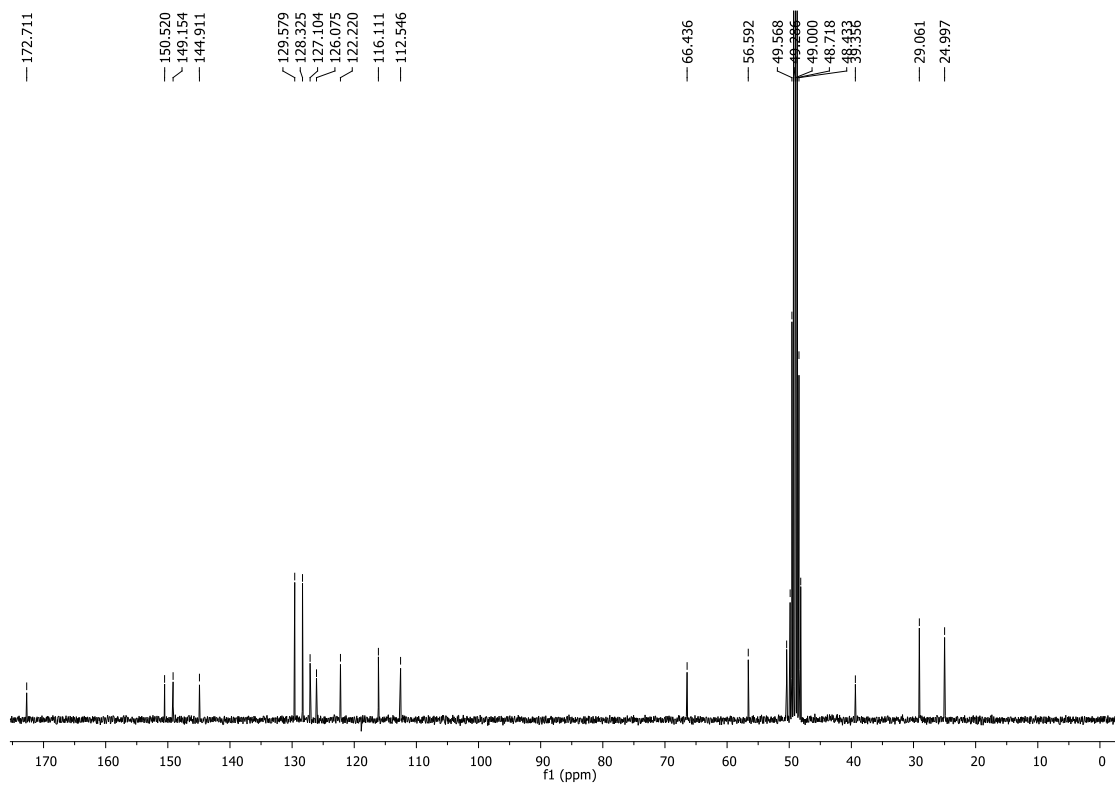
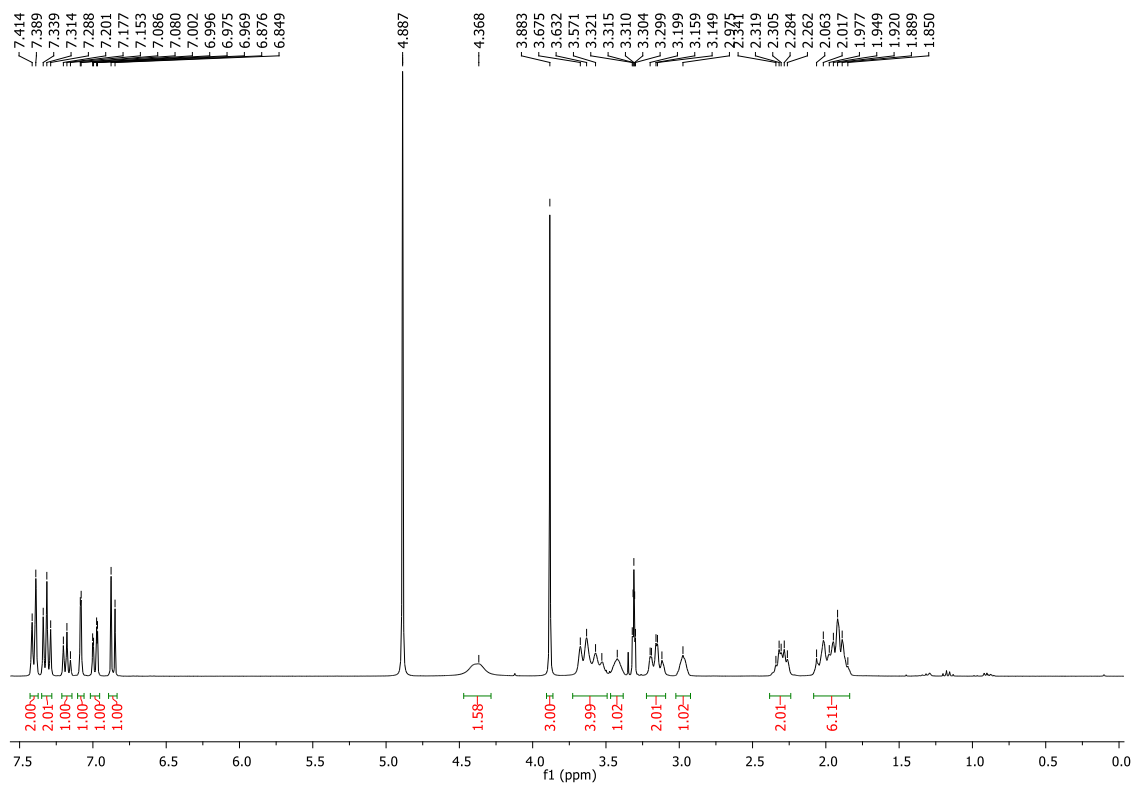


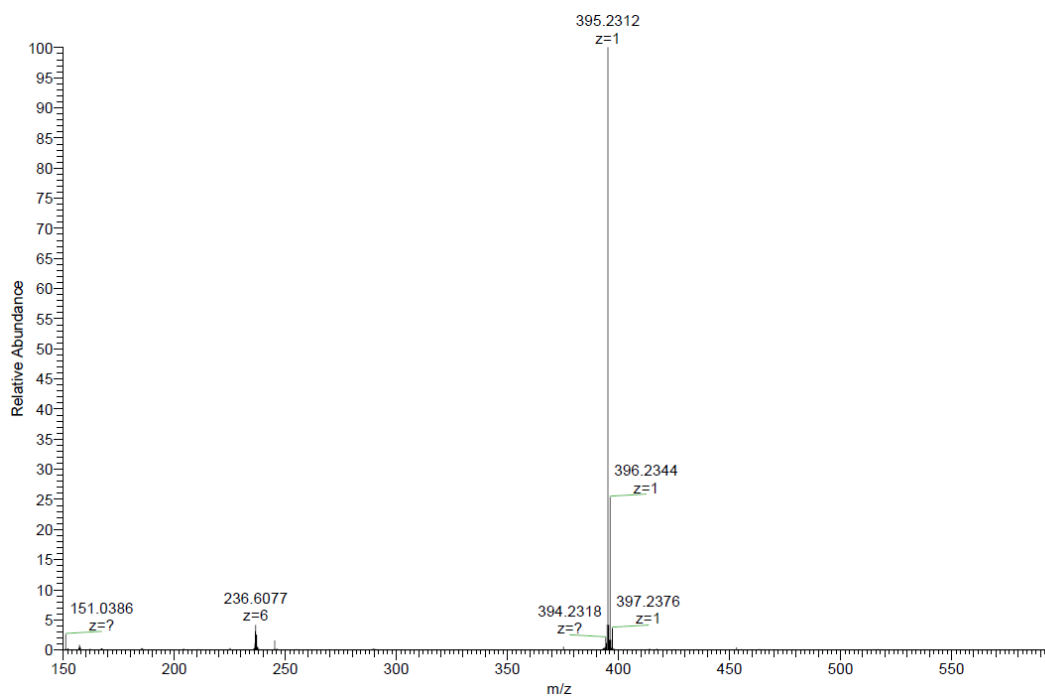
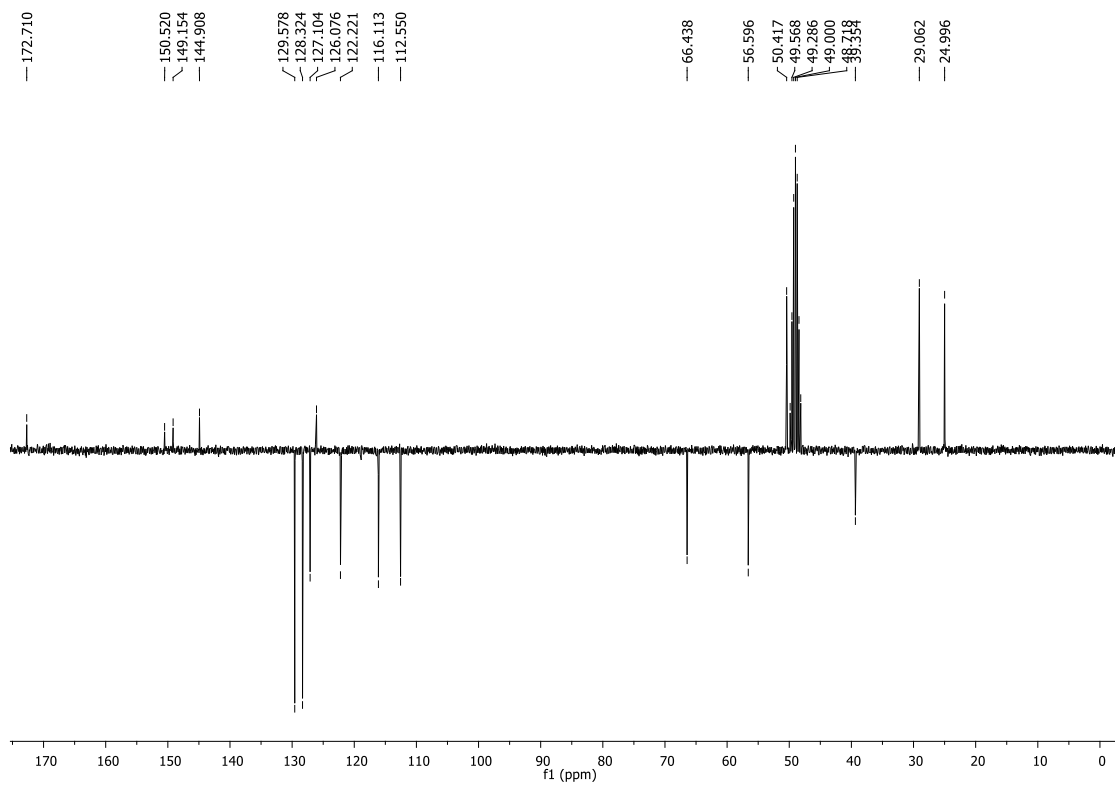


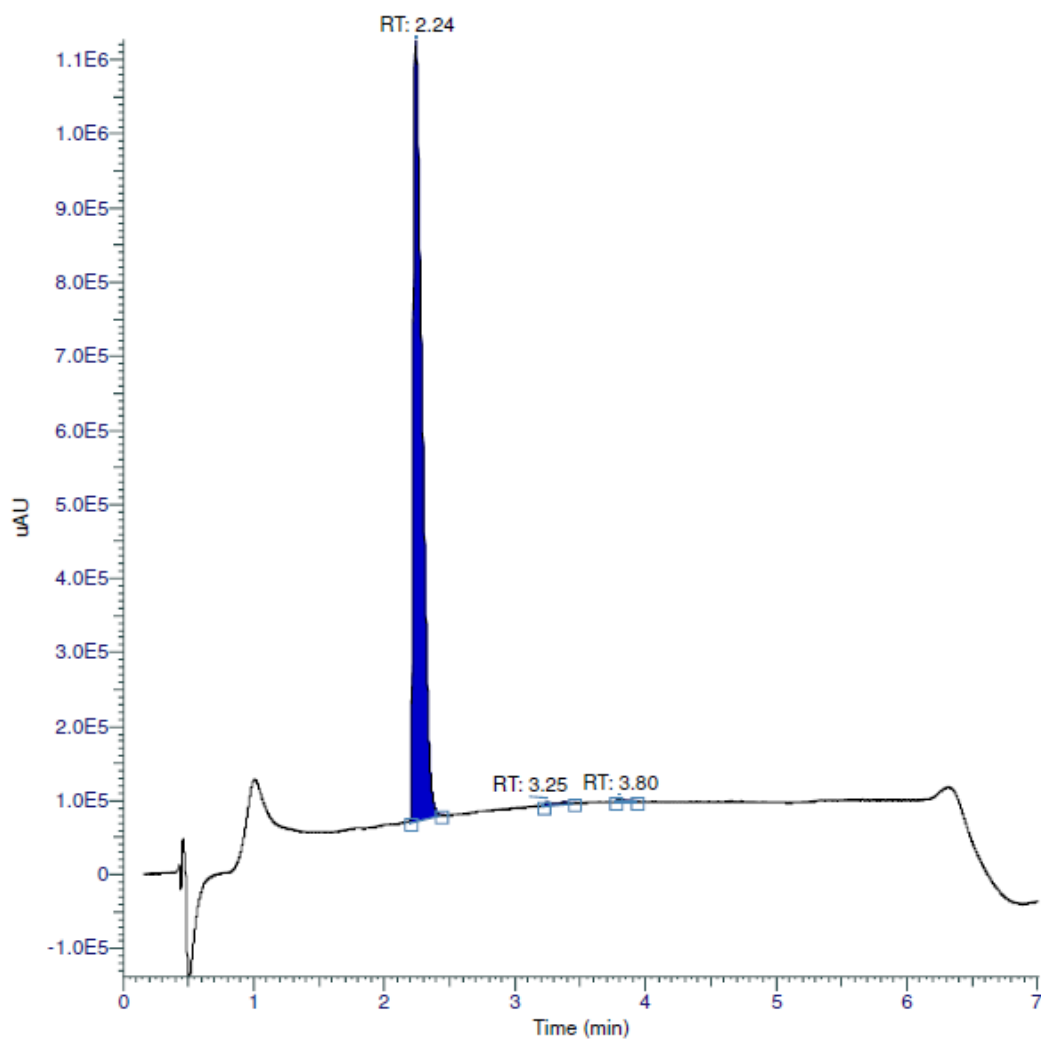


RT (Min)	% Area
2.656666666666667	99.8
3.441666666666667	0.06
4.603333333333333	0.05
5.25	0.09

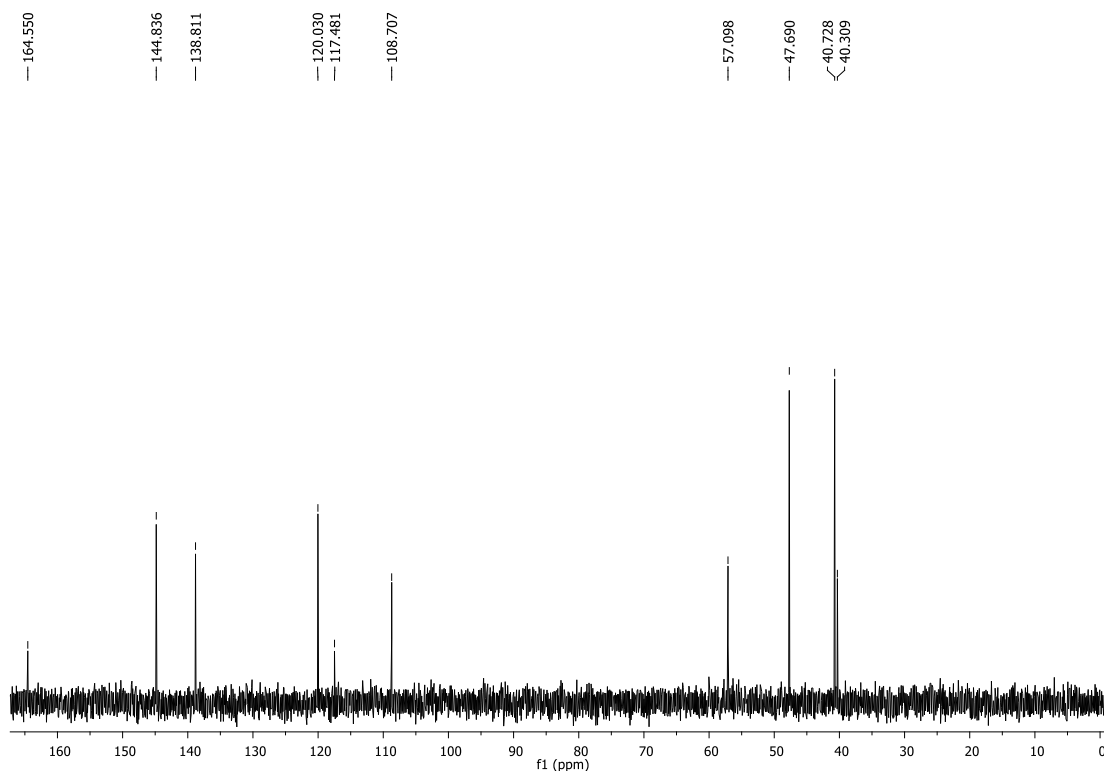
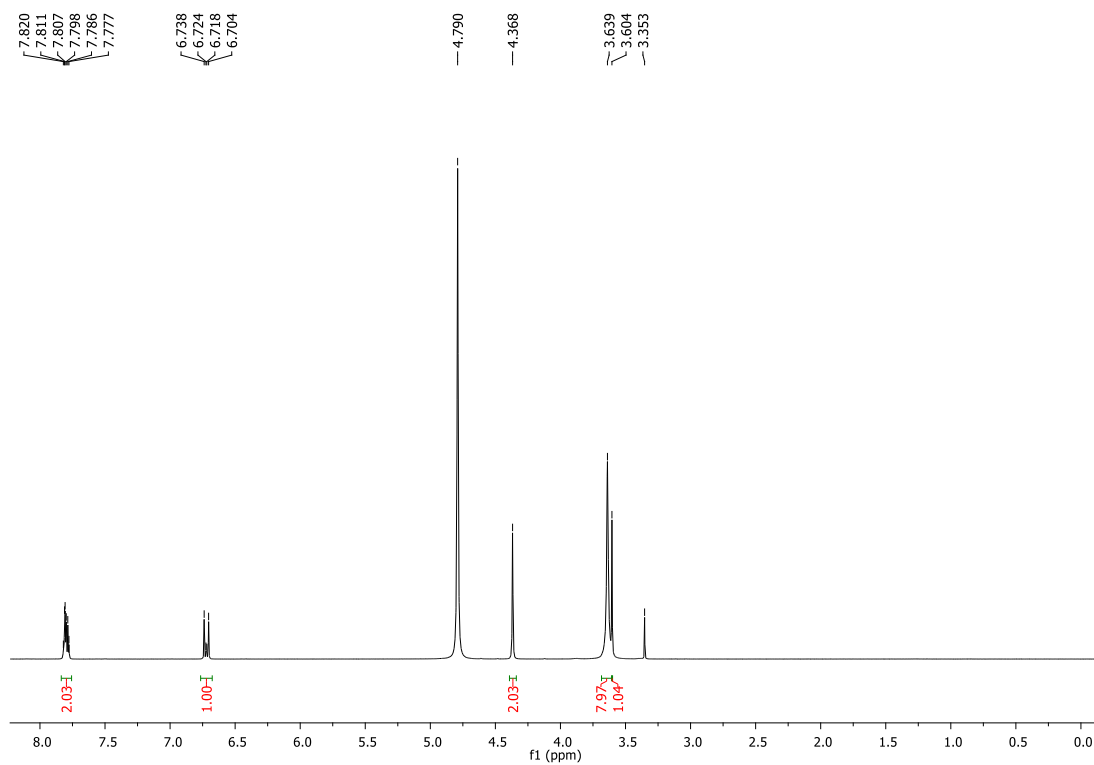
(4-hydroxy-3-methoxyphenyl)(4-((1*S*,4*S*)-4-phenylcyclohexyl)piperazin-1-yl)methanone (28f).



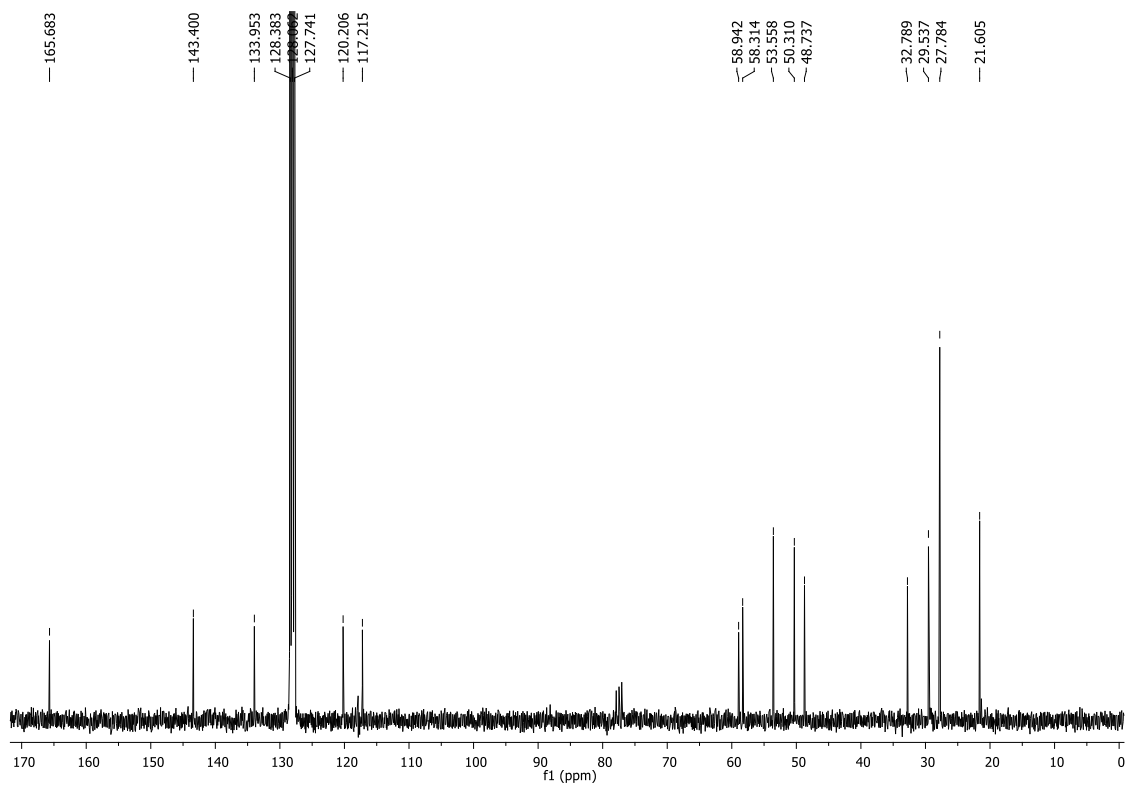
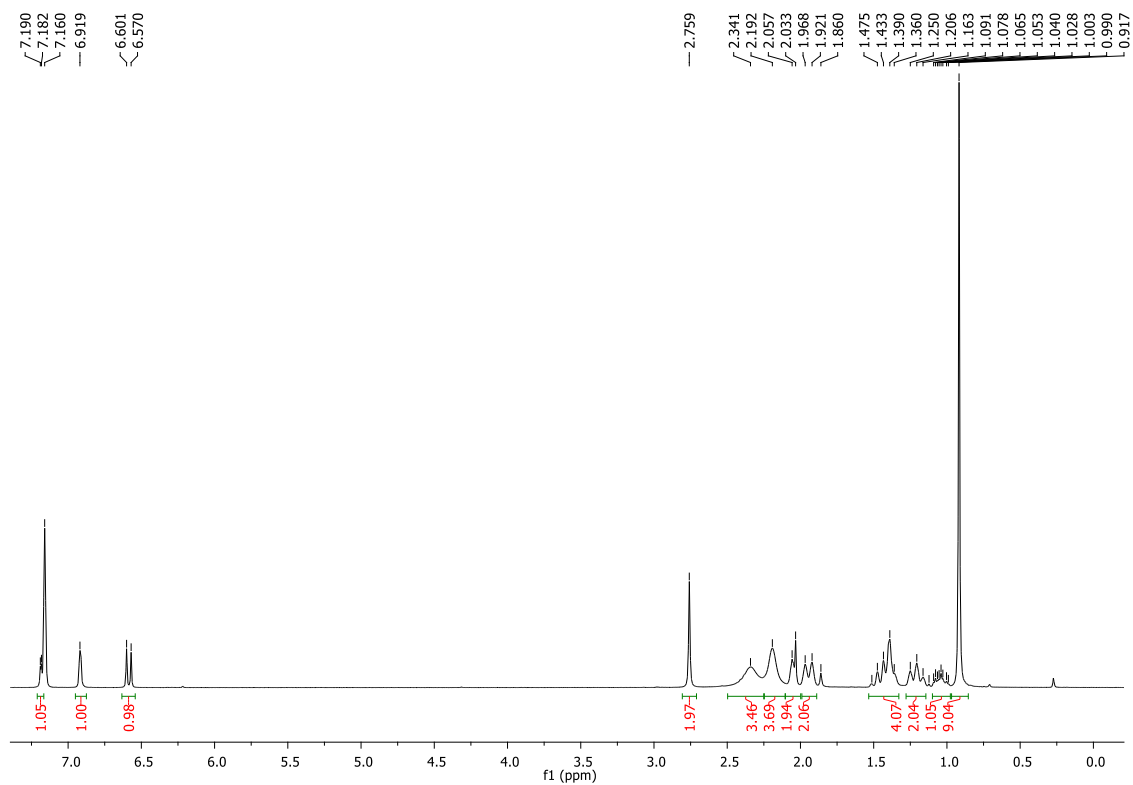


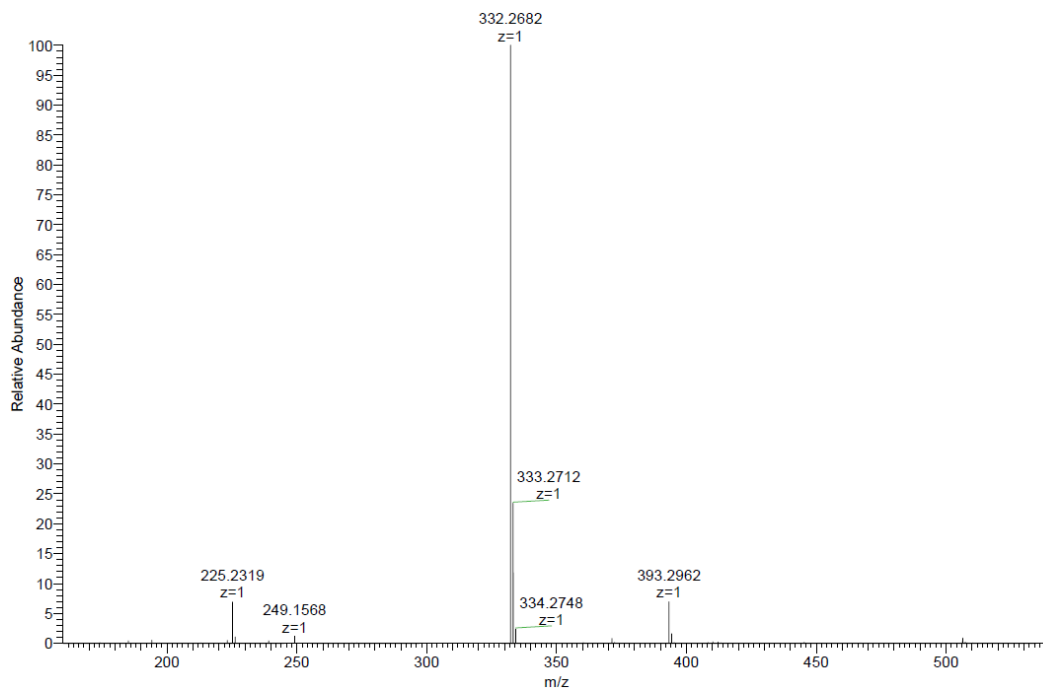
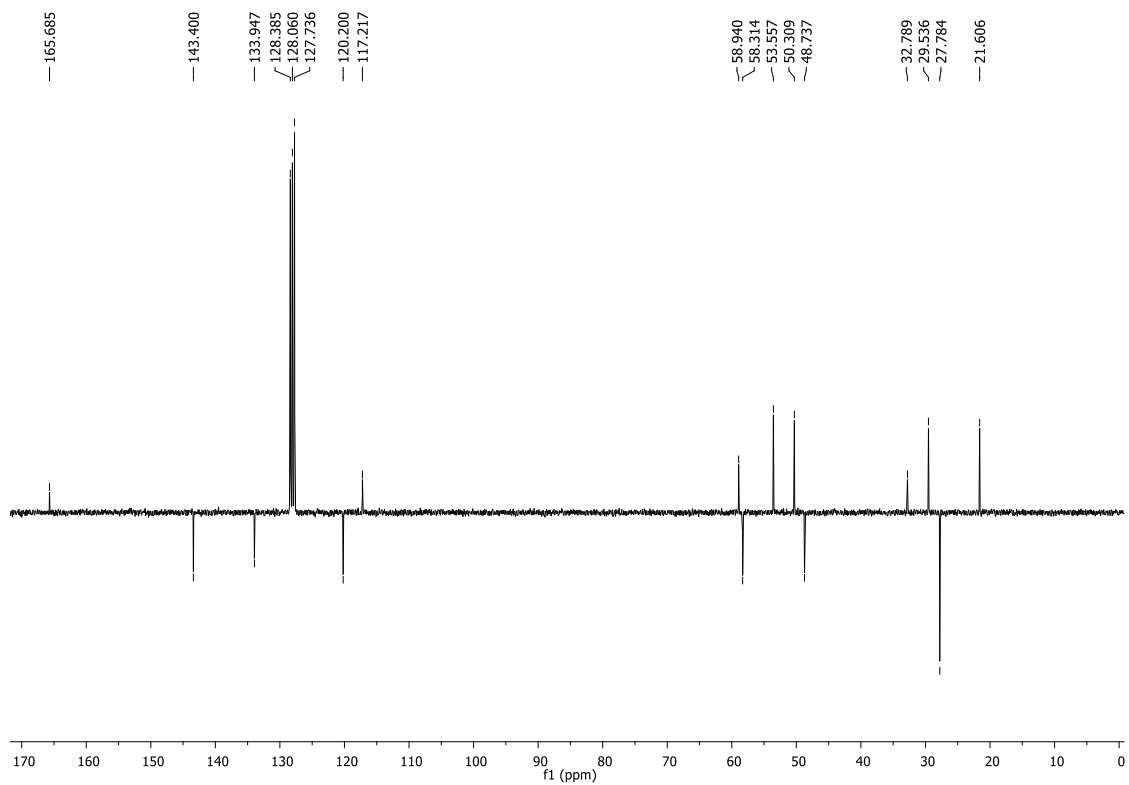


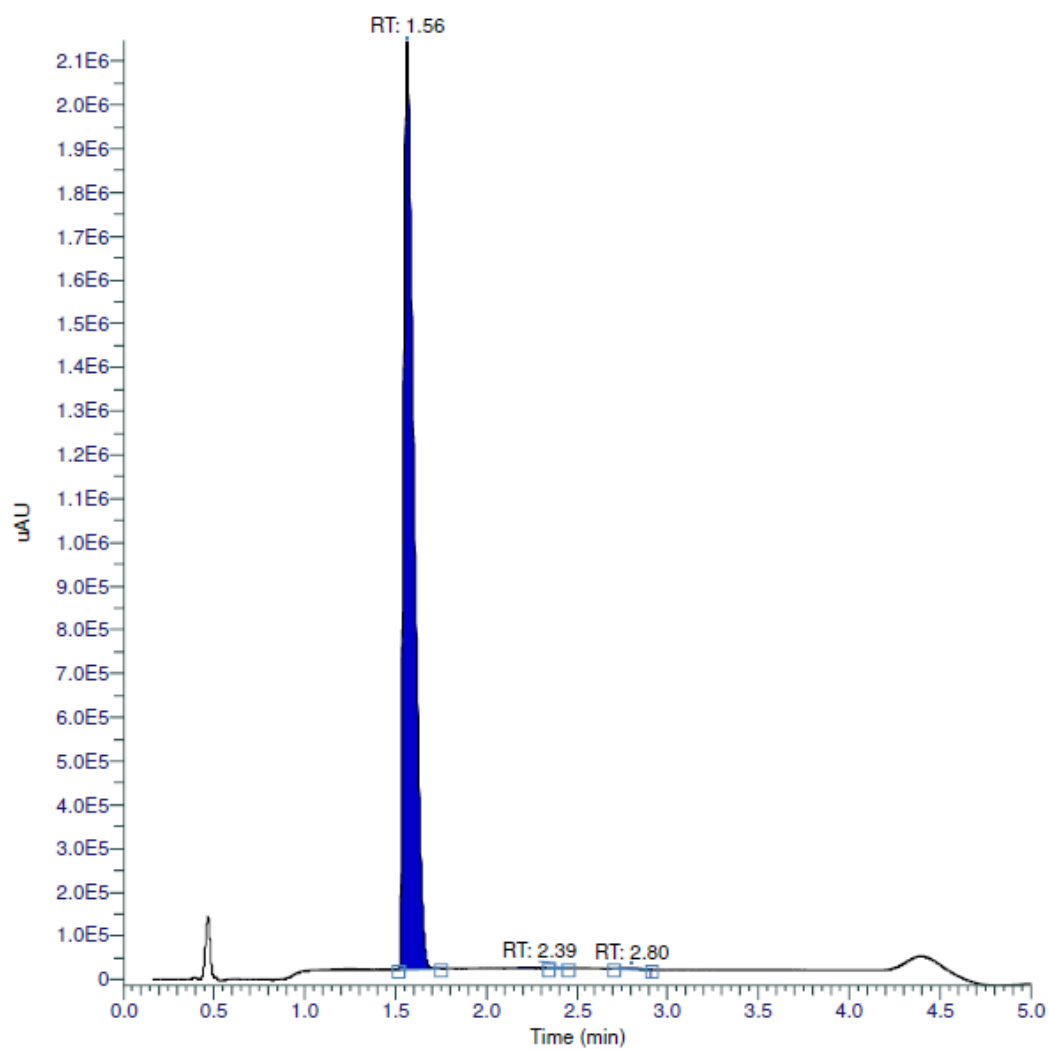
RT (Min)	% Area
2.24166666666667	99.06
3.24666666666667	0.55
3.79833333333333	0.38

**5-(piperazin-1-ylmethyl)pyridin-2(1H)-one (31).**

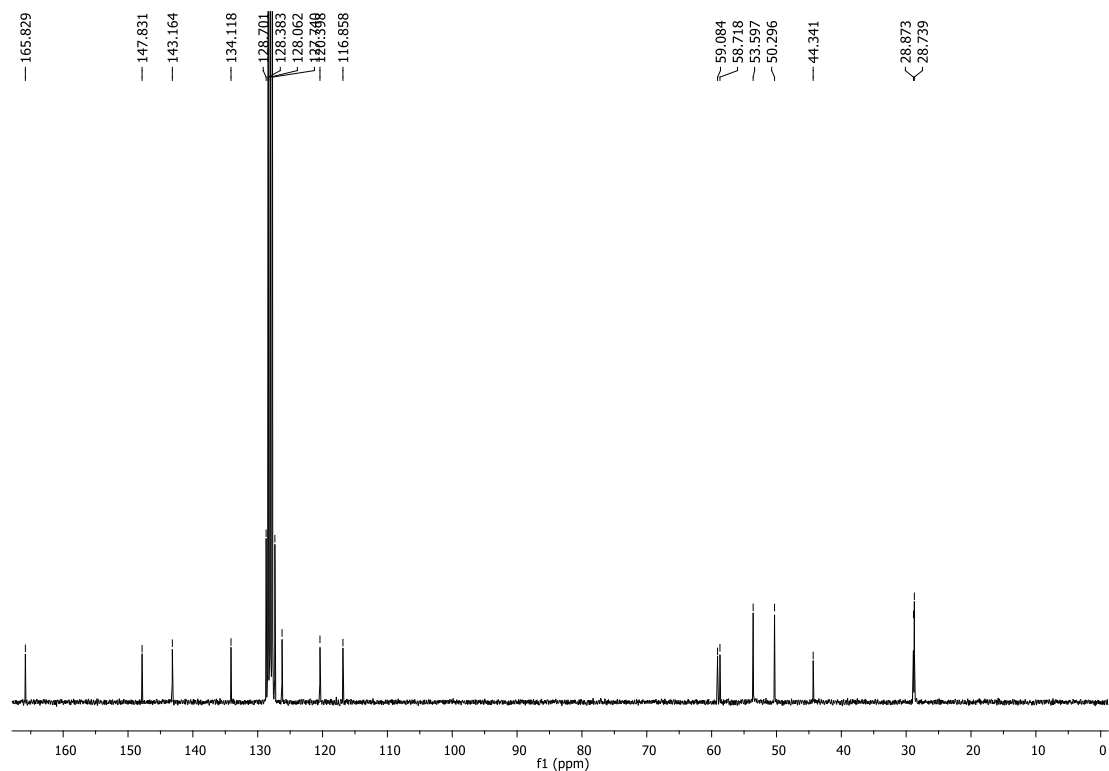
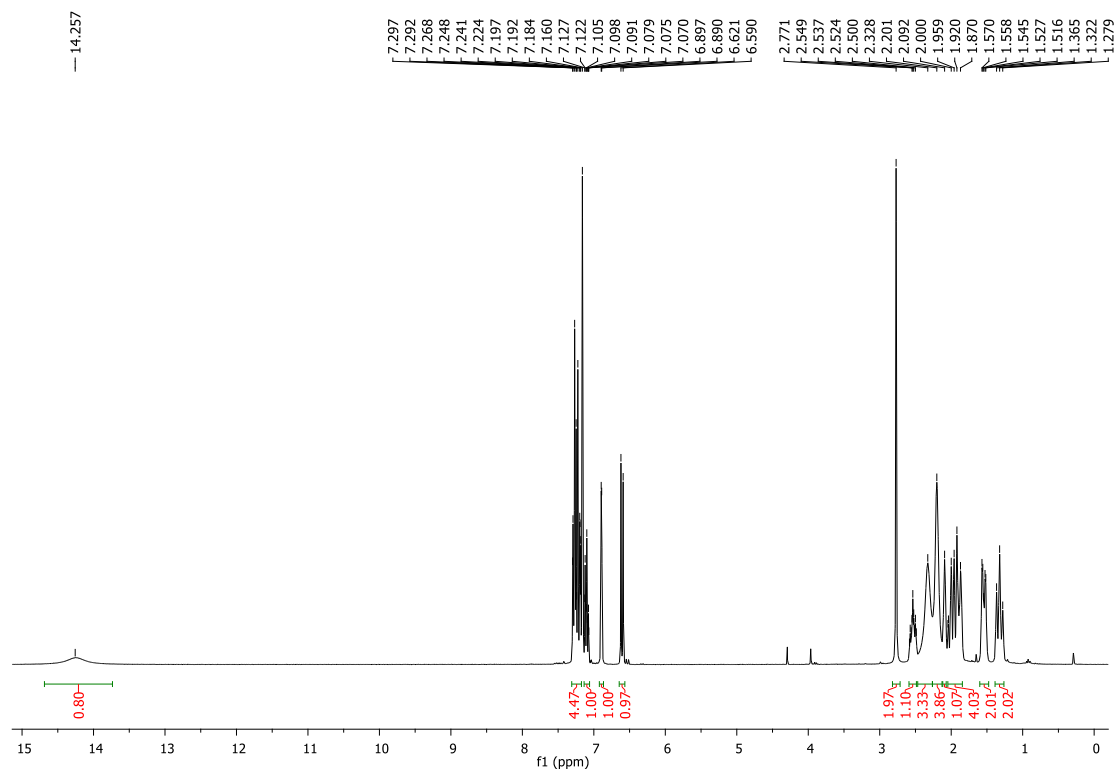
**5-((4-((1*S*,4*S*)-4-(tert-butyl)cyclohexyl)piperazin-1-yl)methyl)pyridin-2(1*H*)-one  
(32e).**

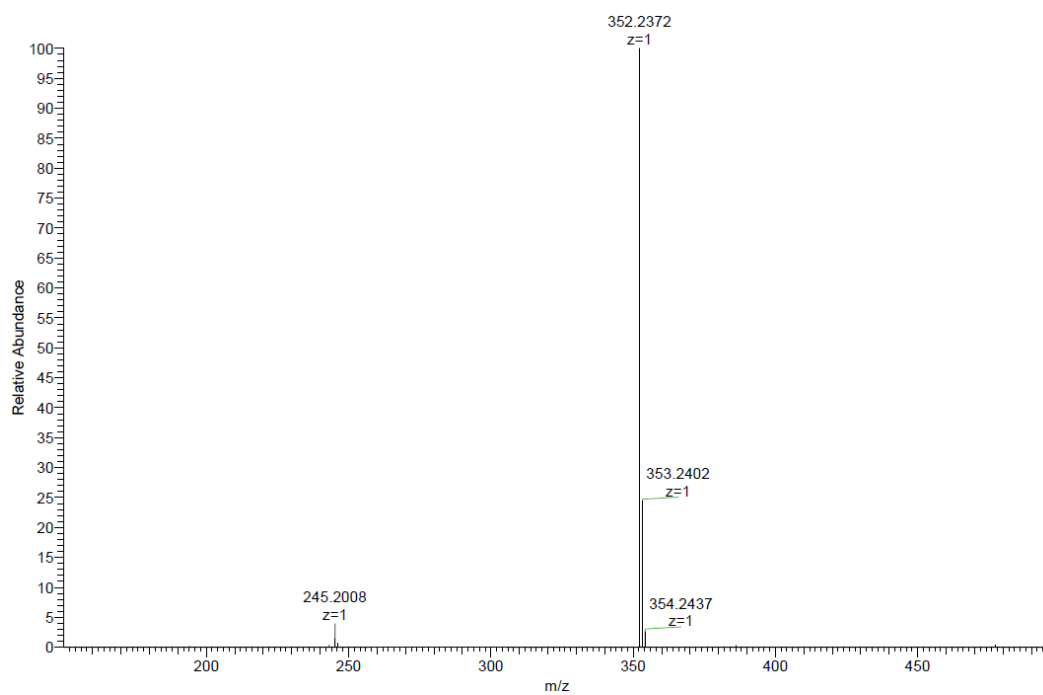
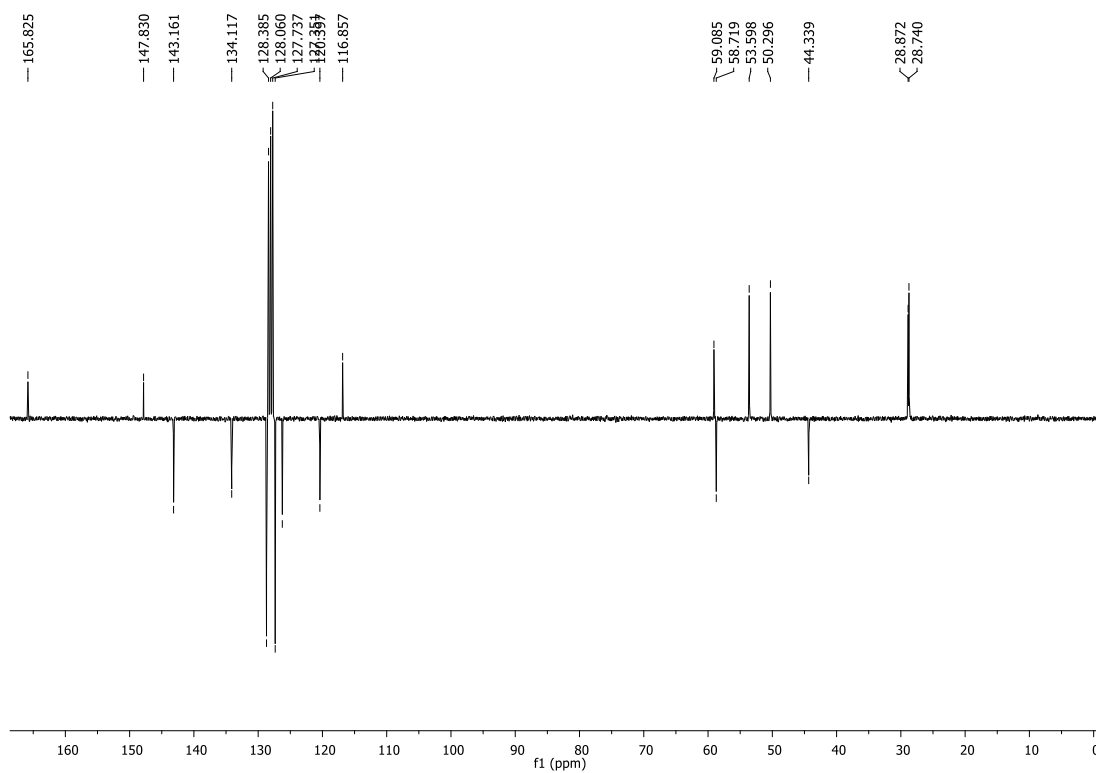


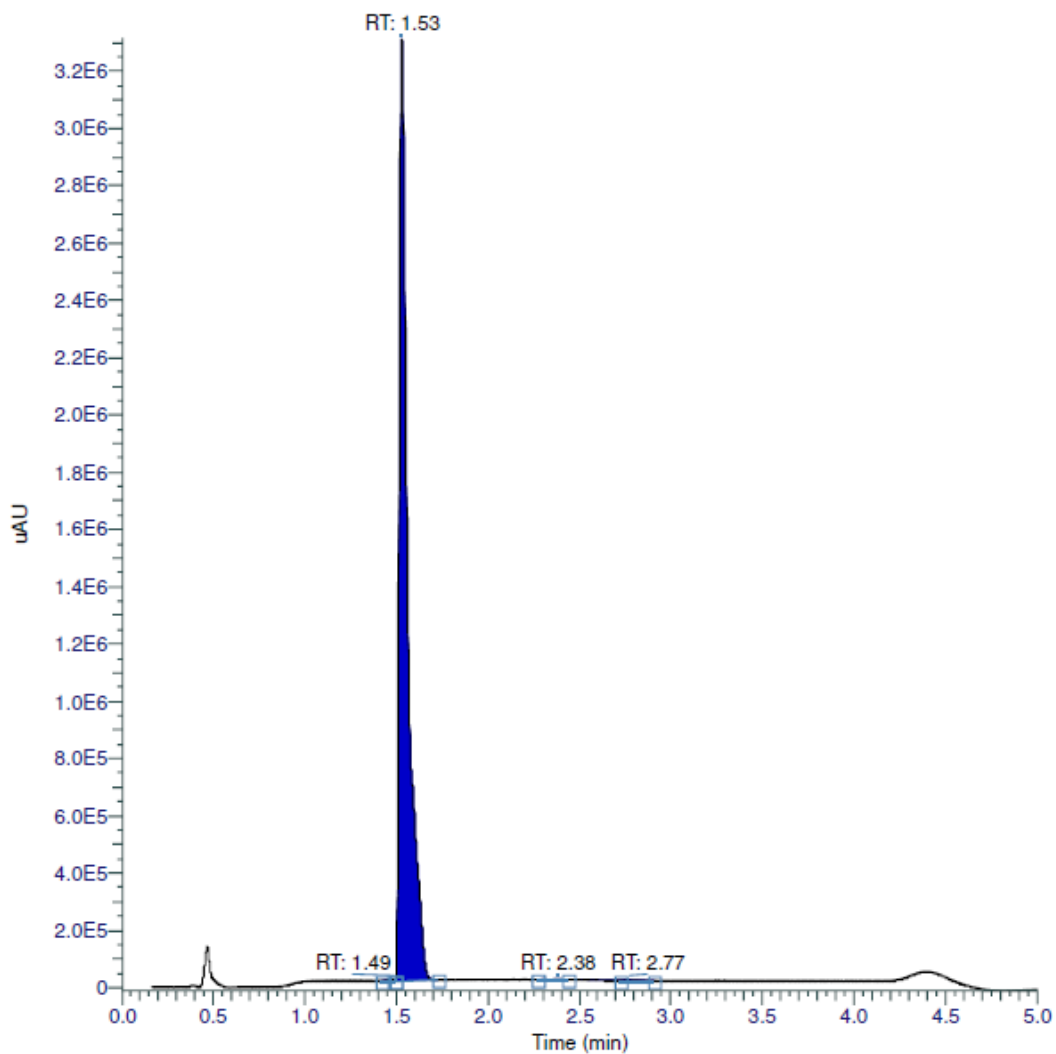




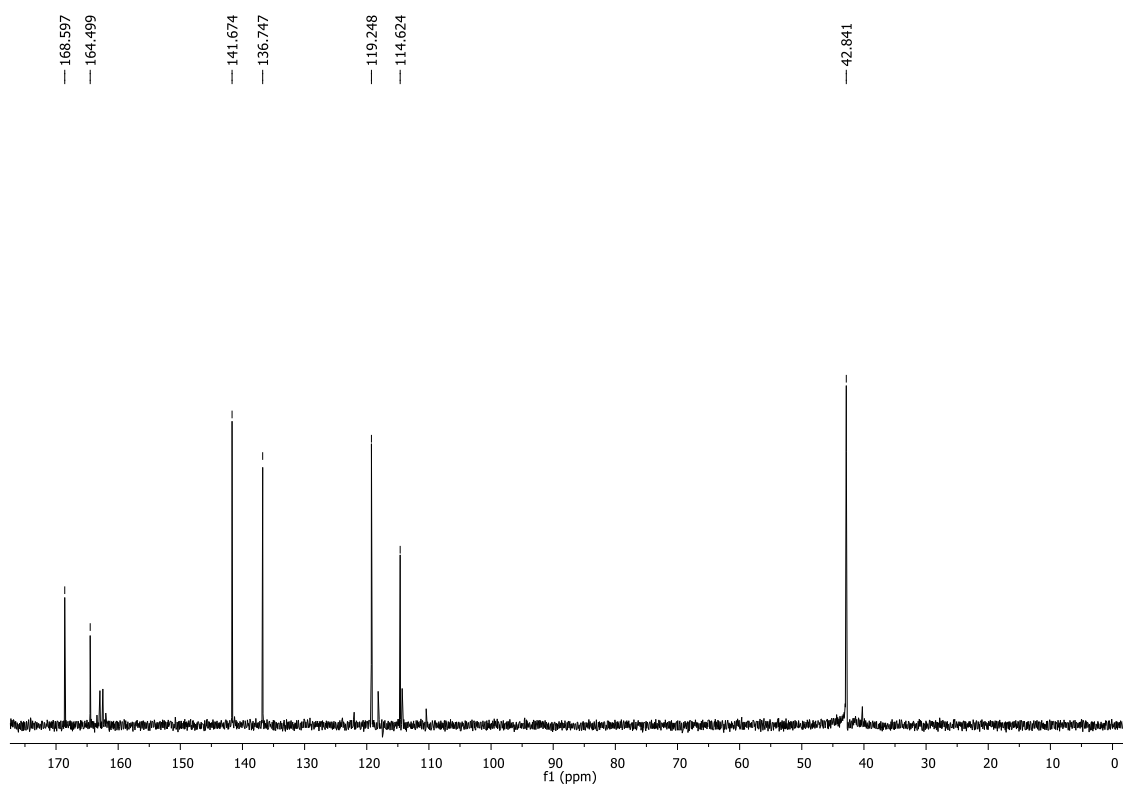
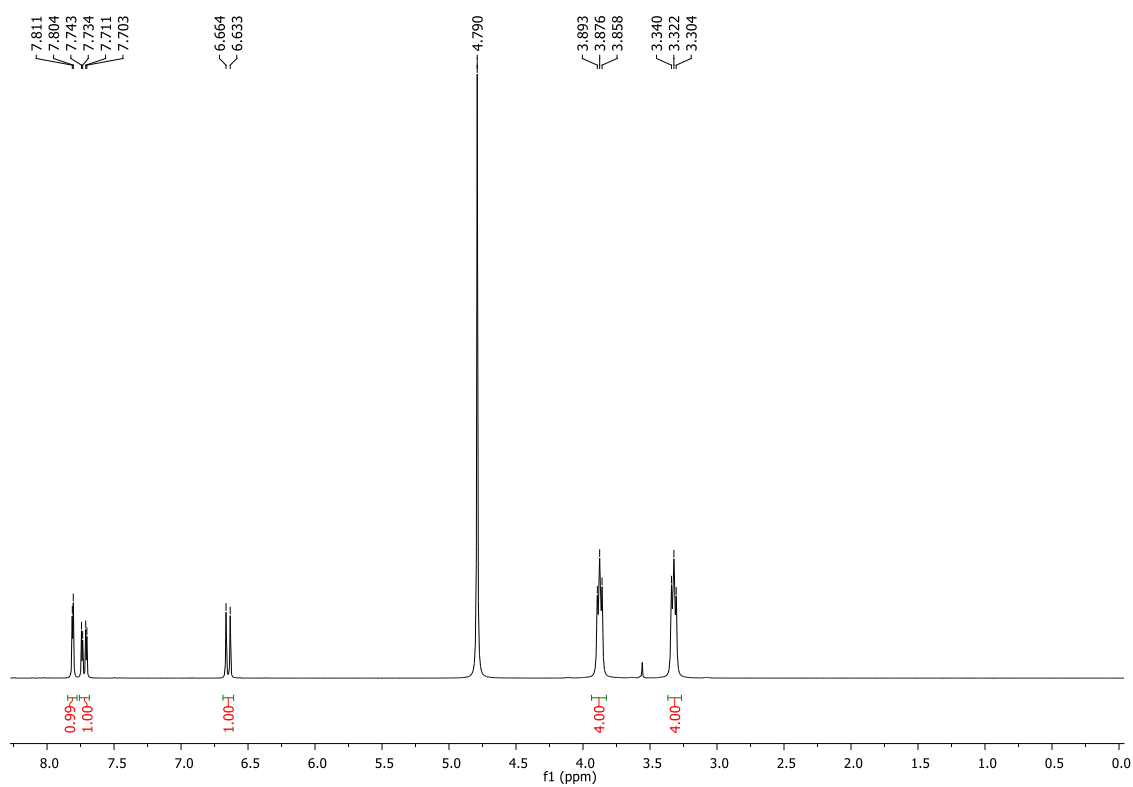
RT (Min)	% Area
1.56333333333333	99.87
2.39	0.04
2.79666666666667	0.09

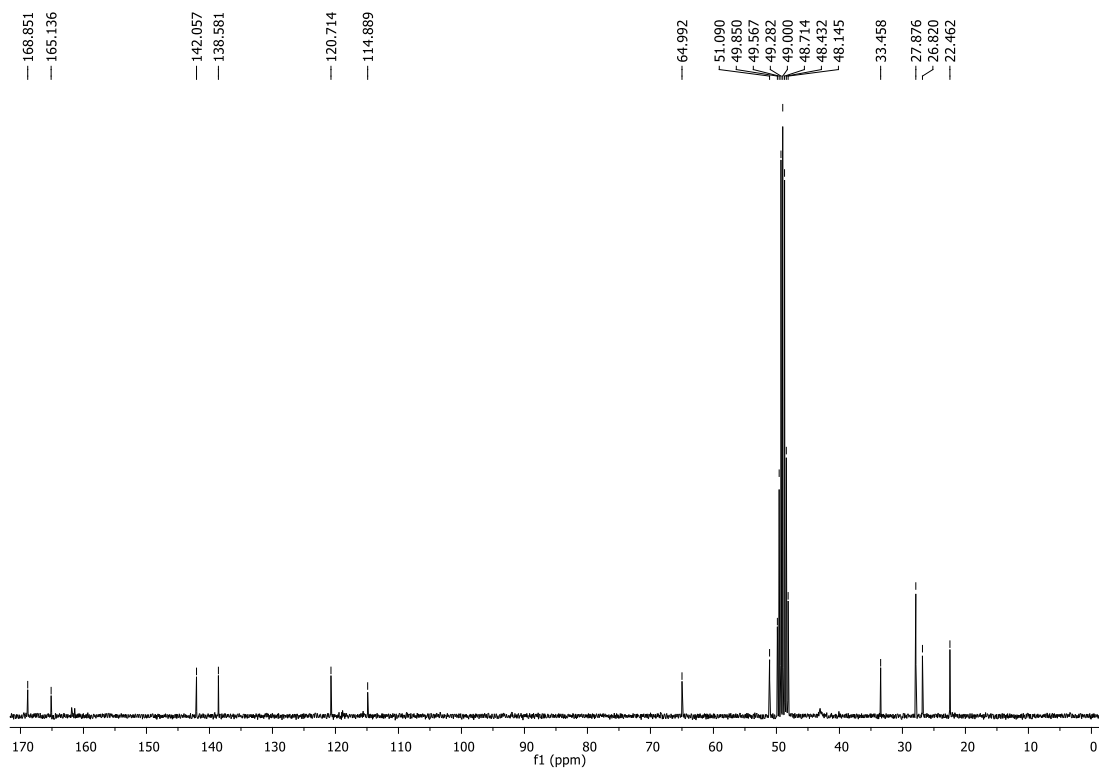
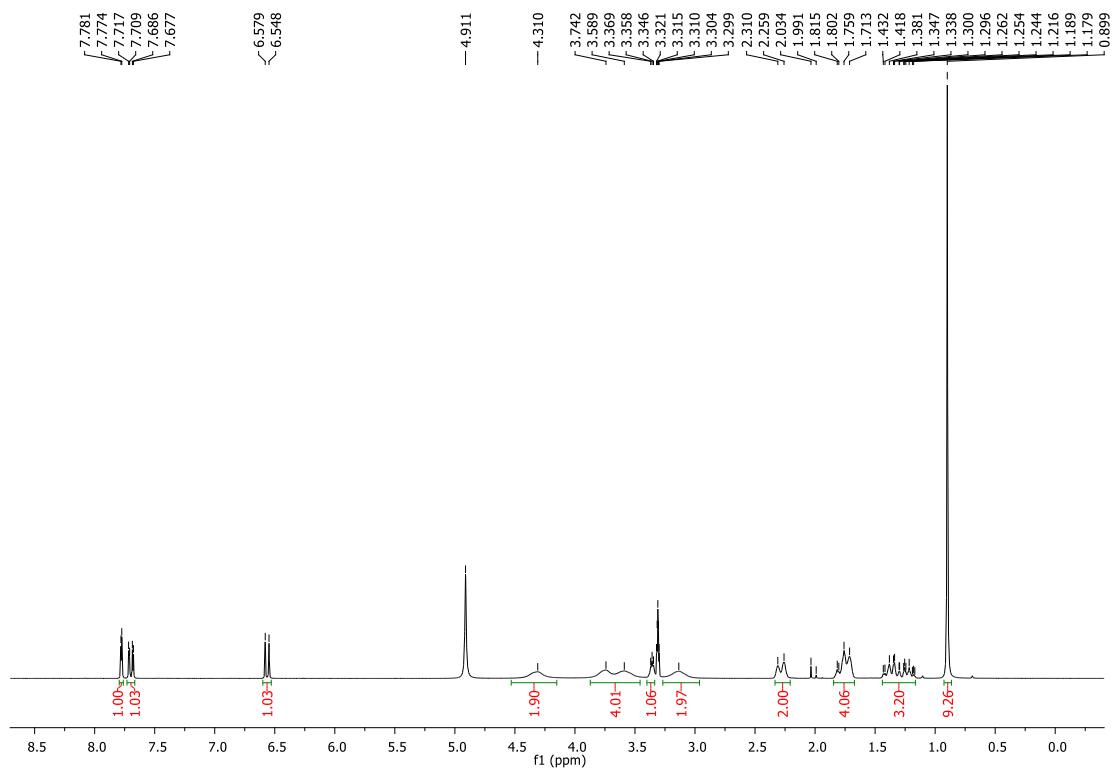
5-((4-((1*S*,4*S*)-4-phenylcyclohexyl)piperazin-1-yl)methyl)pyridin-2(1*H*)-one (32f).

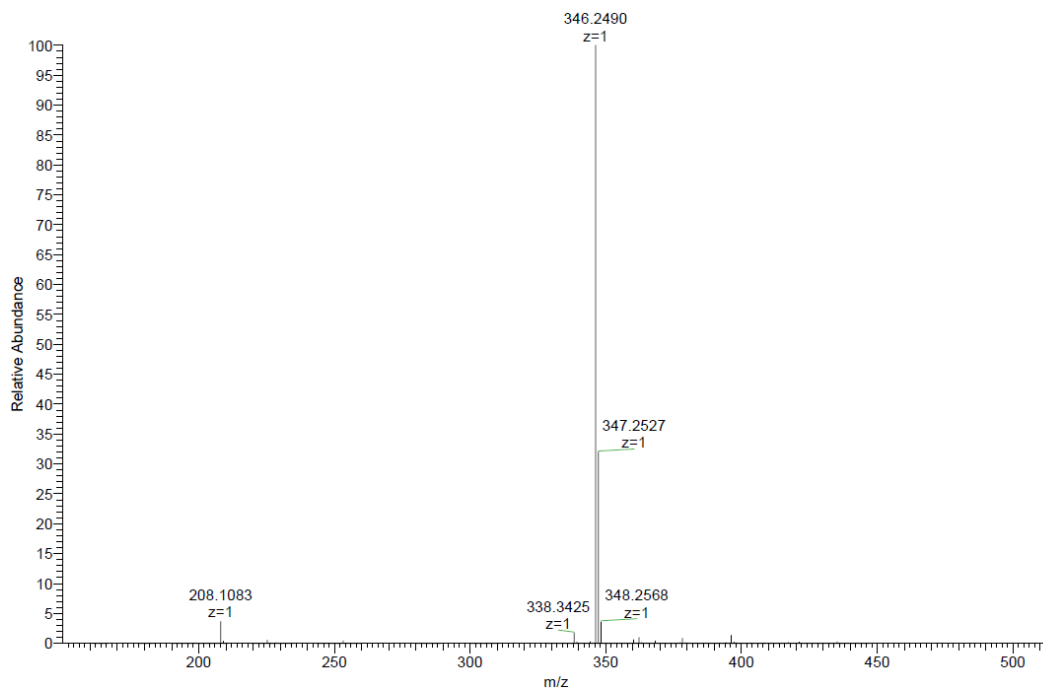
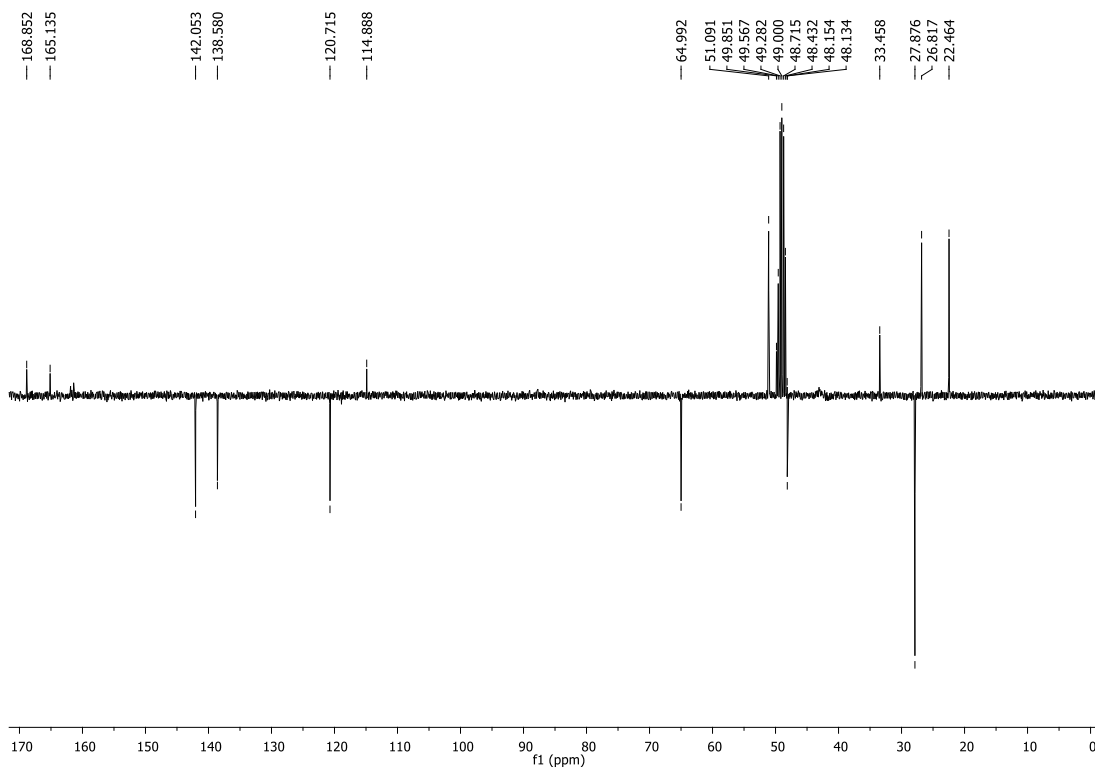


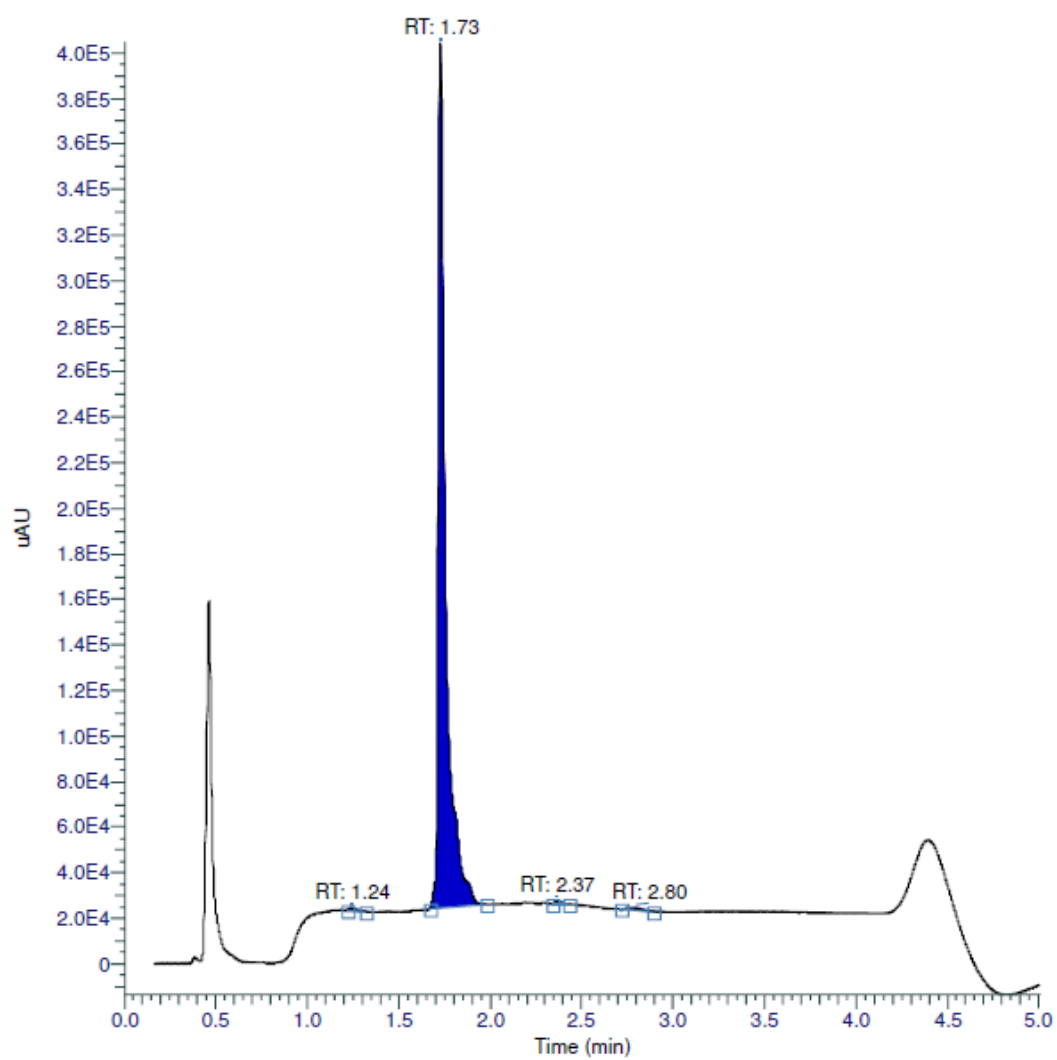


RT (Min)	% Area
1.49333333333333	0.08
1.53	99.84
2.37666666666667	0.05
2.77333333333333	0.04

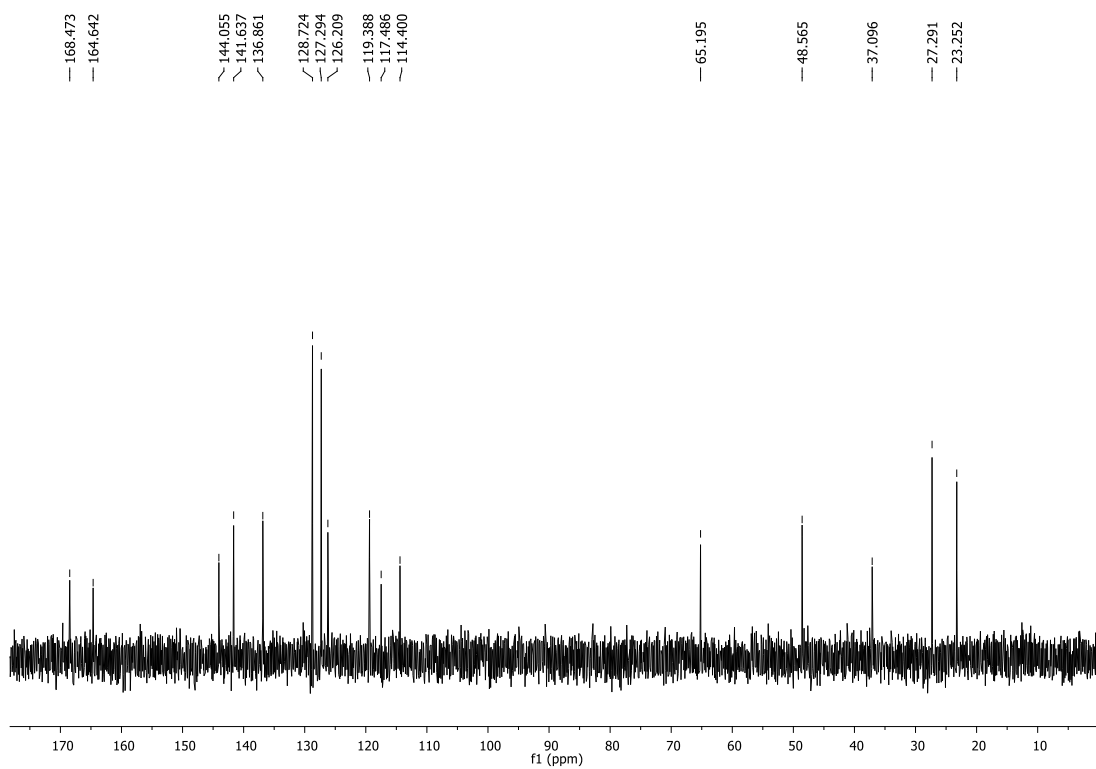
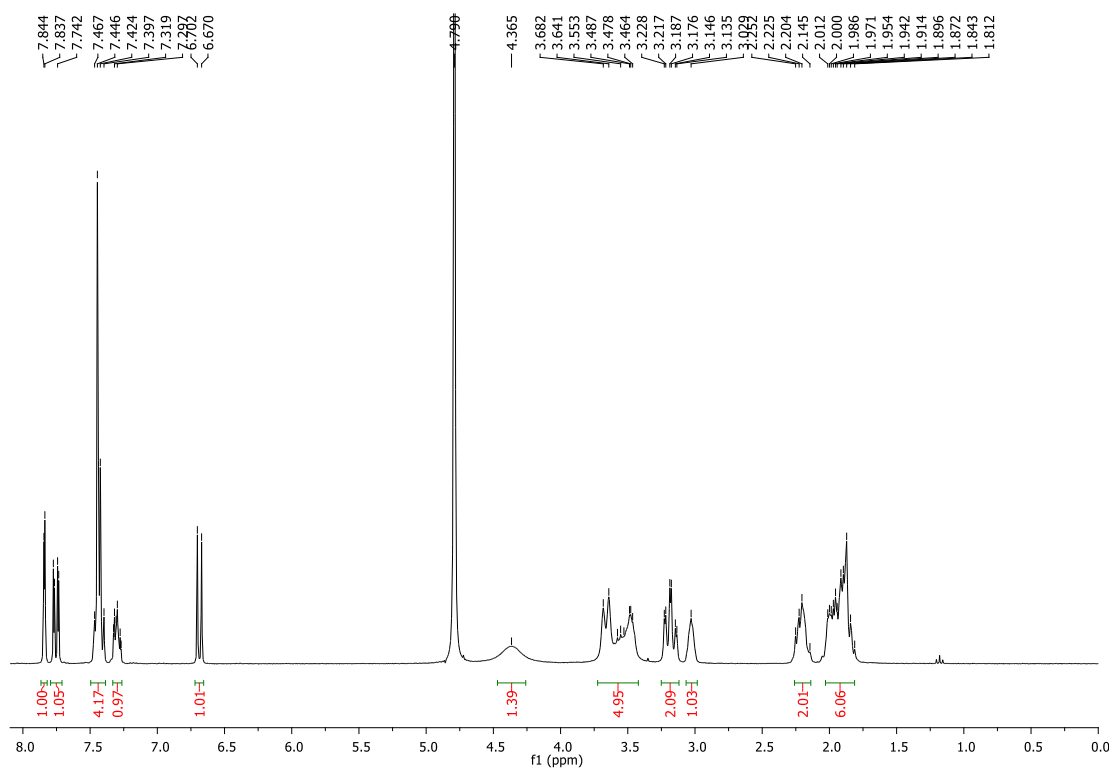
**5-(piperazine-1-carbonyl)pyridin-2(1H)-one (35).**

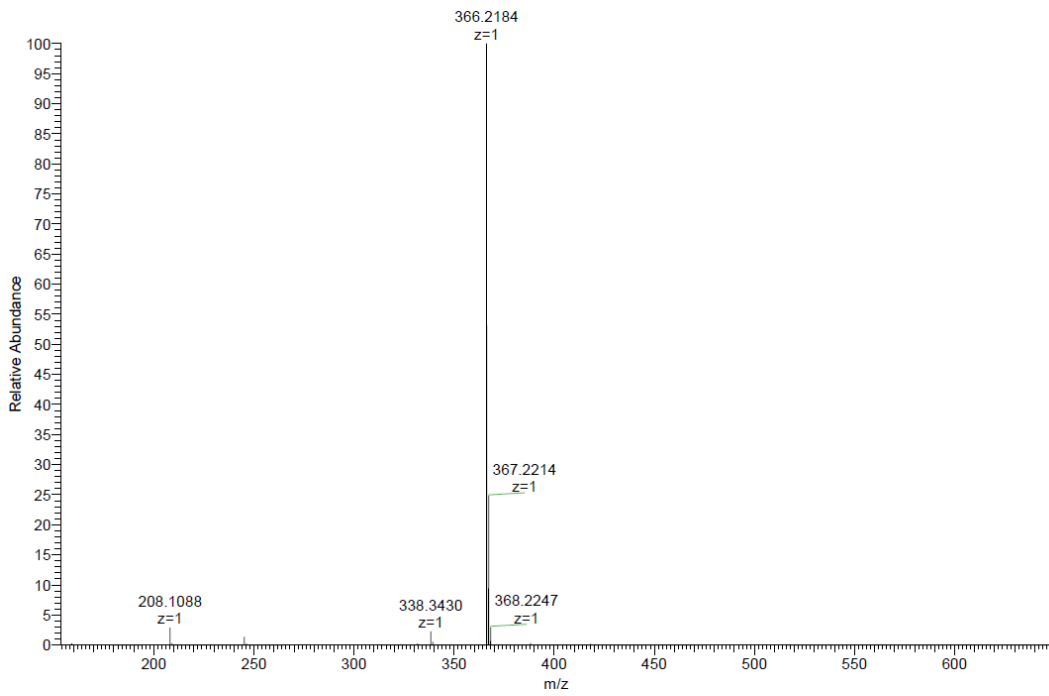
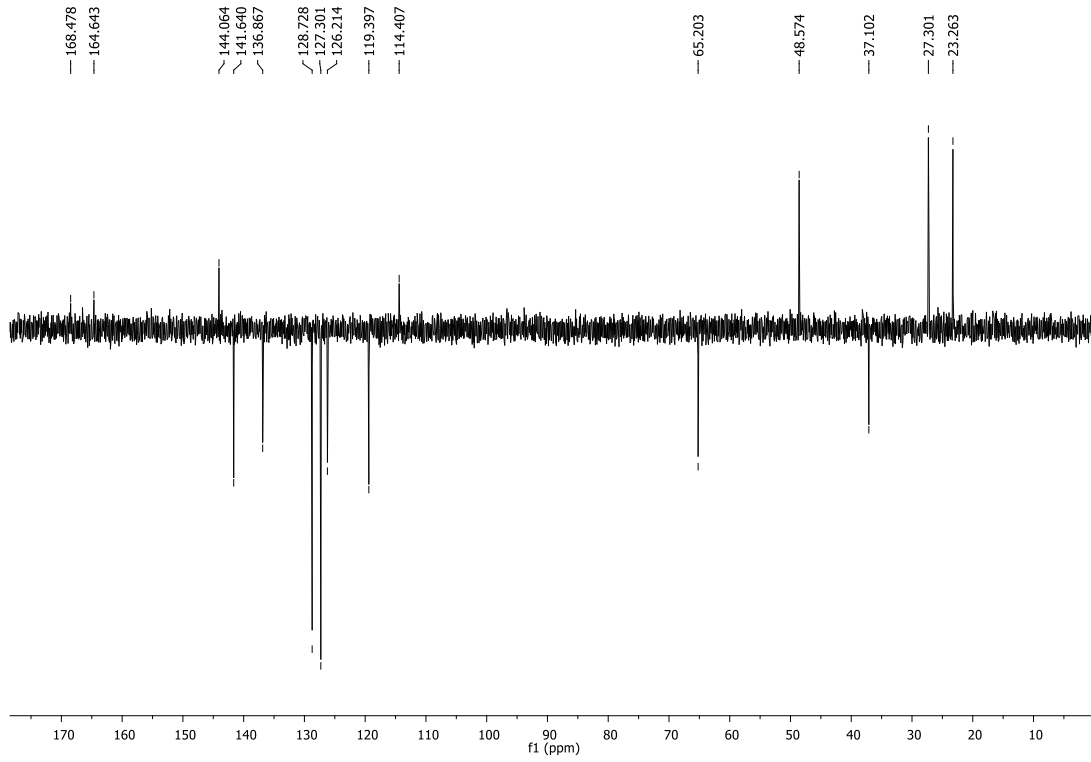
**5-(4-((1*S*,4*S*)-4-(*tert*-butyl)cyclohexyl)piperazine-1-carbonyl)pyridin-2(1*H*)-one (36e).**

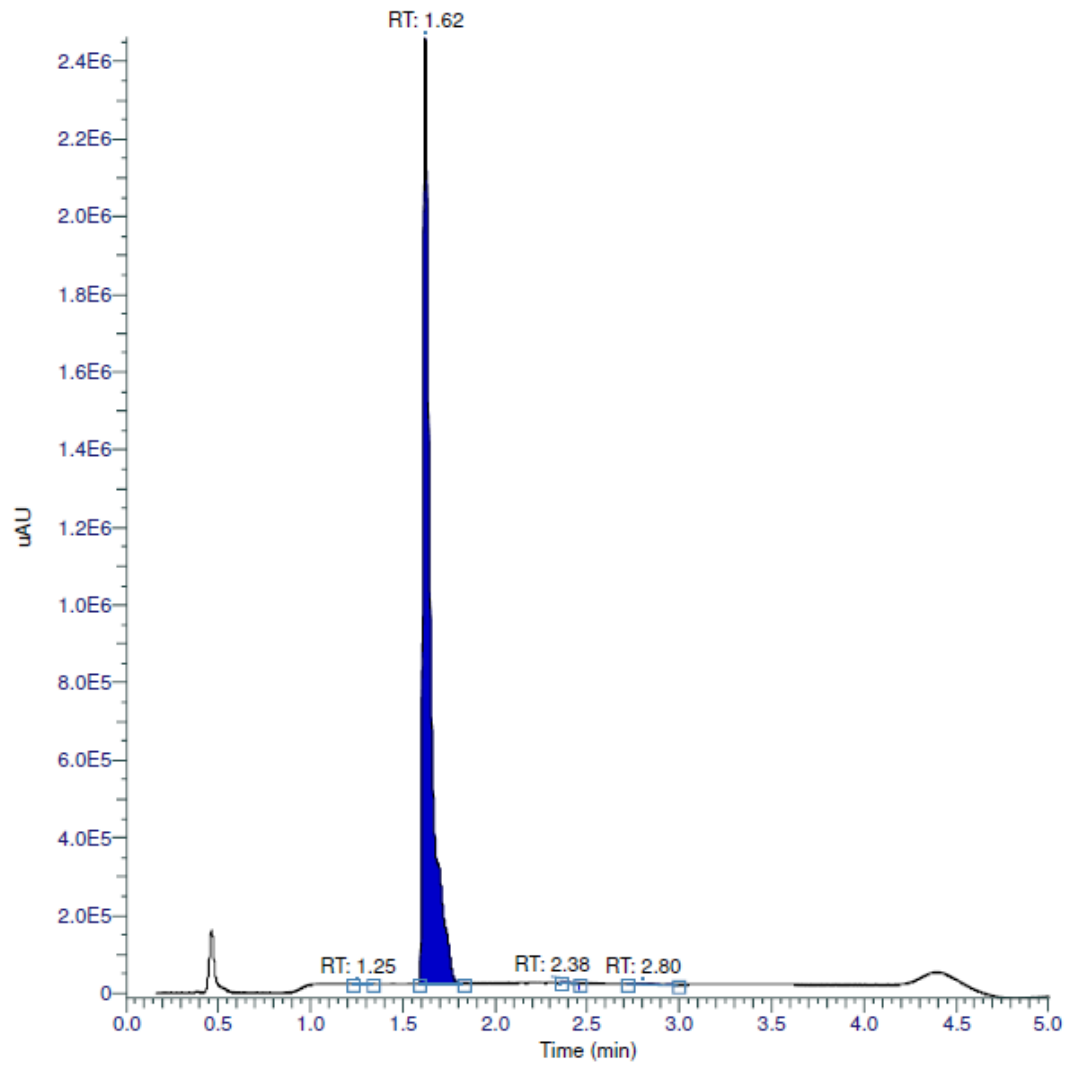




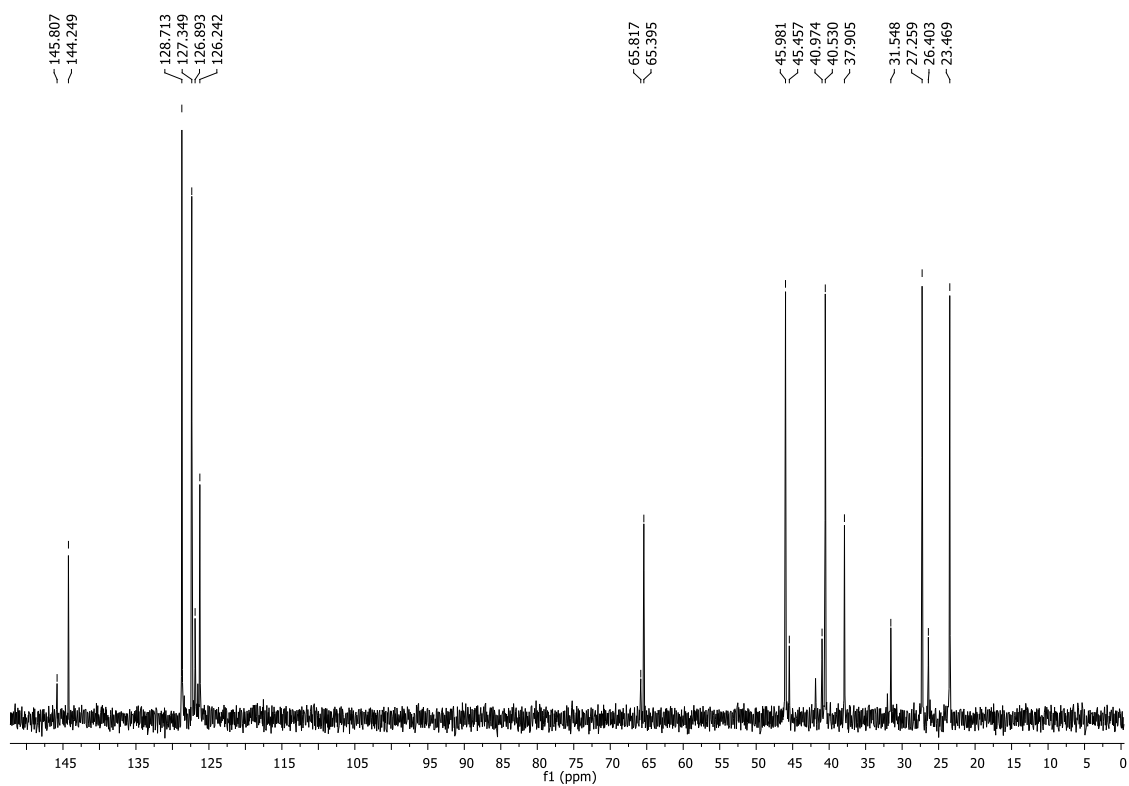
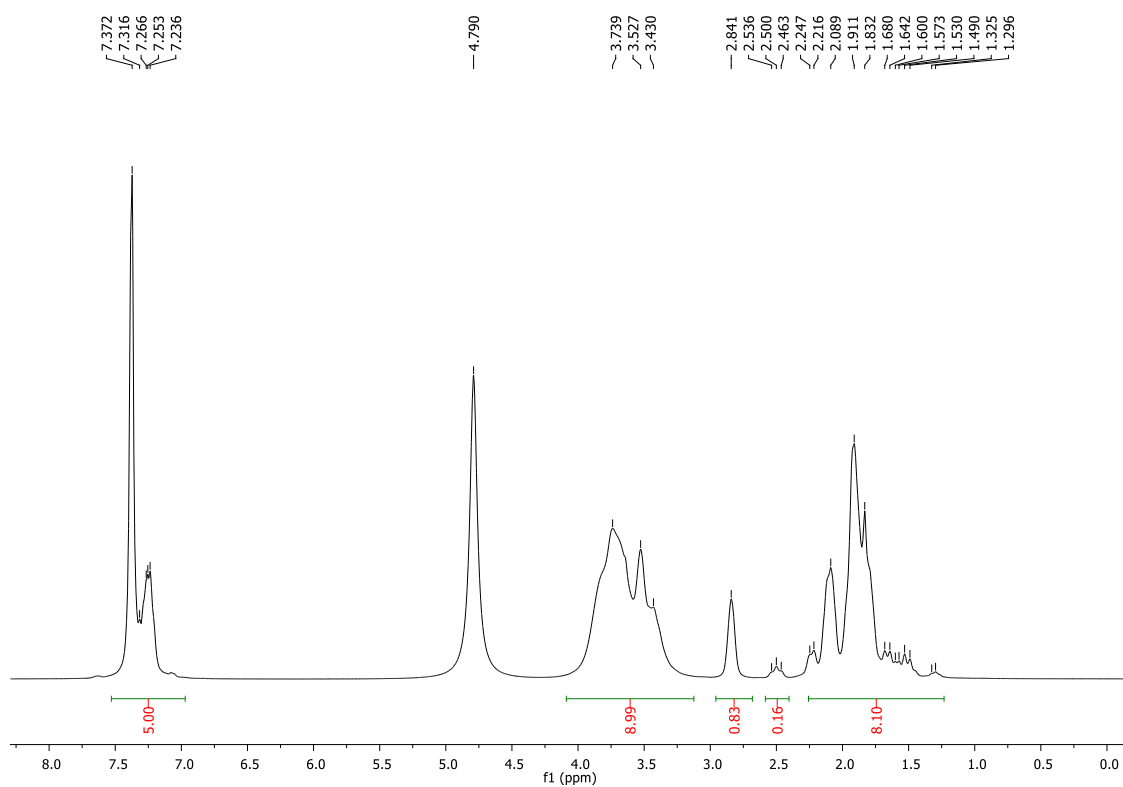
RT (Min)	% Area
1.24	0.3
1.72666666666667	99.02
2.36666666666667	0.23
2.795	0.44

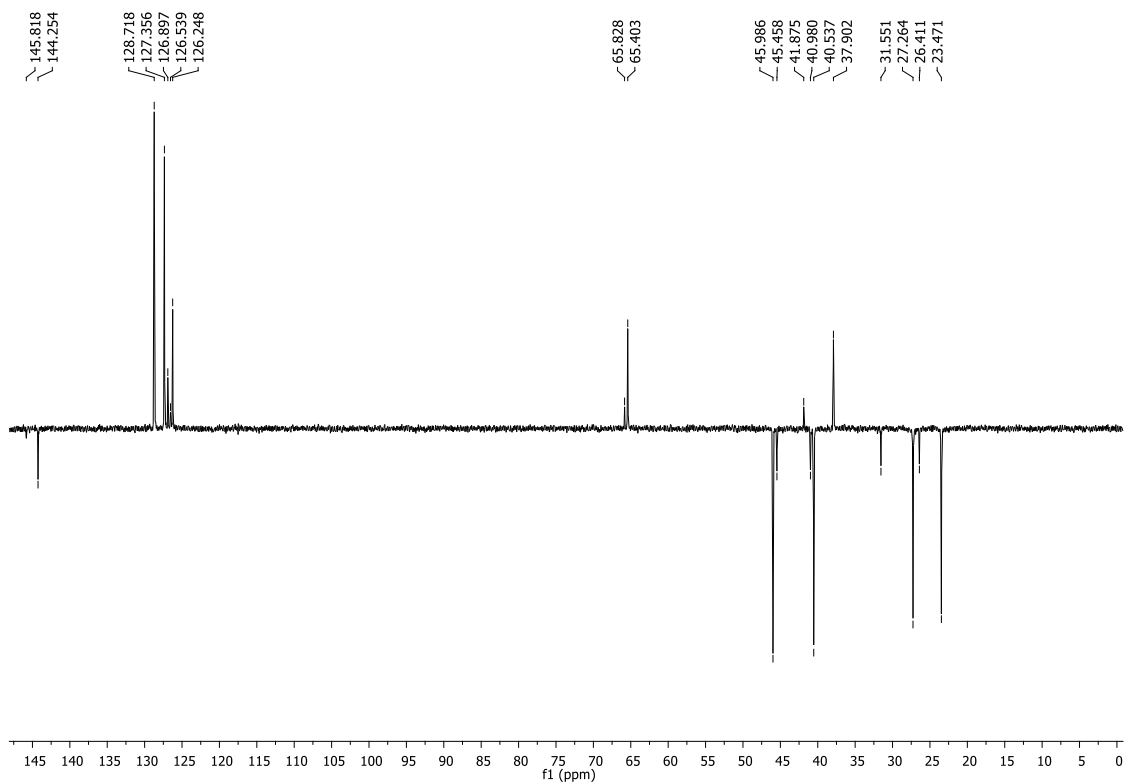
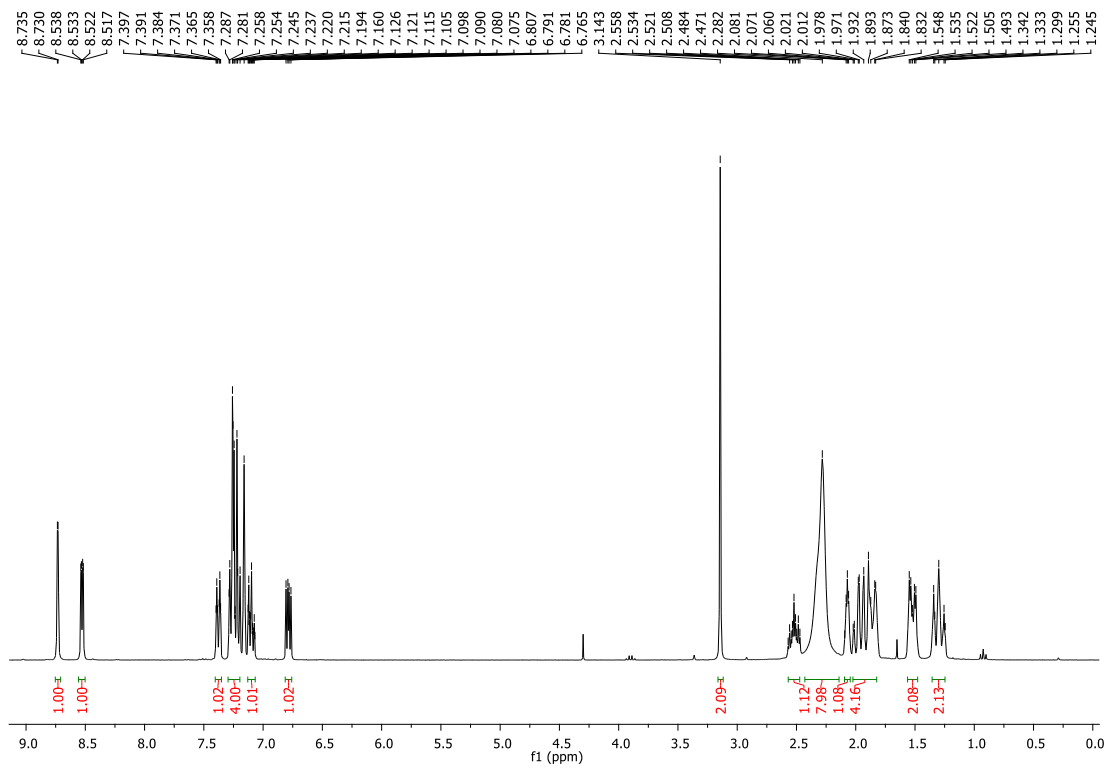
**5-((1*S*,4*S*)-4-phenylcyclohexyl)piperazine-1-carbonylpyridin-2(1*H*)-one (36f).**

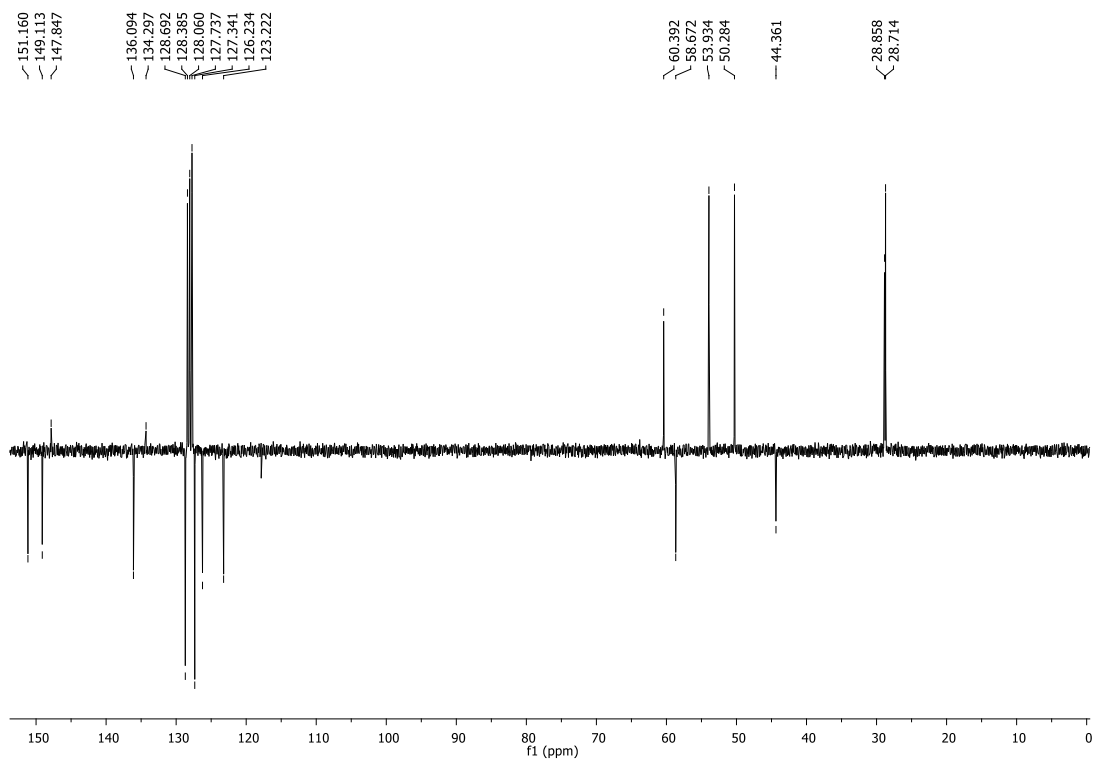
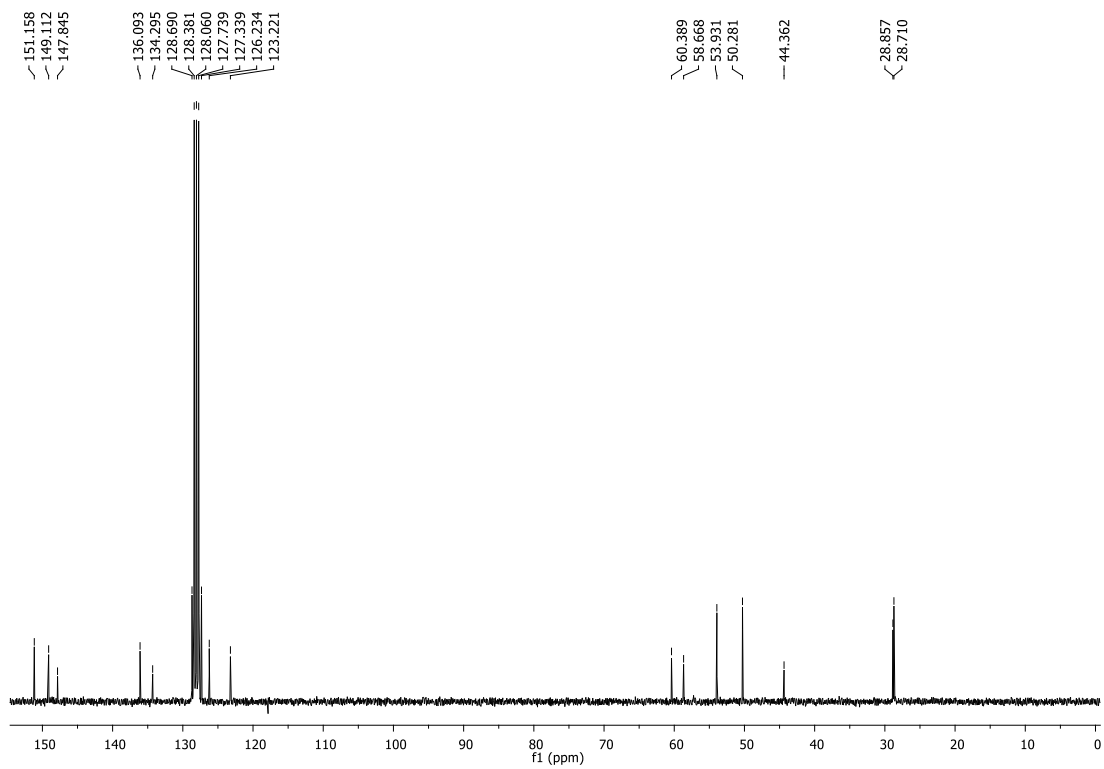


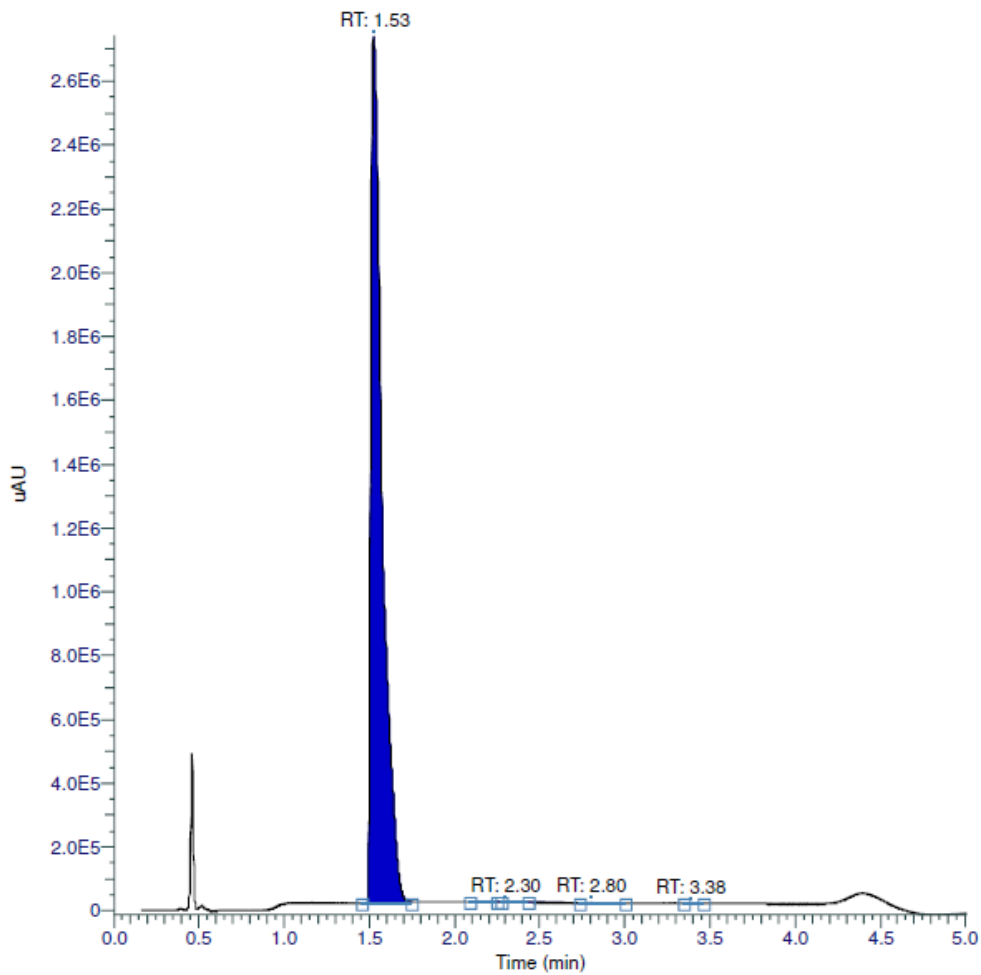
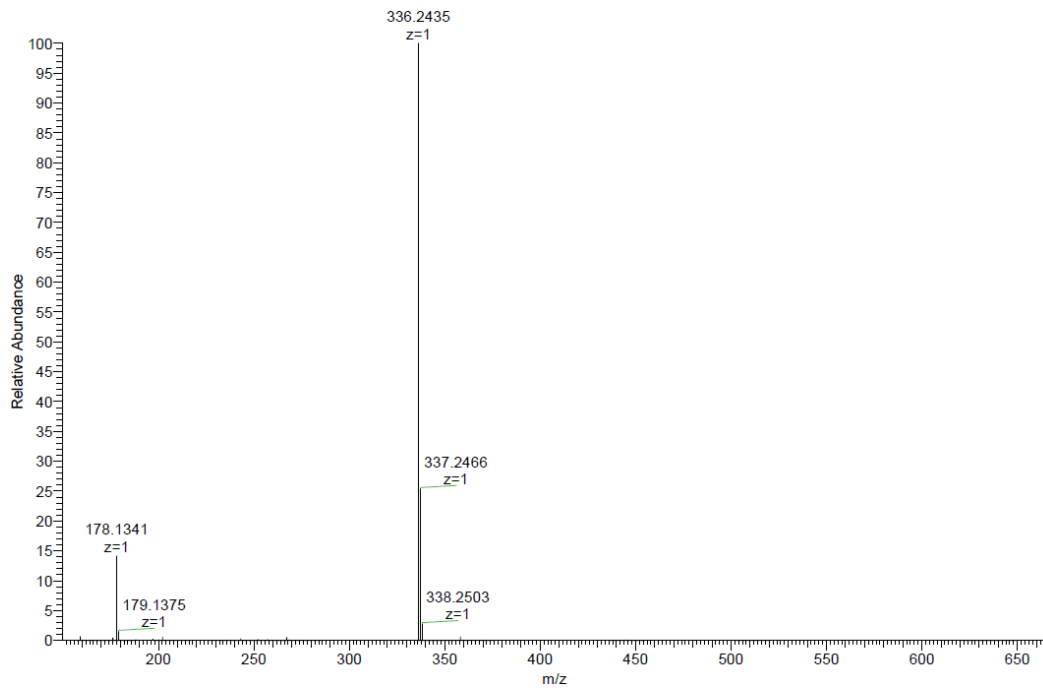


RT (Min)	% Area
1.25	0.04
1.62166666666667	99.85
2.375	0.03
2.8	0.08

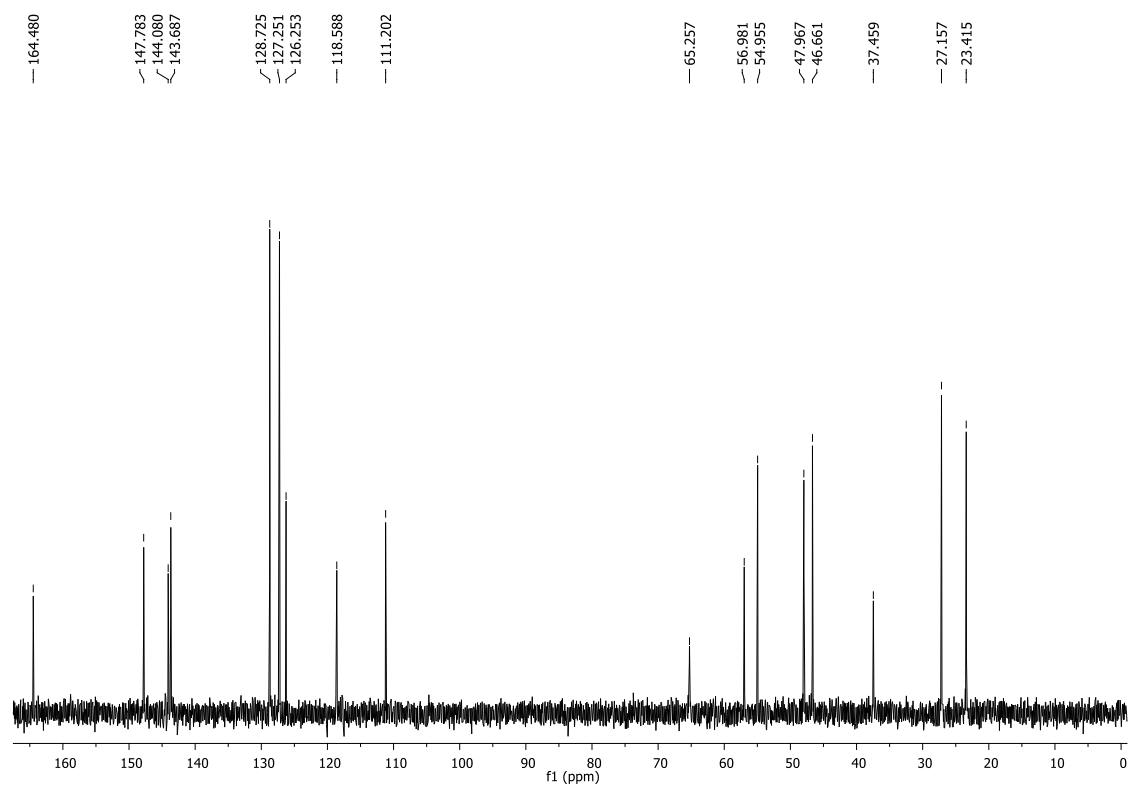
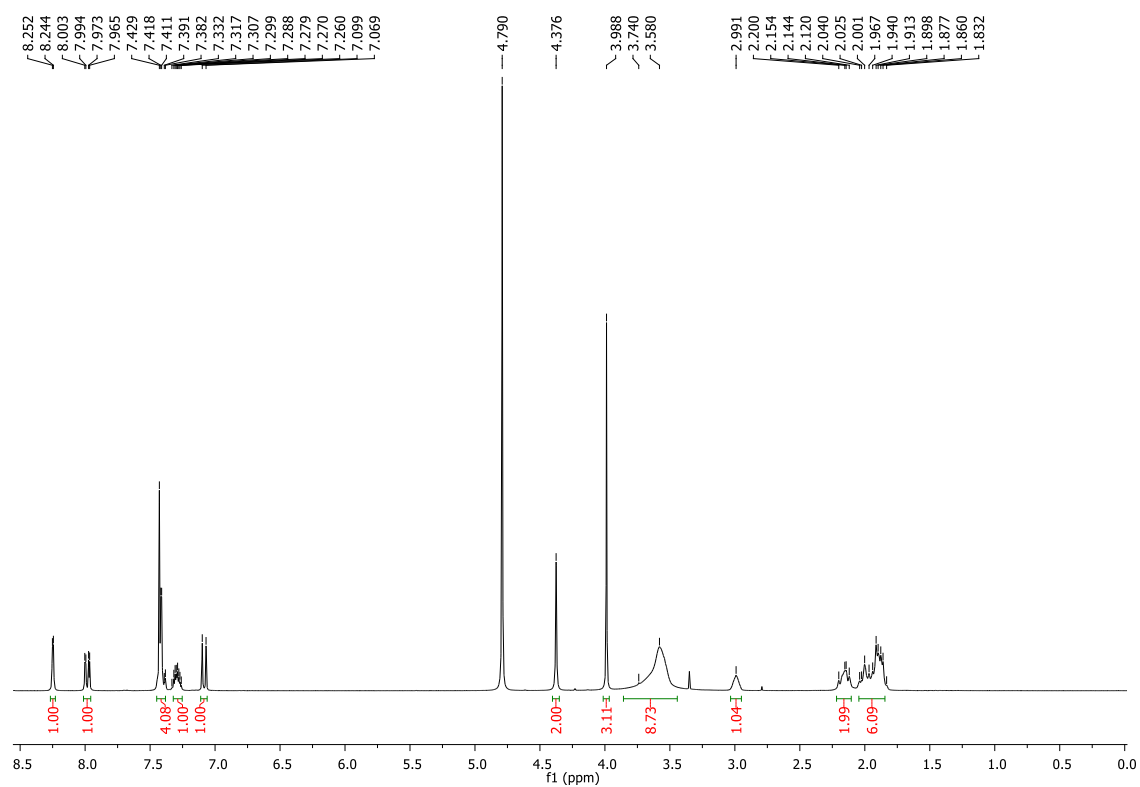
**1-(4-phenylcyclohexyl)piperazine (38f).**

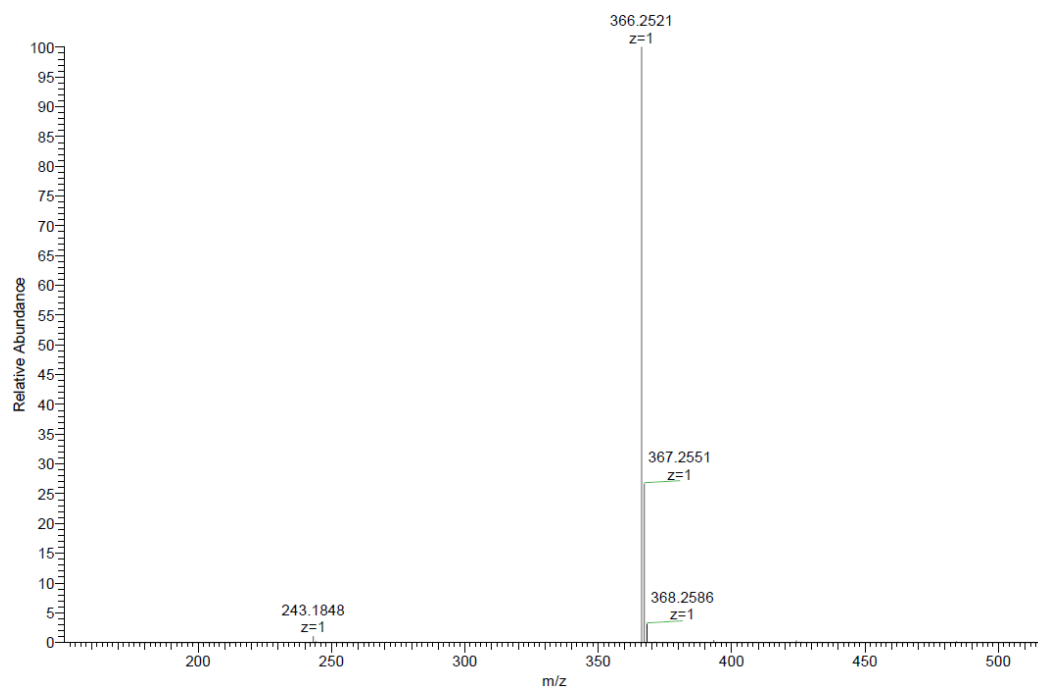
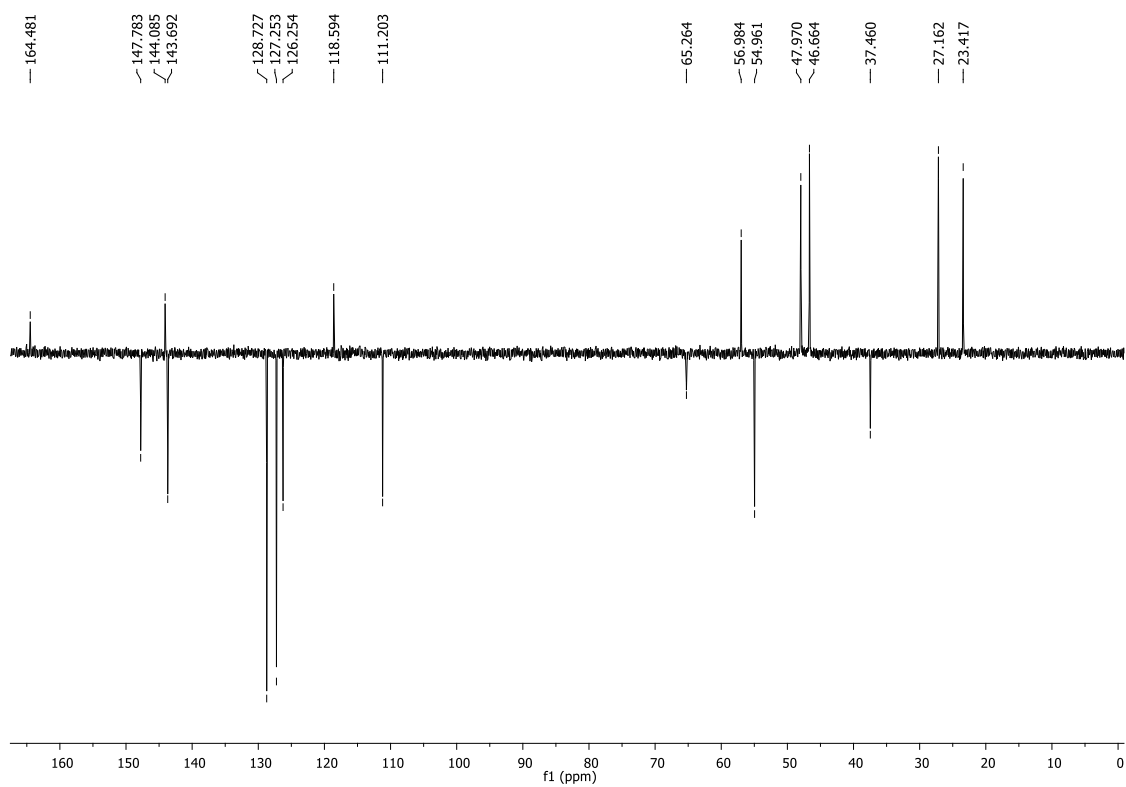
**1-((1*S*,4*S*)-4-phenylcyclohexyl)-4-(pyridin-3-ylmethyl)piperazine (42f).**

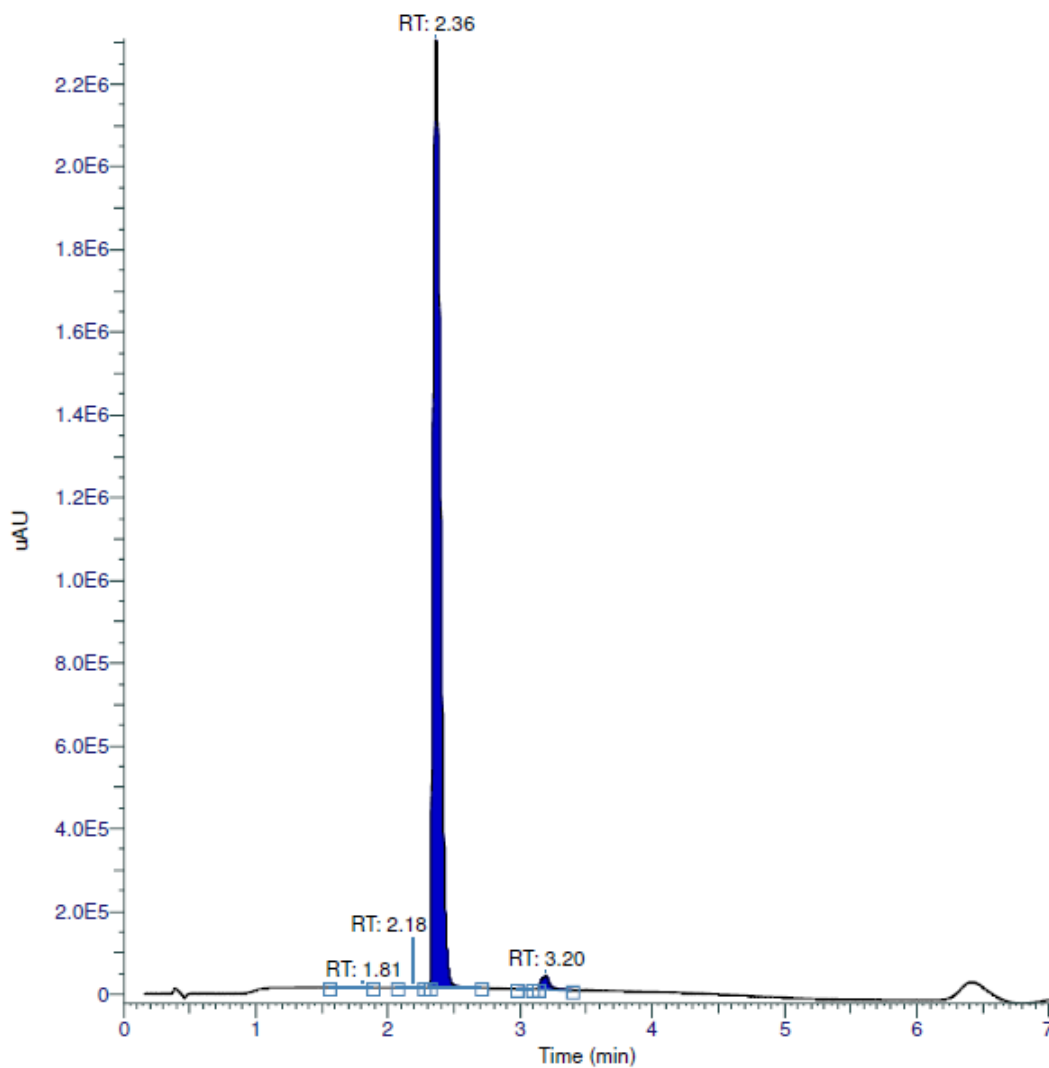




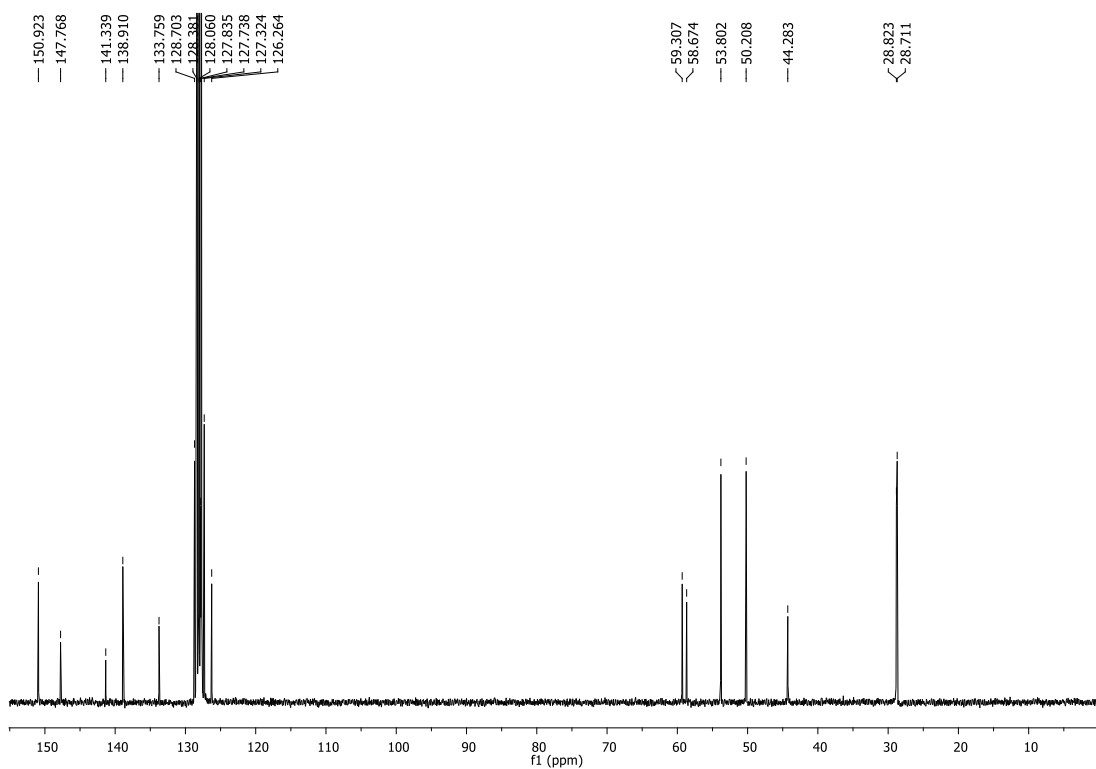
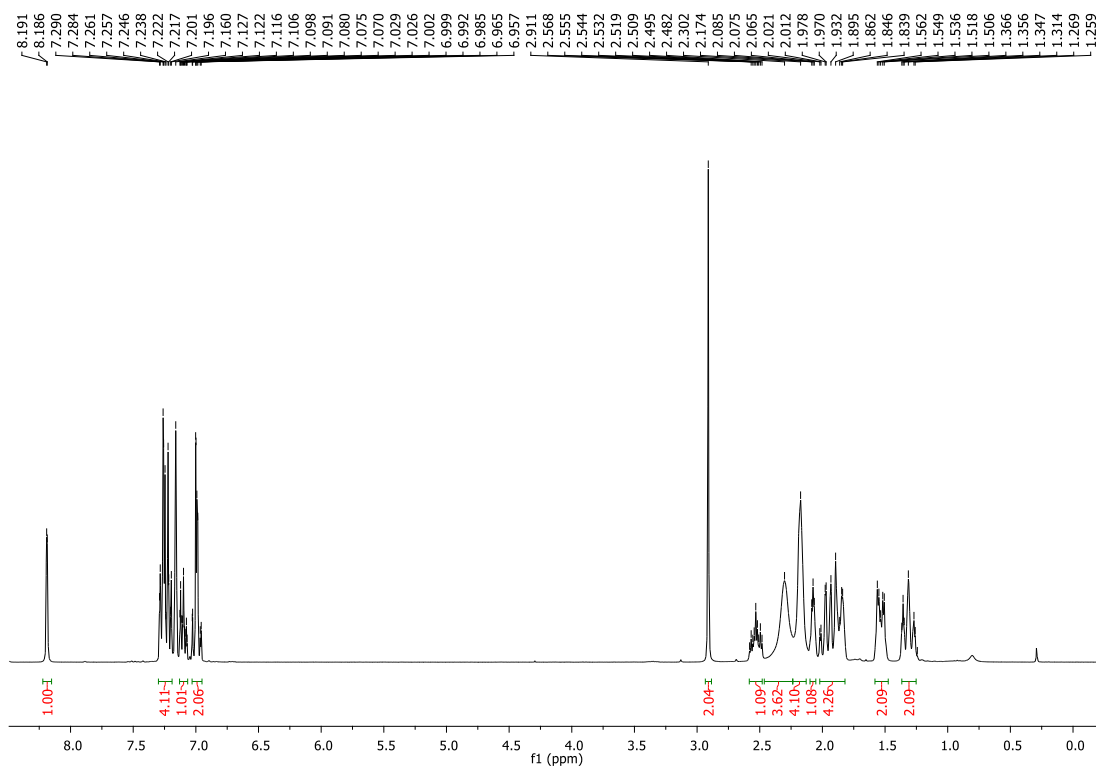
RT (Min)	% Area
1.525	99.85
2.19666666666667	0.02
2.3	0.07
2.80166666666667	0.04
3.38333333333333	0.02

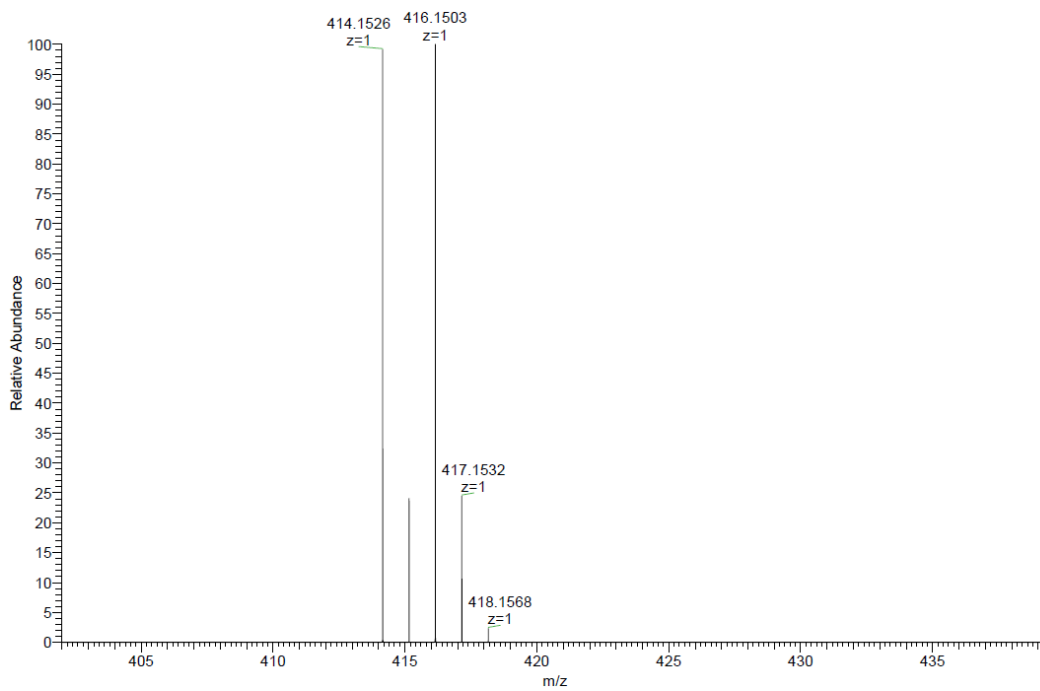
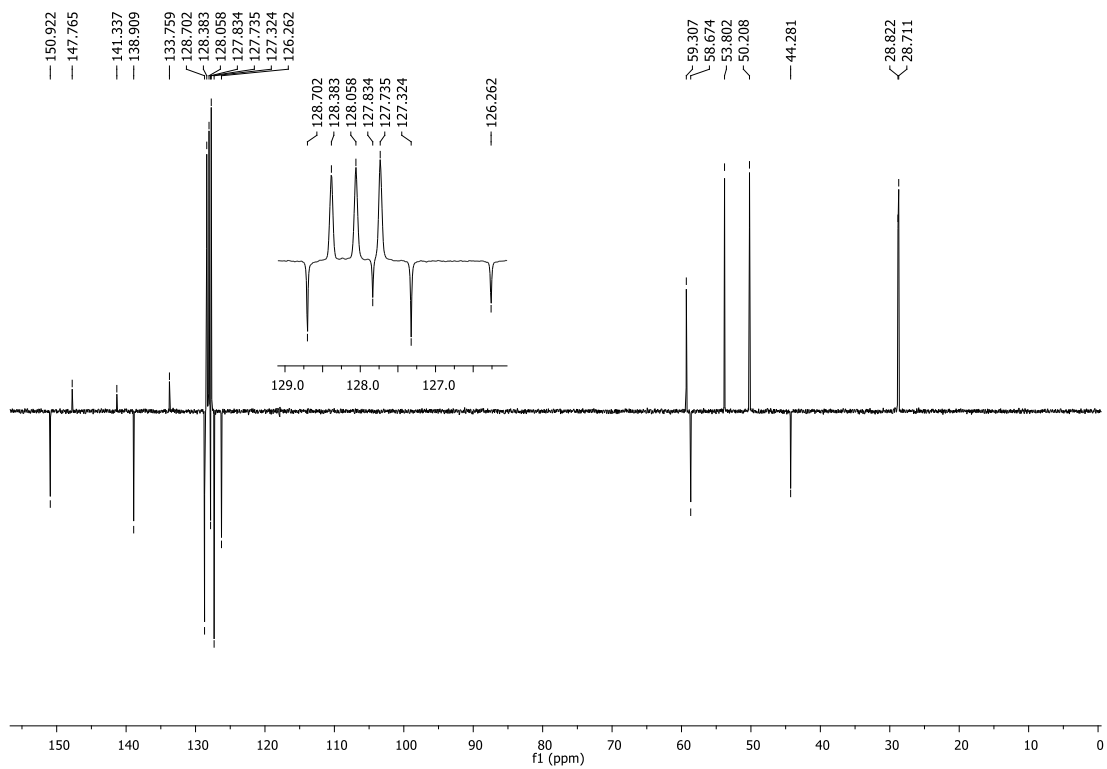
**1-((6-methoxypyridin-3-yl)methyl)-4-((1*S*,4*S*)-4-phenylcyclohexyl)piperazine (43f).**

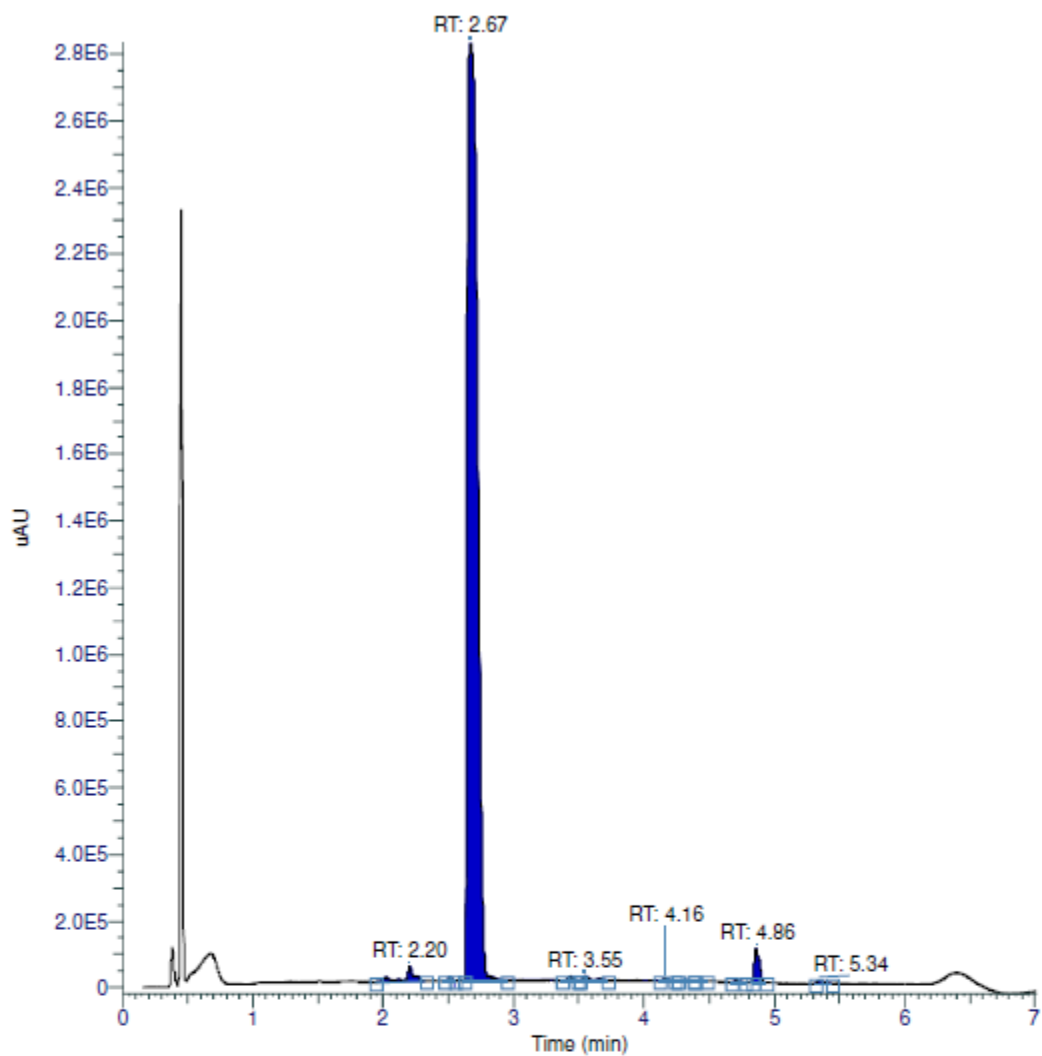




RT (Min)	% Area
1.8085	0.16
2.18183333333333	0.06
2.3635	98.09
3.01683333333333	0.08
3.19516666666667	1.6

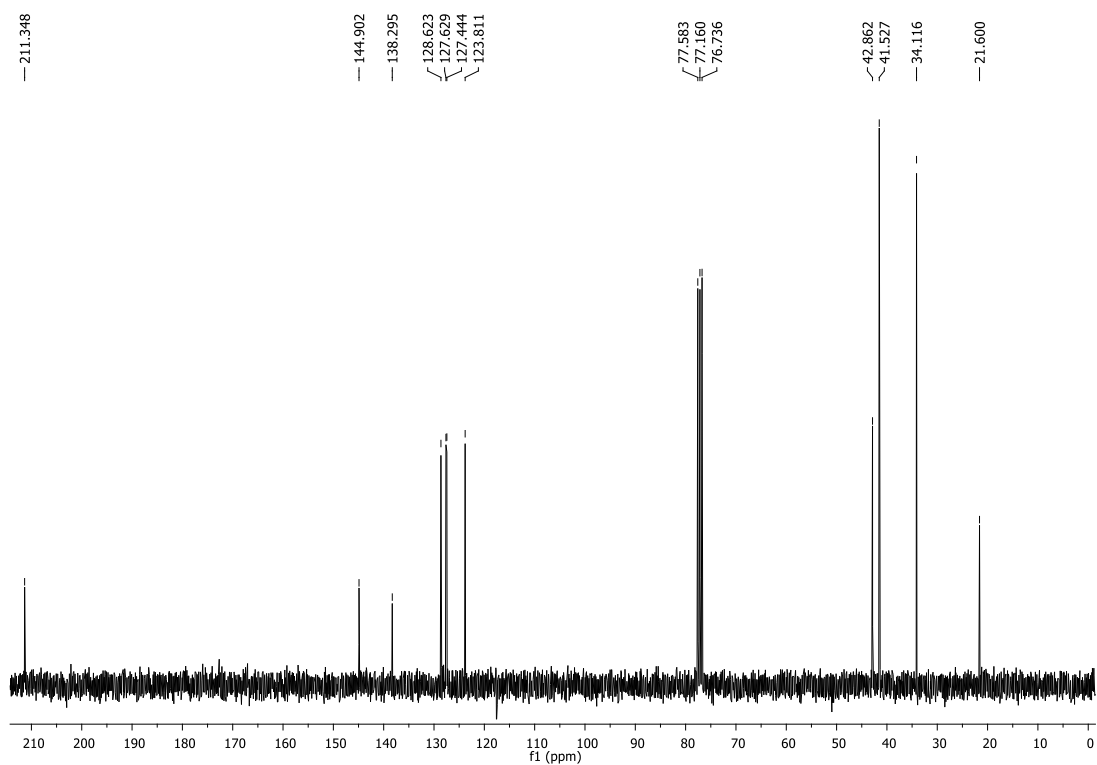
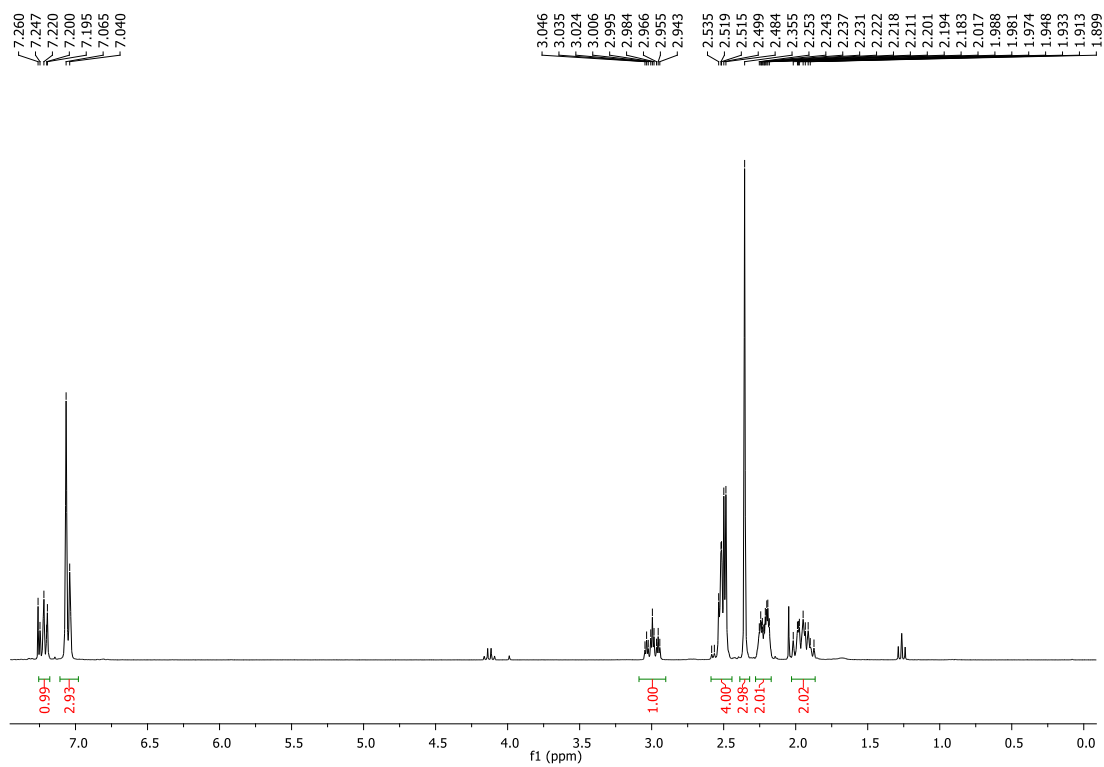
**1-((6-bromopyridin-3-yl)methyl)-4-((1*S*,4*S*)-4-phenylcyclohexyl)piperazine (44f).**



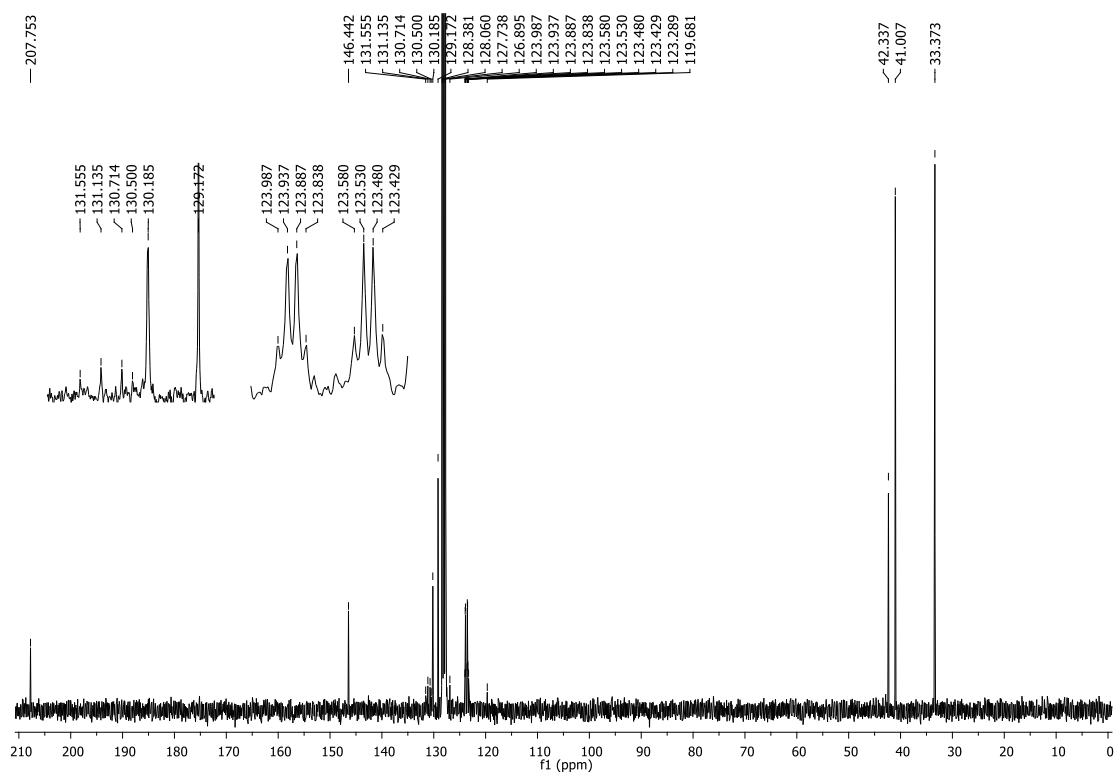
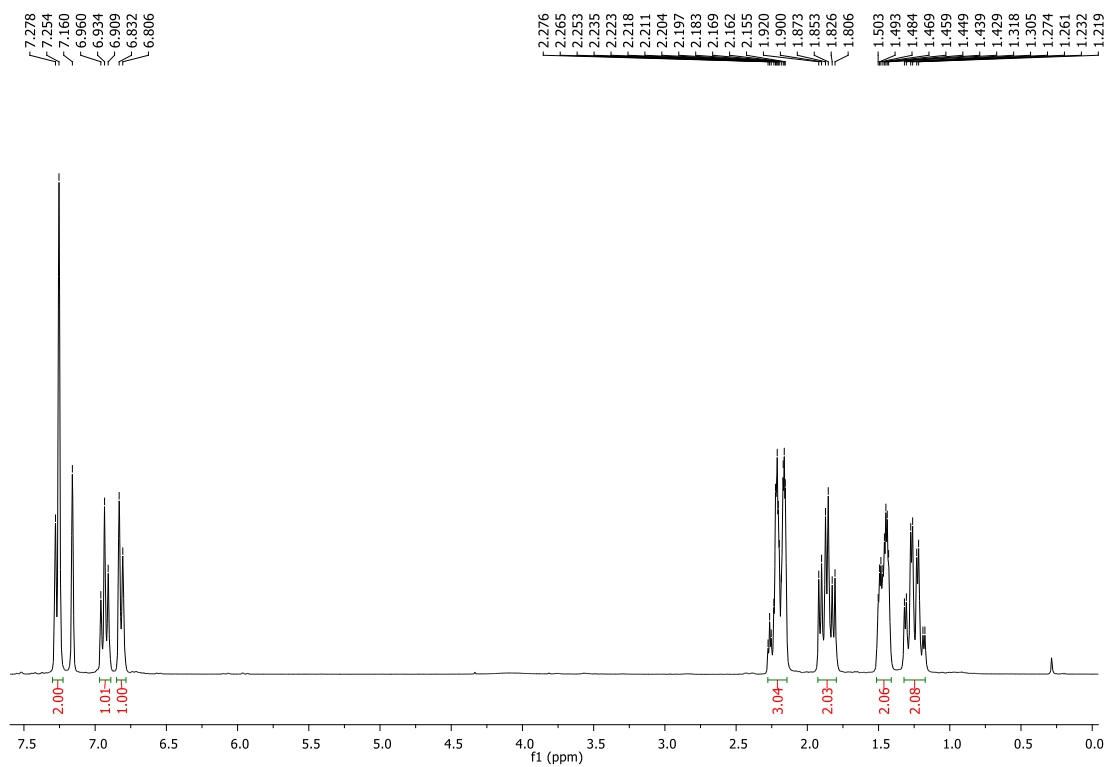


RT (Min)	% Area
2.20016666666667	1.3
2.50683333333333	0.13
2.6685	95.97
3.43183333333333	0.19
3.54683333333333	0.3
4.16183333333333	0.11
4.31683333333333	0.05
4.4285	0.05
4.71016666666667	0.07
4.8585	1.63
5.34016666666667	0.19

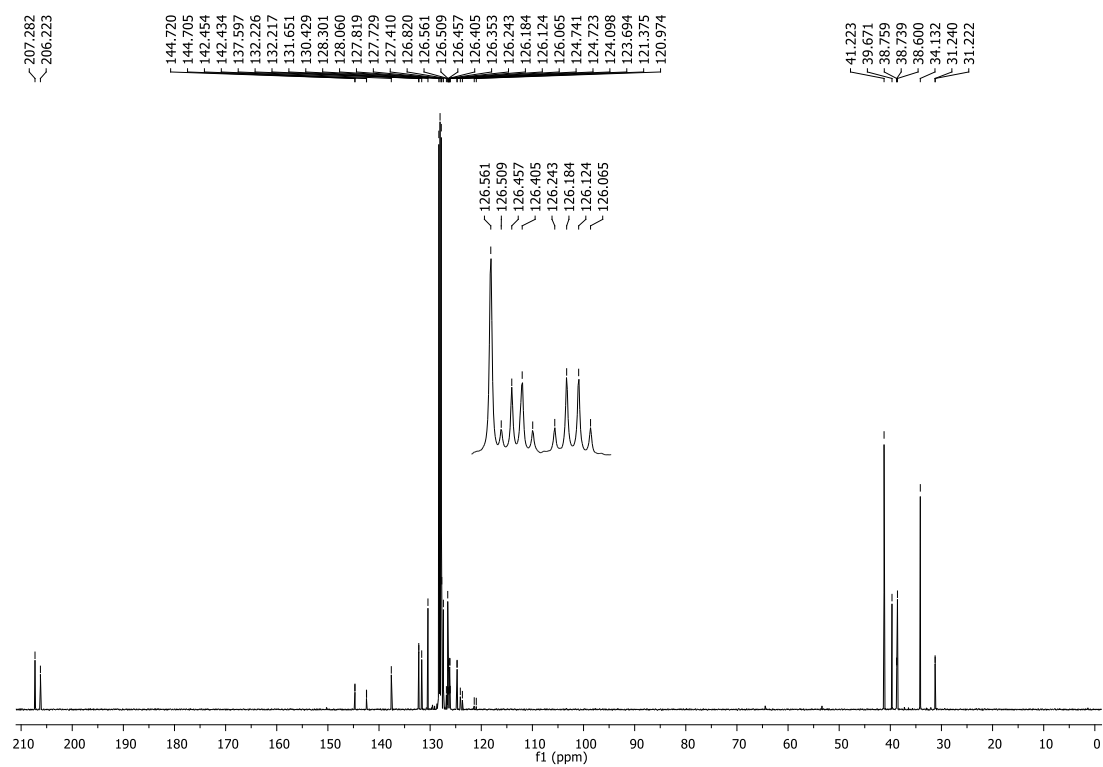
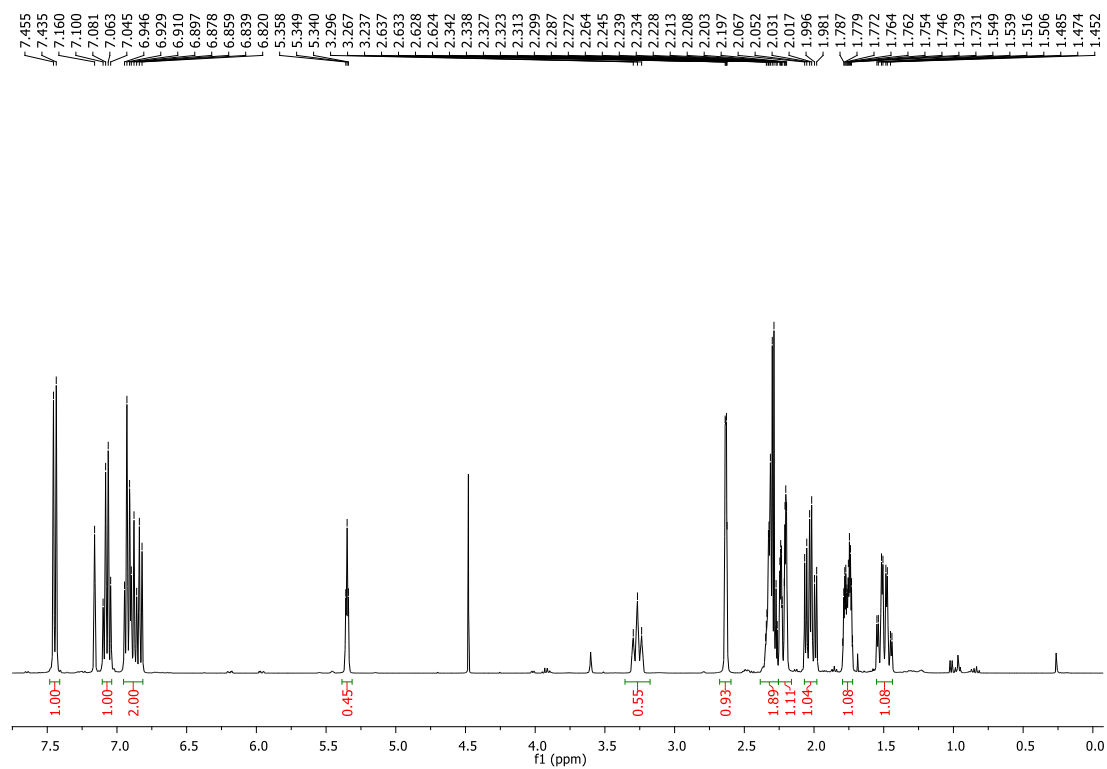
## 4-(m-tolyl)cyclohexan-1-one (50g).

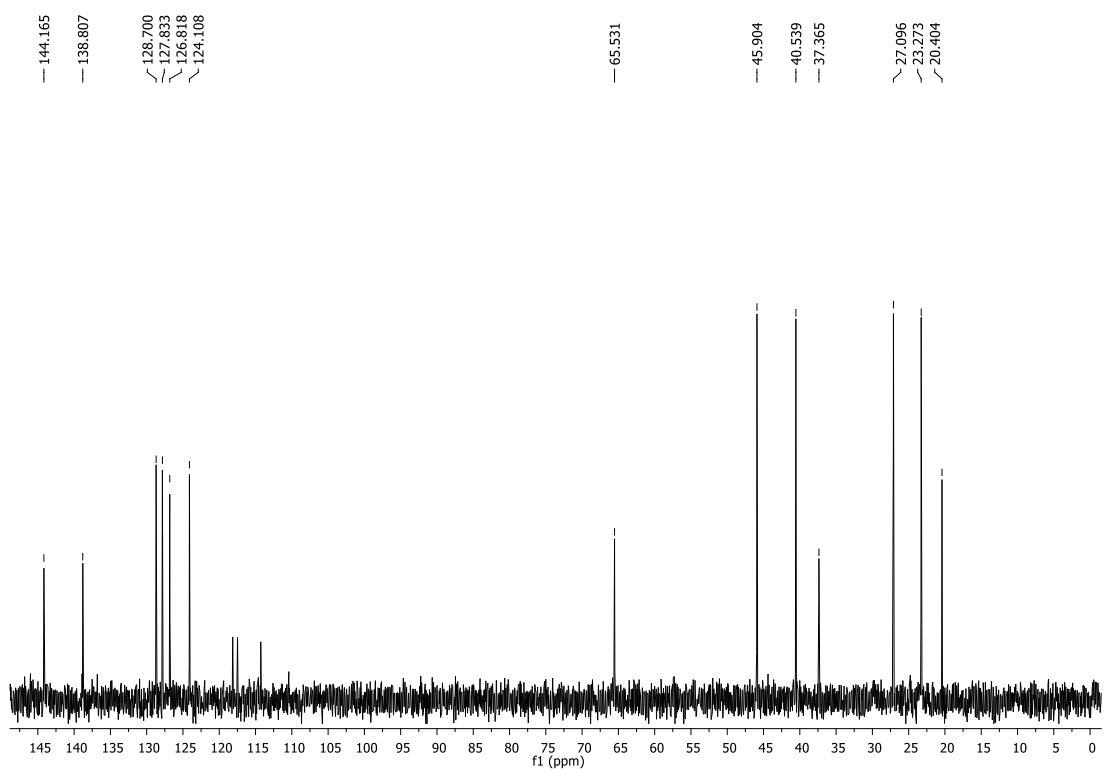
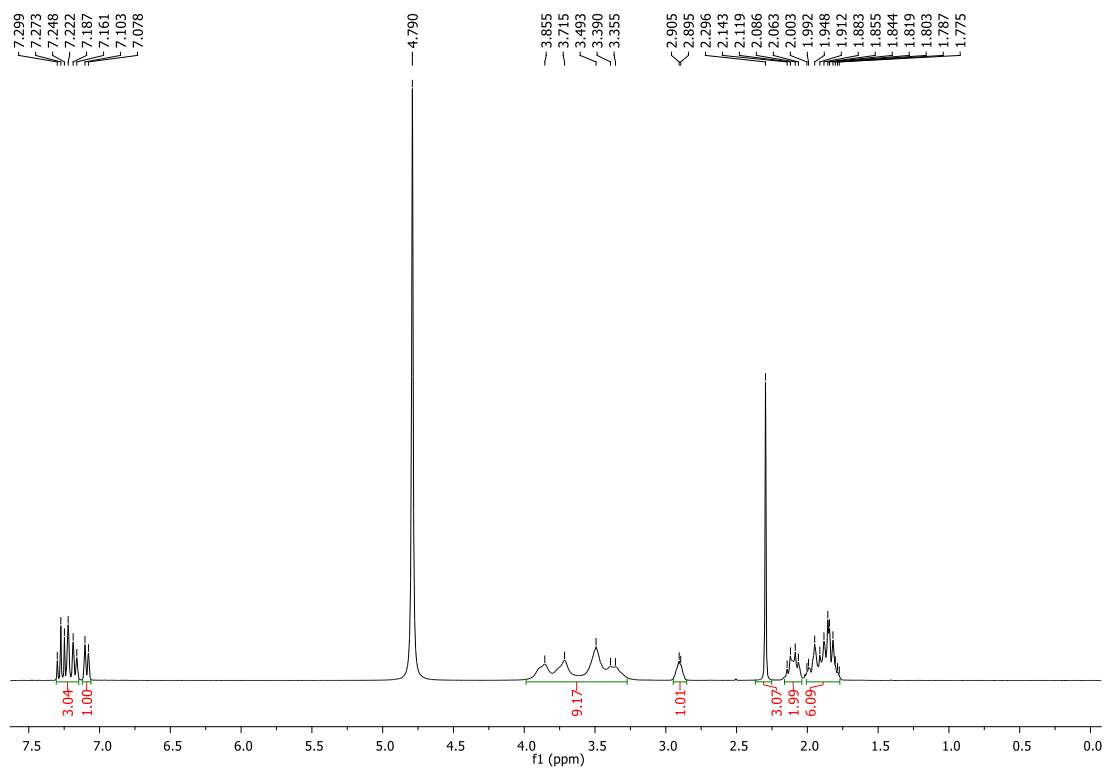


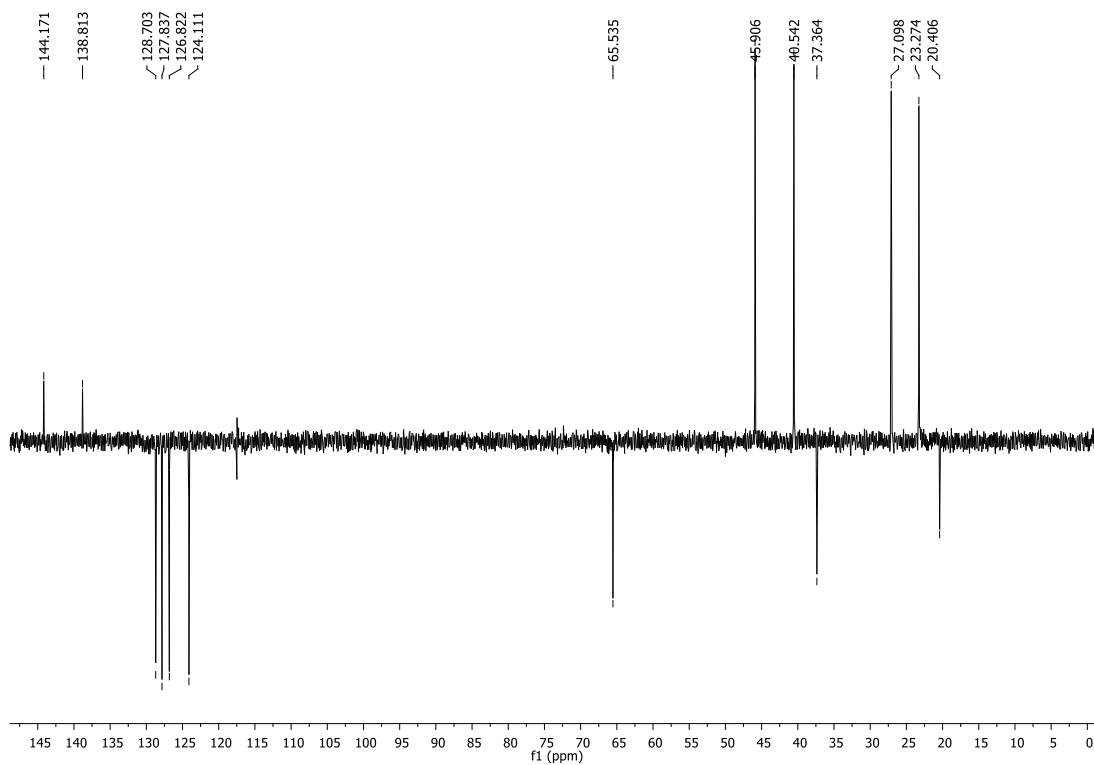
## 4-(3-(trifluoromethyl)phenyl)cyclohexan-1-one (50h).



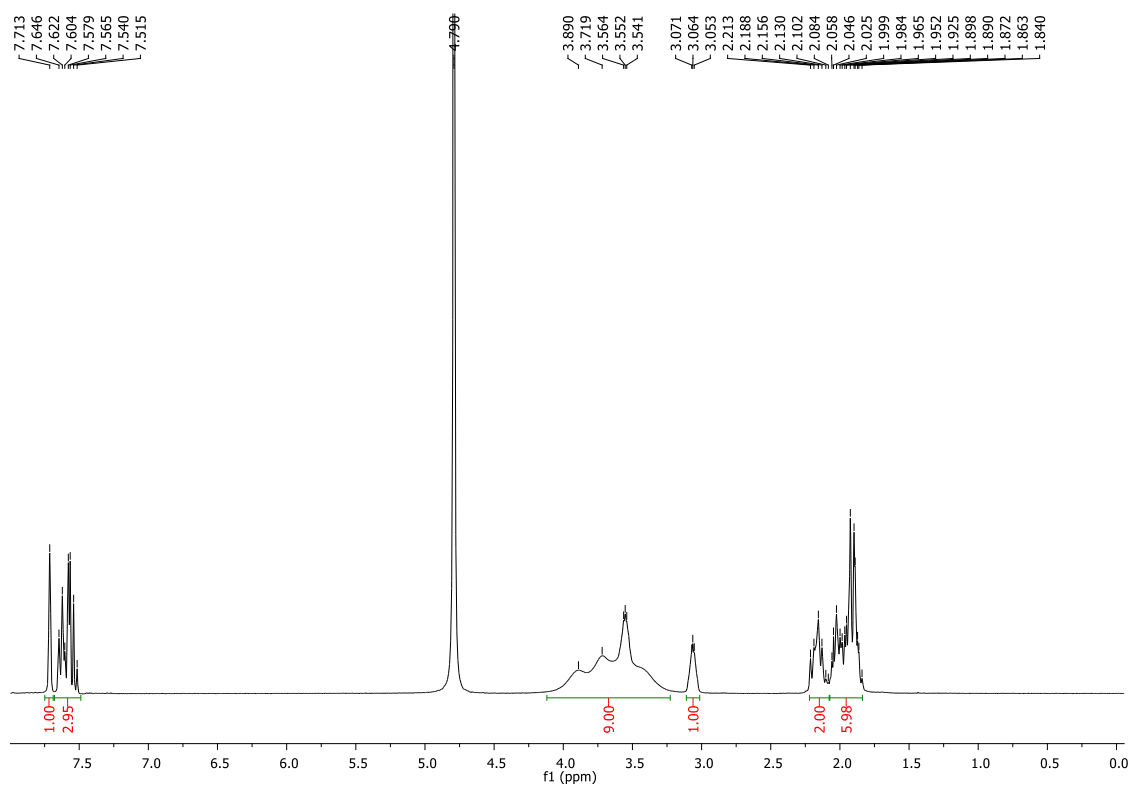
## 4-(2-(trifluoromethyl)phenyl)cyclohexan-1-one (50i).

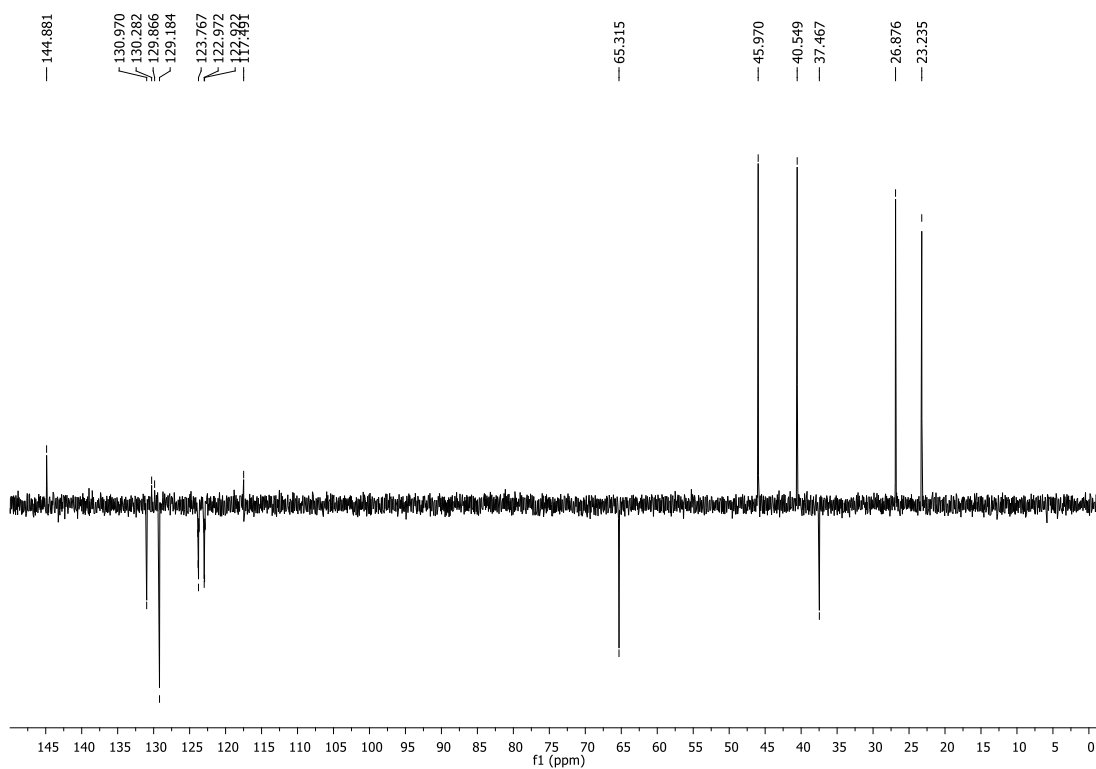
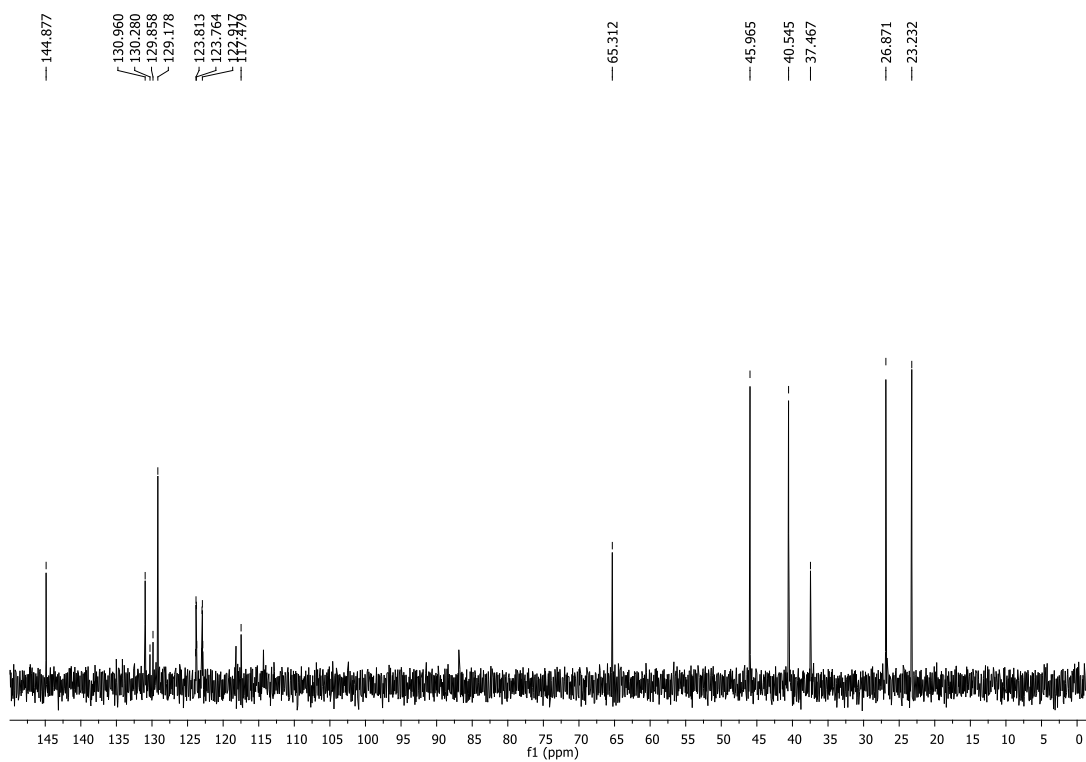


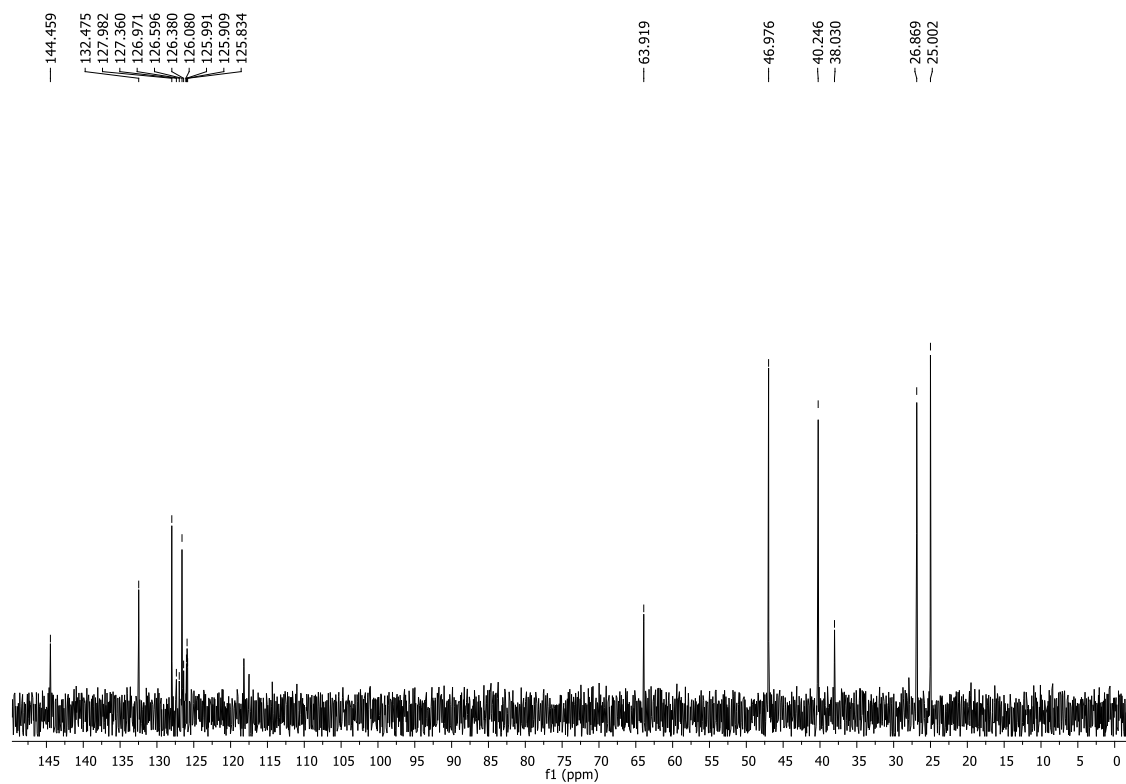
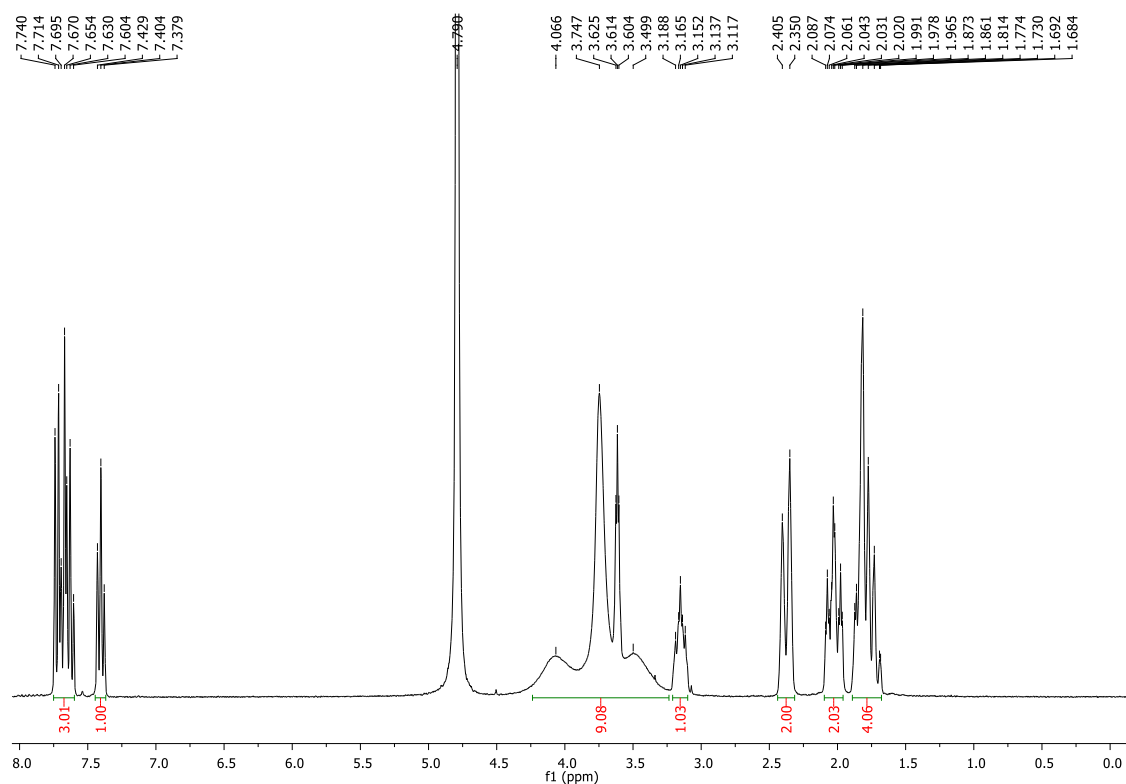
**1-((1*S*,4*S*)-4-(*m*-tolyl)cyclohexyl)piperazine (52g).**

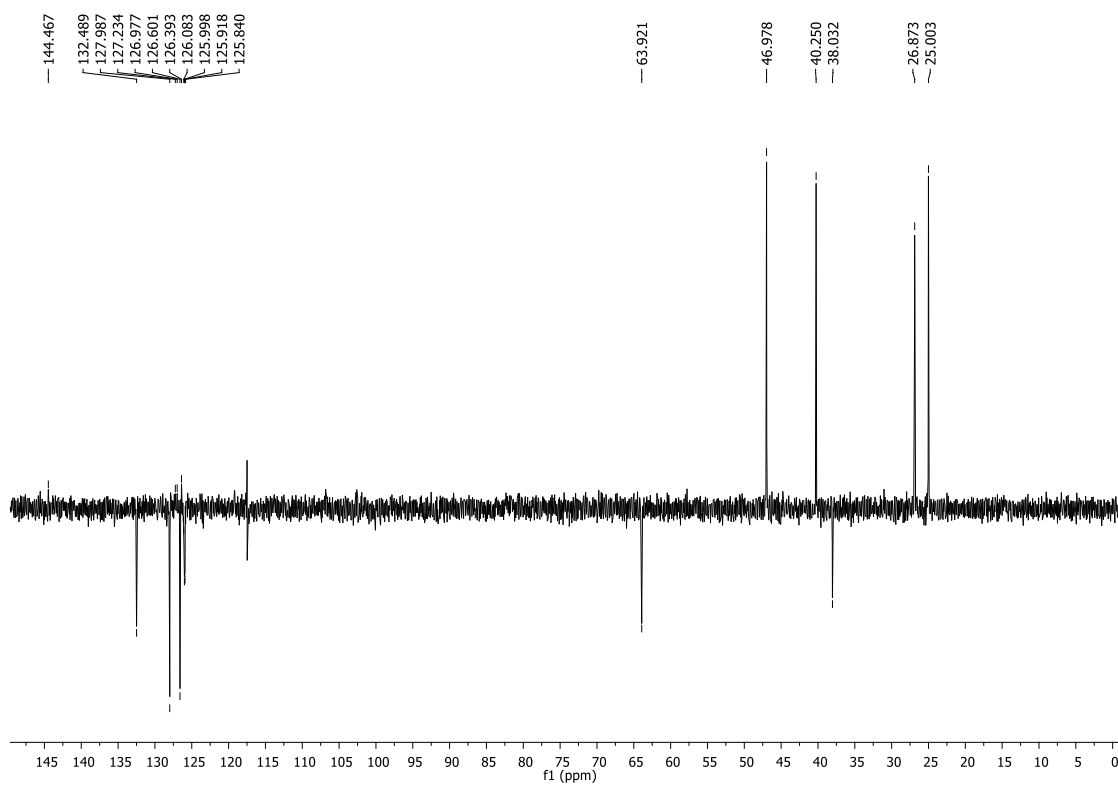


**1-((1S,4S)-4-(3-(trifluoromethyl)phenyl)cyclohexyl)piperazine (52h).**

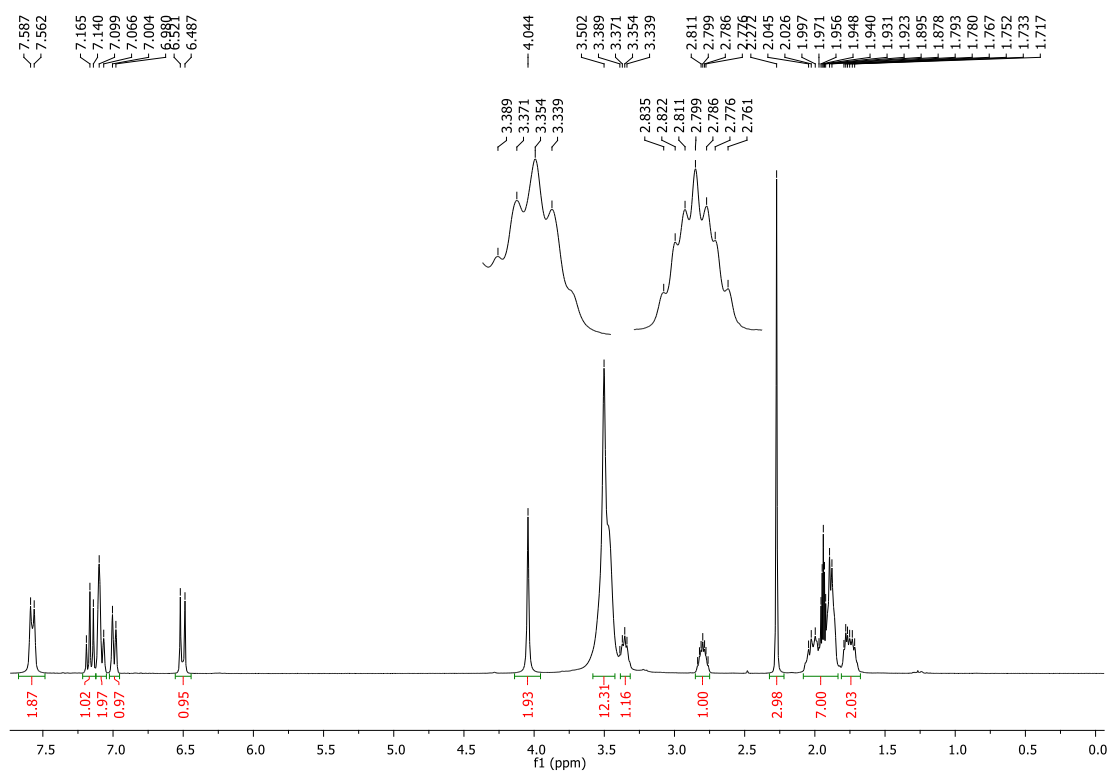


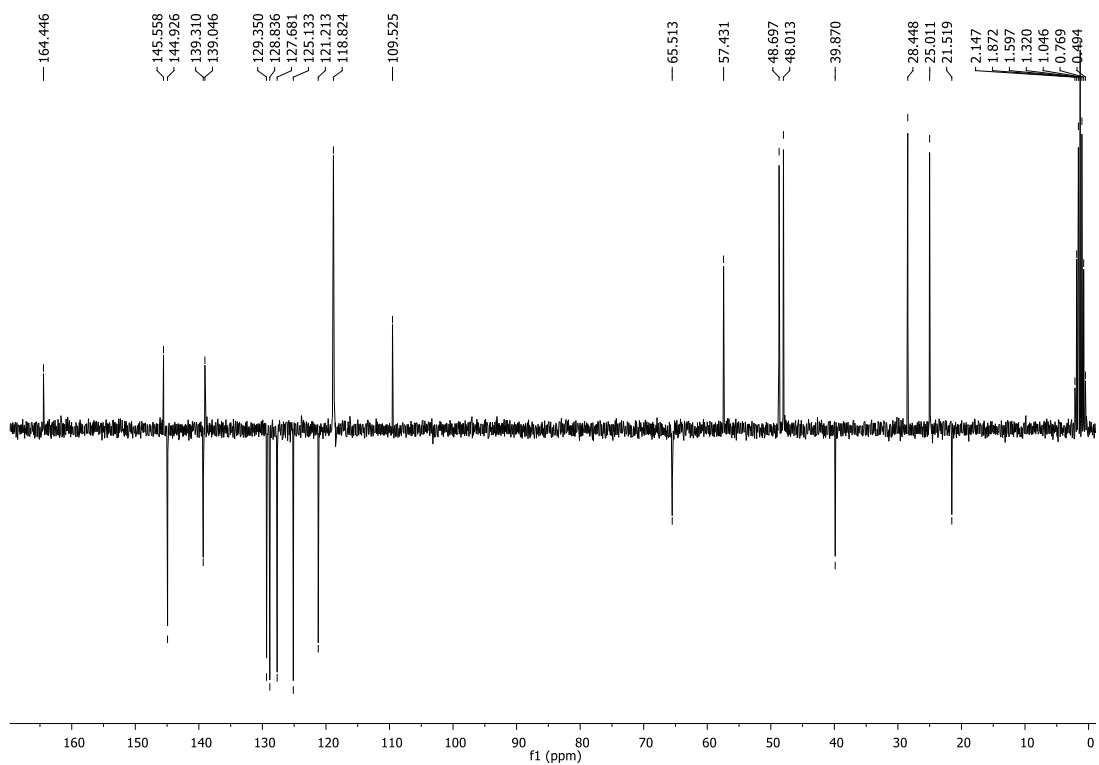
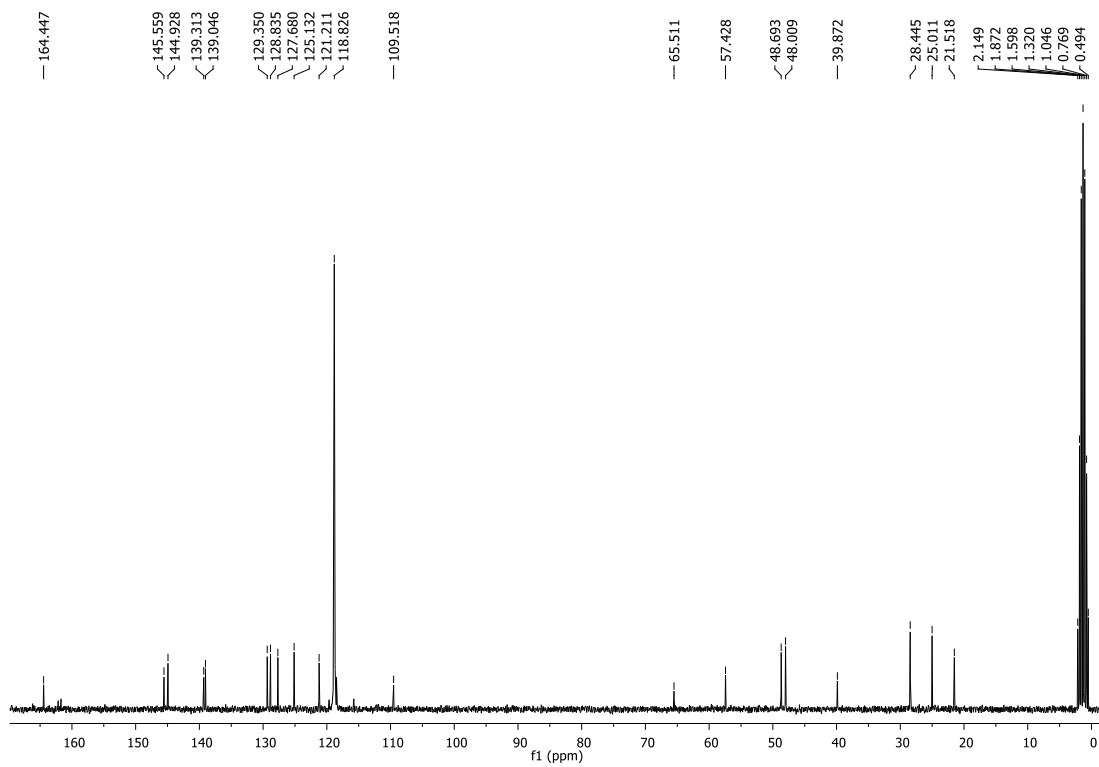


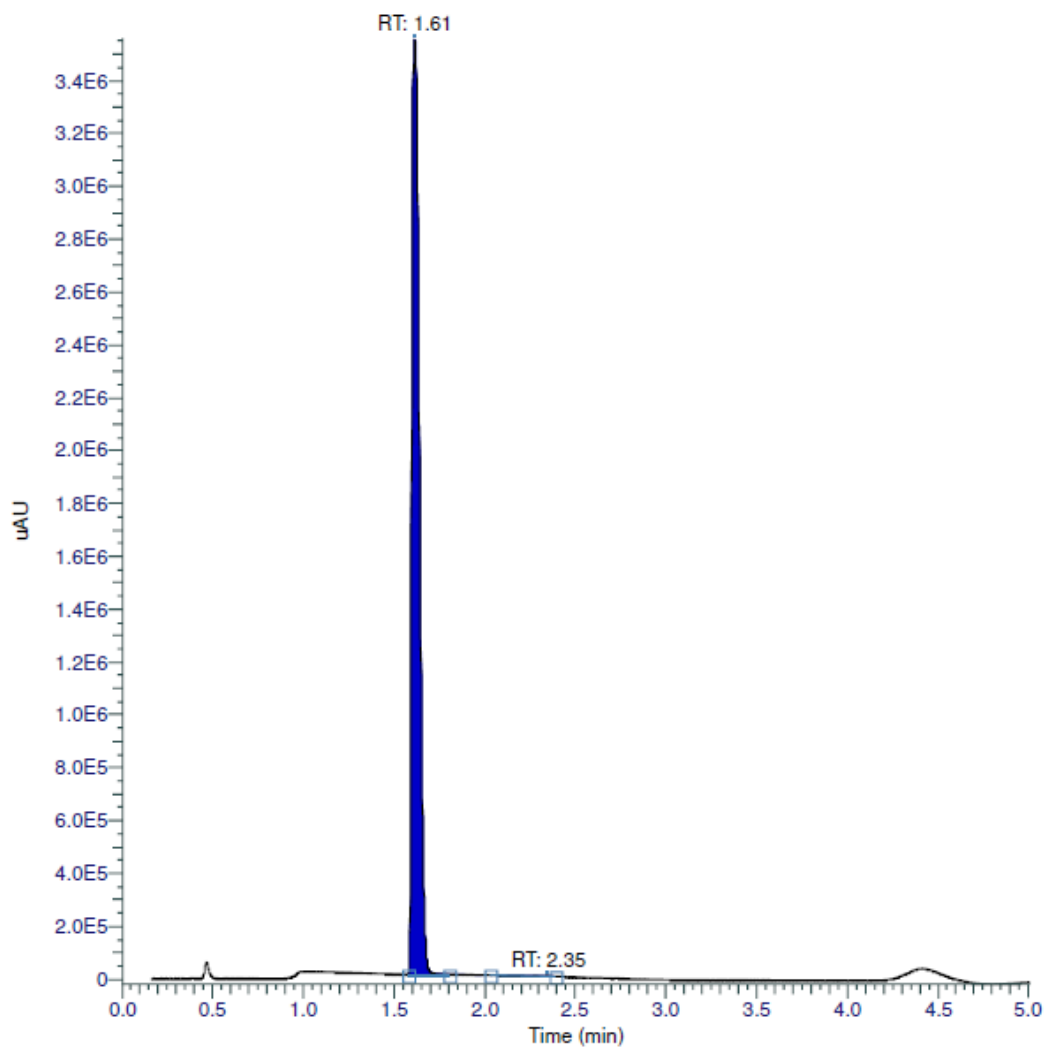
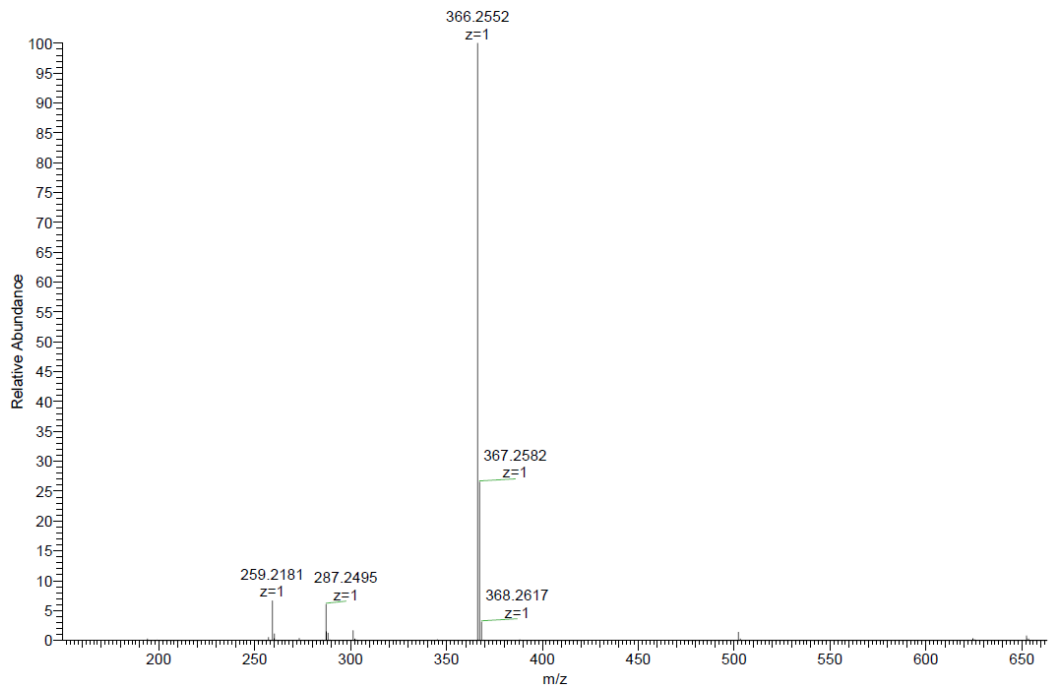
**1-((1*S*,4*S*)-4-(2-(trifluoromethyl)phenyl)cyclohexyl)piperazine (52i).**



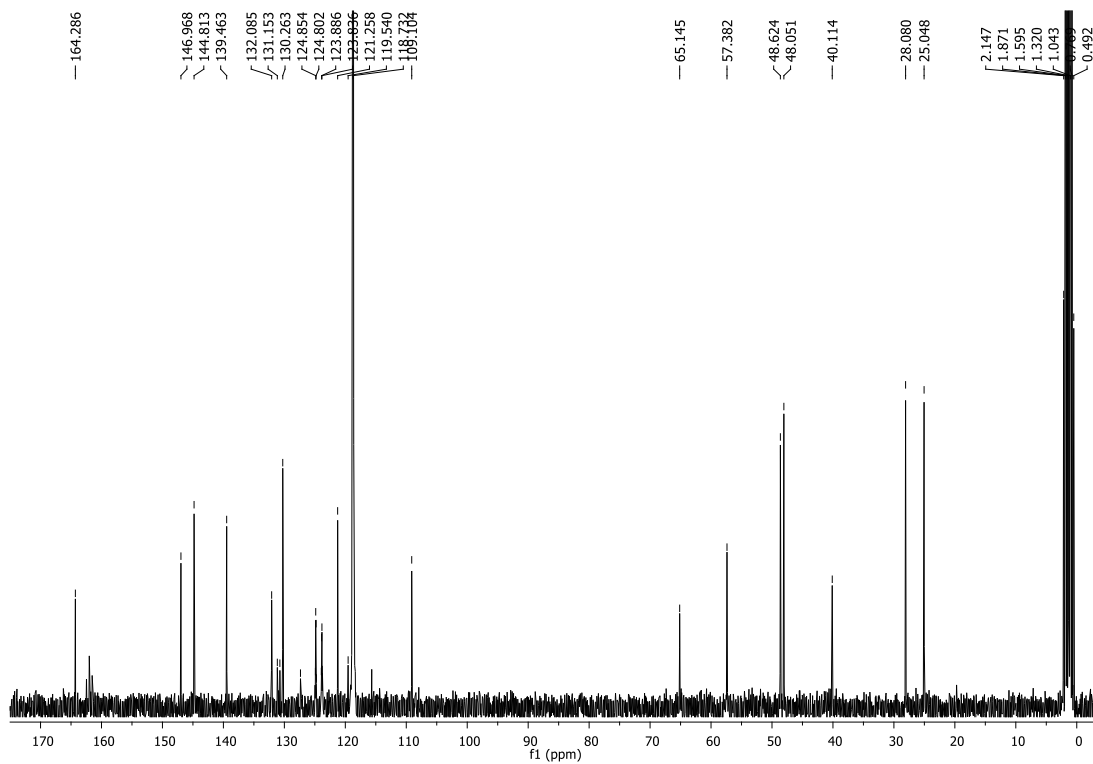
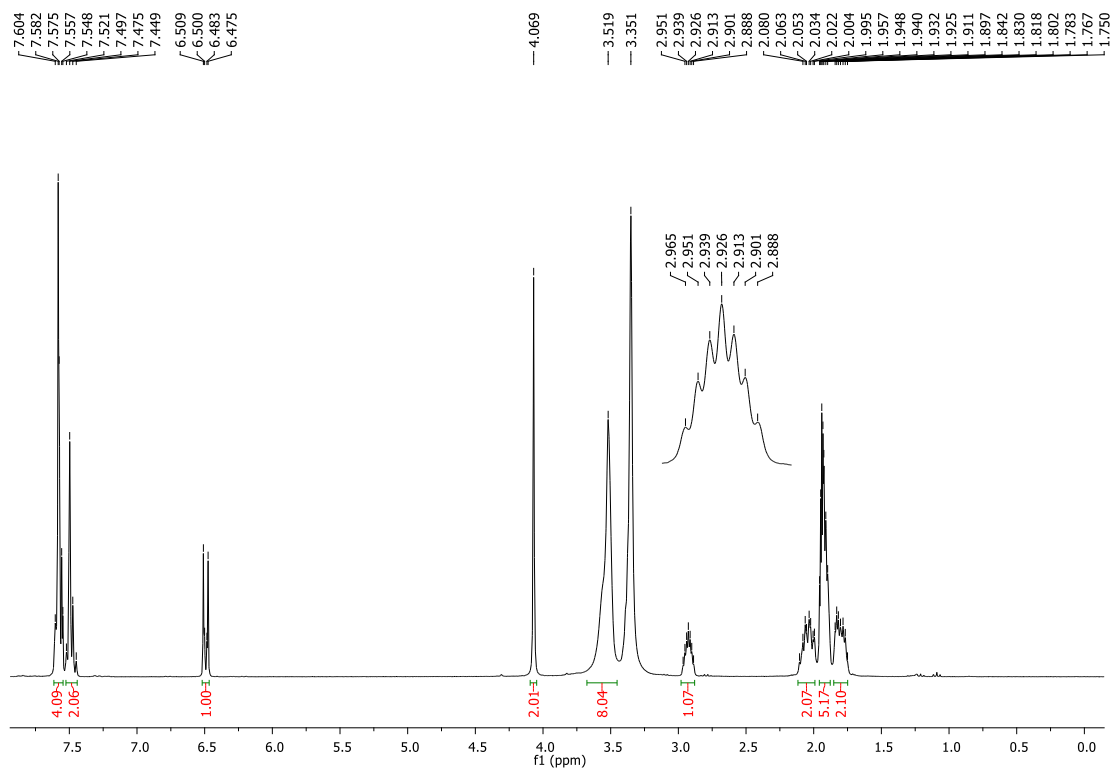
**5-((4-((1S,4S)-4-(m-tolyl)cyclohexyl)piperazin-1-yl)methyl)pyridin-2(1H)-one (53g).**

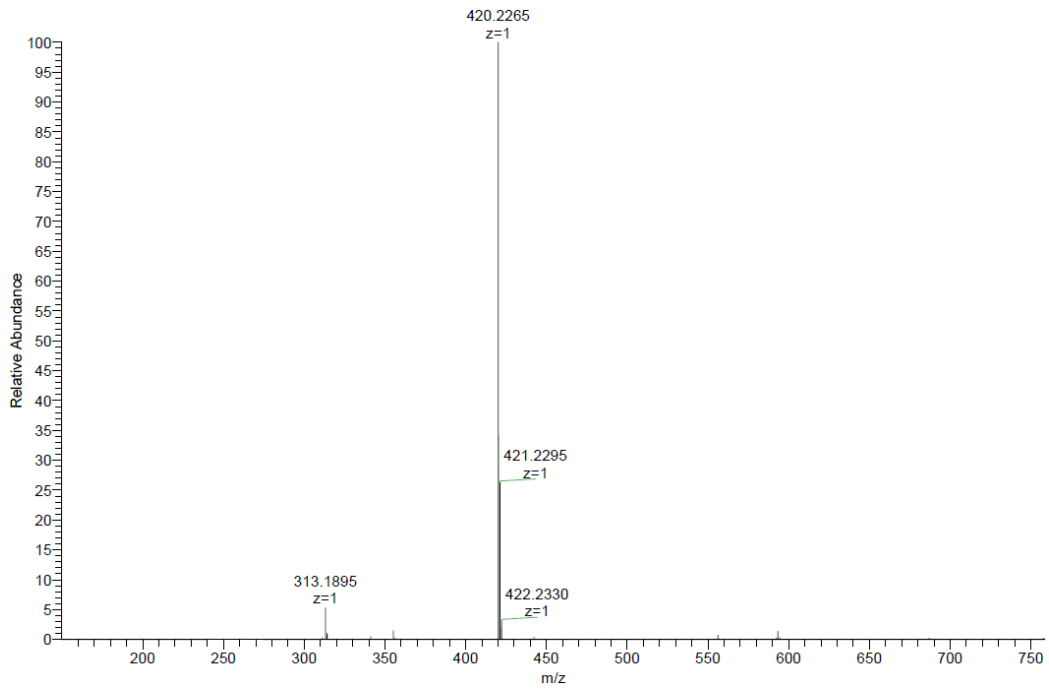
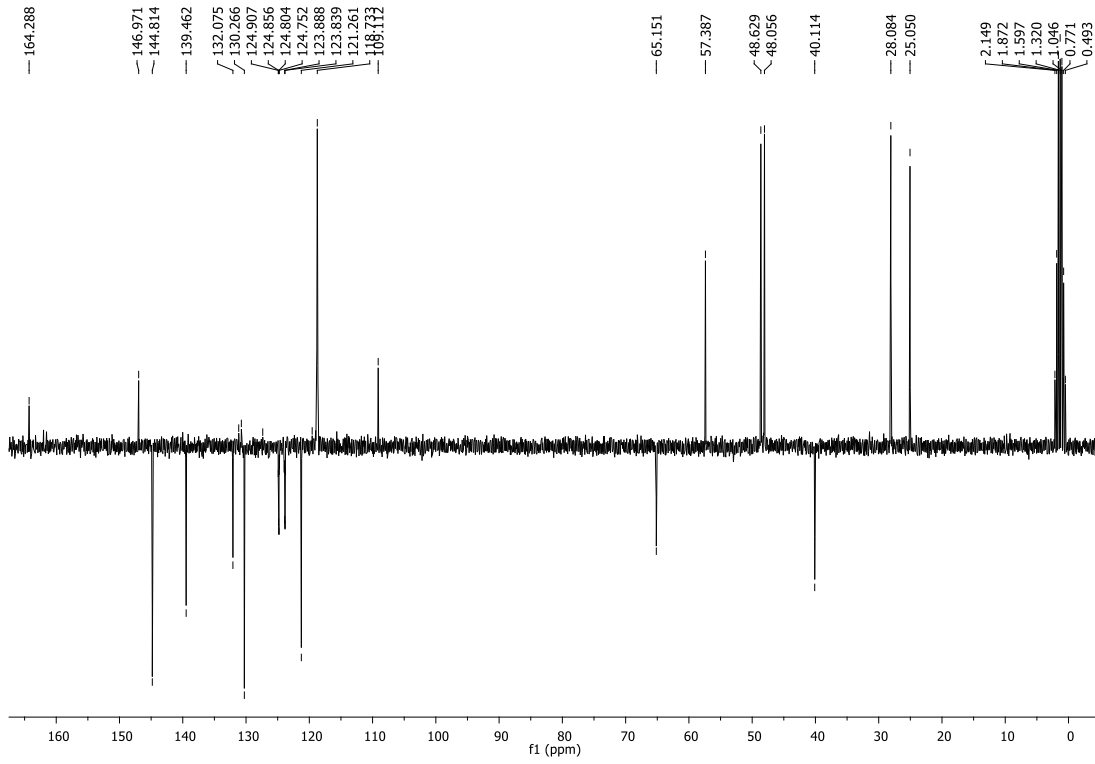


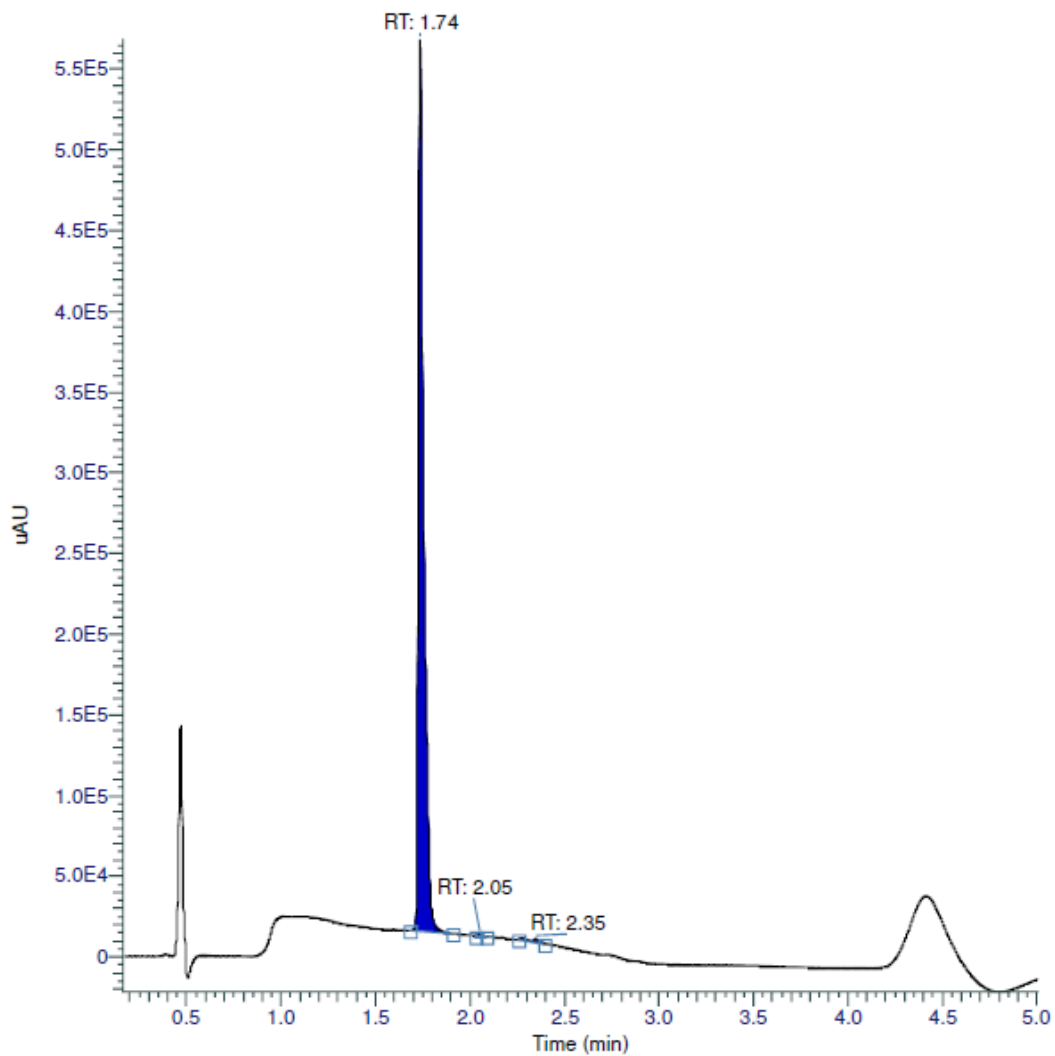




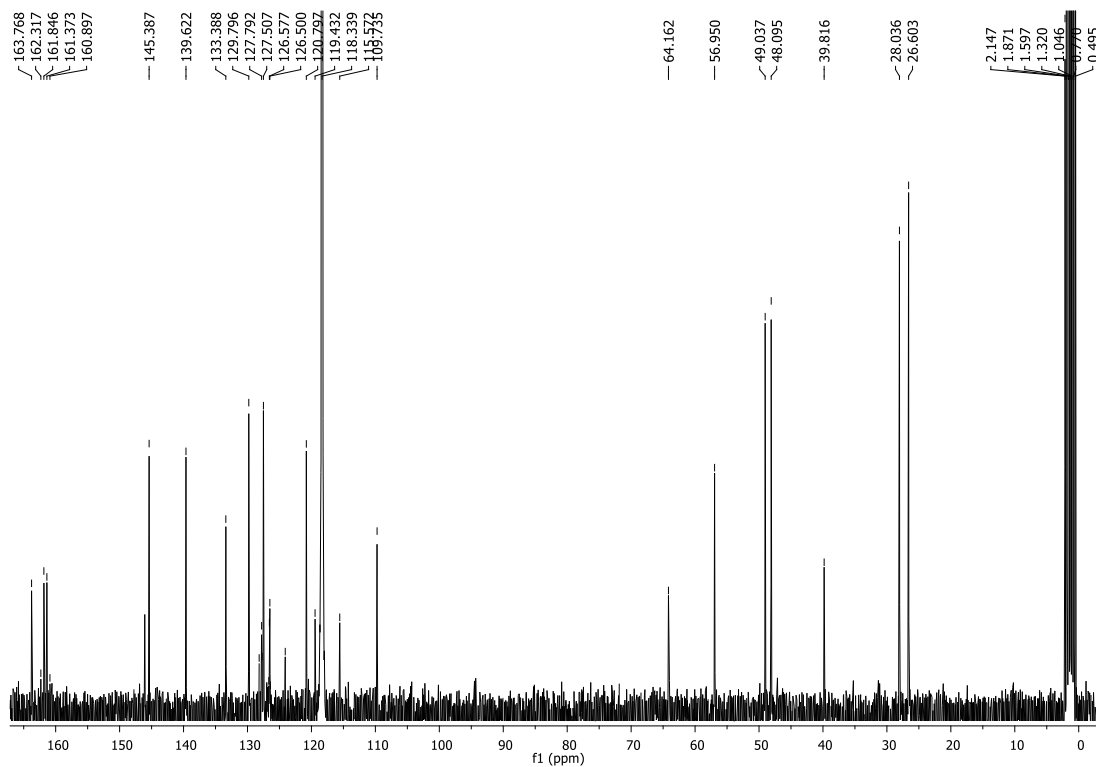
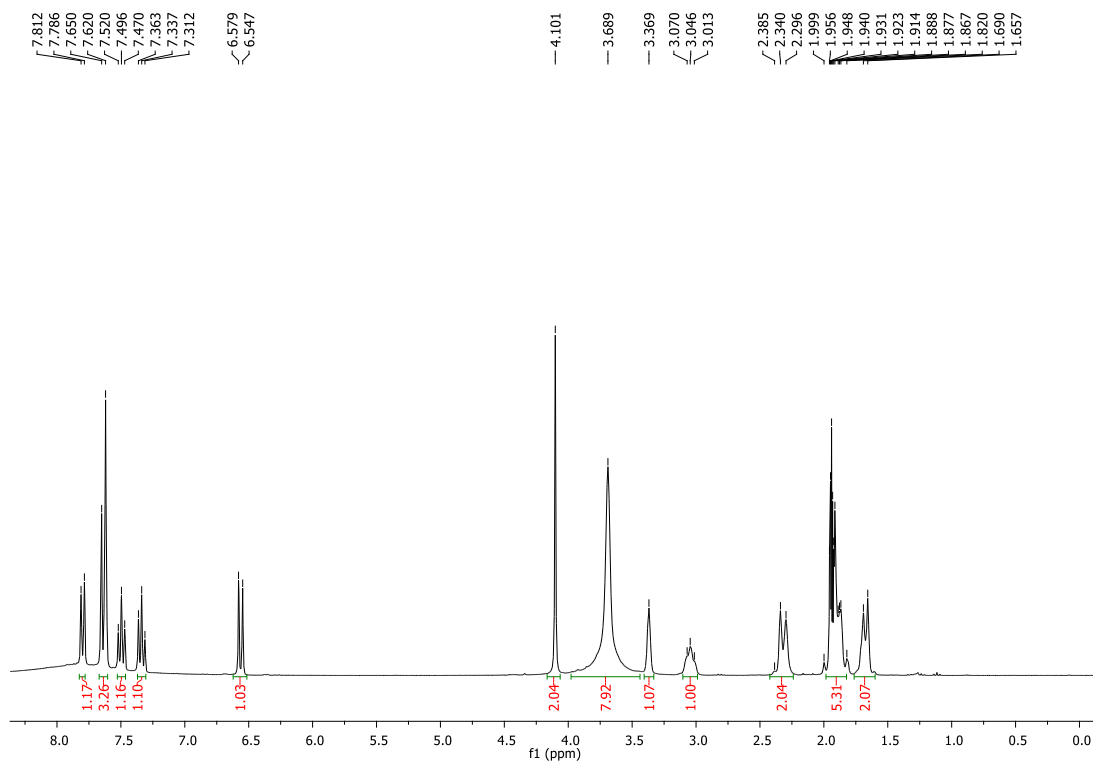
RT (Min)	% Area
1.61166666666667	99.88
2.34666666666667	0.12

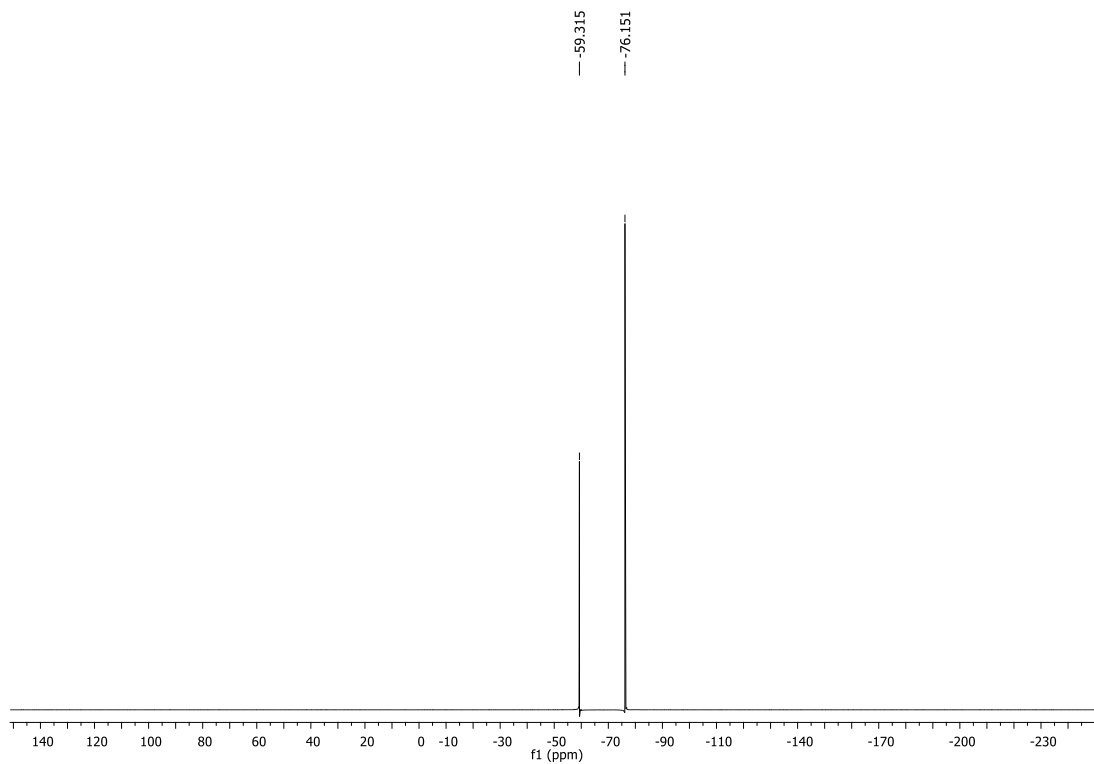
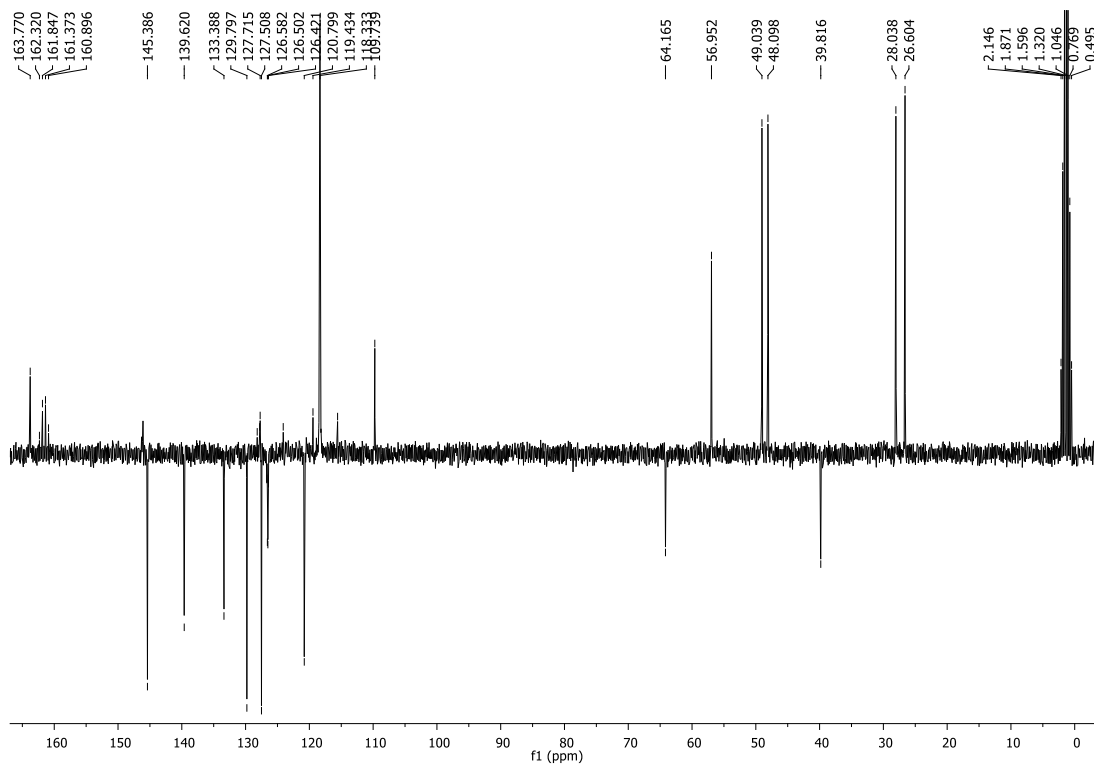
**5-((4-((1*S*,4*S*)-4-(3-(trifluoromethyl)phenyl)cyclohexyl)piperazin-1-yl)methyl)pyridin-2(1*H*)-one (53h).**

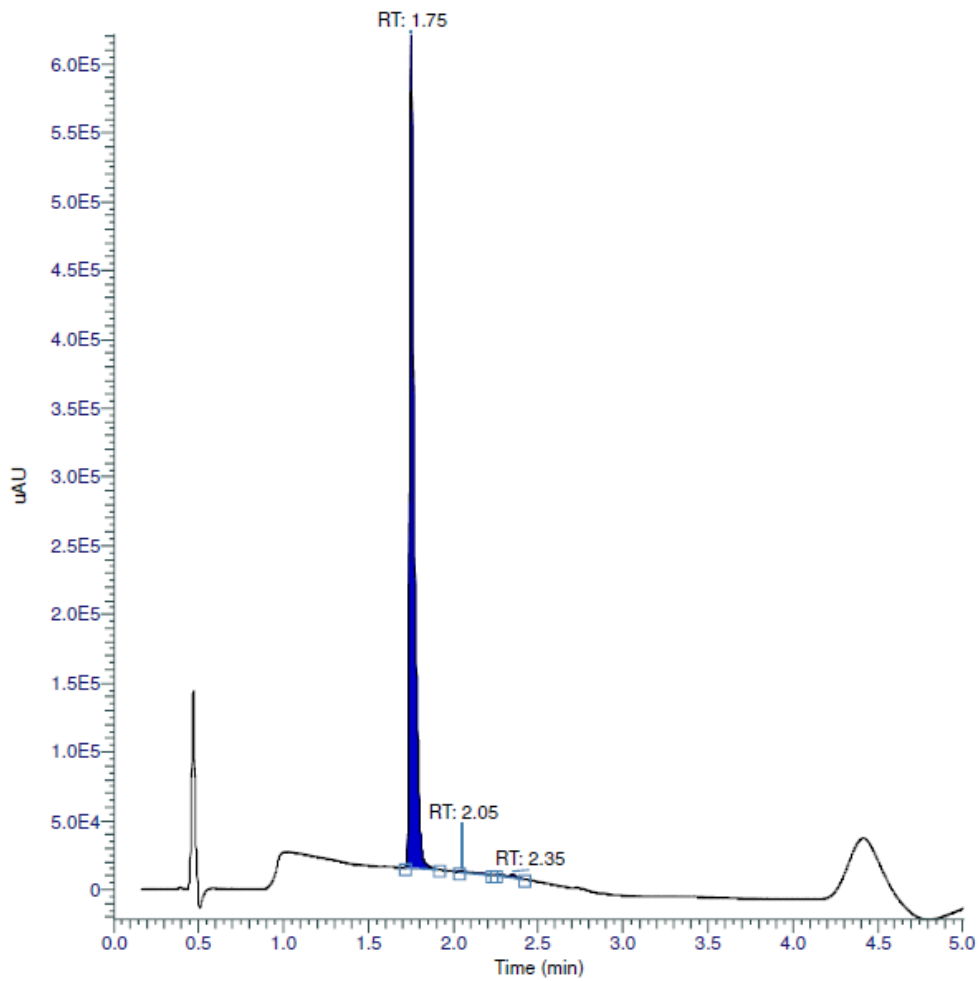
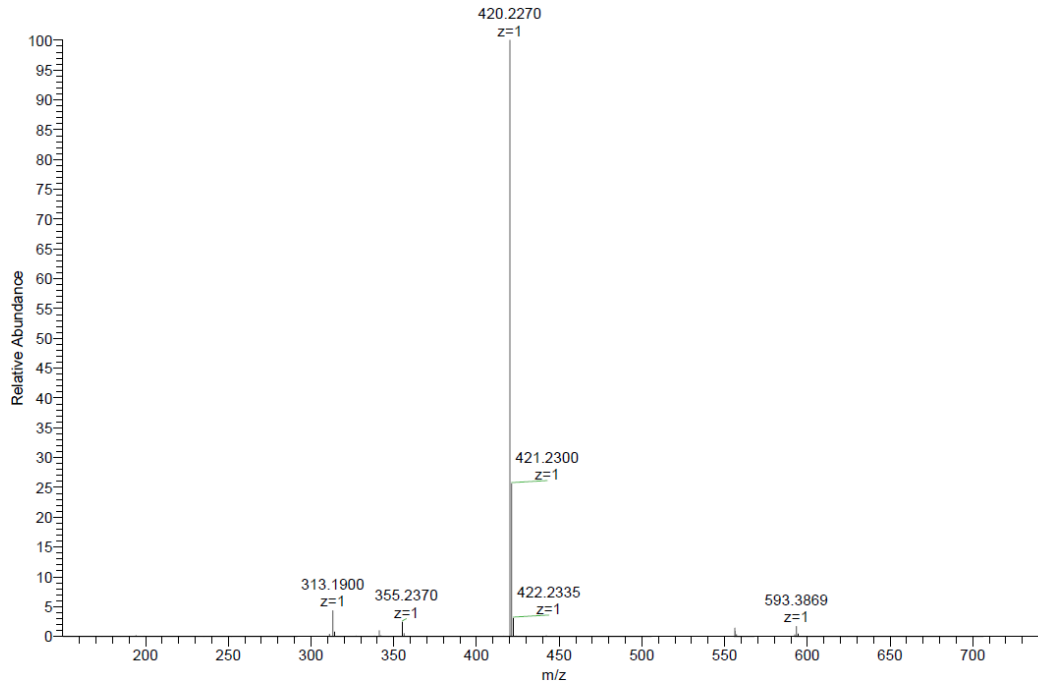




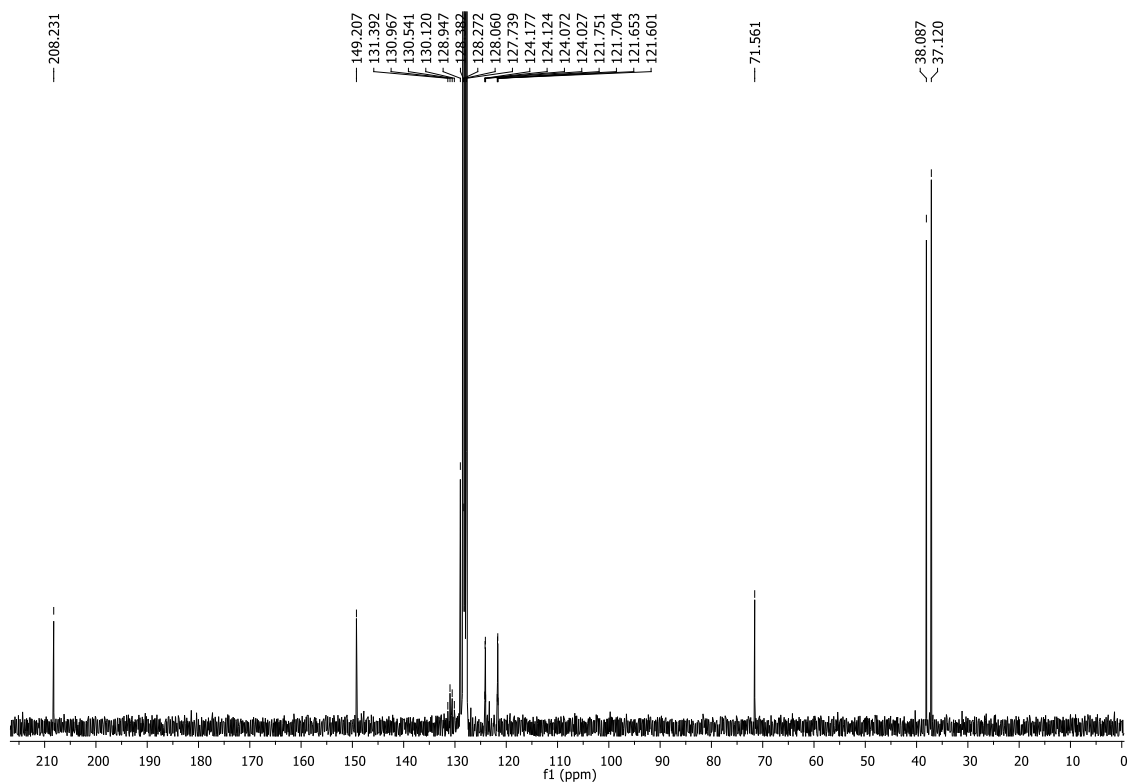
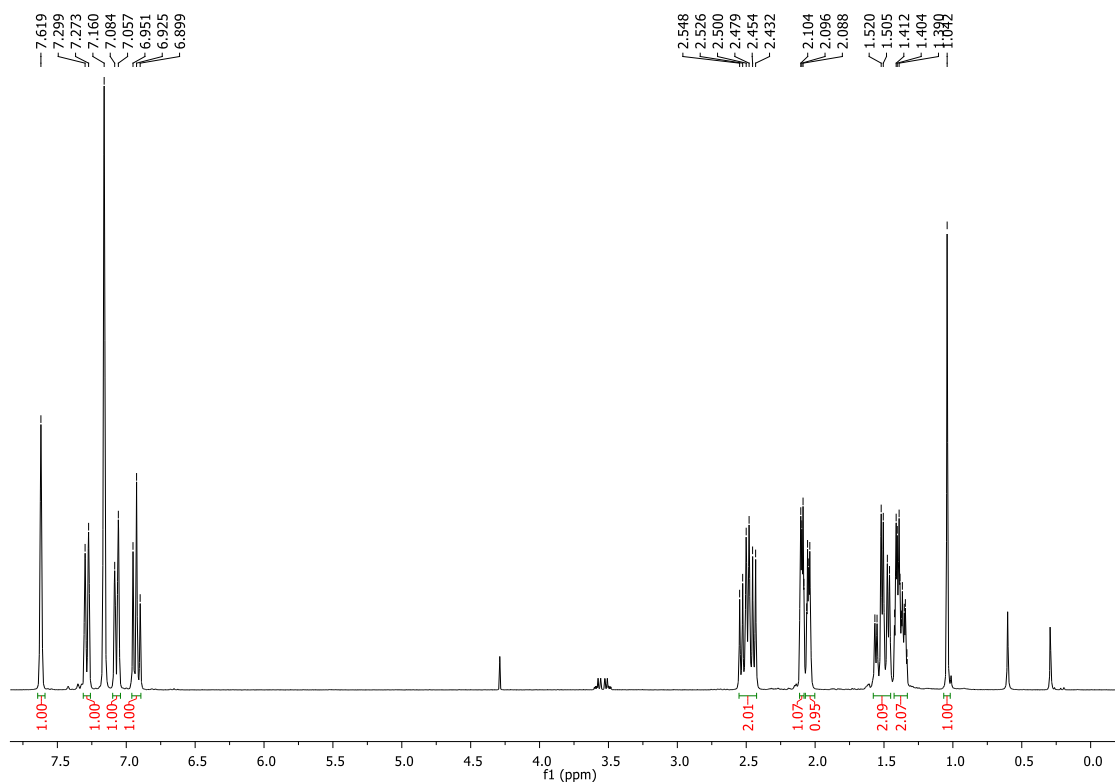
RT (Min)	% Area
1.735	99.25
2.05333333333333	0.14
2.34833333333333	0.61

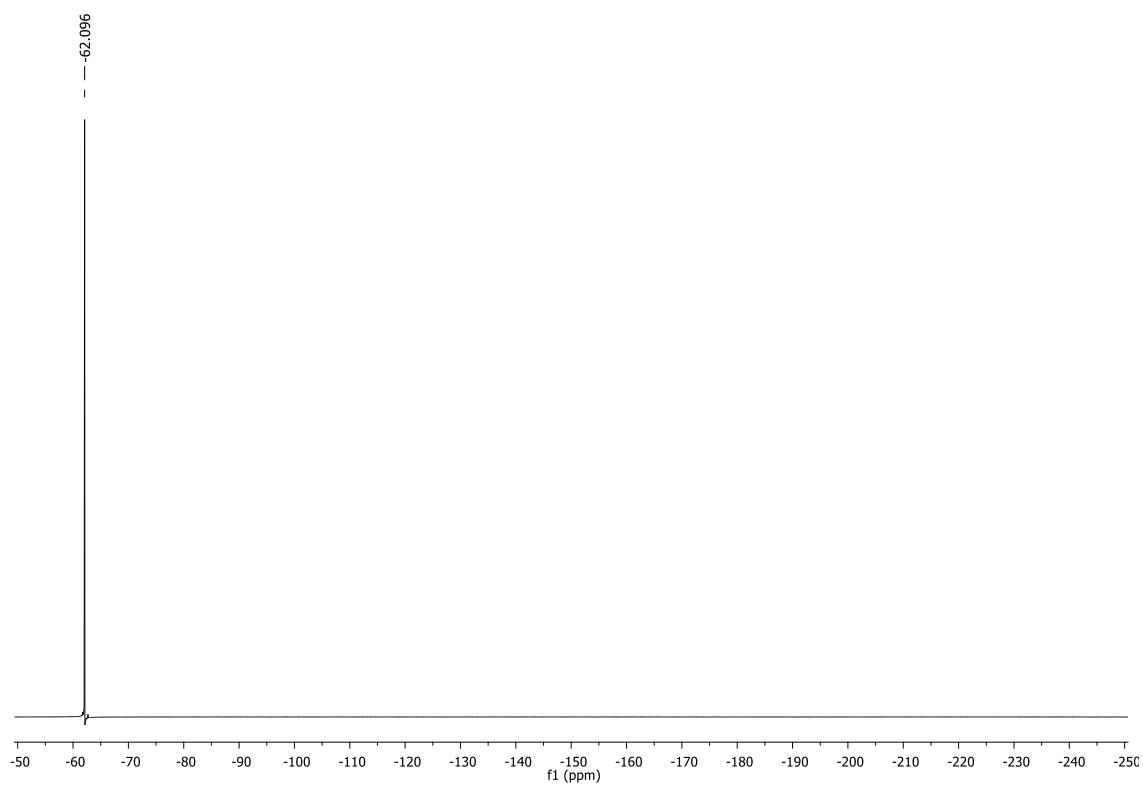
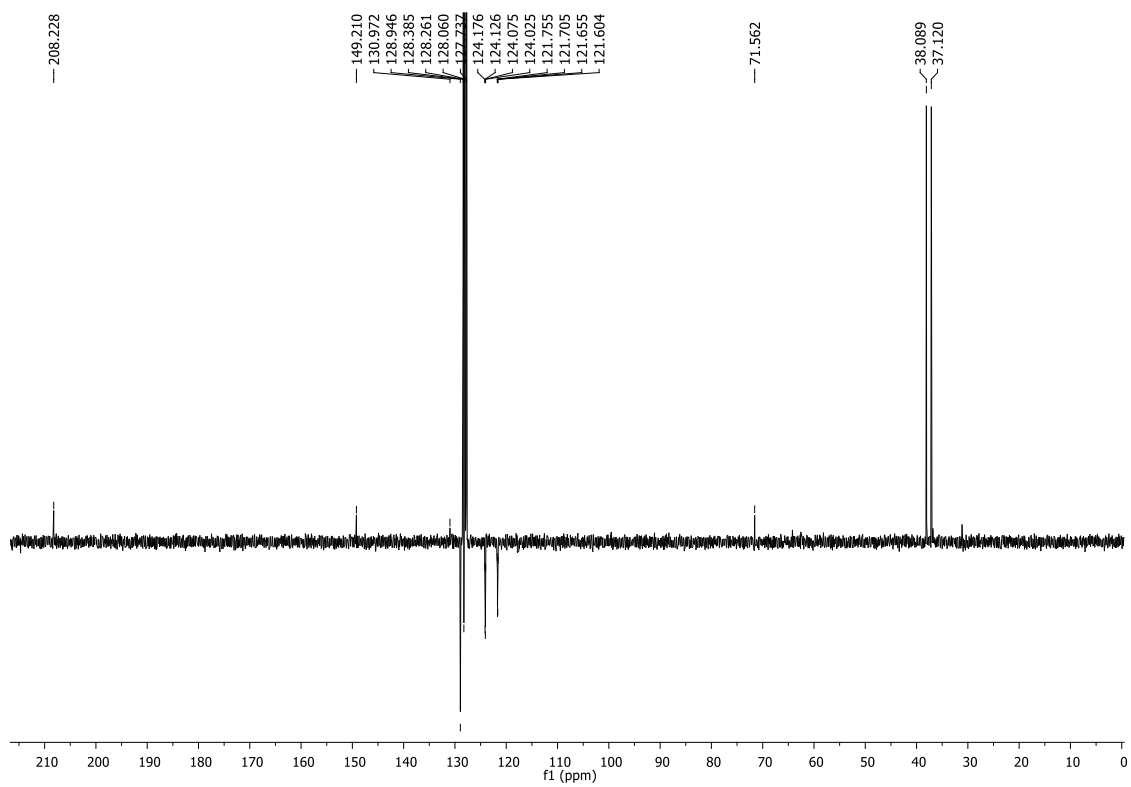
**5-((4-((1*S*,4*S*)-4-(2-(trifluoromethyl)phenyl)cyclohexyl)piperazin-1-yl)methyl)pyridin-2(1*H*)-one (53i).**

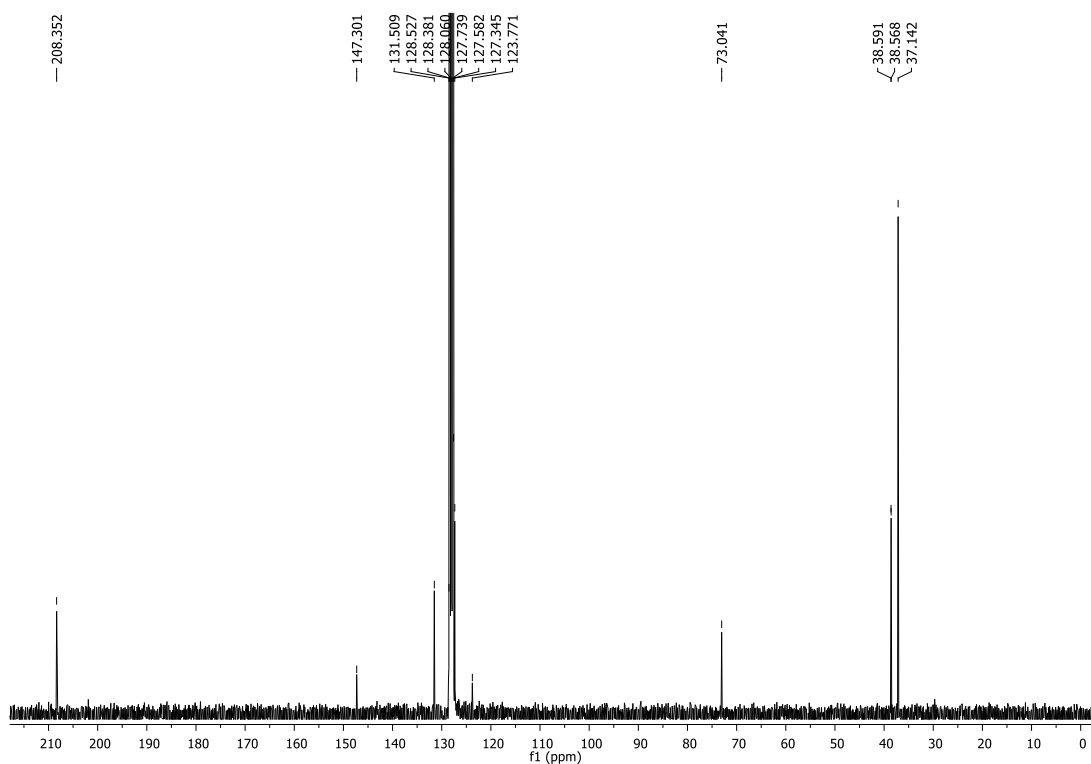
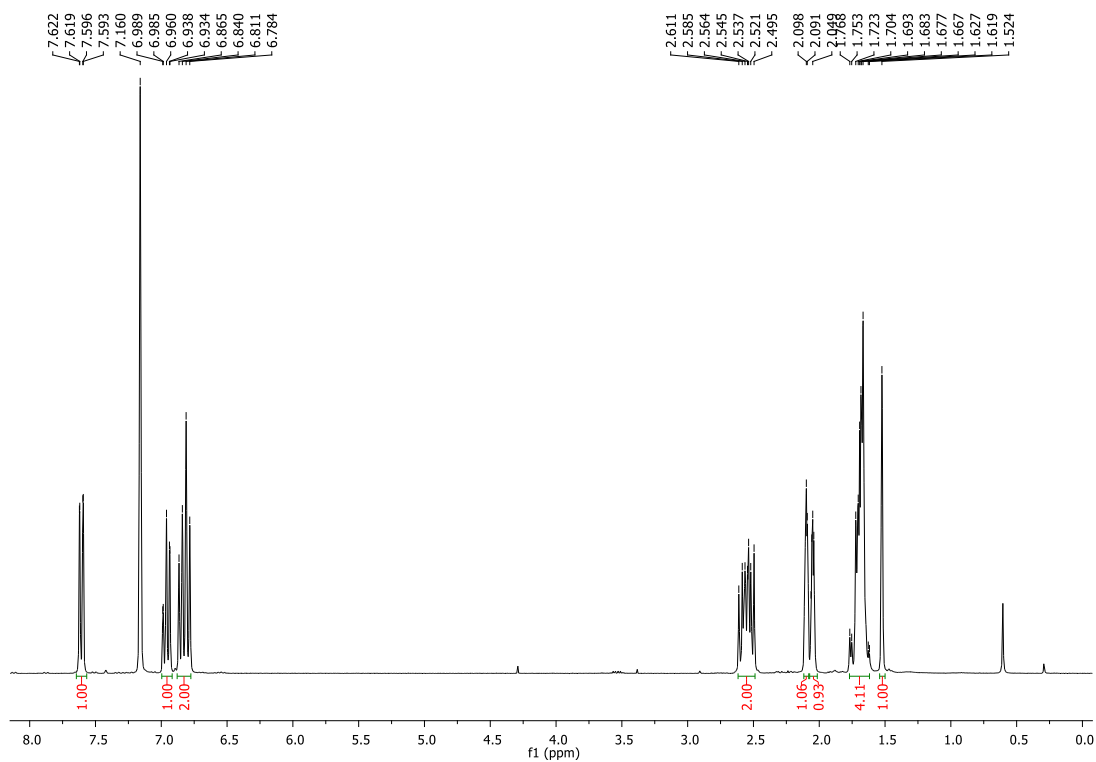


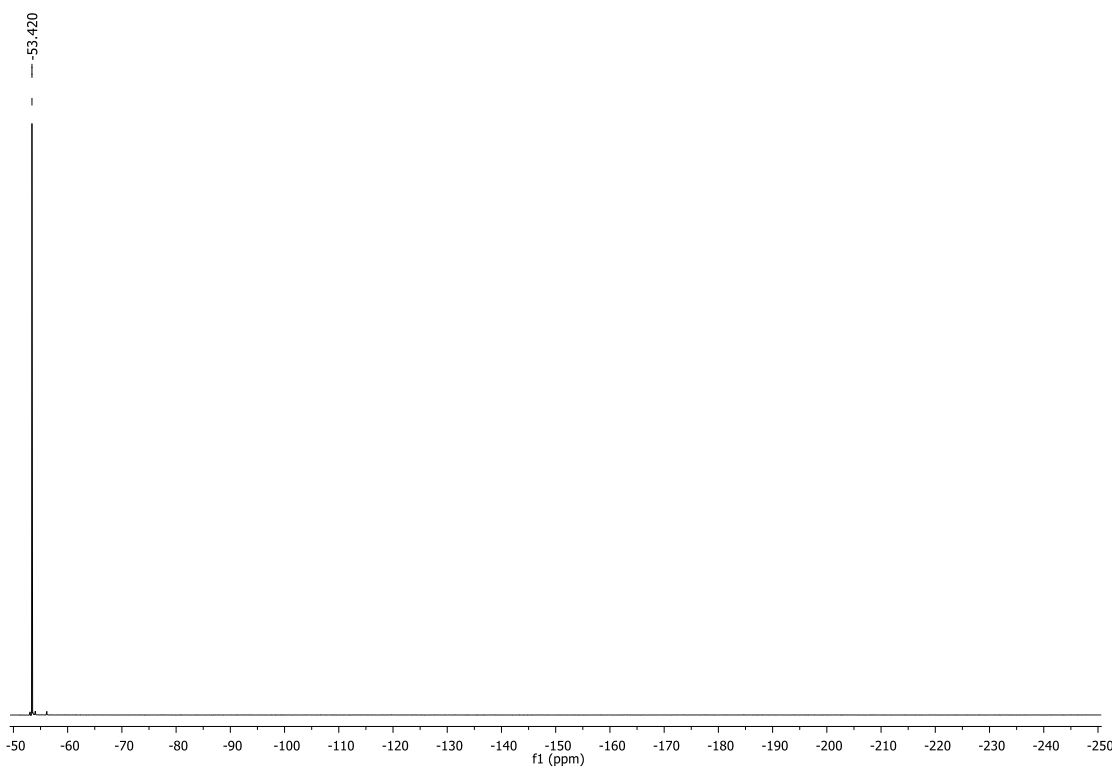
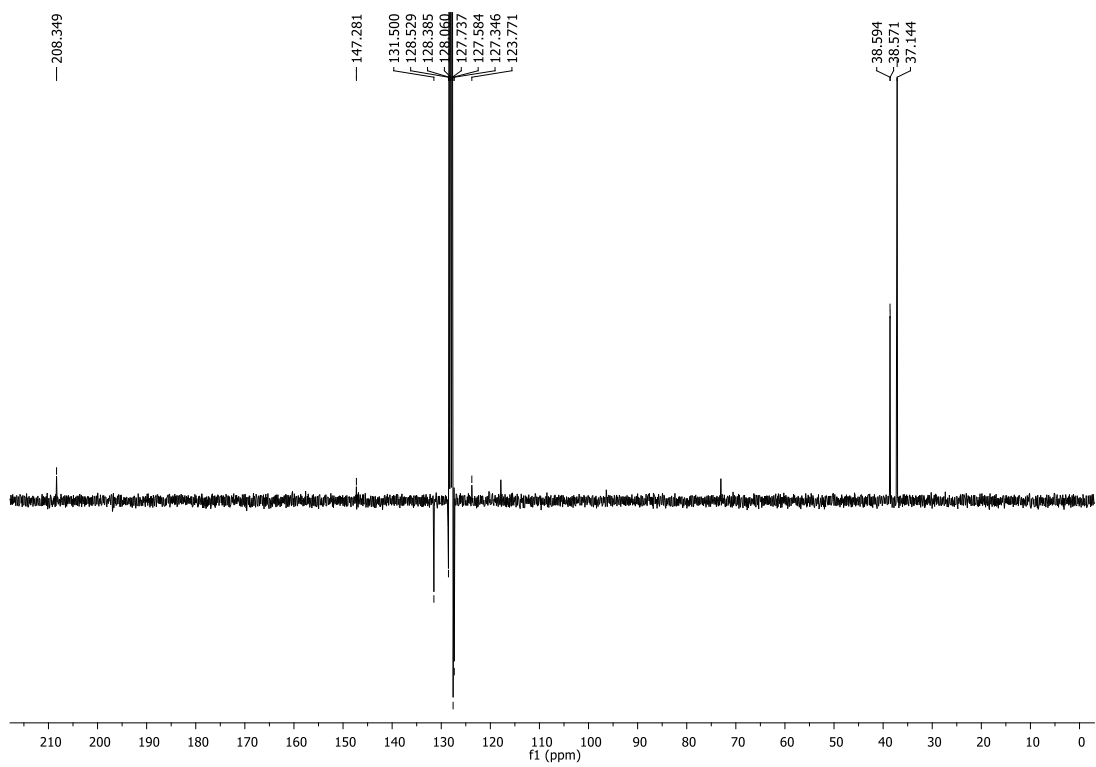


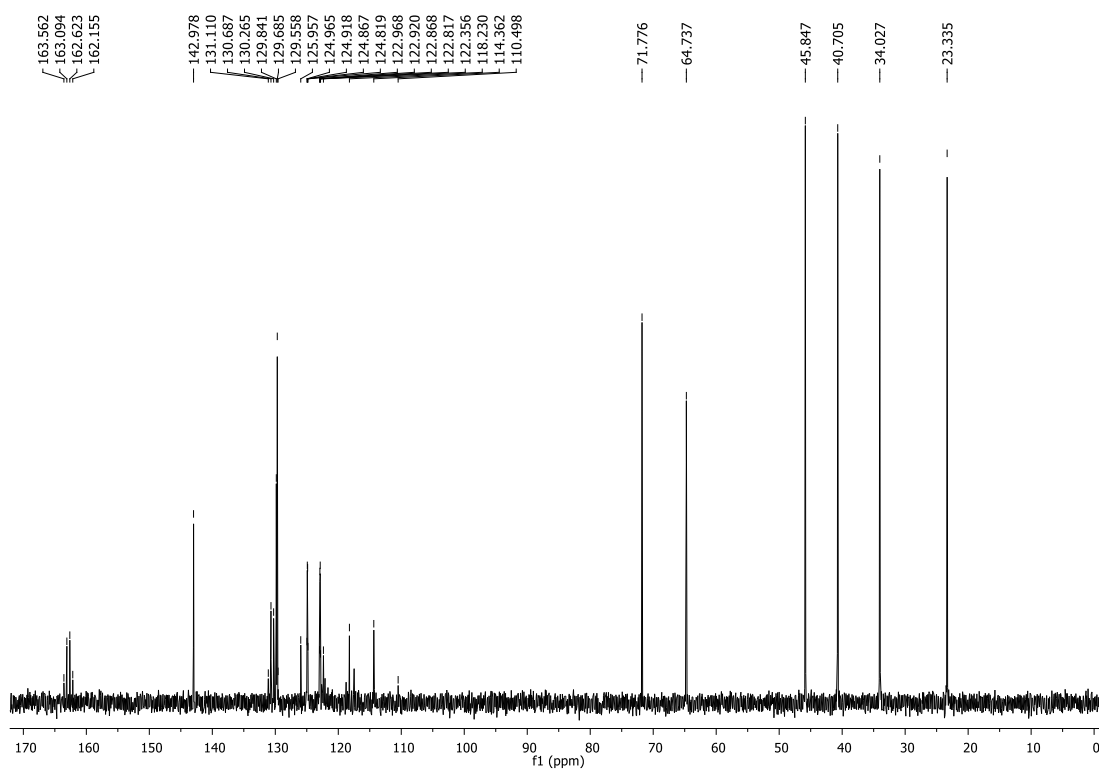
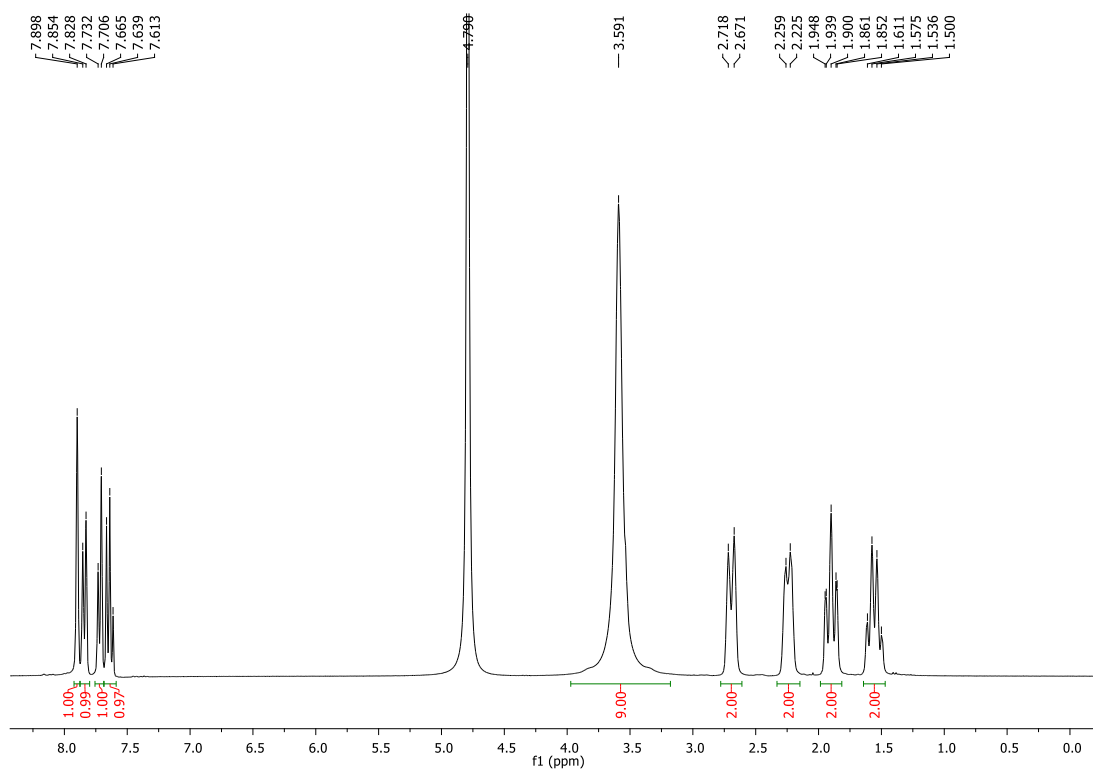
RT (Min)	% Area
1.75166666666667	99.01
2.05333333333333	0.26
2.34833333333333	0.73

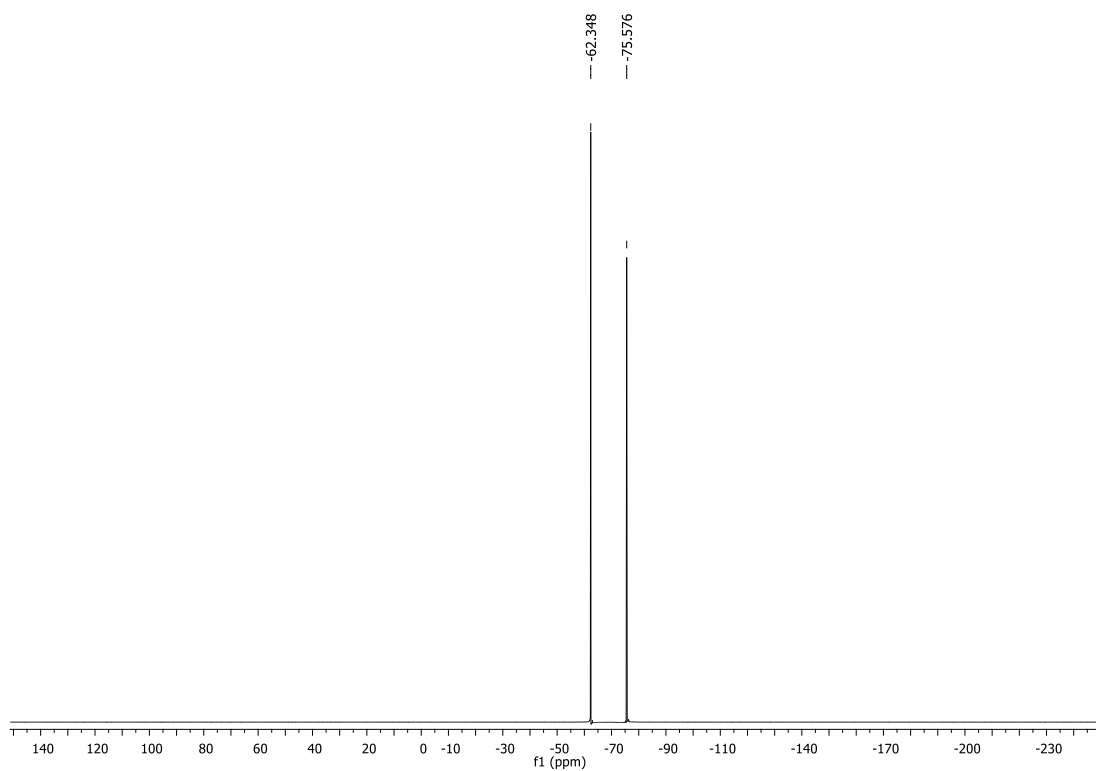
**4-hydroxy-4-(3-(trifluoromethyl)phenyl)cyclohexan-1-one (54h).**



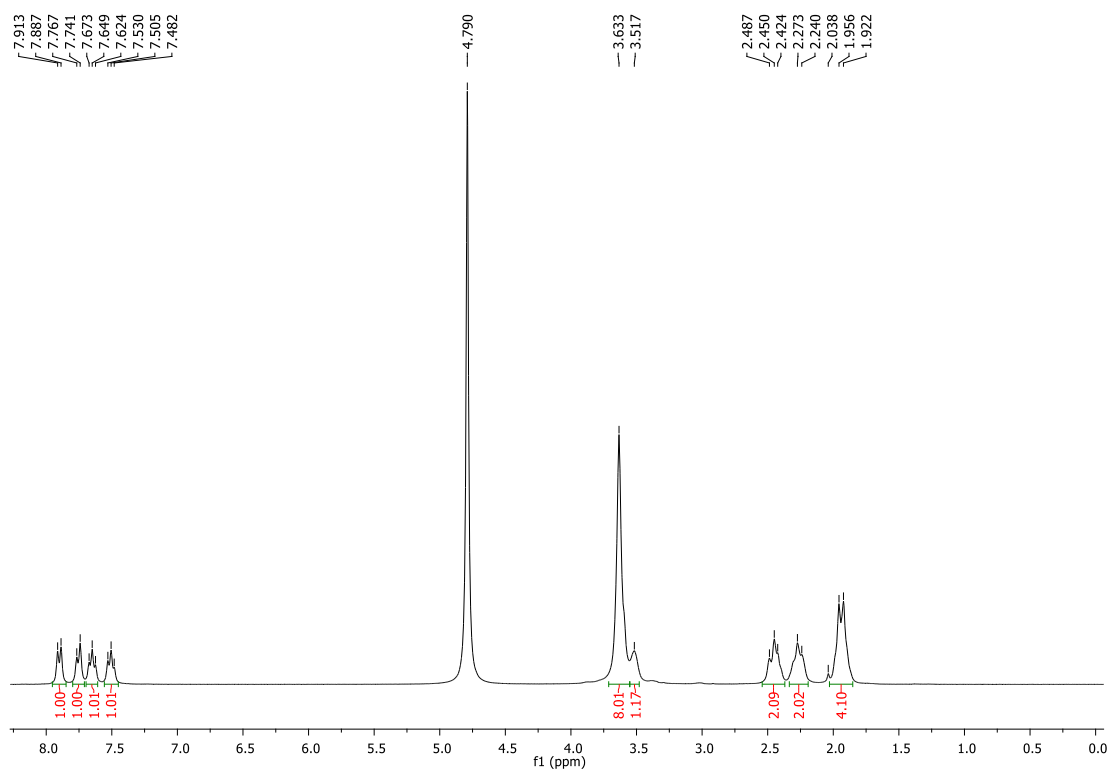
**4-hydroxy-4-(2-(trifluoromethyl)phenyl)cyclohexan-1-one (54i).**

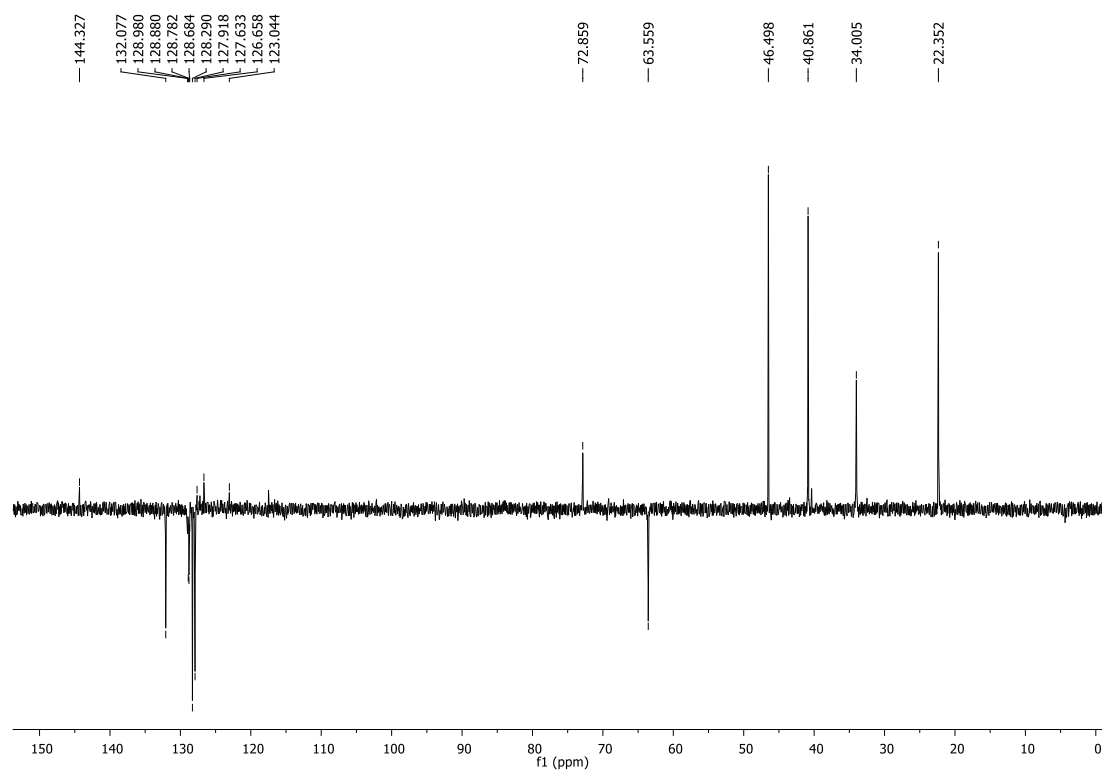
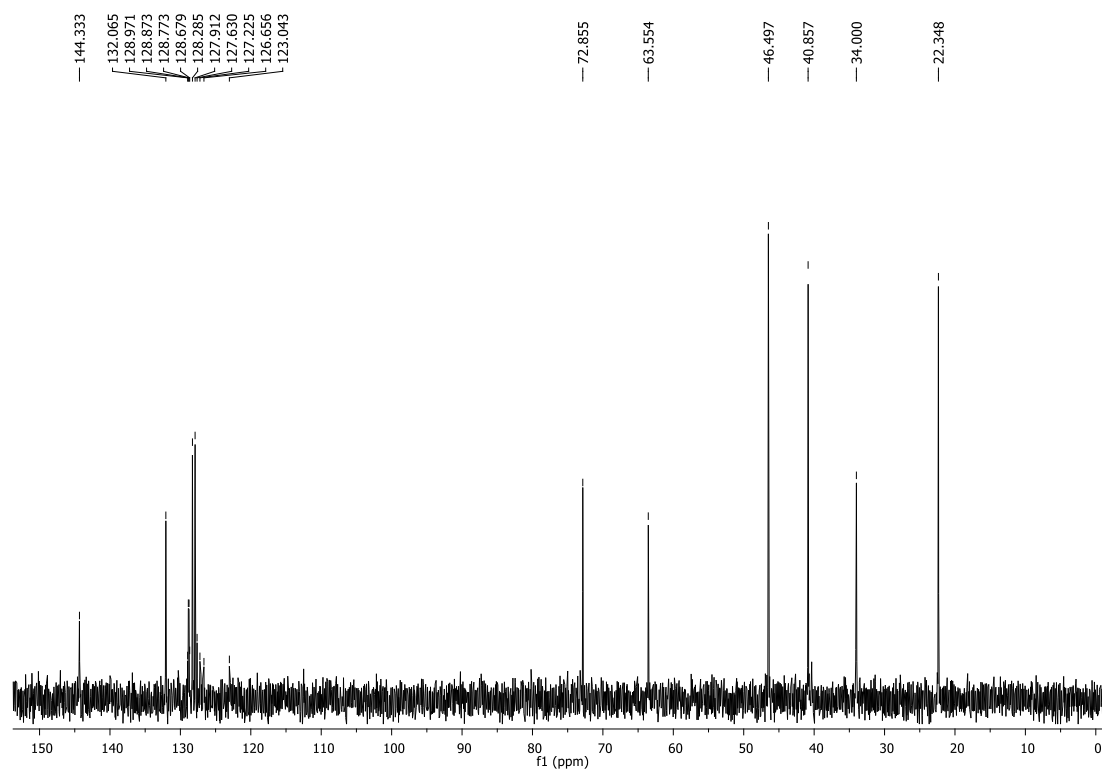


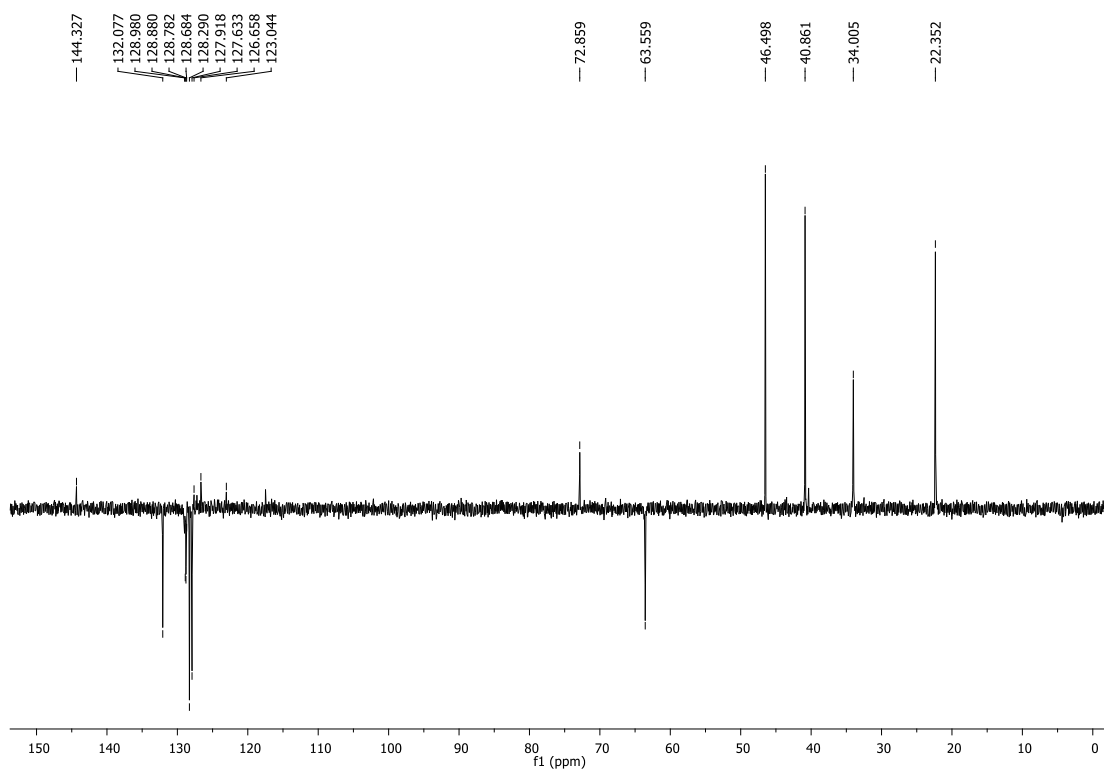
**(1*S*,4*S*)-4-(piperazin-1-yl)-1-(3-(trifluoromethyl)phenyl)cyclohexan-1-ol (55h).**



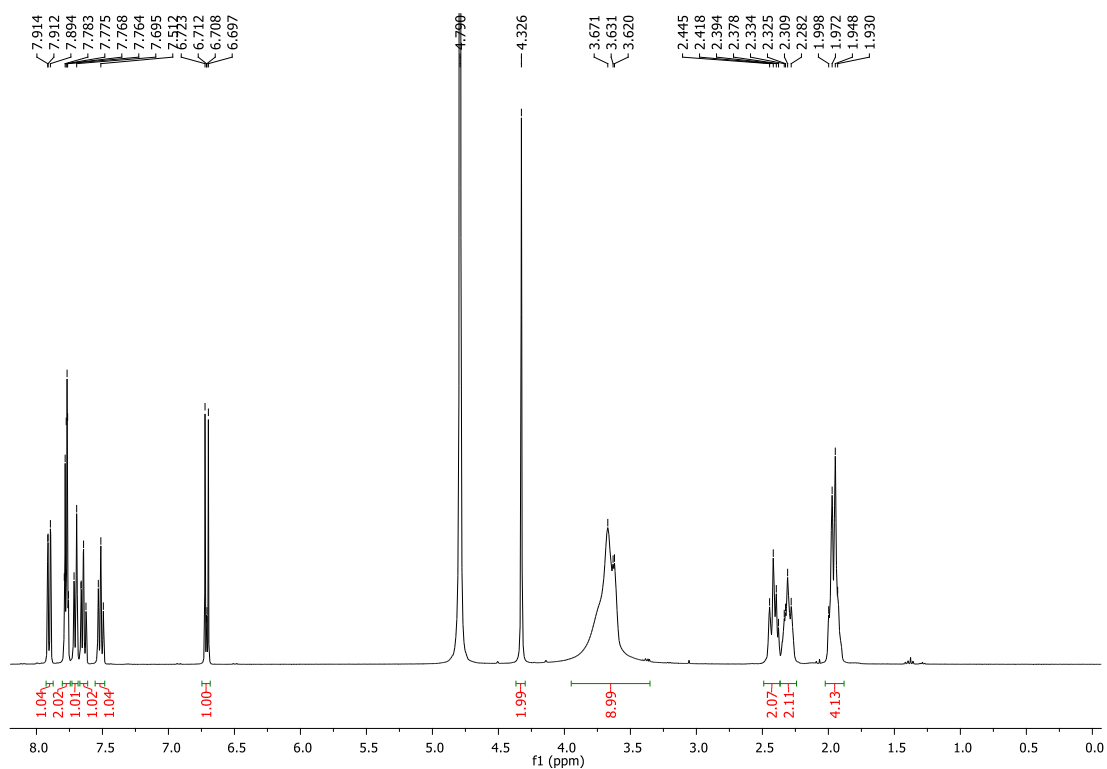
**(1*S*,4*S*)-4-(piperazin-1-yl)-1-(2-(trifluoromethyl)phenyl)cyclohexan-1-ol (55i).**

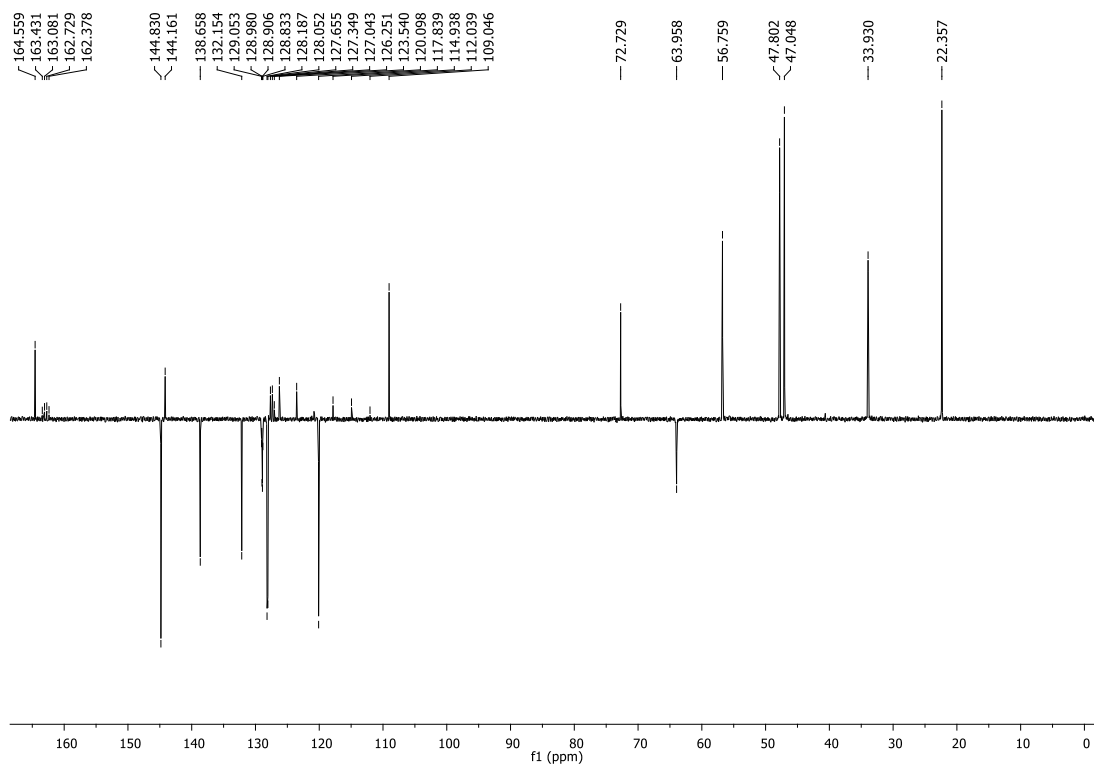
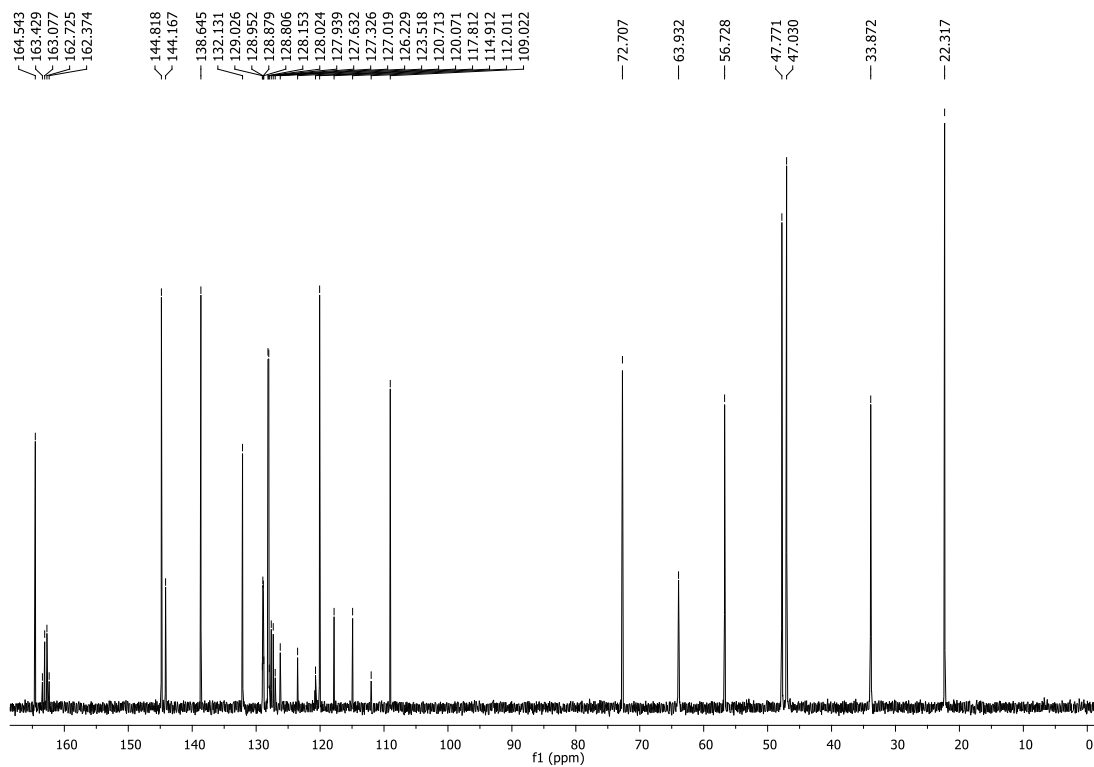


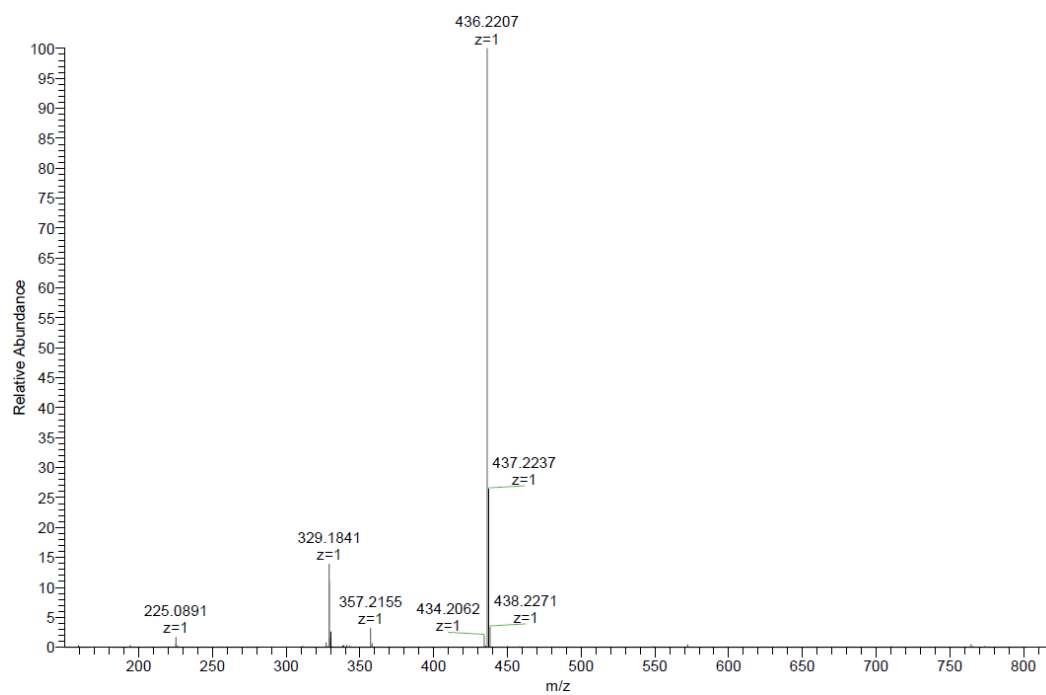
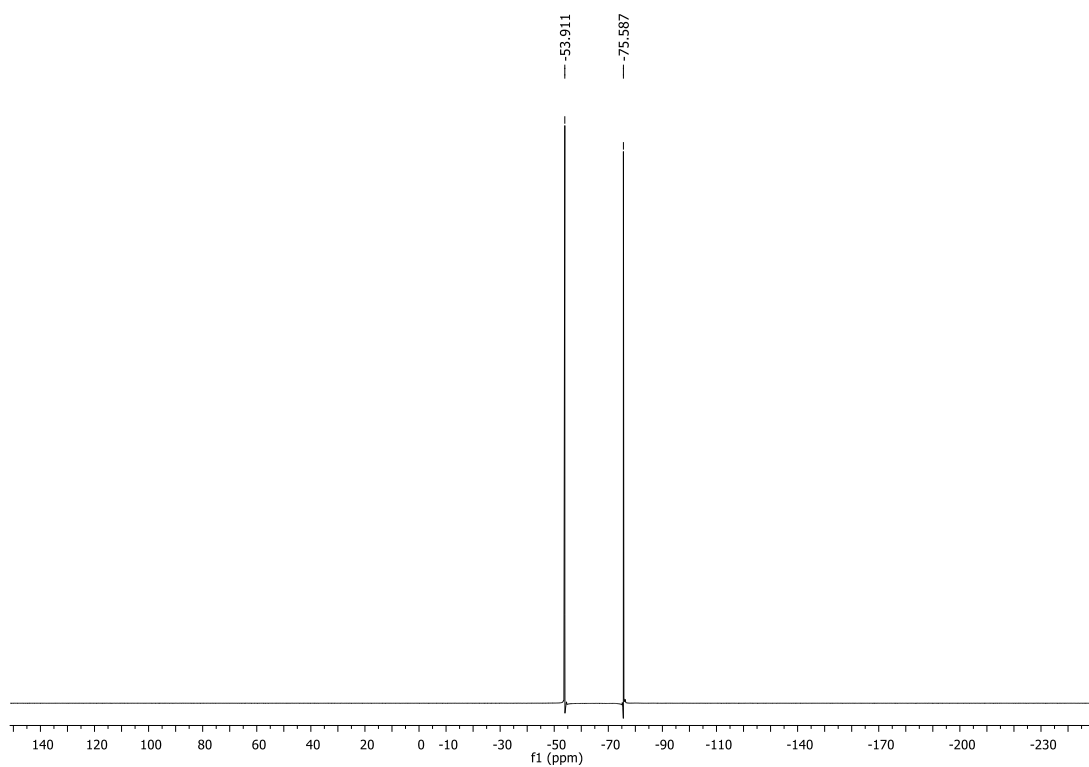


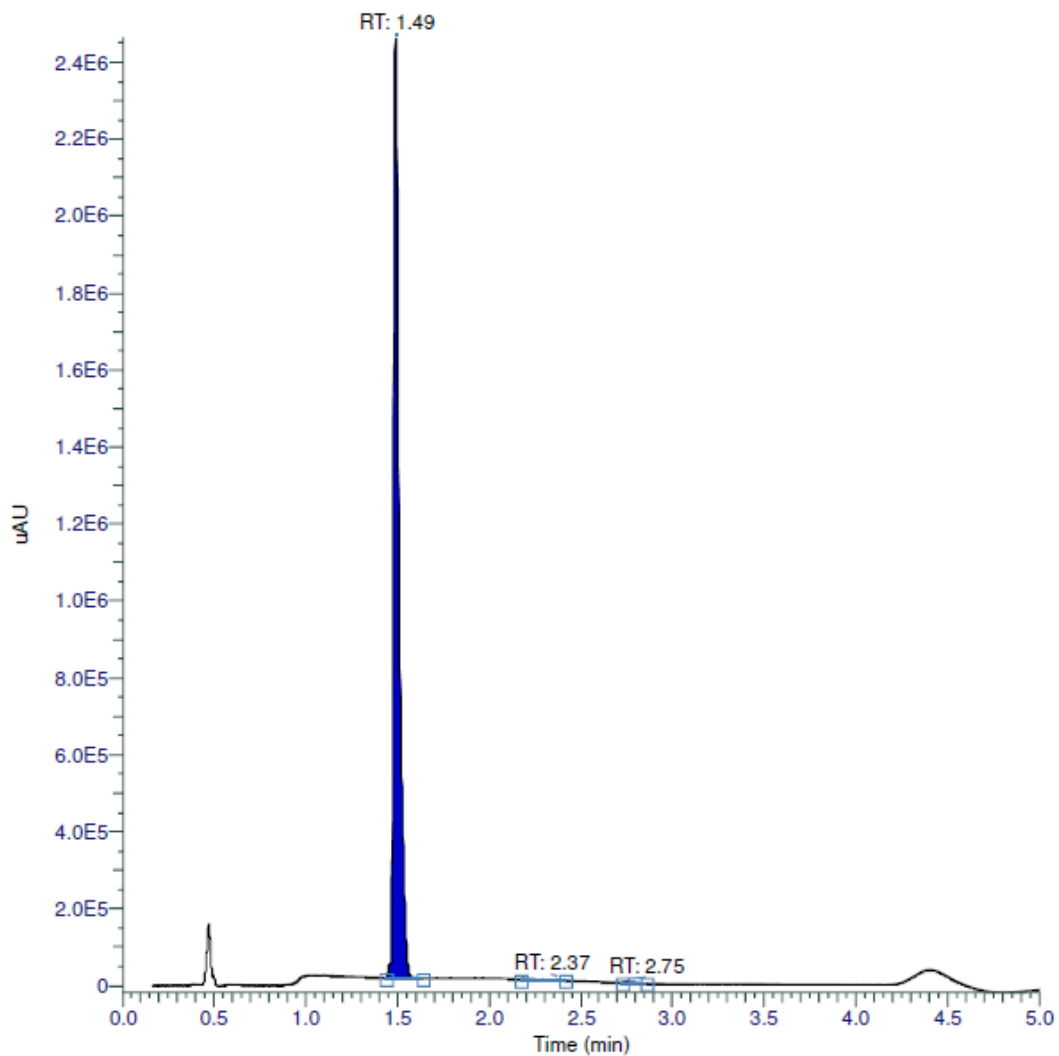


**5-((4-((1*S*,4*S*)-4-hydroxy-4-(3-(trifluoromethyl)phenyl)cyclohexyl)piperazin-1-yl)methyl)pyridin-2(1H)-one (56h).**

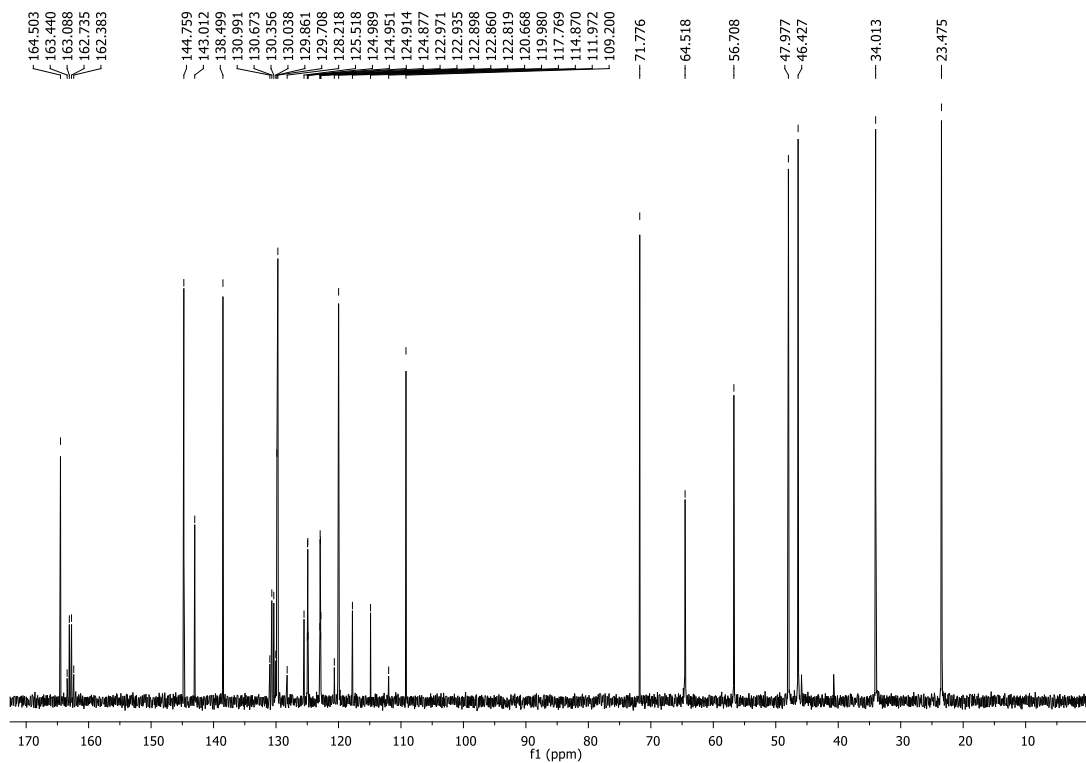
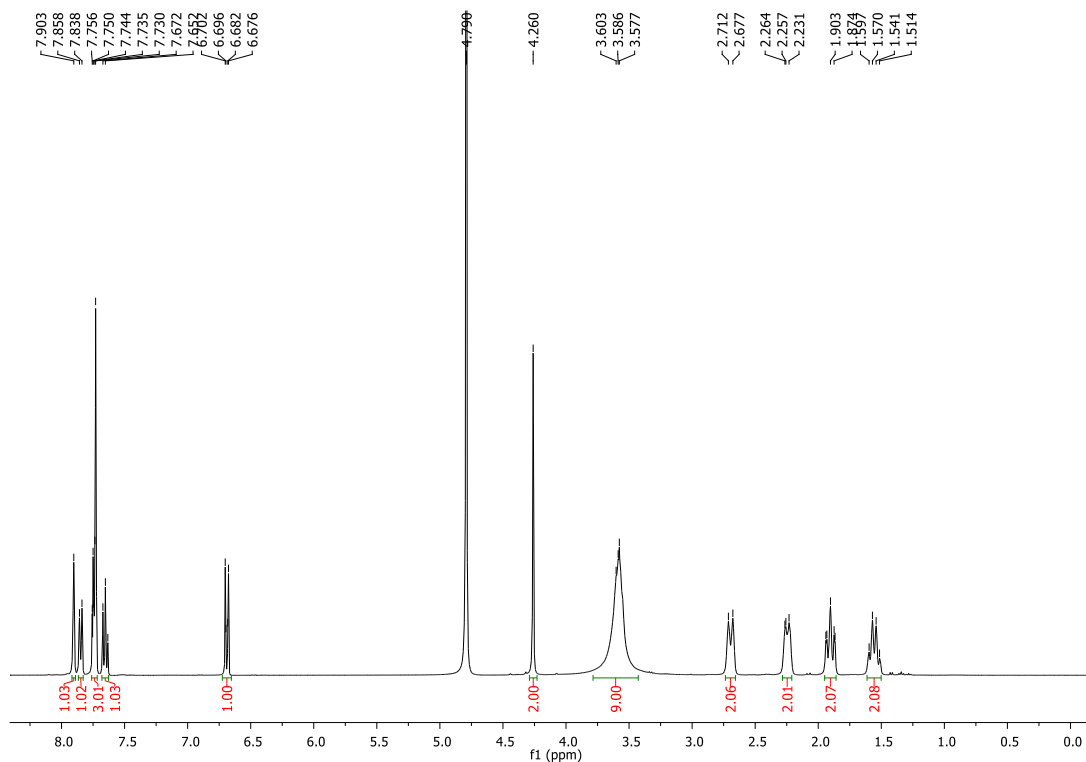


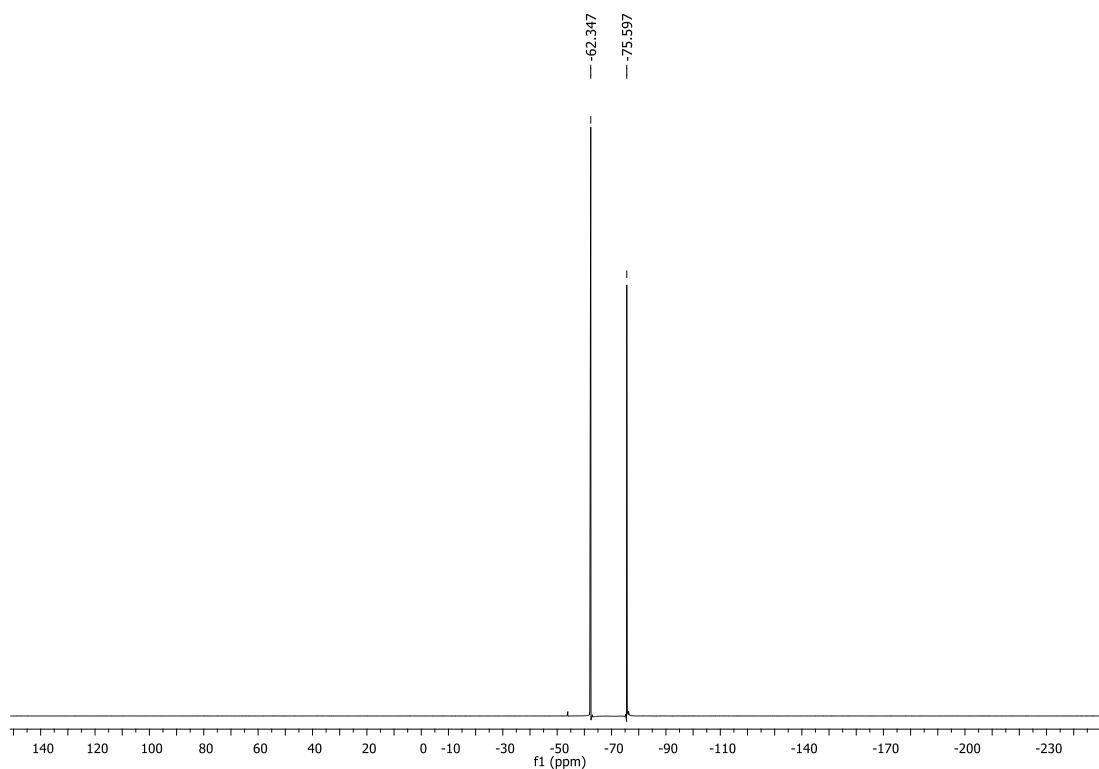
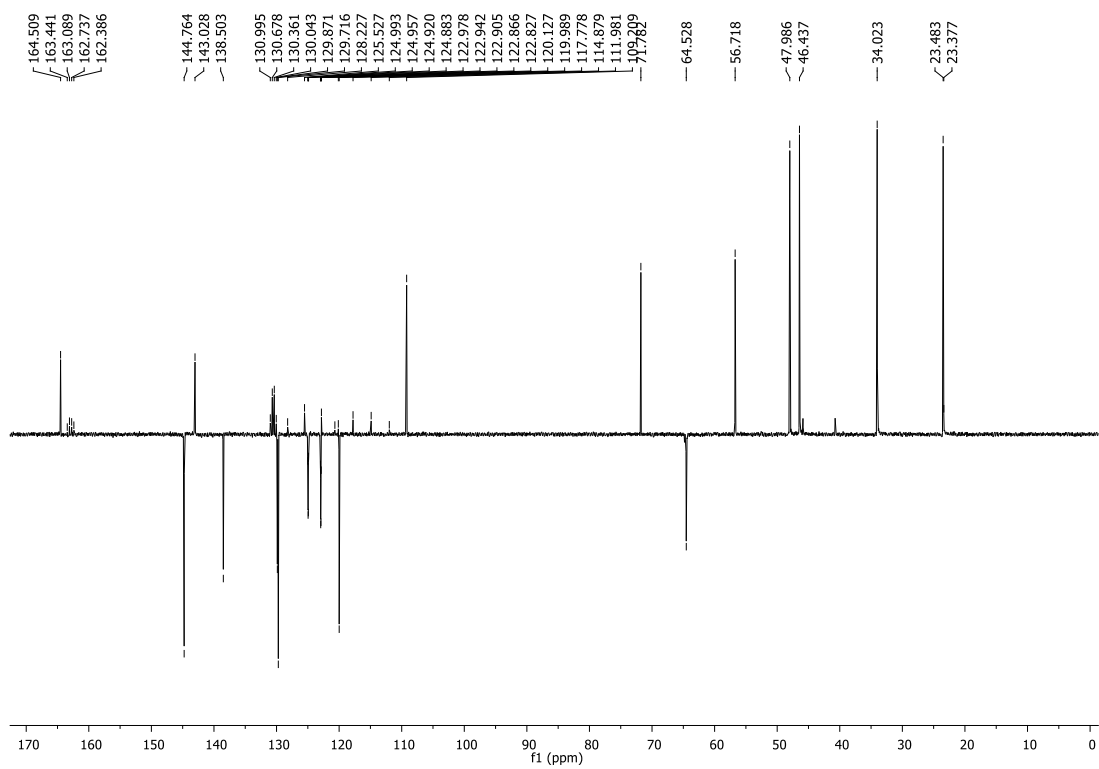


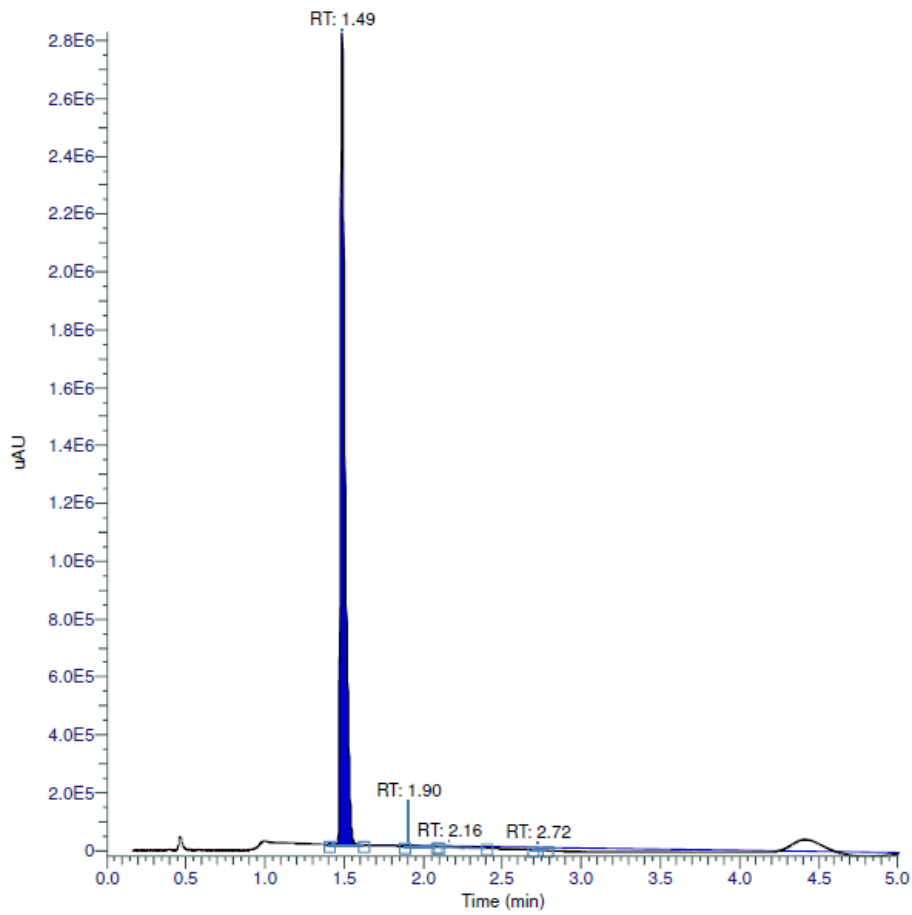
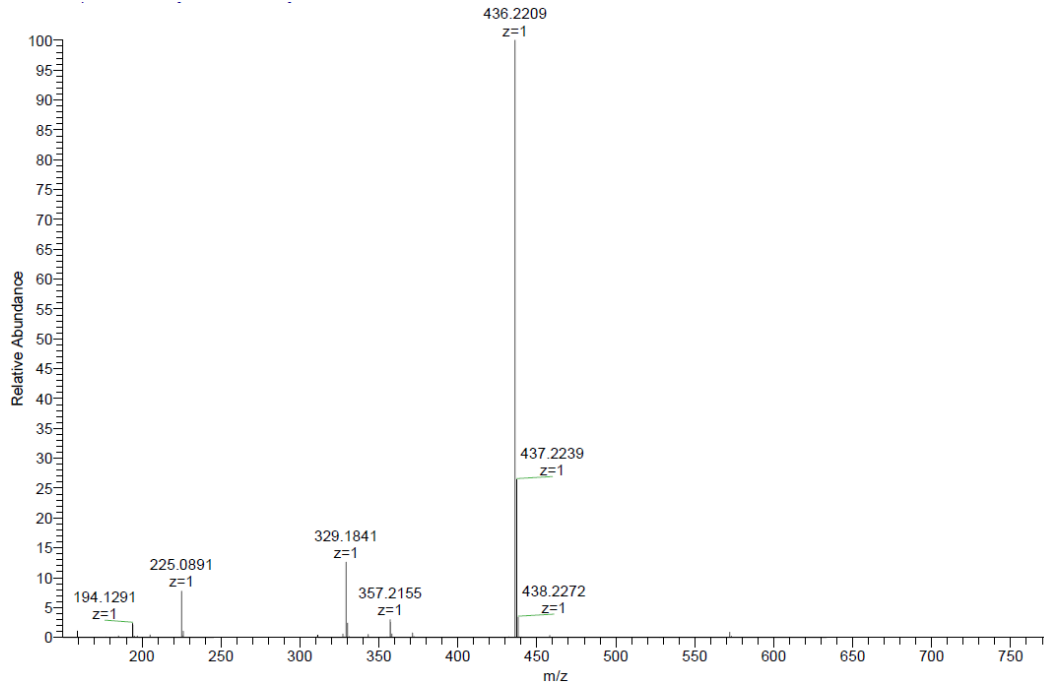




RT (Min)	% Area
1.4883333333333333	99.78
2.3683333333333333	0.11
2.7533333333333333	0.11

**5-((4-((1*S*,4*S*)-4-hydroxy-4-(2-(trifluoromethyl)phenyl)cyclohexyl)piperazin-1-yl)methyl)pyridin-2(1*H*)-one (56i).**





RT (Min)	% Area
1.48666666666667	99.62
1.90166666666667	0.1
2.16333333333333	0.23
2.72	0.05

## 7.5 Curriculum Vitae

19/10/2019

Curriculum System of Curriculum Lattes (Micael Rodrigues Cunha)



Micael Rodrigues Cunha

I have degree in Pharmacy at Mackenzie Presbyterian University (2014) and conduct my PhD at the University of São Paulo, Department of Pharmacy (Brazil). In 2017, I was awarded with the Swiss Excellence Scholarship for Foreign Scholars at the University of Bern, Department of Chemistry and Biochemistry (Switzerland). For almost two years I'd worked within the National Centre of Competence in Research (NCCR) TransCure focused in transmembrane receptors, as part of my exchange PhD. Organized, communicative and committed with project's goals, my main working area involve the Medicinal Chemistry aspects of Drug Discovery: synthesis of small molecules, biological evaluation and molecular modeling (docking and dynamics).  
(Text informed by the author)

Last updated 09/06/2019

06/09/2019

Address to access this CV:  
<http://lattes.cnpq.br/5423655107938989>

### Personal Information

**Name** Micael Rodrigues Cunha

**Bibliographic Citation** CUNHA, M. R.; CUNHA, MICAEL RODRIGUES; CUNHA, MICAEL R.; CUNHA, MICAEL

**Professional Address** Universidade de São Paulo, Faculdade de Ciências Farmacêuticas.  
Cidade Universitária  
Butantã  
05508900 - São Paulo, SP - Brasil  
Phone: (11) 30913793 Extension number: 4

### Formal Education/Degree

- 2015** Ph.D. in progress in Fármaco e Medicamentos .  
Universidade de São Paulo, USP, Brasil.  
with collaborative period in Universität Bern (Advisor: Jean-Louis Reymond ). Advisor: Roberto Parise Filho.  
Grantee of: Coordenação de Aperfeiçoamento de Pessoal de Nível Superior ,CAPES ,Brasil .  
Keywords: Capsaicina; Planejamento de fármacos; Drug design; TRPV.  
Major Area: Health Sciences.  
Major Area: Health Sciences / Área: Pharmacy / Subarea: Química dos Produtos Naturais.  
Activities Sectors: Scientific research and development.
- 2011 - 2014** Graduation in Farmácia .  
Universidade Presbiteriana Mackenzie, MACKENZIE, Brasil.  
Advisor: Jan Carlo Moraes Oliveira Bertassoni Delorenzi.  
Grantee of: Universidade Presbiteriana Mackenzie ,MACKENZIE ,Brasil .
- 2008 - 2010** Secondary Education .  
Colégio Presbiteriano Mackenzie, MACK, Brasil.

### Complementary Education

- 2018 - 2018** ACS Reviewer Lab. (Credit Hours: 30h).  
American Chemical Society, Estados Unidos.
- 2015 - 2015** Continuing education in Pesquisa e Inovação em Fármacos e Medicamentos. (Credit hours: 30h).  
Universidade de São Paulo, USP, Brasil.

### Scientific Journal Referee

- 2015 - 2015** Journal: African Journal of Pharmacy and Pharmacology

### Areas of Expertise

1. Major Area: Health Sciences / Área: Pharmacy / Subarea: Química Farmacêutica.

### Languages

- Portuguese** Comprehends Well, Speaks Well, Reads Well, Writes Well.
- Spanish** Comprehends Reasonably, Speaks Reasonably, Reads Reasonably, Writes Reasonably.
- English** Comprehends Well, Speaks Well, Reads Well, Writes Well.

### Awards and Titles

- 2019** RSC Advances Poster Prize, Royal Society of Chemistry.
- 2018** Best Poster in Chemical Biology, Swiss Chemical Society.
- 2017** Swiss Government Excellence Scholarships for Foreign Scholars and Artists, Swiss Confederation.
- 2015** Paulo Minami Award, Regional Pharmacy Council of São Paulo.

## Scientific, Technological, Artistic and Cultural Production

## Bibliographical Production

## Articles in Scientific Journals

1. [doi>](#) PEREIRA, GUSTAVO JOSÉ VASCO ; TAVARES, M. T. ; Azevedo, R. A. ; Martins, B. B. ; CUNHA, MICAEL R. ; BHARDWAJ, R. ; Cury, Y. ; ZAMBELLI, V. O. ; BARBOSA, E. G. ; HEDIGER, M. A. ; PARISE-FILHO, R. . . BIOORGANIC & MEDICINAL CHEMISTRY **JCR**, v. 27, p. 2893-2904, 2019.
2. [doi>](#) CHAVES, OTÁVIO ; TAVARES, MAURÍCIO ; CUNHA, MICAEL ; PARISE-FILHO, ROBERTO ; SANT'ANNA, CARLOS ; NETTO-FERREIRA, JOSÉ . Multi-Spectroscopic and Theoretical Analysis on the Interaction between Human Serum Albumin and a Capsaicin Derivative-RPF101. *Biomolecules* **JCR**, v. 8, p. 78, 2018.
3. [doi>](#) FERNANDES, T. B. ; CUNHA, MICAEL RODRIGUES ; SAKATA, R. P. ; CANDIDO, T. M. ; BABY, A. R. ; TAVARES, M. T. ; GUIMARAES, E. ; ALMEIDA, W. P. ; PARISE-FILHO, R. . Synthesis, molecular modeling, and evaluation of novel sulfonylhydrazones as acetylcholinesterase inhibitors for Alzheimer's disease.. *ARCHIV DER PHARMAZIE* **JCR**, v. 350, p. 1-16, 2017.
4. [doi>](#) TAVARES, MAURÍCIO T. ; PRIMI, MARINA C. ; SILVA, NUNO A. T. F. ; CARVALHO, CAMILA F. ; CUNHA, MICAEL R. ; PARISE-FILHO, ROBERTO . Using an in Silico Approach To Teach 3D Pharmacodynamics of the Drug-Target Interaction Process Focusing on Selective COX2 Inhibition by Celecoxib. *JOURNAL OF CHEMICAL EDUCATION* **JCR**, v. 94, p. 380-387, 2017.
5. [doi>](#) MELO, TAHIRA SOUZA ; GATTASS, CERLI ROCHA ; SOARES, DEIVID COSTA ; CUNHA, MICAEL RODRIGUES ; FERREIRA, CHRISTIAN ; TAVARES, MAURÍCIO TEMOTHEO ; SARAIVA, ELVIRA ; FILHO, ROBERTO PARISE ; BRADEN, HANNAH ; DELORENZI, JAN CARLO . Oleanolic acid (OA) as an antileishmanial agent: Biological evaluation and in silico mechanistic insights. *Parasitology International* **JCR**, v. 65, p. 227-237, 2016.
6. [doi>](#) CUNHA, MICAEL RODRIGUES ; TAVARES, MAURÍCIO TEMOTHEO ; CARVALHO, CAMILA FELIX ; PEREIRA, GUSTAVO JOSÉ VASCO ; SOUZA, ALFREDO DANILO FERREIRA ; SILVA, NUNO ALBUQUERQUE TAVARES ; FERREIRA, FABIO FURLAN ; PARISE FILHO, ROBERTO . An environmentally safe condition for the synthesis of aryl and alkyl sulphonyl hydrazones via one-pot reaction. *ACS SUSTAINABLE CHEMISTRY & ENGINEERING* **JCR**, v. 4, p. 1899-1905, 2016.
7. [doi>](#) CUNHA, M. R. ; MELO, T. S. ; MAGRI, F. M. M. ; DELORENZI, J. C. . Analgesic activity of *Ruta graveolens* L. (Rue) extracts. *African Journal of Pharmacy and Pharmacology* **JCR**, v. 9, p. 1-5, 2015.

## Articles accepted for publication

1. [doi>](#) CUNHA, MICAEL RODRIGUES ; BHARDWAJ, RAJESH ; LINDINGER, SONJA ; BUTORAC, CARMEN ; ROMANIN, CHRISTOPH ; HEDIGER, MATTHIAS A. ; REYMOND, JEAN-LOUIS . A Photoswitchable Inhibitor of the Calcium Channel TRPV6. *ACS Medicinal Chemistry Letters* **JCR**, 2019.

## Technical Production

## Other Kinds of Technical Production

1. CUNHA, M. R. ; LEAL, S. W. ; CERVONE, A. ; CARVALHO, A. Y. O. M. . Young Pharmacists and Perspectives. 2016. (Radio or TV Program/ Roundtable).

## Events

## Participation in events

1. .Design, synthesis and photochemical properties of a new photoswitchable TRPV6 inhibitor. 2019. (Participation In Events/ Congresses).
2. .Lead-Optimization of 1-(4-aryl)cyclohexyl-4-(3-pyridyl)piperazine as TRPV6 Inhibitors. 2019. (Participation In Events/ Symposium).
3. .Design, synthesis and photochemical properties of a new photoswitchable TRPV6 inhibitor. 2018. (Participation In Events/ Congresses).
4. .Design, synthesis and photochemical properties of a new photoswitchable TRPV6 inhibitor. 2018. (Participation In Events/ Congresses).
5. .Practical Drug Discovery in Chemical Space Using TransCure Online Tools. 2017. (Participation In Events/ Seminary).
6. .Design, Synthesis and Antitumor Evaluation of Bioisosteric Capsaicin-Like Compounds. 2016. (Participation In Events/Other).
7. .A facile and industrial scalable one-pot synthesis of aryl/alkylsulphonyl hydrazones. 2015. (Participation In Events/ Meetings).
8. .Congress of Bible School Teachers and Leaders. 2013. (Participation In Events/ Congresses).
9. .Study of the Potential Analgesic Effect of *Ruta graveolens* (rue).. 2013. (Participation In Events/ Seminary).

## Organization of Events

1. FERRAZ, H. G. ; CUNHA, M. R. ; SOUZA, A. D. F. ; HUBNER, A. ; WRÓBLEWSKA, K. B. ; BARBOSA, E. J. ; GONZAGA, R. V. . Winter School: Research and Innovation in Drugs and Medicines. 2016. (Event Production/ Other).
2. FERREIRA, E. I. ; PARISE-FILHO, R. ; CUNHA, M. R. . IV Symposium on Drug Design and Development for Neglected Diseases. 2015. (Event Production/Congress).
3. FERREIRA, E. I. ; PARISE-FILHO, R. ; CUNHA, M. R. . XIII National Meeting of Medicinal Chemistry Professors. 2015. (Event Production/Congress).

## 7.6 Student's Record

Janus - Sistema Administrativo da Pós-Graduação



Universidade de São Paulo  
Faculdade de Ciências Farmacêuticas

Documento sem validade oficial

FICHA DO ALUNO

9138 - 9265072/2 - Micael Rodrigues Cunha

**Email:** micaelrc@usp.br  
**Data de Nascimento:** 20/11/1993  
**Cédula de Identidade:** RG - 41.858.247-6 - SP  
**Local de Nascimento:** Estado de São Paulo  
**Nacionalidade:** Brasileira  
**Graduação:** Farmaceutica Bioquimica - Universidade Presbiteriana Mackenzie - São Paulo - Brasil - 2014  
**Graduação:** Farmácia - Universidade Presbiteriana Mackenzie - São Paulo - Brasil - 2015

**Curso:** Doutorado Direto  
**Programa:** Fármaco e Medicamentos  
**Área:** Insumos Farmacêuticos  
**Data de Matrícula:** 14/07/2015  
**Início da Contagem de Prazo:** 14/07/2015  
**Data Limite para o Depósito:** 11/11/2019  
**Orientador:** Prof(a). Dr(a). Roberto Parise Filho - 14/07/2015 até o presente. Email: roberto.parise@usp.br  
**Proficiência em Línguas:** Inglês, Aprovado em 14/07/2015  
**Prorrogação(ões):** 120 dias  
 Período de 14/07/2019 até 11/11/2019  
**Data de Aprovação no Exame de Qualificação:** Aprovado em 29/06/2017  
**Data do Depósito do Trabalho:**  
**Título do Trabalho:**  
**Data Máxima para Aprovação da Banca:**  
**Data de Aprovação da Banca:**  
**Data Máxima para Defesa:**  
**Data da Defesa:**  
**Resultado da Defesa:**  
**Histórico de Ocorrências:** Primeira Matrícula em 14/07/2015  
 Prorrogação em 11/03/2019

Sigla	Nome da Disciplina	Início	Término	Carga Horária	Cred.	Freq.	Conc.	Exc.	Situação
FBF5777-3/5	Tópicos Gerais de Fármaco e Medicamentos I	13/08/2015	25/11/2015	45	3	93	A	N	Concluída
FBF5779-2/3	Preparo de Artigos Científicos na Área de Farmácia	04/09/2015	05/11/2015	90	6	100	A	N	Concluída
FBF5734-7/4	Mecanismos de Ação dos Fármacos aos Níveis Molecular e Eletrônico	16/02/2016	30/05/2016	90	6	100	A	N	Concluída
FBF5704-6/4	Análise Espectrométrica de Fármacos	02/03/2016	14/06/2016	150	10	95	A	N	Concluída
FBF5805-2/2	Delineamento de Experimentos e Ferramentas Estatísticas Aplicadas às Ciências Farmacêuticas	10/03/2016	19/05/2016	90	6	100	A	N	Concluída
FBF5824-1/1	Introdução à Modelagem Molecular como Ferramenta no Estudo e Desenvolvimento de Moléculas Biotivas	04/07/2016	24/07/2016	90	6	100	A	N	Concluída
FBF5826-1/1	Relação entre Estrutura Química e Atividade Biológica	09/08/2016	31/10/2016	120	8	100	A	N	Concluída
FBA5728-4/3	Aprimoramento Pedagógico	16/08/2016	12/09/2016	60	4	100	A	N	Concluída

	Créditos mínimos exigidos		Créditos obtidos
	Para exame de qualificação	Para depósito de tese	
<b>Disciplinas:</b>	0	25	49
<b>Estágios:</b>			
<b>Total:</b>	0	25	49

Créditos Atribuídos à Tese: 167

Conceito a partir de 02/01/1997:

A - Excelente, com direito a crédito; B - Bom, com direito a crédito; C - Regular, com direito a crédito; R - Reprovado; T - Transferência.

Um(1) crédito equivale a 15 horas de atividade programada.

Última ocorrência: Matrícula de Acompanhamento em 01/07/2019

Impresso em: 19/10/2019 14:26:12